Loughborough University

This item was submitted to Loughborough University as a PhD thesis by the author and is made available in the Institutional Repository (https://dspace.lboro.ac.uk/) under the following Creative Commons Licence conditions.

creative commons

COMMONS DEED

Attribution-NonCommercial-NoDerivs 2.5

You are free:

- to copy, distribute, display, and perform the work

Under the following conditions:

Attribution. You must attribute the work in the manner specified by the author or licensor.

Noncommercial. You may not use this work for commercial purposes.

No Derivative Works. You may not alter, transform, or build upon this work.

- For any reuse or distribution, you must make clear to others the license terms of this work.
- Any of these conditions can be waived if you get permission from the copyright holder.

Your fair use and other rights are in no way affected by the above.

This is a human-readable summary of the Legal Code (the full license).

Disclaimer

For the full text of this licence, please go to:
http://creativecommons.org/licenses/by-nc-nd/2.5/

BLDSC No. DX/81050

LOUGHBOROUGH
UNIVERSITY OF TECHNOLOGY
LIBRARY

AUTHOR/FILING TITLE
HEUMANN, T O

ACCESSION/COPY NO.
016719/02

VOL. NO. | CLASS MARK

LOAN COPY

12 FEB 1993
03 JUN 1994
30 JUN 1995
20 FEB 1996

13 NOV 1992

001 6719 02

Elastic Properties and Failure Mechanisms in Hybrid Composites with Differing Resin Matrices

by

TIMOTHY O. HEUMANN

A Doctoral Thesis submitted in partial fulfilment
of the requirements for the award of
Doctor of Philosophy
of the Loughborough University of Technology

1987

Supervisor: Mr J.F. Harper
Institute of Polymer Technology and Materials Engineering

© by Timothy Heumann, 1987

Loughborough University
of Technology Library
Date Mar 88
Class
Acc. No. 016719/02

SYNOPSIS

Previous work on tensile and compressive failure of both monofibre and hybrid unidirectional composites is reviewed, together with a summary of some of the more important works on the variation of elastic modulus.

A series of hybrid composite laminates was made up using the Derakane 411 and 470 vinyl ester resins and the Ciba-Geigy Fibredux 913 and 914 epoxy resin prepreg systems, with E-glass and Grafil XA-S carbon fibre reinforcement. Tensile and compressive tests were performed together with some further inter-laminar shear and transverse tensile tests. Emphasis was placed on the study of failure mechanisms in monofibre composites. This was necessary as a basis from which hybrid behaviour could be analysed.

The elastic moduli of the composites varied with respect to both tensile and compressive strain. The large variation in the CFRP modulus is explained in terms of the variation in fibre modulus, while the smaller reduction in modulus of GRP with respect to tensile strain is interpreted as the result of some debonding occurring before failure. The elastic moduli of hybrids obeyed the rule-of-mixtures throughout the strain range.

The vinyl esters form poorer bonds with the fibres than do the epoxies, but this was not reflected in their tensile strengths. The tensile failure strains exhibited a positive hybrid effect which was greater in laminates with a lower carbon:glass reinforcement ratio. The tensile failure strains of laminates with GRP outer layers were greater than those with CFRP outer layers.

Compressive failure results were analysed on a similar basis. Compressive strengths were better than those of some previous workers due to the increased Celanese specimen width adopted, but they were lower than the tensile strengths, even when the shear mechanism of failure occurred. This is due to stress raising effects as a result of compressive specimen geometry. Unlike the tensile failure results, several different mechanisms of failure occurred, the active one being dependent on the type of matrix/composite system and the type of fibre reinforcement. As in tension, a positive hybrid effect was observed which increased with decreasing proportion of carbon fibre, and the compressive failure strains of laminates with GRP outer layers were greater than those with CFRP outer layers.

Failure mechanisms of hybrid laminates resembled those of the respective parent materials in both tension and compression. Characteristic curves describing the failure strain of hybrid lay-ups with respect to the fibre reinforcement ratio V_{fc}/V_{ft} are established.

The most significant matrix effect was the poor compressive strengths recorded in vinyl-ester CFRP specimens. This was reflected in the hybrid lay-ups. It is explained in terms of the observed failure mechanisms.

Some suggestions for further work are included.

ACKNOWLEDGEMENTS

The author wishes to express his thanks to the following, for their help in the accomplishment of this work.

- Professor I.A. Menzies of the Institute of Polymer Technology and Materials Engineering for the provision of laboratories and research facilities

- Supervisor Mr J.F. Harper for his continuous guidance and encouragement.

- The Ministry of Defence for the provision of funds.

- Dr G. Dorey of RAE for assistance and useful comments throughout the course.

- Mr N.A. Miller for his instruction and assistance in using the mechanical test equipment.

- Fellow research workers, especially Dr M. Naeem for helpful discussions and practical assistance.

- Mrs Janet Smith for her care and attention in typing this thesis.

TABLE OF CONTENTS

		Page No
Synopsis		i
Acknowledgements		iii
Contents		iv
List of Tables		viii
List of Figures		xi
List of Plates		xx
Principal Notation		xxiii
CHAPTER 1:	INTRODUCTION	1
CHAPTER 2:	LITERATURE REVIEW	6
2.1	Introduction	6
2.2	Resin Chemistry	7
	2.2.1 Polyester Resins	7
	2.2.2 Epoxy Resins	9
	2.2.3 Vinyl Ester Resins	12
2.3	Tensile Behaviour of Unidirectional Fibre Composites	15
	2.3.1 Monofibre Composites	15
	2.3.2 Hybrid Composites	29
2.4	Compressive Behaviour of Unidirectional Fibre Composites	46
	2.4.1 Monofibre Composites	46
	2.4.2 Hybrid Composites	64
2.5	Elastic Modulus Variation	70
CHAPTER 3:	EXPERIMENTAL WORK	77
3.1	Introduction	77
3.2	Materials	80
	3.2.1 Glass Fibres	80
	3.2.2 Carbon Fibres	80

Page No

	3.2.3	Epoxy Resin Prepregs	81
	3.2.4	Vinyl Ester Resins	81
3.3	Equipment		82
	3.3.1	Laminate Manufacturing Equipment .	82
	3.3.2	Volume Fraction Analysis Equipment .	84
	3.3.3	The Celanese Compression Test Fixture	84
	3.3.4	Mechanical Testing Equipment . . .	86
3.4	Techniques		86
	3.4.1	Manufacture of Composite Slabs . .	86
	3.4.2	Preparation of Test Specimens . . .	89
	3.4.3	Volume Fraction Analysis	91
	3.4.4	Environmental Conditioning	94
	3.4.5	Strain Measurement	95
	3.4.6	Mechanical Testing and Data Acquisition	99
	3.4.7	Resin Density Measurement	100
	3.4.8	Determination of Strain Gauge Requirement on Compressive Test Specimens	101
	3.4.9	Poisson's Ratio Measurement	103
CHAPTER 4:	RESULTS		105
4.1	Introduction		105
4.2	Tensile Properties		106
	4.2.1	Observations from the Tensile Tests	106
	4.2.2	Tensile Failure Strain	108
	4.2.3	Ultimate Tensile Strength	109
4.3	Compressive Properties		110
	4.3.1	Observations from the Compressive Tests	110
	4.3.2	Compressive Failure Strain	111
	4.3.3	Ultimate Compressive Strength . . .	112

Page No

4.4 Elastic Modulus 112

4.4.1 Methods of Elastic Modulus Measurement 112

4.4.2 Secant Modulus Results 114

4.4.3 Tangent Modulus Results 114

4.5 Other Properties 115

4.5.1 Inter-Laminar Shear Strength . . . 115

4.5.2 Transverse Tensile Strength 116

4.5.3 Poisson's Ratio 117

CHAPTER 5: DISCUSSION 118

5.1 The Rule of Mixtures and Hybrid Effects . . 118

5.2 The Variable Elastic Modulus 124

5.2.1 Modulus Variation and the Rule of Mixtures 124

5.2.2 The Effect of a Composite Modulus which Varies with Strain 126

5.2.3 The Causes of the Variation in Modulus 128

5.3 Tensile Failure 137

5.3.1 Tensile Failure and Bond Strength . 137

5.3.2 Analysis of the UTS Results 140

5.3.3 A Model for Tensile Failure 144

5.3.4 Tensile Failure of Hybrid Laminates 147

5.4 Compressive Failure 151

5.4.1 Introduction to Compressive Failure Modes 151

5.4.2 Compressive Failure of Monofibre Composites 152

5.4.3 Compressive Failure of Hybrid Composites 173

5.4.4 An Assessment of the Celanese Compression Test Fixture and Specimen Geometry 178

Page No

5.5	Resin Effects	181
	5.5.1 Introduction	181
	5.5.2 Bond Strength	182
	5.5.3 914 CFRP	182
	5.5.4 Tensile Strength	184
	5.5.5 Compressive Strength	185
	5.5.6 Elastic Modulus	188
	5.5.7 The Hybrid Effect	189
5.6	Characterisation of the Hybrid Effect . .	191
CHAPTER 6:	CONCLUSIONS	198
6.1	Composite Modulus	198
6.2	Tensile Failure	199
6.3	Compressive Failure	200
6.4	The Hybrid Effect	202
6.5	Resin Effects	204
CHAPTER 7:	RECOMMENDATIONS FOR FURTHER WORK	206
References	. . . . .	209
Tables	. . . . .	221
Figures	. . . . .	249
Plates	. . . . .	337
Appendices:		
1.	Individual Test Results	363
2.	Statistical Significance Tests for the Hybrid Effect	376
3.	Quantification of the Variation of Modulus with Respect to Strain	384

LIST OF TABLES

1. Properties of the glass fibres
2. Properties of the carbon fibres
3. The epoxy resin prepreg compression moulding cure conditions
4. The vinyl-ester resin curing system
5. Properties of the cured resins
6. Details of the strain gauges used in the compressive tests
7. Results of resin density measurement
8. Secant modulus results demonstrating the effect of using either one or two strain gauges on each compressive specimen
9. Primary tensile failure strain results, 913 matrix
10. Primary tensile failure strain results, 914 matrix
11. Primary tensile failure strain results, 411-45 matrix
12. Primary tensile failure strain results, 470-36 matrix
13. Ultimate tensile strength results, 913 matrix
14. Ultimate tensile strength results, 914 matrix
15. Ultimate tensile strength results, 411-45 matrix
16. Ultimate tensile strength results, 470-36 matrix
17. Compressive failure strain results, 913 matrix
18. Compressive failure strain results, 914 matrix
19. Compressive failure strain results, 411-45 matrix
20. Compressive failure strain results, 470-36 matrix
21. Compressive strength results, 913 matrix
22. Compressive strength results, 914 matrix
23. Compressive strength results, 411-45 matrix
24. Compressive strength results, 470-36 matrix
25. Tensile secant modulus results, 913 matrix
26. Tensile secant modulus results, 914 matrix
27. Tensile secant modulus results, 411-45 matrix
28. Tensile secant modulus results, 470-36 matrix
29. Compressive secant modulus results, 913 matrix
30. Compressive secant modulus results, 914 matrix
31. Compressive secant modulus results, 411-45 matrix
32. Compressive secant modulus results, 470-36 matrix

33. Inter-laminar shear strength results from vinyl-ester and epoxy-GRP materials
34. Inter-laminar shear strength results from vinyl-ester and epoxy-CFRP materials
35. Transverse tensile strength results from epoxy-GRP materials
36. Transverse tensile strength results from epoxy-CFRP materials
37. Poisson's ratio results from 913 GRP and CFRP material
38. Average tensile and compressive modulus results from GRP and CFRP composites of the four resin systems employed
39. A comparison of the single carbon fibre modulus results of Johnson (from Ref. 67) normalised to represent a 60% V_{ft} laminate with those of 913 CFRP laminates
40. The K-factors of the GRP and CFRP laminates, calculated from the tensile strength results
41. Expected values of longitudinal compressive strength of GRP and CFRP composites using transverse tensile strength as the failure criterion. (Strengths are not normalised to represent 60% fibre volume fraction)
42. The hybrid effect resulting from an increase in fibre volume fraction of CFRP, from equation 5.25, based on the Rosen theory[44] of fibre buckling in the shear mode
43. A summary comparison of uniaxial strength results obtained from the parent material composites
44. A comparison of the epoxy-CFRP compressive strength data with that of other workers
45. A comparison of the tensile hybrid effects in each of the four composite systems studied
46. A comparison of the compressive hybrid effects in each of the four composite systems studied
47. The data used for calculation of the constants A, B, C and D in failure strain characterisation ($x = V_{fc}/V_{ft}$)

Appendices Tables:

Individual tensile test results:

A48 913 matrix

A49 914 matrix

A50 411-45 matrix

A51 470-36 matrix

Individual compressive test results:

A52 913 matrix

A53 914 matrix

A54 411-45 matrix

A55 470-36 matrix

Results of statistical significance tests for the hybrid effect:

A56 913 tensile tests

A57 914 tensile tests

A58 411-45 tensile tests

A59 470-36 tensile tests

A60 913 compressive tests

A61 914 compressive tests

A62 411-45 compressive tests

A63 470-36 compressive tests

A64 The constants A and B (in equation A3.1) which define the straight lines through the tangent modulus vs strain results

LIST OF FIGURES

1. Synthesis of a polyester resin from a dibasic acid and a diol

2. Production of a simple linear polyester from ethylene glycol and maleic acid

3. The action of the peroxide free radicals with styrene

4. The crosslinking action of a simple polyester resin with styrene

5. The molecular structure of the epoxide group

6. The molecular structure of epichlorohydrin

7. The molecular structure of bisphenol-A

8. The bisphenol-A/epichlorohydrin epoxy (otherwise known as DGEBA or MY-750)

9. The crosslinking action of a primary amine with an epoxy resin

10. Dicyandiamide, a latent curing agent used in epoxy resins

11. The molecular structure of MY-720 epoxy resin

12. The reaction of methacrylic acid with DGEBA to produce the Derakane 411 vinyl-ester resin

13. Comparison of the structures of a polyester and a vinyl-ester resin

14. The molecular structure of the Derakane 470 vinyl ester resin, based on the epoxy novolak structure

15. The rule of mixtures relationship: modulus vs fibre volume fraction

16. The rule of mixtures relationship for the strength of unidirectional composites in which $\hat{\varepsilon}_f > \hat{\varepsilon}_m$

17. The rule of mixtures relationship for the strength of unidirectional composites in which $\hat{\varepsilon}_m > \hat{\varepsilon}_f$

18. Rosen's model for the analysis of tensile strength in monofibre composites (from ref 22)

19. The stress/strain curves of cured and semi-cured CFRP and fibre bundles obtained by Fuwa et al (from ref 28). The frequency distribution of their cured CFRP failure strains is shown

20. Hayashi's model for a hybrid composite system (from ref 31)
    a) Stress/strain properties of the three composite materials
    b) Stress/strain response of the resulting hybrid

21. The tensile stress/strain diagram of a hybrid carbon glass-epoxy composite of Aveston and Sillwood, in comparison with their debonded theory (from ref 33)

22. Zweben's model for the analysis of tensile strength in hybrid composites (from ref 34)

23. Rosen's analytical model for the compressive strength of unidirectionally reinforced fibre composites involving fibre microbuckling (from ref 44)

24. The compressive strength of glass reinforced epoxy composites as predicted by the Rosen buckling model (from ref 44)

25. Hayashi's rule of mixtures relationship for the compressive strength of unidirectionally reinforced fibre composites (from ref 46)

26. The variation of longitudinal and constrained transverse compressive strength of HT-S CFRP with temperature, observed by Ewins and Ham (from ref 49)

27. An arrested compressive failure specimen of Chaplin, showing propagation of the kink-band (from ref 52)

28. Piggott's consideration of interface and matrix failure as a result of sinusoidally buckled fibres (from ref 57)

29. Non rule of mixtures results obtained by Piggott and Harris with HM-S carbon/glass hybrids (from ref 62) for
    a) compressive modulus
    b) compressive strength

30. Cross section of a leaky mould used in the wet lay-up of vinyl ester composites

31. The acid digestion process of volume fraction measurement

32. Cross section of the Celanese compression test fixture

33. Composite laminates made by:
    a) wet lay-up technique for vinyl ester laminates
    b) prepreg compression moulding technique for epoxy laminates (dimensions in mm)

34. The lay-up of a prepreg laminate in the compression moulding process

35. A fibre wound steel frame ready for resin impregnation by the wet lay-up technique

36. The tensile test specimen

37. The compressive test specimen

38. The strain gauge bridge circuit

39. Primary tensile failure strain results as a function of V_{fc}/V_{ft}, 913 matrix

40. Primary tensile failure strain results as a function of V_{fc}/V_{ft}, 914 matrix

41. Primary tensile failure strain results as a function of V_{fc}/V_{ft}, 411-45 matrix

42. Primary tensile failure strain results as a function of V_{fc}/V_{ft}, 470-36 matrix

43. Ultimate tensile strength results as a function of V_{fc}/V_{ft}, 913 matrix

44. Ultimate tensile strength results as a function of V_{fc}/V_{ft}, 914 matrix

45. Ultimate tensile strength results as a function of V_{fc}/V_{ft}, 411-45 matrix

46. Ultimate tensile strength results as a function of V_{fc}/V_{ft}, 470-36 matrix

47. Compressive failure strain results as a function of V_{fc}/V_{ft}, 913 matrix

48. Compressive failure strain results as a function of V_{fc}/V_{ft}, 914 matrix

49. Compressive failure strain results as a function of V_{fc}/V_{ft}, 411-45 matrix

50. Compressive failure strain results as a function of V_{fc}/V_{ft}, 470-36 matrix

51. Compressive strength results as a function of V_{fc}/V_{ft}, 913 matrix

52. Compressive strength results as a function of V_{fc}/V_{ft}, 914 matrix

53. Compressive strength results as a function of V_{fc}/V_{ft}, 411-45 matrix

54. Compressive strength results as a function of V_{fc}/V_{ft}, 470-36 matrix

55. Tensile modulus results as a function of V_{fc}/V_{ft}, 913 matrix

56. Tensile modulus results as a function of V_{fc}/V_{ft}, 914 matrix

57. Tensile modulus results as a function of V_{fc}/V_{ft}, 411-45 matrix

58. Tensile modulus results as a function of V_{fc}/V_{ft}, 470-36 matrix

59. Compressive modulus results as a function of V_{fc}/V_{ft}, 913 matrix

60. Compressive modulus results as a function of V_{fc}/V_{ft}, 914 matrix

61. Compressive modulus results as a function of V_{fc}/V_{ft}, 411-45 matrix

62. Compressive modulus results as a function of V_{fc}/V_{ft}, 470-36 matrix

63. A tensile stress/strain curve from a GRP laminate, 913 matrix

64. A tensile stress/strain curve from a CFRP laminate, 913 matrix

65. A tensile stress/strain curve from a G_2C_6/C_6G_2 hybrid laminate, 913 matrix

66. A tensile stress/strain curve from a G_4C_4/C_4G_4 hybrid laminate, 913 matrix

67. A tensile stress/strain curve from a G_6C_2/C_2G_6 hybrid laminate, 913 matrix

68. A tensile stress/strain curve from a G_7C/CG_7 hybrid laminate, 913 matrix

69. A tensile stress/strain curve from a C_4G_4/G_4C_4 hybrid laminate, 913 matrix

70. A tensile stress/strain curve from a $G_2C_4G_2/G_2C_4G_2$ hybrid laminate, 913 matrix

71. A compressive stress/strain curve from a GRP laminate, 913 matrix

72. A compressive stress/strain curve from a CFRP laminate, 913 matrix

73. A compressive stress/strain curve from a G_4C_4/C_4G_4 hybrid laminate, 913 matrix

74. The variation of tangent modulus as a function of tensile and compressive strain in GRP, CFRP and G_4C_4/C_4G_4 hybrid laminates, 913 matrix

75. The variation of tangent modulus as a function of tensile and compressive strain in GRP, CFRP and G_4C_4/C_4G_4 hybrid laminates 914 matrix

76. The variation of tangent modulus as a function of tensile and compressive strain in GRP and CFRP laminates, 411-45 matrix

77. The variation of tangent modulus as a function of tensile and compressive strain in GRP and CFRP laminates, 470-36 matrix

78. A comparison of the tangent modulus variation between G_4C_4/C_4G_4 and C_4G_4/G_4C_4 hybrid laminates as a function of tensile and compressive strain, 913 matrix

79. The proportional contributions of the components of a glass-carbon hybrid system to the modulus, for composites of constant V_{ft}

80. The theoretical stress/strain curve of a hybrid composite, showing $\hat{\varepsilon}_{ROM}$

81. The theoretical stress/strain curve of a hybrid composite, showing $\hat{\sigma}_{ROM}$ and $\hat{\sigma}_H$

82. The expected increase in tensile failure strains of hybrid laminates as a result of thermal contraction effects, in comparison with observed failure strains, 913 laminates ($\Delta T = 115^{o}C$)

83. The method of modulus measurement employed by Piggott and Harris in which machine displacement/applied force is plotted as a function of specimen length (from ref 53)

84. The stresses in the individual components of hybrid laminates due to cooling from the cure temperature, 913 matrix ($\Delta T = 115^{o}C$)

85. A tensile failure model for unidirectional GRP material
   a) Unstressed composite which contains defects
   b) Debonding begins to occur due to defects
   c) Fibre failure begins to occur, and crack propagation is halted by the debonding
   d) Final failure due to fibre tensile failure and fibre-matrix splitting

86. A tensile failure model for unidirectional CFRP material
   a) Unstressed composite
   b) As fibre failure begins to occur there is considerably less debonding than in GRP
   c) Final failure due mainly to fibre and resin tensile failure

87. The variation of compressive stress in a loaded compression specimen

88. A comparative representation of the stress ranges of unidirectional hybrid composites containing equal volumes of glass and carbon fibres

89. The difference in the failure strains between hybrid laminates with GRP in the outer layers and those with CFRP in the outer layers, 913 matrix
   a) tensile failure
   b) compressive failure

90. Characterisation of the 913 tensile failure results for laminates with GRP outer layers
   a) failure strain
   b) strength

91. Characterisation of the 913 tensile failure results for laminates with CFRP outer layers
   a) failure strain
   b) strength

92. Characterisation of the 913 compressive failure results for laminates with GRP outer layers
   a) failure strain
   b) strength

93. Characterisation of the 913 compressive failure results for laminates with CFRP outer layers
   a) failure strain
   b) strength

LIST OF PLATES

1. The Dartec servohydraulic test machine with which tensile tests were performed

2. The Mand servo-screw test machine with which compressive tests were performed

3. The tensile failure of an epoxy GRP specimen 913 matrix

4. The tensile failure of a vinyl-ester GRP specimen, 411-45 matrix

5. The tensile failure of a vinyl-ester GRP specimen, 470-36 matrix

6. The tensile failure of an epoxy CFRP specimen, 913 matrix

7. The tensile failure of a vinyl-ester CFRP specimen, 411-45 matrix

8. The tensile failure of a vinyl-ester CFRP specimen, 470-36 matrix

9. The tensile failue of an epoxy C_4G_4/G_4C_4 hybrid specimen, 914 matrix

10. The splitting mode of compressive failure observed in many of the GRP specimens, 913 matrix

11. The splitting mode of compressive failure observed in many of the GRP specimens, 470-36 matrix

12. The kink-band mode of compressive failure observed in some of the GRP specimens, 411-45 matrix

13. The shear mode of compressive failure observed in the epoxy CFRP specimens, 913 matrix. The 45° failure plane is visible but not distinct because of the influence of the end tabs on the path of the fracture

14. A high magnification SEM micrograph of the surface of the shear failure observed in epoxy CFRP specimens, 914 matrix

15. The microbuckling mode of compressive failure observed in the vinyl-ester CFRP specimens, 411-45 matrix. The characteristic 70° plane of the fracture surface is clearly visible

16. A high magnification SEM micrograph of part of the surface of a microbuckling failure observed in vinyl-ester CFRP specimens, 411-45 matrix

17. A high magnification SEM micrograph of the fibres from an epoxy GRP inter-laminar shear failure, 913 matrix

18. A high magnification SEM micrograph of the fibres from an epoxy CFRP inter-laminar shear failure, 913 matrix

19. A high magnification SEM micrograph of the fibres from a vinyl-ester GRP inter-laminar shear failure, 411-45 matrix

20. A high magnification SEM micrograph of the fibres from a vinyl-ester CFRP inter-laminar shear failure, 411-45 matrix

21. The tensile failure of an epoxy CFRP specimen, 914 matrix

22. A high magnification SEM micrograph of a fibre from an epoxy GRP transverse tensile failure, 913 matrix

23. A high magnification SEM micrograph of a fibre from an epoxy GRP transverse tensile failure, 914 matrix

24. An SEM micrograph of the compressive failure surface of a vinyl-ester CFRP specimen, 470-36 matrix. The characteristic steps which are the result of fibre microbuckling are clearly visible

25. A high magnification SEM micrograph of the end of a carbon fibre from a vinyl ester CFRP compressive failure, 470-36 system. The fibre microbuckling failure has resulted in well defined tensile and compressive regions of fracture being visible

26. The splitting mode of compressive failure in the GRP outer layers of a G_4C_4/C_4G_4 hybrid specimen, 470-36 matrix

27. The kink-band mode of compressive failure in the GRP outer layers of a G_4C_4/C_4G_4 hybrid specimen, 470-36 matrix

28. The compressive failure of an epoxy C_4G_4/G_4C_4 hybrid specimen, 914 system. The influence of the end tabs on the path of the fracture is evident, but the 45° shear plane in the CFRP outer layers is also visible in places

29. An SEM micrograph of part of the tensile failure surface of an epoxy CFRP specimen, 913 matrix

30. An SEM micrograph of part of the tensile failure surface of a 914 epoxy CFRP specimen. Comparison with Plate 29 reveals that in the 914, crack propagation through fibres and matrix has been aided

PRINCIPAL NOTATION

Unless otherwise defined, the principal notation used is as follows:

1. Symbols and Abbreviations

A	cross-sectional area
a	dimensionless parameter defining amplitude of sinusoidal buckling (in fibre diameters)
AE	acoustic emission
CFRP	carbon fibre reinforced plastic
CO	laminate with CFRP outer layers
CSA	cross-sectional area
CV	coefficient of variation
d	diameter
E	elastic modulus
G	shear modulus
GO	laminate with GRP outer layers
GRP	glass reinforced plastic
HE	high extension
HMS	high modulus (carbon fibre)
HTS	high tensile strength (carbon fibre)
K	factor accounting for imperfect fibre strength utilisation
k	stress/strain intensity factor
KRP	Kevlar reinforced plastic
L	length
LE	low extension
P	general material property
R	radius of curvature of fibre
r	radius
ROM	rule of mixtures
R_ε	ratio of lower bound of hybrid failure strain to that of a composite of the same length containing LE fibres only
S	inter-laminar shear strength

T	temperature
UCS	ultimate compressive strength
UTS	ultimate tensile strength
V	volume fraction
α	coefficient of thermal expansion
γ	surface work of fracture
δ	ineffective length
ΔT	temperature difference
$\Delta\hat{\varepsilon}_o$	theoretical difference in failure strain between GO and CO laminates, obtained from hybrids extrapolated to $V_{fc}/V_{ft}=0$
ε	strain
$\hat{\varepsilon}$	failure strain
$\hat{\varepsilon}_{GRP-CO}$	theoretical failure strain of GRP laminate obtained from results of CO hybrids, extrapolated to $V_{fc}/V_{ft} = 0$
$\hat{\varepsilon}_{GRP-GO}$	theoretical failure strain of GRP laminate obtained from results of GO hybrids, extrapolated to $V_{fc}/V_{ft} = 0$
λ	dimensionless parameter defining wavelength of sinusoidal buckling (in fibre diameters)
ν	Poisson's ratio
ρ	density
σ	(direct) stress
$\hat{\sigma}$	strength
σ_b	bending stress
σ_{fl}	stress in fibres at strain of $\hat{\varepsilon}_m$
$\hat{\sigma}_H$	rule of mixtures strength defined as stress in composite at failure strain of LE component
σ_{my}	matrix yield stress
σ_{ml}	stress in matrix at strain of $\hat{\varepsilon}_f$
σ_1^*	predicted compressive strength based on transverse tensile failure criterion
τ	shear stress
ϕ_o	misalignment angle

Subscripts

a	adhesion
C	CFRP value
c	composite
f	fibre
fc	carbon fibre
fg	glass fibre
fK	Kevlar fibre
ft	total fibre content
G	GRP value
m	matrix
ROM	rule of mixtures value
1	axial direction
2	transverse direction

Superscripts

*	critical value
^	maximum value
ˇ	minimum value

2. Fibre Lay-up Configurations

All laminates contained 16 layers of reinforcement.

Glass or carbon fibre reinforcement was denoted by 'G' or 'C' respectively.

The number of layers of a particular fibre type within each ply is denoted by a subscript.

The centre of the laminate is denoted by '/'.

Therefore G_4C_4/C_4G_4 defines a 3 ply, 16 layer laminate with GRP outer layers and 8 layers of CFRP in the centre.

3. Direction Vector Notation

The three directions within a specimen are denoted as shown.

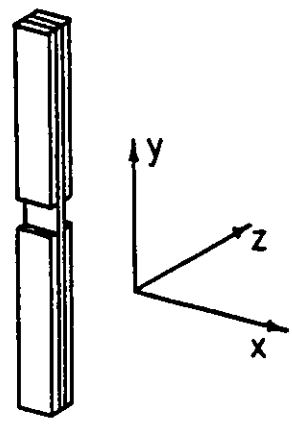

CHAPTER 1

INTRODUCTION

In recent years, the use of fibre reinforced plastic (FRP) materials in engineering applications has been growing rapidly. Composites are now seen in many types of structure, both large and small, where previously metals would have been employed. The combination of high strength, together with low weight, has attracted designers from various industries, the most notable being perhaps the aircraft industry where weight savings are a primary consideration. While many different types of FRP are available having a considerable range of mechanical and environmental resistance characteristics, a greater diversity of properties can be achieved by using two or more different constituent materials in the structure or laminate. These compound structures are known as hybrid composites. They can take on many forms but in this work the definition is limited to fibre composites which contain more than one type of reinforcing fibre.

The structures of hybrid fibre composites can be split into two main categories:

i) Intraply or Dispersed Fibre Hybrids

These consist of an intimate mixture of individual fibres or fibre tows of two or more types of reinforcing fibre within a resin matrix. The dispersion of the fibres can be either random or orderly.

ii) Interply or Segregated Ply Hybrids

In these composites the two or more different types of reinforcing fibre are segregated into separate layers or plies within a common resin matrix. The individual layers may be varied in terms of thickness, orientation angle, and fibre type. Laminates of this type

are nearly always symmetrical so that distortion does not occur after cooling from an elevated cure temperature or from changes in environmental conditions in service.

Although dispersed fibre hybrid composites are not uncommon, the segregated ply hybrids are much more often encountered due to their greater ease of manufacture and in some ways more adaptable properties. (A better flexural modulus for example, can be achieved by putting the stiffer fibres in the outer layers). It is this latter category of hybrid composites which forms the subject of the current investigation. All the materials manufactured and tested can be considered to consist of sixteen layers of either glass reinforced plastic (GRP) or carbon fibre reinforced plastic (CFRP). Although the plies are considered as individual layers of FRP material, it should be noted that the resin is always a common and homogeneous matrix throughout the laminate structure. Individual layers are only segregated in terms of the fibre reinforcement they contain.

The rule-of-mixtures (ROM) is often used as a baseline for determining the expected mechanical properties of these hybrid composites. However it has been found in practice that hybrids do not always behave as might be expected. Undirectional hybrid fibre composite test pieces can be loaded to strains which are significantly higher than those at which the lower extension components alone, would fail. This synergistic strengthening is commonly known as the "hybrid effect". Clearly it can be of advantage to the designer, but further research is required for a fuller understanding of the hybrid effect in quantitative terms, the factors which affect it, and the mechanics of failure associated with it.

In order to present a meaningful analysis of the mechanical properties of these composite materials, it is necessary to define precisely what is meant by the terms "rule-of-mixtures" and "hybrid effect". In some instances confusion has arisen from the fact that different authors have used different definitions, resulting in both positive and negative hybrid effects being reported in similar composites, due simply to the difference in terminology (for example in references 1 and 2 respectively).

The rule of mixtures is defined as the average value of a property of individual components of the composite, each of which has been normalised in proportion to its relative volume fraction within the composite. This definition could be alternatively described as the linear variation of a property (P) with respect to a change in the volume fractions of the constituents. The rule of mixtures is commonly used to describe the relationship between the properties of a unidirectional monofibre composite and the volume fraction of fibre present (P vs V_f). In this work, the majority of the composite lay-ups under consideration are hybrids in which the two types of reinforcing fibre (glass and carbon in this case) each have independent volume fractions upon which the property P is dependent. If P is a function of two independent variables the graphical representation of the relationship is three-dimensional. In order to simplify the analysis, the extra independent variable is eliminated by considering only total fibre volume fractions of 60% (V_{ft} = 0.6). The volume ratio of the two types of reinforcing fibre present within the composite (V_{fc}/V_{ft}) becomes the new independent variable and the rule of mixtures defines the relationship P vs (V_{fc}/V_{ft}) as a straight line. It should be noted that a modification to this definition is employed when composite strength is defined. The failure of the composite is expected when the lowest extensible

component reaches its failure stress rather than at an average of the strengths of the components. The equations are developed in Sections 2.3.1 and 2.3.2.

The term "hybrid effect" is defined as any deviation in the properties of a hybrid composite from what may reasonably be expected to occur, as a result of considering the properties of each of the constituents. Essentially it is used to describe a departure in failure strain from that expected but is sometimes used when considering modulus and strength deviations from their expected values. The hybrids tested contain two types of fibre - a low extension component (carbon fibre) and a high extension component (glass fibre). In a hybrid lay-up containing both of these types of fibre, one could reasonably expect the lower extension component to continue to fail at its usual failure strain. Primary failure of a hybrid is therefore expected at the failure strain of the CFRP and any deviation from this would constitute a hybrid effect. An increase in strain (tensile or compressive) is defined as a positive hybrid effect, while a decrease from that of the low extension component would be defined as negative. The elastic moduli of hybrid composites are expected to follow a rule of mixtures relationship related to the elastic moduli of the individual components. A hybrid effect on modulus can therefore be defined as any deviation in the elastic modulus of the hybrid from the rule of mixtures prediction. To define the hybrid effect in terms of the ultimate strength of the composite is a little more complex because failure is not necessarily expected to occur at either of the failure strengths of the individual parent materials or at the average value. For most hybrids, ultimate strength expectations can be represented by the product of elastic modulus and failure strain ($E \times \hat{\varepsilon}$) and the hybrid effect will be any deviation from this function. Further discussion

and explanation of this is presented in Section 5.1.

There were several main objectives in this work:

- to identify and precisely quantify the hybrid effect
- to investigate the relative effects of using vinyl ester matrix resins in hybrid glass/carbon composites in comparison with epoxy resins
- to add to the understanding of the macro-and micro-mechanical events which contribute to the failure of these materials.

The resins used consisted of two epoxies which were in preimpregnated fibre form (prepreg) and two vinyl esters which were in simple resin form. Both tensile and compressive tests were carried out on composites containing various relative proportions of glass and carbon fibre reinforcement, and the stress vs strain curves were analysed in detail. Further information about failure mechanisms was obtained by means of examination of the failed specimens. Compressive properties, being more matrix dominated than tensile properties, give more information about the effects of using different matrix resins. Tensile properties however give basic fibre and composite strength information and an indication of fibre-resin bond strength. This is useful in assessing the composites tested in comparison with other data, and to provide further information which aids in the interpretation of the compressive test results. In addition, some inter-laminar shear strength, and transverse tensile strength tests were performed. The results from these clarified the interpretation of some of the data obtained in the main series of tests.

2. LITERATURE REVIEW

2.1 INTRODUCTION

2.2 RESIN CHEMISTRY

2.2.1 Polyester Resins

2.2.2 Epoxy Resins

2.2.3 Vinyl Ester Resins

2.3 TENSILE BEHAVIOUR OF UNIDIRECTIONAL FIBRE COMPOSITES

2.3.1 Monofibre Composites

2.3.2 Hybrid Composites

2.4 COMPRESSIVE BEHAVIOUR OF UNIDIRECTIONAL FIBRE COMPOSITES

2.4.1 Monofibre Composites

2.4.2 Hybrid Composites

2.5 ELASTIC MODULUS VARIATION

2.1 INTRODUCTION

The term reinforcement phase is often used to describe a material within a polymer matrix which has been added for its high strength and modulus characteristics. Fibre reinforced materials can be divided into two categories. These are known as low performance and high performance composites. The former group of materials contain small amounts of short lengths of fibrous material and would be employed in applications where ease of processing must be maintained. High performance composites however contain a high volume fraction of continuous fibres which are added with a view to achieving high strength and stiffness. It is this latter category of composite materials which form the subject of this investigation and which are therefore reviewed in the survey of previous work done.

Though the majority of the stress applied to a high performance composite material is carried by the reinforcing fibres, the matrix gives the structure rigidity and provides a medium through which load can be transferred between fibres. It also serves to protect the fibres from both mechanical and chemical damage, and is therefore a very important part of the composite structure. There are many different matrix materials in existence today, each offering different advantages in terms of processing requirements and composite performance. However in the field of high performance composites, thermosetting resins are the most widely used group. Curing of these resins involves a chemical crosslinking reaction which transforms the viscous liquid into a rigid solid. The nature and properties of thermosetting resins can vary considerably, being dependent on the structure of the molecule and on the type of crosslinking action employed. Some properties of the composites can

be understood in terms of the molecular characteristics of the matrix resin. For this reason a review is included of the chemistry of polyester, epoxy, and vinyl ester resins. Polyesters are included because of their close relationship with vinyl esters and epoxies, both of which are employed in this work. They also form a helpful guide for comparison purposes.

It is clear that mechanisms involved in compressive failure are different from those in tensile behaviour, and the reviews of previous investigative work for each mode are therefore presented separately. A considerable amount of work has been done on the tensile properties of unidirectional composites both for hybrid and non-hybrid laminates, and much data is available on tensile strength and stiffness. Compression data however, is not so plentiful and failure processes are not so well understood. Much of the work by previous researchers has involved single fibre type composites (monofibre composites) of various forms. Compression data on unidirectional hybrids is extremely limited and interpretation of the behaviour of carbon fibre/glass fibre hybrid systems must relate to that observed in the GRP and CFRP parent composites.

2.2 RESIN CHEMISTRY

2.2.1 Polyester Resins

Polyester resins account for a very important sector of the thermosetting resin industry. Indeed, due to their widespread use it has been said that they helped to lay the foundations of modern composite technology[3]. One of the main reasons for this is the fact that they are relatively easy to make, both in terms of manufacture of the resin, and of curing it to obtain the hard, crosslinked structure. The polyesters used in thermosetting fibre reinforced

composites are called unsaturated polyesters because they always contain points of unsaturation or double bonds within the polymer chain. These double bonds, or vinyl groups, are reactive and become the points where crosslinking takes place between the molecules in the presence of the curing agent. Although other forms of polyester do exist, such as the fibre forming type[4], they are not important in the fibre reinforced plastics (FRP) industry because they do not form a crosslinked thermoset structure. The term "polyester" will be used in this work to denote an "unsaturated polyester".

Preparation of the uncured polyester resin has been covered in detail in a number of books and documents[3,5,6]. The process consists of a condensation reaction involving dibasic acids and diols. (One of the acids must be unsaturated so that an unsaturated polyester is produced). Both of the reactants are bifunctional, being able to form an ester link at either end, so the esterification reaction proceeds step by step building up the linear chain molecule, and releasing a water molecule at each step. A typical example of this reaction is shown in Figure 1. Many variations of polyester resins can be made, the resulting structure being determined by the structures of the reactants used to produce them. The properties of the polyester resin can therefore be controlled at the manufacturing stage by using mixtures of different diacids and diols and by altering their molar proportions. A typical example of a simple linear polyester is that produced from ethylene glycol and maleic acid as shown in Figure 2. The vinyl groups from the unsaturated acid become part of the polyester chain so that reactive sites occur regularly along its length. Since the polyester is often a solid, a diluent is required. This is usually styrene, which takes part in the crosslinking reaction.

Addition of a free radical curing agent such as methyl ethyl ketone peroxide (MEKP) causes polymerisation to take place. Though on its own this would require a temperature of about 150°C, upon addition of a small amount of cobalt naphthanate or other activator, the polyester will cure at room temperature. The peroxide is broken down into two free radicals, each of which forms a new free radical with the styrene. This is shown in Figure 3. These free radicals then react with the vinyl groups in the polyester chain and build up the crosslinked structure. Typically two or three styrene monomers are contained in the chains which link up the polyester molecules. The polymerisation process of a simple polyester with styrene is shown in Figure 4.

2.2.2 Epoxy Resins

Although epoxy resins are more expensive than polyesters[6], and present some fabrication problems which do not occur with polyesters, they exhibit many favourable properties. For this reason they are now used in a wide variety of industrial applications. When used as adhesives or matrices in composite materials, advantage is taken of their high adhesive strength, low shrinkage during cure, and their good resistance to environmental attack. There are now many different types of epoxy resin systems with a wide range of material properties and cure procedures. By definition, an epoxy resin can be identified by the presence of two or more epoxide groups in the molecule. The epoxide group is shown in Figure 5. Chemically, this is a very reactive group of atoms because the ring is under strain and will readily open[4]. It is by means of a ring opening mechanism that curing will take place in the presence of a catalyst.

The epoxide group is introduced into the molecule by means of a reaction with the chemical epichlorohydrin. This is shown in Figure 6. The epoxy resin is made from the reaction of epichlorohydrin with any mono- or poly-hydric phenol. This reaction will take place in the presence of an alkaline catalyst such as caustic soda[7,8]. Two examples of phenol compounds in common use for this purpose are bisphenol-A as shown in Figure 7, which is the one most commonly used, or a novolak made from phenol and formaldehyde. The alkaline catalyst initiates the reaction in which the glycidyl group joins onto the phenol group, eliminating a molecule of hydrochloric acid in the process. Clearly, for the diepoxide, two molecules of epichlorohydrin would be needed for each molecule of bisphenol-A, but competing reactions tend to cause an increase in the length of the molecule formed. If the proportion of bisphenol-A were increased, the resulting average molecular weight of the polymer would be higher. In order to ensure that the polymer chains are terminated with epoxide groups, an excess of epichlorohydrin is generally used. The epoxy resin produced from the reaction of bisphenol-A with epichlorohydrin is known as the diglycidyl ether of bisphenol-A (DGEBA). It is shown in Figure 8. The molecule has the lowest molecular weight when n=0. For the liquid versions, n varies from zero to about three. Beyond this, increasing molecular weight results in soft, then brittle solids. The viscosity of epoxy resins does generally tend to be higher than that of polyesters, which is one reason why they are more difficult to lay-up in composite slabs. It is possible to reduce the viscosity by the addition of a reactive diluent, but the mechanical and thermal properties are impaired[5]. It is important to note that while the DGEBA epoxy described is bifunctional because it contains two epoxide groups, others such as that based on the novolak structure are multifunctional and the

number of remnant epoxide groups is dependent on the value of n, the number of repeating units.

Unlike polyesters, epoxy resins are very stable in the absence of a curing agent and can be stored for long periods. There are a large number of potential curing agents available, amines or acid anhydrides being commonly used in structural composite applications. A primary amine, for example, would cause crosslinking to take place[5] as shown in Figure 9. This type of curing reaction will occur at room temperature. In many cases, however, a latent curing agent is preferred, such as that in the Ciba-Geigy prepreg materials used in this work. These contain a complex amine hardener, dicyandiamide (DICY)[9]. The structure of DICY is shown in Figure 10. This is just one example of many types of latent curing agent that have been produced for curing epoxy resins[10]. They do not react with the epoxy resin at normal room temperatures so that the resin, containing the curing agent, has a long shelf life. When curing is required it is simply carried out by raising the temperature.

The Ciba-Geigy prepreg materials used contain more than one type of epoxy resin structure and have been commercially developed to suit end-use requirements. Good quality laminates can be easily prepared with a high fibre volume fraction (0.6 - 0.7). 913 is made up of a DGEBA epoxy resin as the main constituent, and a secondary constituent in a smaller proportion which has very good high temperature properties. These epoxy resins are known by the trade names of MY 750 and MY 720 respectively. (See Figures 8 and 11). A further additive is present together with DICY hardener. The make-up of 913 gives it a combination of good environmental resistance combined with good mechanical properties. 914 prepreg material contains the MY 720 epoxy resin in the greater proportion which

gives the cured structure its excellent thermal resistance. It also contains many small spheres (ranging from 0.5 - 2.5 μm diameter) which give the resin added toughness by restricting crack propagation[11]. It is cured at a higher temperature than 913, and in addition a post-cure is required to stabilise the structure for its high temperature service.

2.2.3 Vinyl Ester Resins

Vinyl esters are a new class of resins which became available commercially in about 1970. They are related to both polyester and epoxy resins and exhibit some of the more favourable properties of both of these groups. Because they contain unsaturated vinyl groups in the chain, they can be cured with vinyl monomers such as styrene in the same way as polyesters, therefore making fabrication by hand lay-up techniques at room temperature practicable. The backbone of a vinyl ester resin molecule however, is identical with that of an epoxy and therefore the good mechanical properties exhibited in epoxies are also characteristic of vinyl esters.

Manufacture of the resin, as detailed by Pritchard[6], is carried out by means of a reaction between an epoxy resin and an ethylenically unsaturated carboxylic acid. The particular epoxy resin used determines the backbone structure of the resulting vinyl ester resin molecule. Various epoxies can be used, a common one being the diglycidyl ether of bisphenol-A (DGEBA), for which the reaction is shown in Figure 12. It is a fairly simple reaction between the epoxy resin and the acid and can be catalysed by amines or phosphines. The basic difference in synthesis between vinyl esters and polyesters means that the precise polymer structure and relatively low molecular weight of the former is in contrast with

the high molecular weight random structure of the latter group of resins[12]. As with polyesters, styrene is often used as the reactive diluent and takes part in the crosslinking reaction. Polymerisation is the same as for polyesters (as described in Section 2.2.1) and laminates can easily be cured at room temperature using the MEKP/cobalt octoate system. However, unlike the crosslinking of a polyester, the reaction takes place only from the ends of the chains, and a much more uniform structure is produced. The epoxy resin backbone imparts toughness to the cured resin[6], and the length of this chain or the molecular weight can be controlled by controlling the amounts of the reactants used when the epoxy resin is made. Since physical properties such as tensile strength, tensile strain and heat distortion temperature are related to the molecular weight, it means that these properties can be controlled at the resin synthesis stage with a view to the end requirements.

Comparing the molecular structure of a bisphenol-A-fumaric acid polyester with that of the Derakane 411 vinyl ester helps to explain the improvement in chemical and mechanical properties that can be achieved by using vinyl ester resins. Figure 13 shows a comparison of the two molecular structures. The vinyl ester differs from the polyester in two important ways. Firstly, it does not have any ester groups within the repeating unit so that they do not occur within the main polymer chain. Secondly, the reactive vinyl sites, unlike in the polyester molecule, are situated at the ends of the vinyl ester chain. Since these ester groups are subject to hydrolytic attack, this makes the polyesters much more vulnerable, and once attacked the chain is split up leaving it open to further chemical attack[13]. In the vinyl ester however, not only are there fewer ester groups, but also even if they are attacked the main body of the molecule remains unaffected. Together with this, the pendant

methyl groups, which can be seen in Figure 12, tend to have a shielding effect on the ester groups, offering the molecule further protection. The terminal unsaturation of the vinyl ester molecules results in a much more uniform crosslinked structure and can even enable homopolymerisation of the resin molecules to occur. The availability of reactive sites along the polyester chain results in a partially reacted, non-uniform structure leaving some of the vinyl sites open to chemical attack and again making the resin molecule vulnerable along its length. The resiliency (resistance to cracking and crazing) of vinyl esters is better than that of polyesters because the absence of reactive sites along the chain give it a more stable structure enabling it to act as an energy absorber. Polyesters on the other hand tend to be more brittle as a result of their internal vinyl groups. Another advantage of the vinyl ester structure is the presence of hydroxyl groups along the chain. This improves the wetting and bonding properties of the resin to glass reinforcement[9]. Adhesion to glass is better than for polyesters but somewhat poorer than epoxies[14].

Because of the reduced number of ester linkages giving the vinyl ester a greater resistance to hydrolytic attack, the majority of early applications were in glass fibre reinforced chemical plants[12,13]. However, in 1974 Phillips and Murphy[15] presented the results of experiments which showed that vinyl esters exhibit far better adhesion properties than polyesters when using carbon fibres as a reinforcing medium. This opened up a new field of wet lay-up work to carbon fibre laminates, and also to hybrids.

Vinyl ester resins, which are marketed under the trade name "Derakane"* come in a variety of different types, each having a

* Derakane is a registered trade name of the Dow Chemical Company

different molecular structure which has been tailored to meet specific end-use requirements. In this work, composites made with the Derakane 411 and 470 vinyl ester resin systems are under analysis. Although both of these resin systems contain all the characteristics of vinyl esters, their overall structures are quite different as a result of their having been made from different epoxy resins. The Derakane 470 resin structure, shown in Figure 14, can be compared with the 411 resin structure, shown in Figure 13. The main difference is that the 470 resin is based on an epoxy novolac structure and contains side chains in the repeating unit, while the 411 structure is a linear molecule. A higher crosslink density is achieved from the 470 type of molecule which results in better heat resistance and thermal stability. It retains the excellent corrosion resistance of the 411 resin but tensile elongation and strength are reduced[6,16]. A flame retardant vinyl ester resin is available which is just a modified form of the 411 structure, containing bromine atoms on each of the phenol groups. It is manufactured under the name Derakane 510.

2.3 TENSILE BEHAVIOUR OF UNIDIRECTIONAL FIBRE COMPOSITES

2.3.1 Monofibre Composites

Since unidirectional composites were first introduced, strength predictions have often been based on the simple rule of mixtures (ROM). This is not satisfactory for any accurate determination of expected composite behaviour since the mechanics involved is in reality much more complex than the ROM takes into consideration. In this review developments in failure theories are presented which give a deeper understanding of the mechanical behaviour than this simple model. Firstly however, the ROM is considered. It is important because of its wide usage, and due to its simplicity it

forms a very good basis with which other theories can be compared. A summary description of the ROM can be found in much of the literature dealing with fibre composite materials[17,18].

The basis of the ROM is the principle that each constituent of the composite will contribute to the material property in proportion to the volume fraction it occupies within the composite. If the fibres and matrix are considered to be loaded in parallel, then

$$\sigma_c = \sigma_f V_f + \sigma_m V_m \tag{2.1}$$

This is the general equation of the stress distribution in a monofibre composite. It defines the stress before any failure has occurred. Since

$$\varepsilon_c = \varepsilon_f = \varepsilon_m$$

it follows that:

$$E_c = E_f V_f + E_m V_m \tag{2.2}$$

This is the equation of the elastic modulus in a monofibre composite. It is represented graphically in Figure 15.

Composite strength predictions are based on the failure strains of the components. Two cases are possible:

i) When $\hat{\varepsilon}_f > \hat{\varepsilon}_m$

Figure 16 shows the rule of mixtures behaviour of a composite in which the failure strain of the fibres is greater than that of the matrix. At low fibre contents, the strength is attributable to that of the matrix, and the equation for failure is:

$$\hat{\sigma}_c = \sigma_{f1} V_f + \hat{\sigma}_m V_m \tag{2.3}$$

When the fibre content is high, matrix failure does not cause complete composite failure, and the load is transferred to the fibres until their failure strain is reached. The strength of the composite is then:

$$\hat{\sigma}_c = \hat{\sigma}_f V_f \tag{2.4}$$

ii) When $\hat{\varepsilon}_m > \hat{\varepsilon}_f$

In the case of many thermosetting resin systems such as those used in this work, the matrix failure strain is greater than that of the reinforcing fibres. ROM behaviour for this type of system is shown in Figure 17. At very low fibre volume fractions the fibres do not improve the load carrying capacity of the matrix, and failure occurs at the matrix failure strain. However because of the presence of the fibres, the matrix strength is reduced. Up to a certain fibre volume fraction, the addition of fibres reduces the strength of the composite. At low fibre contents it is defined by the equation:

$$\hat{\sigma}_c = \hat{\sigma}_m V_m \tag{2.5}$$

If a high volume fraction of fibre is present, the fibres carry the majority of the load. When they fail, it is transferred to the matrix which cannot support the extra load so that total failure occurs. For this situation, composite strength is defined by the equation:

$$\hat{\sigma}_c = \hat{\sigma}_f V_f + \sigma_{ml} V_m \tag{2.6}$$

Equation 2.6 is often used as a guideline for determining the strength of a real composite system[19]. From Figure 17, it is apparent that a critical fibre volume fraction exists, below which the strength of the composite is lower than the matrix alone. This critical volume fraction is termed V_{fcrit}. The volume fraction at which composite strength is lowest is known as V_{fmin}.

Experimental work has shown that the rule of mixtures will predict the elastic modulus of a unidirectional composite to a generally acceptable level of accuracy[19]. However when we are representing a fibre reinforced plastic by a homogeneous anisotropic medium, we are neglecting all microstructure effects, and the ROM is not always suitable for describing certain properties in composites, especially in dynamic situations, and fracture behaviour.

If the elastic response of a fibre composite material is to be modelled, it can be represented by a homogeneous but anisotropic material having the same average stress/strain response. The elastic constants which describe this material are a simple function of the constituent material properties of the composite. The relationship between elastic moduli and constituent material properties is reasonably well understood. However if a fracture criterion is required, since all the fibres in the composite do not fail simultaneously, consideration must be give to internal irregularities in the state of stress; average stress/strain response is no longer sufficient.

Parratt[20] described in 1960, how the strength of a fibre is dependent on surface flaws. The tensile strength of a fibre therefore increases as its length is decreased. He also described how shorter fibres can carry less stress due to the limiting

adhesion and friction between fibre and matrix. Failure, Parratt suggested, occurs when the accumulation of fibre fractures has reduced the effective lengths to a point where the applied stress in each fibre reaches the maximum allowable value due to the limiting shear transfer.

Rosen[21,22] followed up this work by considering fibre strength to be represented by a statistical distribution function. The model Rosen used is shown in Figure 18. It consists of a set of parallel fibres, both strong and stiff with respect to the matrix. Their strengths are dependent on the degree of surface imperfection which is described by the statistical distribution function. As the load is increased, a fracture occurs at one of the flaws so that the axial stress in that fibre is zero at the break. Due to load transfer through shear from the matrix, the axial stress builds up along the fibre, back to its undisturbed stress value. Shear stress on the other hand builds up from zero to a maximum value at the fibre break. These stress patterns are shown in Figure 18. Upon such a break occurring, several possibilities exist for the future behaviour of the composite: firstly, the high interface shear stress could cause interface failure which would propagate along the fibre, reducing the effectiveness of that fibre over a substantial length. This could be overcome by having either a stronger bond or a more ductile matrix material, which would allow redistribution of the shear stress. Secondly the crack could propagate across the composite due to poor fracture toughness of the matrix material and increased tensile stress in adjacent fibres. Thirdly, it is possible that the local stress field does not cause further fracture, and increasing the load simply causes a distribution of fibre fractures corresponding to the initial distribution of weak points. Continued accumulation of these fractures would eventually produce a weak

cross-section at which the unbroken fibres could no longer transmit the applied load and tensile failure would occur. In the vicinity of one of these individual breaks, a small portion of the fibre (length δ) may be considered ineffective for load transfer. This is known as the ineffective length. Assuming the former two failure modes are halted, Rosen carried out his analysis by considering each fibre to be represented by a series of links, each of length δ. After applying the mathematical analysis to the model he produced the equation:

$$\frac{\delta}{d_f} = \frac{1}{2} \left[\frac{(1 - V_f^{\frac{1}{2}})}{V_f^{\frac{1}{2}}} \left(\frac{E_f}{G_m}\right) \right]^{\frac{1}{2}} \cosh^{-1} \left[\frac{1 + (1 - \phi)^2}{2\,(1 - \phi)} \right] \qquad (2.7)$$

where ϕ = the fraction of the undisturbed stress, below which the fibre is considered ineffective

δ = the ineffective length of a broken fibre

G_m = matrix shear modulus

d_f = the fibre diameter

Using this result for the fibre link length, Rosen deduced the statistical strength distribution of the links from fibre test data and he produced the equation for failure stress:

$$\hat{\sigma} = V_f\,(\alpha\delta\beta e)^{-\frac{1}{\beta}} \qquad (2.8)$$

where α and β are constants defining link strength deduced from experimental tests, for fibre strength versus length data.

Rosen carried out an experimental programme[22] to support the validity of his failure model. The experimental techniques he used

were designed to observe the failure mechanism within a composite during loading. Very thin specimens were made with a single layer of large diameter (approximately 90 μm) glass fibres embedded in an epoxy resin matrix, and loaded in tension parallel to the fibre direction. The specimens were observed photoelastically during the test in such a way that the unloaded specimen appeared black and the loaded specimen bright. The glass fibres are the major contributors to the photoelastic effect so as they are loaded up they brighten up but in the vicinity of a break a dark area is visible where the tensile stress has been relieved. This is the ineffective length. To identify matrix effects, two series of tests were carried out in which one set of specimens had a flexibilizer added to the matrix to give lower Youngs modulus and increased strain to failure. Fibre fractures were observed at loads less than 50% of the UTS as dark areas appeared at random locations. Rosen stated that even with stress concentrations in the vicinity of the breaks, the variation in fibre strength generally more than offset the effect of such concentrations. Hence the breaks occurred randomly rather than cumulatively. The effects of the different matrix properties were also clearly evident, the ineffective lengths being substantially longer in the low modulus epoxy, and the number of breaks smaller. However, since the ineffective lengths are longer it takes fewer to produce a weak cross-section and hence composite failure. Rosen concluded that although a ductile matrix is desirable from the point of view of alleviating shear stress and hence interface failure, a strong and stiff matrix is more effective in confining the perturbations in the stress field and therefore has a beneficial effect for this statistical failure model.

Although Rosen reasoned that increased stress in adjacent fibres is outweighed by the random distribution of weak points, it would have

been very difficult to observe any failure sequence of the fibres in the composite as complete failure had taken place. This reasoning may not therefore have held at the onset of failure.

Zweben[23] postulated that the discrepancy between Rosen's theory and experimental data might be a result of such simplifications. He used Rosen's geometrical model to study the influence of fibre breaks on two-dimensional composites. The formula Zweben used for the static load concentration (k_r) in the two fibres adjacent to a run of r broken fibres was:

$$k_r = \frac{4.6.8 \text{ ---- } (2r+2)}{3.5.7 \text{ ---- } (2r+1)} \qquad (2.9)$$

For a single fibre break therefore the load concentration was 4/3. Zweben showed that stress concentrations have a significant effect on strength, and his theoretical predictions of the number of fibre breaks vs fibre stress were in good agreement with experimental data.

Zweben and Rosen, together took the theory further[24], by considering the local increases in stress level in the vicinity of fracture sites in three-dimensional composites, and went on to develop general failure criteria. The geometrical model used was based upon that suggested by Gücer and Gurland[25] in which the material is considered to be an aggregate of "representative volume elements" arranged in cross-sectional layers. The strength of the representative volume elements is taken to be a statistical variable which corresponds to the statistical distribution of weak points in the fibres. As the material is loaded, elements fracture randomly due to the statistical scatter of their strength levels and this causes an increase in stress in the elements adjacent to the failed

ones rather than a uniform redistribution of the stress throughout the layer. The load concentration factors used in the analysis were from Hedgepeth and Van Dyke[26].

Zweben and Rosen showed how these localised load concentrations are of great importance to the prediction of macroscopic material strength. The probabilities of multiple breaks occurring at various stress levels were determined. Upon comparison with experimental data, the stress at which the first multiple fracture break has a probability of one was found to be a good failure criterion, though perhaps on the conservative side. Stress at first fibre break could provide a lower bound on strength, while Rosen's cumulative weakening theory[22] gave a good upper bound. It was suggested that failure may be caused by the propagation of fibre breaks, which would provide a reasonable explanation of the discrepancy between ROM predictions and actual composite behaviour.

As composite failure theories were developed, the significance of the statistical approach to fibre strength became widely recognised. Harris[27] in 1972 stated that since the strength of a composite depends upon the breaking stresses and strains of all the fibres contained within it, strength prediction is going to be a statistical problem. However he still considered that the strength in tension of carefully prepared (aligned) composites is almost always sufficiently closely predicted by the simple rule of mixtures for the more sophisticated treatments to be ignored. This is significant because he felt that even after complex statistical failure theories had been developed, the ROM outweighed them as a simple and convenient guide to composite strength, and was sufficiently accurate for most purposes.

In 1975, the work of Fuwa, Bunsell and Harris[28] was of considerable value in developing understanding of tensile failure mechanisms. They examined the modes of fracture in specimens of cured and semi-cured carbon fibre reinforced plastic (CFRP) and in fibre bundle specimens. Acoustic emission (AE) techniques were used to monitor the failure processes and the specimens were examined microscopically after the tests. The stress-strain curves for the semi-cured and fibre bundle specimens showed that the absence of a rigid matrix resulted in a lower initial modulus and a non-linear stress/strain response. The stress strain curves of the bundles then became linear up to about 0.35% strain, after which the slope began to fall off. The partial contribution of the matrix in the semi-cured specimens caused the decrease in slope of the stress-strain curve to be smaller and the maximum load to be greater, though catastrophic failure of both bundles and semi-cured specimens occurred at about 0.53% strain. This is shown in Figure 19. AE results showed that the fall in the stress-strain curve slope was related to the failure of fibres. The stress-strain curves of the cured CFRP were linear with an abrupt brittle failure and a much higher scatter of failure strains. Fuwa et al pointed out the significant fact that the CFRP specimen which had the greatest extension reached a strain beyond that at which all the fibres in the bundle specimens had failed. This meant that each fibre in that fully-cured composite specimen must have failed at least once. Also the AE results showed that fibre failure rates in the cured composite specimens reached a peak at a strain close to that at which the bundle moduli showed marked deviations from linearity. At this stage several observations were made:

i) the weakest fully-cured specimen failed at a strain of 0.32%, close to the strain at which the results for bundles and semi-

cured samples suggested significant numbers of fibre failures begin to occur;

ii) about 80% of the cured specimens failed before the maximum failure strain for bundle specimens;

iii) some cured specimens survived to strains greater than 0.55% at which level all the fibres in the semi-cured specimens and bundles had broken.

Fuwa et al reasoned that since 60% of the fully cured specimens failed at strains lower than 0.45%, a level at which only an estimated 10% of the fibres in the bundles had failed, the fibres do not fail in isolation but rather that a progressive failure mechanism such as related fibre breakage or crack propagation could be occurring. Alternatively, since some failed at strains greater than that which the bundles could sustain, a random fibre failure mechanism could be occurring and the ultimate failure of the specimens is a statistically determined quantity. The variability in strength results may therefore be an inherent characteristic of the material rather than a result of poor experimental technique. The condition of the fibres in the surface layers of broken CFRP specimens was examined by removing the surface layers of matrix with sulphuric acid. In all samples, fibre fractures were found in apparently intact portions of the specimens. It appeared that adjacent fractures occurred in bundles and that these bundle failures were linked together by matrix shear failure. Adjacent fracture therefore does occur, though it is apparently confined to sub-bundles containing only a few fibres. These associated fibre failures, it was suggested, may possibly be limited by matrix shear failure, which could act as a blunting mechanism. This situation would result in a distribution of weak regions in the specimen. It is then probable that those samples which fail near the bottom of

the scatter band do so because of a chance accumulation of weak points in a cross-section, while the upper limit of the scatter band would be defined by a more even distribution.

Fukuda and Kawata[29] in 1977 returned to the statistical approach for an estimate of composite tensile strength. However unlike previous authors[21,23,24] who had used a Weibull distribution, Fukuda and Kawata assumed the fibre irregularities to be represented by a normal distribution. They produced a simulation of a fracture process in a composite material which demonstrated crack propagation through the model cross-section. However they explained that this predicted fracture may not accurately reflect the actual fracture phenomena because the debonding mode is not considered in their model. They made it clear that relative strength of the composite is dependent upon specimen length, volume fraction and the ratio of fibre to matrix moduli. Their predicted composite strength is always lower than the rule of mixtures and they suggested that if the rule of mixtures is to be used, a multiplication factor should be applied to $\hat{\sigma}_f$, the fibre strength, so that equation 2.6 becomes:

$$\hat{\sigma}_c = K\hat{\sigma}_f V_f + \sigma_{ml} V_m \qquad (2.10)$$

where K is somewhat less than 1.

Barry in 1977[30] extended the work done by Zweben and Rosen[24] by proposing a model which could be used to predict the range of possible composite strengths. In Barry's model, the composite consists of a number of transverse slices and he considered that the composite would fail when any of these failed. The fibre length in one of these slices is the positively affected length (PAL) of an adjacent intact fibre rather than the ineffective length. The

effects of fibre modulus, matrix modulus and volume fraction of fibres on the characteristic fibre length were considered and in addition the length of debonding of a failed fibre was considered to affect it. Both static and dynamic stress concentration influences were considered, the dynamic effects being the more important ones for determining whether further fibre failures will occur in the vicinity of a broken fibre. Barry used a computer simulation of the loading of the model slice to failure which directly gave him a possible strength distribution without requiring experimental fibre strength data. This computer simulation showed typical fibre failure patterns that existed in the model slice just prior to failure, for various coefficients of variation of the fibres. The percentages of fibres that had failed just before catastrophic failure of the composite took place varied from about 0.5% for a CV_f value of 10% to about 7% for a CV_f value of 25%. This means that even for a fairly small specimen, the number of individual fibre breaks occurring before composite failure, is very large. The computer simulation also showed that many multiple fibre fractures can occur before complete composite failure takes place which would suggest that Zweben and Rosen's[24] failure criterion of the first multiple fibre break is conservative especially where the coefficient of variation of fibre strength is greater than 10%. Barry expressed the model strength results graphically as a function of CV_f and the ratio L/L_r (which is dependent on debond length) where L is the model fibre length and L_r is the model fibre length for the case of zero debonding. This was done for the upper and lower limits of strength and these predictions were compared with experimental data from composite tensile specimens. A small number failed above the predicted upper limit but a larger number failed below the lower limit for the case of the estimated maximum debond length. Barry suggested that this discrepancy arises from the fact that the

maximum debond lengths chosen were those which appeared to account for the majority of the fibre pull-out lengths. For many specimens however these were exceeded in some fibres by up to 50% and, although initially neglected because of the small number of fibres involved, Barry reasoned that they may not be negligible and the estimated average pull-out length should be higher.

Summarising the above works, it is clear that although the rule of mixtures will always give a reasonable approximation of the tensile strength of a unidirectional composite, it does not take into account specimen size, failure mode, or any statistical variation in the strength of the reinforcing fibres. It does not give any indication of the range of scatter of tensile strengths to be expected which Fuwa et al[28] concluded is an inherent characteristic of this type of material. From the analyses it is clear that the strength of unidirectional composites is dependent on many factors, including:

i) the statistical characteristics of the fibre strengths
ii) the relative fibre and matrix moduli
iii) the fibre-matrix bond strength
iv) the fibre volume fraction

These considerations can make the analysis very complex and it may be appropriate to recall Harris's comment[27] in 1972 that, "the strength in tension of carefully prepared (aligned) composites is almost always sufficiently closely predicted by a simple rule of mixtures for us to ignore the more sophisticated treatments." The rule of mixtures is important because of its simplicity which has led to its widespread usage and because it does not require determination of the less readily known properties of composites

such as effective fibre pull-out length at a break or the statistical function describing the distribution of weak points. Also, if a more accurate prediction of composite strength is required it may still be possible to use the ROM by applying a simple multiplication factor such as that proposed by Fukuda and Kawata[29].

2.3.2 Hybrid Composites

With a desire to obtain a better all-round combination of properties in fibre composites, a move has been made from using one type of fibre alone to using hybrid reinforcement. GRP has a fairly large elongation to failure and a low modulus, while type II CFRP relatively has a much lower elongation to failure together with a higher modulus and strength. When used separately, the inherent properties of these materials cause limitations on their applications while combining them in hybrids enables more advanced properties to be exploited. There is the implicit assumption that if several different types of fibres are used to reinforce a composite material, the resultant properties of that composite should be an average of the properties of the parent composites made from the constituent materials. This is known as the "rule of mixtures" as applied to hybrids. Because of the simplicity of this rule, it is universally applied to the study of hybrids as a baseline from which any synergistic effect is measured. To consider the tensile behaviour of unidirectional hybrid fibre reinforced plastics the composite is defined as a series of plies of fibre reinforced material rather than a single matrix containing several fibre types. Each layer of fibre reinforcement can then be considered to fail at the characteristic failure strain of that particular material.

The equations describing the rule of mixtures are applied to hybrids as follows. If the composite contains two types of reinforcing fibres A and B, equation (2.1) becomes:

$$\sigma_c = \sigma_{fA}V_{fA} + \sigma_{fB}V_{fB} + \sigma_m V_m \qquad (2.11)$$

where σ_{fA} and σ_{fB} denote the stress in fibres A and B respectively
V_{fA} and V_{fB} denote the volume fractions of fibres A and B respectively

Equation (2.11) is the general equation of the stress distribution in a two-fibre type unidirectional hybrid composite before any failure occurs. Similarly, equation (2.2) becomes:

$$E_c = E_{fA}V_{fA} + E_{fB}V_{fB} + E_m V_m \qquad (2.12)$$

where E_{fA} and E_{fB} denote the elastic moduli of fibres A and B respectively.

Equation (2.12) is the equation of elastic modulus in a two-fibre type unidirectional hybrid composite. If fibre type A has a lower failure strain ($\hat{\varepsilon}_{fA}$) than fibres B ($\hat{\varepsilon}_{fB}$) and the matrix, then the failure criterion for this type of composite is:

$$\hat{\sigma}_c = \hat{\sigma}_{fA}V_{fA} + \sigma_{fB1}V_{fB} + \sigma_{m1}V_m \qquad (2.13)$$

where σ_{fB1} denotes the stress in fibres B when fibres A fail
σ_{m1} denotes the stress in the matrix when fibres A fail

Equation (2.13) is a prediction of first failure or primary failure. It does not consider the fact that the remaining materials, after fibres A have failed, may be able to support the load and attain strains higher than $\hat{\varepsilon}_{fA}$. Alternatively, the equations decribing the ROM in monofibre composites can be used in a two fibre system by considering the hybrid as low extension (LE) fibre reinforcement in a matrix of resin and high extension (HE) fibres (for example, carbon fibres in a GRP matrix).

The characteristics of this type of rule of mixtures behaviour were clearly defined by Hayashi[31] in 1972 when he considered a material design problem for a tie member. Studying the problem of a three fibre system, Hayashi defined the stress-strain characteristics of each of the constituent materials A, B and C as shown in Figure 20(a). He considered a symmetrical hybrid laminate to consist of each of these materials A, B and C from the centre to the outer layers respectively, and with each layer having the appropriate volume fractions V_A, V_B and V_C. If each layer fails at its own fracture strain, and the modulus is calculated from a combination of the moduli of the remaining intact layers, then the resulting stress-strain curve would be as shown in Figure 20(b). Hayashi set about verifying this by making up some glass and carbon fibre reinforced hybrid tensile specimens together with some separate GRP and CFRP specimens to estabish the behaviour of the component materials. It was found that the CFRP part of the hybrids broke first as expected and the initial and final elastic moduli and final strengths and strains corresponded closely to the predicted values. Primary fracture strength and strain however were about 40% higher than expected, an observation which Hayashi explained as the greater ductility of the surrounding GRP causing the fracture occurrence of the CFRP layer to retard. This was the first reported observation

of the hybrid effect. Although Hayashi did not present the equation in this form, his criterion for primary failure was:

$$\hat{\sigma}_H = \hat{\sigma}_A V_A + \sigma_{B1} V_B + \sigma_{C1} V_C \qquad (2.14)$$

where $\hat{\sigma}_H$ denotes expected strength of the hybrid if material A has the lowest failure strain

In Hayashi's model, the brittle layers do not contribute to the load shearing once they have failed so that the resulting extension behaviour is solely that of the more extensible components. Bunsell and Harris[32] suggested in 1974 that this need not always be so, provided that the layers are well bonded. They believed that the interlayer bond could contribute to the composite's behaviour, enabling the CFRP layers to contribute to the rigidity and the load bearing capacity of the composite even after first failure had taken place. They also attempted to explain the hybrid effect in terms of residual strains in the laminate due to thermal contraction on cooling from the cure temperature. The differences in the coefficients of thermal expansion result in the CFRP layer being put into compression and the GRP layers in tension in the cooled laminate. They suggested therefore that if the initial compressive strain in the CFRP is $\Delta\varepsilon_C$, then fracture of the CFRP layer should be expected at a strain of $(\hat{\varepsilon}_C + \Delta\varepsilon_C)$. This of course would appear as an apparent increase in the tensile failure strain of the carbon fibre layers of a hybrid over that of plain CFRP. In order to explore this possibility, Bunsell and Harris[32] manufactured a series of GRP, CFRP and hybrid tensile specimens from prepreg materials, and in some of the hybrids they inserted silicon paper between the layers so that the effect of unbonded plies could be determined. Elastic moduli obeyed the mixture rule in both bonded and unbonded

specimens up to the point of first failure, and there was an increase in strain to this first failure over plain CFRP. Bunsell and Harris interpreted this increase in strain as being a result of the residual thermal compression in the CFRP layer from the cure. After initial fracture had taken place there was a considerable deviation in the results of the unbonded specimens from those of the well bonded ones. Since in bonded hybrids the CFRP continued to carry some load, the drop in load after initial fracture was much less than for unbonded specimens. Bunsell and Harris suggested that a "critical length" exists in a broken carbon fibre which extends either side of the fracture. Beyond this critical length the load sharing capacity is the same as that of an unbroken fibre, which enabled multiple fractures to occur. These were observed in the failed specimens. Final failure occurred at a strain less than that expected for GRP alone. The reason suggested for this was that the glass fibres were only able to extend in the short regions around fractures in the carbon fibres. There was no obvious difference in strength behaviour of hybrids with either glass or carbon fibre layers on the outside.

After this early work on hybrids, there was much controversy about their mechanical behaviour and the mechanisms involved. Indeed there was even doubt about whether the hybrid effect actually exists or whether it was simply the apparent effect caused by differences in thermal contraction as proposed by Bunsell and Harris[32]. In a short paper in 1976, Phillips[1] summarised the controversies that were taking place, and in an attempt to avoid further theoretical argument presented experimental results from his own investigations. He found that in tensile tests, the hybrids did indeed fail considerably later than predicted. He drew the conclusion that load sharing does take place between the glass and carbon fibre layers.

Phillips commented on the great potential usefulness of this phenomenon.

Aveston and Sillwood[33] in 1976 considered a hybrid composite to be made up of a low extension fibre within a matrix composed of resin and high extension fibres. The expected failure strain of the low extension fibres was predicted by considering the work of fracture required to produce new fibre failure surfaces. This was done for the two cases of a good elastic bond and a purely frictional bond between the fibres and matrix. The equations they used for the limiting case of failure strain were, for the bonded case:

$$\hat{\varepsilon}_{fc}^{2} = \frac{2\,\gamma_f}{E_f(1+\frac{1}{\alpha})\,r_f}\left(\frac{G_m}{E_f}\right)^{\frac{1}{2}} \cdot \frac{V_f^{\frac{1}{4}}}{(1-V_f^{\frac{1}{2}})^{\frac{1}{2}}} \qquad (2.15)$$

and for the unbonded case:

$$\hat{\varepsilon}_{fc}^{2} = \frac{6\,\gamma_f\,\alpha V_m}{E_c\,\delta} \qquad (2.16)$$

where $\hat{\varepsilon}_{fc}$ = failure strain of brittle fibres within matrix

γ_f = surface work of fracture of fibre

α = the ratio $\frac{E_m V_m}{E_f V_f}$

δ = the ineffective length of the debonded fibre.

To support their proposed model, Aveston and Sillwood carried out experimental tensile tests on hybrid composites containing 3.5 vol% type I carbon fibre and 35 vol% glass fibre. It was found that the stress-strain curve results fitted the predictions for the debonded case very closely. The initial and final slopes, the strain displacement separating them ($\hat{\varepsilon}_f/2\alpha$) and the mean fibre breaking strain ($\hat{\varepsilon}_f$) were all reflected in the experimental stress-strain curve. These results are shown in Figure 21 where OABC is the

theoretical prediction for the debonded case and ε_{HM} is the failure strain for the plain carbon fibre composite. The only significant difference between the theory and experiment was the fact that the fibres did not all break together, but instead broke over a range of strains which meant that the initial departure from linearity of the stress-strain curve was difficult to determine. Quite clearly, as predicted by the theory, initial breaking strain of the carbon fibres had risen from 0.5% for a CFRP laminate to over 1% for the hybrid, leaving little doubt that a real increase in the effective fibre strength had been achieved. Aveston and Sillwood determined that their theory for good elastic bonding was inapplicable since it predicted failure strains very much lower than those achieved in practice and evidence of debonded regions were observed in the composite after testing. They pointed out that comparison with previous work in which little or no synergistic effect was observed may not be entirely relevant since the laminate configurations that previous workers such as Bunsell and Harris[32] used consisted of relatively massive layers of CFRP and GRP.

In 1977, Zweben[34] presented an approximate statistical analysis for the tensile strength of unidirectional hybrid composites. In this paper he derived an equation to predict the amount of synergistic strengthening one might expect in the failure strain of a hybrid over that of the lower extension component monofibre composite. Zweben included a review of previous work done in this area and he had noted how previous authors had observed a so called "hybrid effect" as an increase in failure strain of the LE component. In his reference to Bunsell and Harris'[32] work, Zweben commented on how their explanation of the hybrid effect in terms of differential thermal contraction of the different fibre layers could only account for approximately 10% of the actual observed increase in strain.

Zweben[34] carried out some tensile tests on both undirectional and bidirectional graphite, Kevlar, and hybrid graphite/Kevlar composites. He found that a hybrid effect on strain of approximately +4% occurred in the unidirectional laminates and of approximately +32% in the bidirectional laminates. With the particular materials in question one would have expected a slight reduction in failure strain from that of the graphite if only thermal effects were to be considered. It was becoming quite clear therefore, that the hybrid effect could not be totally accounted for by thermal contraction effects alone.

Zweben's model[34] for hybrid composite strength was based on the fact that the strength of a reinforcing fibre is a statistical quantity. Fibre strength in general shows significant scatter at a fixed gauge length and mean fibre strength decreases with increasing gauge length. The model was a development of that proposed by Rosen[22] and Zweben[23] for monofibre composites. A two dimensional hybrid composite is considered, of axial length L and made from a single layer of N fibres. The layer of fibres consisted of alternately a high modulus LE fibre and a low modulus HE fibre as shown in Figure 22. In real composites the fibres are not so finely mixed. The individual fibres in Zweben's model could therefore be considered as yarns or tows of each type of fibre, thus accounting for less intimate mixing. The statistical strength characteristics used in the calculations would then be those of the tows rather than of individual fibres. In the following discussion, the term "fibres" is used with the understanding that it represents either fibres or tows.

Zweben's analysis[34] followed the procedures developed in his earlier work[23]. As the load is increased, breaks occur randomly throughout

the material but there will clearly be many more breaks in the LE fibres than in the HE ones. Assuming Weibull distributions for failure strain in the two fibres:

$$F_1(\varepsilon) = 1 - \exp(- p\ell\varepsilon^q) \tag{2.17}$$

$$F_2(\varepsilon) = 1 - \exp(- r\ell\varepsilon^s) \tag{2.18}$$

where p, q, r and s are Weibull parameters, and ℓ is the length of a fibre.

Zweben applied strain concentration factors (k_h) to the HE fibres adjacent to the LE fibre breaks, and he obtained an expression for ε_{2h}, the strain at which fracture of the first overstressed HE fibre is expected:

$$\varepsilon_{2h} = [NLpr\ \delta_h\ (k_h^s - 1)]^{-1/(q+s)} \tag{2.19}$$

where δ_h = the ineffective length associated with a broken LE fibre in the hybrid.

This was compared with the equivalent expression for a monofibre composite containing just LE fibres:

$$\varepsilon_2 = [2NLp^2\ \delta(k^q - 1)]^{-1/2q} \tag{2.20}$$

(The subscripts 1 and 2 refer to LE and HE fibres respectively, and h to the hybrid).

Zweben was therefore able to obtain an expression for R_ε, the ratio of the lower bounds of failure strain of a hybrid to that of a

composite of the same length containing only LE fibres. Zweben then compared this with his experimental data. His theory predicted a hybrid effect on strain of 22% for both unidirectional and bidirectional laminates. The actual results of 4% and 31% respectively clearly lay well to either side of this prediction. Zweben acknowledged that his analysis was a very simplified approach to a complex problem. However it did offer some explanation for the occurrence of considerable increases in failure strain of hybrids over their LE component parent composite materials.

With this paper, Zweben[34] was the first to look at the strength of hybrid composites from a statistical point of view and from this viewpoint it was a major step forward. However, although he defined the hybrid effect as an increase in strain of the LE fibres when contained within a hybrid lay-up, in the mathematical analysis he used the break of the first HE fibre as a lower bound for composite strain. Clearly the failure criterion should rather be determined by further failure of LE fibres. This is perhaps the area where the theory could best be improved.

A helpful guide to the properties of hybrid laminates was published in 1978 by Lovell[35]. In his paper, Lovell summarised the characteristics of hybrids in terms of the following properties: load/deflection curves, modulus, tensile stength, impact strength, fatigue strength, vibration damping, electrical conductivity, thermal expansion and conductivity, and corrosion resistance. Useful data was included giving typical modulus and strength values for composites made from various resin systems, including epoxies and vinyl esters. At the same time, Summerscales and Short[36] also published a paper which summarised the behaviour of hybrid composites. Information was presented under the following headings:

applications, impact behaviour, compressive properties, tensile properties, flexural properties, interlaminar shear strength, fatigue, and other properties. The two papers[35,36] gave a good outline of the general understanding of the nature and properties of hybrid fibre composite materials based on the work of previous authors.

Marom, Fischer, Tuler and Wagner[2] in 1978 investigated some possible parameters other than relative fibre volume fraction which might control the hybrid effect in hybrid composites. These included the relative moduli and strengths of the reinforcing fibre, the nature of the fibre-matrix interface, and the arrangement of the fibres within the composite. Initially, tests were performed on two different hybrid carbon/carbon composite systems in which the two different types of carbon fibre were in each case chosen so that the effect of the fibre-matrix interface was minimised. The surfaces of the constituent fibres were similar while their mechanical properties differed greatly, so that the source of any possible hybrid effect could be associated with the mechanical properties of the fibres rather than with the fibre-matrix bond. Assuming that the rule of mixtures is represented by the mean of the strengths of the parent composites (in all hybrids equal volumes of each type of fibre were used) Marom et al found that essentially no synergistic hybrid effect existed in these carbon/carbon hybrids. This was true of modulus, strength and fracture toughness results. They considered this to be an important observation since it focussed the discussion of the existence of a hybrid effect on to the fibre-matrix interface. In view of the above results, Marom et al continued their work by considering another hybrid system, containing glass and carbon fibre reinforcement. In this case, both the mechanical properties of the fibres and the fibre-matrix

interface properties differed considerably in the two different types of fibre. The elastic moduli of these hybrids again obeyed the rule of mixtures, as expected, but strength properties were consistently lower, as were the fracture energies. Marom et al did not consider this to be a significant synergistic effect and noted that each of these properties was independent of the construction of the layers within the hybrid. However a significant negative synergistic effect was observed in the values of the fracture surface energy (γ_I), the integral of the load/deflection curve (γ_σ) and the work of fracture (γ_F). They explained this phenomenon by examining the values of the work of fracture. Assuming pull-out is the main contribution to the work of fracture, the case is considered where the critical length of one type of fibre is very much greater than that of the other. Marom et al suggested that in this situation the pull-out lengths of the fibres adjust themselves. In one extreme case the glass fibre pull-out length reduces to that of the carbon fibre, resulting in a negative hybrid effect on γ_F, and in the other extreme case, the carbon fibre pull-out length increases to that of the glass, resulting in a positive hybrid effect. Electron micrographs of the fracture surface supported this view. By observing the fibre pull-out in fractured specimens and considering the experimental strength data, Marom et al concluded that a negative hybrid effect on γ_F should be expected in composites where there is a high degree of intimate mixing of the components, while more distinct and segregated layers within the composite will result in a positive hybrid effect.

Marom et al[2] had shown that a prerequisite for a hybrid effect is that the two types of reinforcement differ in both their mechanical properties and in the nature of the interface they form with the matrix. The existence of a positive or negative hybrid effect is

then determined by the following factors:

i) the relative volume fractions of the two types of fibre
ii) the arrangement of the two types of fibre within the hybrid and, it was presumed, by a third factor
iii) the loading configuration.

A further paper by Fischer, Marom and Tuler[37], published in 1979 considered the influence of this latter factor on the hybrid effect. They tested hybrid specimens in both an interlaminar and a translaminar mode of testing. It was found that the hybrid effect is indeed dependent on the mode of testing because a different mechanism of failure was prevalent in the different types of test. Delamination was a dominant mechanism in the case of interlaminar loading, and because delamination failure is more difficult when the fibres are more intimately mixed, segregation of the layers resulted in a negative hybrid effect. In the case of translaminar loading however, fibre pull-out was the dominant mode of fracture and, as discussed in the previous paper[2], greater segregation of layers resulted in a more positive hybrid effect.

It is important to note that in references (2) and (37), the definition used for the hybrid effect is a deviation from the rule of mixtures, which is simply an average of the properties of the parent composites. By this definition, even if the tensile strain to primary failure of a glass/carbon hybrid composite is higher than that of the CFRP alone it may still be less than the average of CFRP and GRP and therefore considered to be a negative hybrid effect. The importance of defining precisely what is meant by the terms "rule of mixtures" and "hybrid effect" is thus illustrated.

Up until Xing, Hsiao and Chou's[38] work in 1981, all treatments of the hybrid effects in composites had considered only the static aspects of load transfer and concentration. However Xing et al pointed out that acoustic emission recorded during the progressive fracture of low elongation fibres indicated that a dynamic failure process was taking place. An investigation was therefore made into dynamic stress concentration factors which occur in the vicinity of fibre breaks. (A dynamic stress concentration factor considers the maximum momentary stress that occurs in the transient response immediately after a fibre has broken). The model Xing et al used consisted of a layer of LE fibres adjacent to a layer of HE fibres, embedded in a common matrix. The fibres are considered to be of infinite length. The aim of the analysis was to evaluate the dynamic stress concentration in an LE fibre next to an LE fibre break.

After carrying out the mathematical analysis, Xing et al[38] found that the stress concentration factor (k_{HY}) of an LE fibre immediately adjacent to a fibre break in a hybrid is less than that in the parent composite consisting of LE fibres only (k_{LE}). The case of the parent LE fibre composite provides the upper bound to stress concentration in the hybrid since there is no difference in response phase and amplitude. Therefore because $k_{HY} \leqslant k_{LE}$, the LE fibre is less likely to reach its failure stress in the hybrid than in the parent composite, and fibre failure does not propagate. Because the phase difference in the dynamic response of a fibre adjacent to a fibre break is controlled by the fibres' mass per unit length, in hybrids where this is different a phase difference will always exist. This means that a hybrid effect is always expected and that this hybrid effect is always positive, at least as a result of the dynamic stress concentration factor. Xing et al noted that

this differs from Zweben's[34] stipulation of the existence of a negative hybrid effect.

Fukuda[39] had noted the serious shortcoming of Zweben's[34] statistical model (that it considered failure of an HE fibre rather than a second LE fibre, as a lower bound) and in 1983 presented a paper which developed Zweben's theory further by taking this fact into consideration. His model was the same as that used by Zweben with an intraply mixture of fibres or tows. However, after failure of a single LE fibre, Fukuda considered not only the strain in an adjacent HE fibre (as Zweben), but also in the nearest LE fibre. His equations for expected failure strain were:
For the adjacent HE fibre:

$$\varepsilon_{2h} = [NLpr\,\delta_h\,(k_h^{s} - 1)]^{-1/(q+s)} \qquad (2.21)$$

This was the same result as that which Zweben had obtained (equation 2.19).
For the nearest LE fibre:

$$\varepsilon_{1h} = [NLp^2\delta_h\,(k_h^{q} - 1)]^{-1/2q} \qquad (2.22)$$

where the notation used is the same as that in equations 2.19 and 2.20. Fukuda[39] discussed the fact that in order to get a true prediction of the hybrid effect, equation 2.22 should be compared with equation 2.20 rather than equations 2.21 and 2.20.

Using the data of Bunsell and Harris[32] for the fibres used, Fukuda, by the above analysis, calculated that in high modulus graphite/E glass composites, $R_\varepsilon = 1.11$. After taking into consideration the effect of residual thermal strain[32] this figure was modified to

R_ε = 1.21. Bunsell and Harris' experiments yielded a value R_ε = 1.31. Fukuda then calculated that R_ε = 1.13 from Zweben's[34] experimental data for Kevlar 49 and graphite fibres. Zweben's experiments on unidirectional and bidirectional hybrids yielded results of R_ε = 1.04 and R_ε = 1.31 respectively. Although his theory was in fair agreement with the experimental data, Fukuda suggested that further refinement could be achieved by considering a greater number of successive fibre breaks as the failure criterion.

The first published data on the hybrid effect existing in vinyl ester resin composites was by Richardson and Richmond[40] in 1984. After carrying out tensile tests on 3:1 glass/carbon intraply hybrid specimens, they reported that while the elastic modulus obeyed the ROM, a considerable hybrid effect was observed in terms of initial failure strain and strength values. Significant decreases in maximum tensile strain were also reported. They found that an intimate evenly distributed mixture of carbon fibres and E glass fibre tows tended to encourage higher values of first failure strain, high UTS values and a large number of small stress drops between first and final failure. They noted the fact that first failure is predominantly controlled by the ratio V_{fc}/V_{ft}.

In order to summarise the review of hybrid composites, the ROM, which is so widely used in performance predictions is redefined. Strictly, the mixture rule is an average of the properties of the component materials in proportion to their respective volume fractions. In terms of elastic modulus, most authors verify that this rule is obeyed[2,31,32]. However some authors[2,37] have also used this as a failure criterion where strength is concerned. It is generally accepted that by simple theory the LE fibres alone determine the primary failure of the composite. Equation 2.6 is

therefore normally accepted as the definition of the ROM prediction. It can be applied both to monofibre composites and to carbon fibres within a GRP matrix (hybrids). Many researchers have observed a synergistic increase in the failure strain of hybrid glass/carbon composites beyond that of plain CFRP, an effect first reported by Hayashi[31] and which has now become generally known as the hybrid effect. It has been found that this hybrid effect can be dependent upon:

i) the relative volume fraction of the fibres contained in the hybrid[40]
ii) the arrangement of the different types of fibre within the composite (interply or intraply)[2,33]
iii) the speed of testing (strain rate)[2]
iv) the relative thermal expansion coefficients of the two fibre types[32]
v) the degree of bonding between the fibres and matrix[33]
vi) the statistical distributions of fibre flaws within the different fibre types[34,39]
vii) the relative mass per unit lengths of the two fibre types, and the relative extensional stiffnesses (EA)[38].

Still further work is required to give us a fuller understanding of this synergistic effect and why it exists. It must be emphasised that if the hybrid effect is to be studied in any form, specific definition of hybrid composition of the materials used is very important as Phillips[41,42] has discussed. Only then are valid comparisons with the ROM possible.

2.4 COMPRESSIVE BEHAVIOUR OF UNIDIRECTIONAL FIBRE COMPOSITES

2.4.1 Monofibre Composites

There are practical difficulties involved in analysing the compressive behaviour of unidirectionally reinforced fibre composite materials. These include proper interpretation of data which generally displays a considerable amount of scatter as a result of several different mechanisms inducing compressive failure. Also test results can be sensitive to such factors as fibre misalignment, moisture content, test piece fixture, and specimen buckling. Several standard test methods have become established, each of which has its own particular advantages. However these test methods can yield different compressive strength results even on the same material[43]. It is these practical difficulties which are partially to blame for the lack of understanding of compression failure mechanisms.

The rule of mixtures which is a widely used criterion of failure of composites in tension can also be applied to compressive properties in a similar way. For the elastic modulus this is acceptable. However due to the complex combination of failure mechanisms which occur in compression, a simple prediction of strength based on the proportional volumes of the constituents will not be adequate if any degree of accuracy is required. Since the rule of mixtures is based on the strength of the fibres it is also a much more difficult matter to quantitatively define it in compression since compressive fibre strength is not an easily measured quantity.

One of the chief mechanisms associated with the failure of undirectional fibre composites in compression is the buckling of fibres. Expressions for microbuckling of fibres were first derived

by Rosen[44] in 1964. He realised that when glass fibres are embedded in an epoxy resin which is cured at high temperature the shrinkage of the resin as it cools to room temperature results in small wavelength buckling of the fibre. By observing photoelastically the stress pattern produced by this buckling, Rosen verified that the wavelength is linearly dependent on the fibre diameter. He assumed that this type of buckling, analogous to the buckling of a column in an elastic foundation, causes the failure of a unidirectional composite in compression as a basis for his model to predict the compressive strength. He considered a series of parallel fibres, treated as a two-dimensional problem so that his model consists of plates of thickness 2C, as shown in Figure 23. Two possibilities of failure were then considered: firstly, the "extension mode", in which adjacent fibres buckle exactly half a wavelength out of phase with each other, and secondly the "shear mode", in which the buckling of adjacent fibres is exactly in phase. (These modes are so called because the major deformation of the matrix material is either an extension or shear deformation respectively). Rosen then used the energy method to evaluate the buckling stress for each of these modes of failure by comparing strain energy in the compressed but straight deformation pattern with that in the buckled state under the same load.

Rosen's analysis resulted in the following equations to represent compressive strength of the composite:

For the extension mode

$$\hat{\sigma}_c = 2V_f \, [(V_f E_m E_f) \, / \, 3(1 - V_f)] \qquad (2.23)$$

and for the shear mode

$$\hat{\sigma}_c = G_m/(1 - V_f) \qquad (2.24)$$

Rosen expressed these equations graphically, as shown in Figure 24 where composite compressive strength is shown plotted as a function of fibre volume fraction. It is clear from the diagram that at very low volume fractions, the strength of the composite is determined by the extension mode of buckling failure while at higher volume fractions the shear mode predominates, the transformation taking place at about $V_f = 0.25$.

The strengths predicted by Rosen's[44] model are in excess of those measured in actual fibre composites. Since compressive strains of greater than 5% are predicted, which would be beyond the elastic limit of the resin matrix, Rosen considered the effect of modifying the analysis to take into account these inelastic matrix deformations. He replaced the matrix modulus in equations 2.23 and 2.24 by a function which varies linearly from its elastic value at 1% strain down to a zero value at 5%. This is represented by the dotted line in Figure 24. Strength predictions however were still higher than those values obtained in practice. Rosen then expressed his results further by showing compressive failure strain plotted as a function of fibre volume fraction for two different ratios of fibre Youngs modulus to matrix shear modulus. These curves again showed that the shear mode of failure predominates over the extension mode for the major range of interest of volume fractions. Also indicated was the fact that the results are very dependent on the ratio of fibre to matrix moduli, the critical strain being reduced as the matrix stiffness is reduced.

Although Rosen's model gives strength predictions which are too high, it was the first serious attempt at modelling the compressive

failure behaviour of unidirectional fibre composites. Foye[45] in 1966 suggested that compressive failure in a composite material could be linked with shear instability. He showed that failure would occur when the compressive stress becomes equal to the shear modulus. Hayashi[46] in 1970, and Hayashi and Koyama[47] in 1971 discussed this shear instability phenomenon in three-dimensional bulk materials under compression. They considered that an instability occurs and deformation takes place if the mean compressive stress σ reaches the value:

$$\sigma = G(\sigma) \tag{2.25}$$

where $G(\sigma)$ is the shear modulus of the material, which is a variable quantity, dependent upon the compressive stress. Applying this instablity criterion to the matrix material, it was assumed that when the matrix compressive stress σ_m reaches the critical value σ_m^* at which G_m, the matrix shear modulus equals σ_m^*, then the matrix cannot support the fibres elastically and failure occurs. Equation 2.25 then becomes:

$$\sigma_m^* = G_m(\sigma_m^*) \tag{2.26}$$

Data on matrix shear modulus G_m as a function of compressive stress is very limited and since σ_m^* lies very close to the yield stress σ_{my}, Hayashi replaced σ_m^* in the equation with σ_{my}, and produced a rule of mixtures equation for the compressive strength:

$$\hat{\sigma}_c = \sigma_f^* V_f + \sigma_{my}(1 - V_f) \tag{2.27}$$

where σ_f^* is that stress in the fibres corresponding to a matrix stress of σ_m^* or σ_{my}. Figure 25 shows Hayashi's rule of mixtures

relationship of expected compressive stress vs volume fraction of fibres in the composite.

Hayashi and Koyama compared their theory with a range of test results using both previously published test data and their own experimental results for a wide range of fibre volume fractions (0.1-0.7). Agreement was good, verifying the theory, with the exception of their own results for Boron/Epoxy composites which were much lower than the theoretical prediction.

Argon[48] suggested in 1972 that Rosen's model acted as an upper bound prediction applicable only to composites with parallel reinforcing elements perfectly aligned with the loading axis. In practice, imperfections in the fibre alignment always exist and such regions, Argon suggested, form a failure nucleus by undergoing a kinking process. Although this resembles the in-phase buckling of the Rosen model, it operates at a stress level well below the ideal buckling strength.

A region of initial misalignment angle ϕ_o was considered where the applied compressive stress produces an interlaminar shear component of τ such that:

$$\tau = \sigma\phi_o \tag{2.28}$$

When this shear stress τ becomes equal in magnitude to the interlaminar shear strength (S) of the material, then the lamellae in the region will slide and rotate. This movement further increases the resolved shear stress so a local instability is produced and the shear collapse band propagates outwards by means of the stress concentrations at the tips of the band. Thus the

compressive strength is:

$$\hat{\sigma}_c = S/\phi_o \tag{2.29}$$

This is independent of fibre volume fraction over the relatively wide range being considered and neither the elastic resistance of the surroundings of this band nor the bending of the lamellae within it have any effect on the predicted strength. Argon explained that there was considerable evidence to support the view that compressive failure is governed by local imperfections in fibre alignment and indeed observation of failed specimens did reveal this kinking collapse type of failure.

Ewins and Ham[49], in 1973 presented the results of their work to investigate the nature of compressive failure in unidirectional HM-S and HT-S CFRP. They carried out a series of longitudinal compressive tests on CFRP material, and at the same time, a series of transverse compression tests in which the Poisson's expansion in the direction normal to both the fibre axis and the applied load was constrained. Both of these series of tests were carried out for various volume fractions between 0.3 and 0.65. In each case a linear relationship of strength vs volume fraction was obtained and the strength values from the different types of test were in very close agreement.

It is clear that the only mode of failure in a transverse compression test is shear failure of the fibres and matrix. (Buckling modes of failure, for obvious reasons, cannot occur in transverse compression). Analysis of the fracture surfaces revealed to Ewins and Ham that a 45° shear plane occurred in the longitudinal compressive tests as well as in the transverse ones. This fact,

together with the closeness of the strength results to each other, confirmed that the active mode of failure in longitudinal compression was one of fibre and matrix shear failure.

Ewins and Ham then performed two further series of tests in which the longitudinal and constrained transverse compressive strengths were measured at constant volume fraction but at successively higher temperatures. This was done in an effort to identify the microbuckling type of failure that Rosen[44] predicted, in which the matrix shear modulus (which is very temperature dependent) plays a key role. The results showed that up to 100°C the strengths fell gradually with temperature, but over 100°C there was a sudden change in the strength vs temperature relationship of the longitudinal compressive strength. While transverse strength continued to fall gradually, the longitudinal compressive strength fell at a much faster rate. This is shown in Figure 26 for the HT-S composites. Observation of the specimens from this steeper part of the curve confirmed that there had been a change in failure mode from one of shear to one of microbuckling. SEM micrographs of this microbuckling failure surface revealed, at low magnifications a stepped failure surface, and at high magnifications the characteristics of flexural failure on individual fibre ends.

Ewins and Ham concluded that in unidirectional HM-S and HT-S carbon fibre reinforced-epoxy composites longitudinal compressive failure generally occurs by shear on a plane of maximum shear stress, and that this stress forms an upper bound to the composite's strength. At higher temperatures the mode changes to one of microbuckling, but no quantitative agreement with existing theories based on this mode could be demonstrated.

Greszczuk[50] in 1973 presented his work on large diameter rod (2 mm) reinforced composite materials, in a study on compressive failure modes. He concluded that while microbuckling is indeed a valid failure mode in composites it is not the only one which may occur. In composites made with resins having a shear modulus greater than a critical value G_m^*, non-microbuckling compressive failures were observed. The alternative modes of failure included:

- compressive failure of the reinforcement (shear at 45°)
- transverse splitting of the graphite rods, and
- transverse cracking of the composites.

Greszczuk found that both resin and fibre properties influence the failure mode.

Hancox[51] in 1975 carried out some compression tests on type I and type II carbon fibre reinforced epoxy resin specimens. He found that the strengths of all treated fibre specimens were linearly related to fibre volume fraction, as is the case with tensile properties, and that the predominant failure mode in these specimens was one of shear along a plane at 45° to the fibre axis. Hancox also observed that the maximum compressive stress achieved decreased with increasing gauge length, a characteristic which had previously been associated with tensile properties. A critical gauge length however existed, below which the compressive strength levelled out with respect to unsupported gauge length. Hancox contrasted his results with the predicted linear response of Hayashi[46] because Hancox's resin yielded at 4.3% strain, well above tensile and presumably compressive failure strains of either type I or type II fibres. Also, by Hayashi's theory one would have expected type I CFRP compressive strength to be greater than that of type II, in

contradiction to Hancox's experimental results. Because the results appeared to deny the validity of buckling and instability theories and because of a similarity between tensile and compressive strengths, Hancox concluded that the strength in compression of undirectional fibre composites is governed by the same mechanism as the tensile strength, and is an inherent property of the fibre.

Chaplin[52] considered that compressive strengths lower than theory such as Rosen's buckling model[44] were the result of the composite's sensitivity to defects. These could initiate failure which would then be able to propagate through the material. In this light he attempted to understand the compressive behaviour of GRP by performing a number of tests on specimens and analysing the type of failure produced. Some were straightforward specimens to demonstrate failure mode while others were notched from which Chaplin was able to show that specimen failure does propagate from a defect. In some of the notched specimens failure was arrested so a close examination of the material could be made in the region at the tip of the failed zone.

The failed, unnotched samples revealed a band of sheared material in which extensive debonding had taken place. Chaplin found that damage was always entirely restricted to this band. The notched specimens revealed that the failed band, though at an angle to the applied load, propagated in a direction normal to the axis of loading. This is shown in Figure 27. He also discovered that this shear band propagates by means of an initial increase of shear deformation within the fixed band but with no change in orientation. Gradually, as the deformation increases, the bending of the fibres at the boundaries of this band becomes so great as to initiate fracture along the boundary. As the deformation increases still

further, adhesion between fibres and matrix within the shear band breaks down. This interlaminar shear occurring within the shear band is arrested by the fractures at the boundaries. Chaplin commented that this failure is a type of shear instablity and that the term "microbuckling" would seem inappropriate.

Piggott and Harris[53] in 1980 presented the results of their work to investigate the effect, on compressive strength of different matrix and different fibre characteristics. They carried out compressive tests on a series of different polyester resins of various compositions and states of cure. Having established their mechanical properties the same resins were used as matrix materials for a series of unidirectional GRP composites. Their results showed a significant dependence of composite strength on matrix yield strength and microscopic examination suggested that failure mode was also affected. Low matrix yield strengths resulted in very localised composite failure with narrow kink-bands occurring perpendicular to the fibres. However in samples with higher matrix yield strengths, larger scale resin cracking occurred in a "kink/crack/split" type of behaviour. A further series of unidirectional composites was then made using glass, carbon and Kevlar fibre reinforcement to examine the effect of different fibre characteristics on compressive strength. Piggott and Harris noted that the strengths of glass and carbon composites were not significantly different. Failure characteristics however, were. The CFRP specimens for example, separated into two halves after removal from the grips of the test-fixture, while the GRP specimens did not. CFRP composites failed in a brittle manner with a single transverse crack which was perpendicular to the fibre axis, with no splitting occurring, while GRP specimens exhibited multiple kink-bands. On varying the volume fractions of their composites, Piggott

and Harris found that for both modulus and strength properties, rule of mixtures behaviour occurred only at low fibre contents. In the CFRP composites, moduli were significantly lower than predicted by the ROM but they suggested that this could have been a result of fibre misalignment in the pultruded specimens.

Piggott and Harris[53] found that their work did not support any of the existing theories. Certainly the linear relationship between strength and volume fraction could not be compatible with Rosen's[44] model, and since many other results showed this same linear relationship, Piggott and Harris suggested that it may be timely to abandon the Rosen model. The Hayashi theory[46], though it predicts this linear relationship also seemed inapplicable since failure should occur at the matrix yield stress. Composite failure however, according to Piggott and Harris' findings, normally occurred while the matrix was still elastic.

Hull[54] reasoned that Rosen's[44] basic idea of cooperative buckling was valid for some fibre-matrix systems but that it required modification to take into account certain material effects which invalidate some of the assumptions of the model. He listed some factors which reduce the support the matrix will give to the fibres as follows:

i) fibre bunching which results in resin-rich regions
ii) the presence of voids
iii) poor fibre alignment which results in some being preferentially orientated for buckling
iv) differences in Poisson's ratio between fibres and matrix, which can result in fibres debonding
v) viscoelastic deformation of the matrix

vi) non-isotropic properties of the fibres, for example both carbon and Kevlar-49 fibres have low transverse and shear moduli.

All of the above considerations suggest that the prediction of Rosen's theoretical buckling strength would overestimate the actual strength of a real composite. Hull summarised how the buckling type of compresive failure in a laminate can be identified by the bending failures of individual fibres at the boundaries to the kink-band. In contrast to this type of failure, he went on to outline the shear type of failure proposed by Ewins and Ham[49] in which a clean shear failure occurs through the laminate along a plane at 45° to the loading axis. Hull pointed out that the transition in failure that Ewins and Ham observed due to increasing the temperature had also been obtained from moisture uptake in the resin leading to a lower matrix modulus or from an increase in fibre strength[54].

The effect of poorly aligned fibres, which Hull[54] suggested could be one of the reasons why strengths were much lower than the Rosen prediction, was the subject of an investigation by Martinez, Piggott, Bainbridge, and Harris[55]. They carried out compressive tests on glass, carbon and Kevlar fibre specimens containing varying degrees of twist and varying amounts of kinking. They also analysed the relationship between strength and volume fraction for straight fibre specimens and the effect of poor fibre bonding in the GRP.

Elastic moduli in the straight fibre specimens varied linearly up to a value of about 0.5 after which the slope was reduced. This occurred in specimens of all fibre types, and Martinez et al[55] suggested that it may have been due to a change in failure mode. It was also found that strength results varied linearly with volume fraction up to about $V_f = 0.4$ after which strength began to fall

off. While composite moduli extrapolated to reasonable values for the fibres at $V_f = 1.0$, the strengths did not, and in fact compressive strength results were similar in specimens containing each type of fibre reinforcement with the exception of Kevlar. The effect of poor adhesion was clearly to lower the strengths of these composites and Martinez et al commented on the similarity between these strength results and those of Hancox[51], with poor bonding apparently causing strength to fall increasingly further from the ROM expression applied to compressive strength:

$$\hat{\sigma}_c = V_f\hat{\sigma}_f + V_m\sigma_{ml} \qquad (2.30)$$

(This expression assumes that the matrix is still elastic at the instant of composite failure).

From the results of the misaligned fibre specimens in Martinez et al's[55] work, it was clear that if the degree of misorientation exceeded 20° substantial reductions in both strength and modulus occurred. However it was also apparent that considerable displacements from the fibre axial direction could be tolerated without any loss of strength or stiffness. At low angles of twist (10°) an increase in strength was observed in glass and carbon composites over that in the straight fibre specimens. Kinking of fibres reduced composite strength considerably if the minimum radius of curvature of the fibre axes was below 5 mm. Kinking defects in composites could therefore be quite critical while misalignments may not be, to the same extent, if they are kept to within 10° of the fibre axes.

As more experimental work was carried out on different composite systems, it became apparent that none of the existing theories

adequately described their compressive behaviour. Piggott[56] suggested that a number of different mechanisms can cause failure and that the active one in any particular situation would be that which predicts the lowest failure stress. Some of the factors which he considered were fibre strength, matrix yielding, lack of fibre linearity and fibre-matrix adhesion. He noted that modulus as well as strength can be affected by some of these factors. The following modes of failure were described, and in a later piece of work by Piggott[57], experimental data was included to support the theory:

i) fibre failure
ii) matrix yielding
iii) interface failure and matrix tensile failure.

In the fibre failure mode (i), composite strength obeys the ROM relationship:

$$\hat{\sigma}_c = V_f\hat{\sigma}_f + V_m E_m/E_f \hat{\sigma}_f \qquad (2.31)$$

where $\hat{\sigma}_f$ is the compressive stress in the fibres when they fail in the composite. (He pointed out that $\hat{\sigma}_f$ may not necessarily be a true representation of the ultimate compressive strength of the fibres). This type of failure has been observed in Kevlar composites since these fibres have a very low yield stress in compression. In the case of GRP, since this type of failure would give the composite strengths of up to 2.4 GPa, as pointed out by Piggott in the later work[57], it is almost certainly not the governing failure mode. Experimental observation would support this[52,53].

The matrix yielding mode of failure (ii) occurs due to the fact that fibres cannot be perfectly straight. Piggott assumed that the fibre axis is in a sinusoidally buckled shape and that, to start with, there is perfect adhesion with the matrix. On the outer edge of the fibre displacement, a pressure P is created between fibre and matrix. When P reaches the matrix yield stress, an unstable state is reached since further deflection would result in further increasing P. Piggott used these assumptions to derive the following equations which predict composite strength and modulus governed by this failure mode:

$$\hat{\sigma}_c = (2\lambda^2\sigma_{my}/a\pi^3)\ (V_f + V_m E_m/E_f) \qquad (2.32)$$

$$E_1 = V_f/(1/E_f + 1/E_{f1}) + V_m E_m \qquad (2.33)$$

where σ_{my} = matrix yield stress

λd = wavelength of sinusoidal buckling

ad = amplitude of sinusoidal buckling

if d = diameter of fibre

E_f = fibre modulus due to elastic shortening

E_{f1} = fibre modulus resulting from increase in a and decrease in λ due to matrix pressure

(a and λ are dimensionless parameters)

He found that experimental data[53,56] fitted the equations well for GRP up to σ_{my} approximately 60 MPa and for KRP up to σ_{my} approximately 10 MPa. (This failure relationship breaks down at a low value with KRP because a fibre yielding mode takes over).

Another type of failure detailed by Piggott is that of interface failure and matrix tensile failure (iii) as shown in Figure 28. This occurs when the interface is weak, causing separation of the

fibre from the matrix followed by matrix splitting. The same assumption was made as in (ii) above, that the fibre is in a sinusoidal shape except that this time the pressure P under consideration is the negative one on the inside of the fibre curve (i.e. equivalent to a tensile stress). Taking into account the relative areas over which these stresses act, Piggott obtained an equation for the equilibrium of forces, from which he derived the composite strength equation describing this type of failure:

$$\hat{\sigma}_c = \left(\frac{4R}{\pi d}\right) \left(\pi\hat{\sigma}_a + \{\sqrt{(P_f/V_f)} - 2\}\hat{\sigma}_{mt}\right) (V_f + V_m E_m/E_f) \qquad (2.34)$$

where R = radius of curvature of fibre

d = diameter of fibre

$\hat{\sigma}_a$ = adhesion strength

P_f = factor representing fibre packing arrangement ($=2\pi\sqrt{3}$ for hexagonal packing)

$\hat{\sigma}_{mt}$ = matrix tensile strength

Again, Piggott presented experimental data[57] which fitted the equations well. At low volume fractions equation 2.32 gives the lower stress and would therefore define the failure process, while at higher volume fractions equation 2.34 would take over.

In a piece of work by Parry and Wronski[58] in 1981, type III CFRP specimens were tested in flexure and kink-bands were observed in the compressive regions of the failed laminates. In a further paper published in 1982 on the compressive behaviour of these type III CFRP composites, Parry and Wronski[59] were able to analyse the fracture mechanisms by encapsulating specimens in resin, thus causing failure to be arrested during its propagation through the composite. They concluded that the fibres involved in microbuckling

at the edge of a kink-band, fail by a tensile failure mechanism and that this occurs before permanent deformation within the kink-band takes place. Groups of fractured fibres were observed ahead of the propagating kink-band. This observation supported the previous work of Chaplin[52]. On the basis of understanding the failure mechanisms by observation, Parry and Wronski suggested that the strengths of CFRP materials are not related to the moduli of the resins but rather to their strength, ductility and even toughness.

Rosen's buckling model[44] was the first serious attempt at modelling the compressive failure behaviour of unidirectionally reinforced fibre composites. His theory was therefore used as a baseline from which others worked, and many of the early theories of compressive strength were simply modifications of Rosen's buckling theory. This model predicts strengths far in excess of those achieved in practice, and it has been suggested that one of the main reasons for this is flaws and imperfections in the laminate initiating failure at an early stage[48,54]. However the theory does not predict the correct variation of strength with volume fraction as has been observed[47,51]. Other theories were developed[48,52] which modified Rosen's principle of general microbuckling of fibres throughout the composite to one in which microbuckling simply takes place in localised areas such as at the boundaries of a kink-band. These kink-bands are initiated at defects or irregularities in the laminate and propagate through the composite in a direction perpendicular to the fibre axes. There is a considerable amount of experimental evidence to support this[48,52,54,58].

This kink-band type of buckling failure is not however, the only type of failure mechanism which governs the compressive strength of composites. Other workers have observed a shear type of fracture

along a plane inclined at 45° to the fibre axes[49,51,54]. Therefore, depending upon the characteristics of the constituent materials and the conditions of testing, a transition can occur from one type of failure to another[54]. This idea of several different failure mechanisms governing compressive failure in high performance composites has been reinforced by other research[56], and experimental results have backed up the theory[57].

The factors which have been put forward as having an influence on compressive strength and the mode of failure include:

- resin shear modulus
- resin strength
- resin ductility and toughness
- fibre compressive strength
- fibre tensile strength
- volume fraction
- void content
- fibre alignment
- fibre/matrix Poisson's ratios
- fibre-matrix bond strength.

Data on compressive strength is far from plentiful and progress is only beginning to be made in understanding the roles played by the fibres and the matrix in compressive failure mechanisms. Further experimental work is therefore required for a deeper understanding of how closely the above theories describe the behaviour of real composites.

2.4.2 Hybrid Composites

Compressive failure processes in fibre composite materials are still not completely understood, and the use of different reinforcing fibres together, to make hybrid laminates, complicates the issue still further. Little data on compressive properties has been produced and indeed, that which has cannot be fully explained by existing theories. However as in tension, hybrids have the potential to improve on the properties of the parent composites economically and therefore a fuller understanding of their mechanical behaviour is very desirable.

Clearly as an approximate guide, the ROM equations 2.11, 2.12 and 2.13 could be used to describe the compressive properties of these composites. However the limitations of the ROM must always be remembered, especially when it is used to describe a strength relationship for which it may be argued that ROM behaviour cannot necessarily be expected. Since the compressive properties of fibres, upon which the ROM is based are difficult to determine experimentally, and due to the nature of compressive failure mechanisms, the ROM approach may be less applicable than with tensile behaviour and is not generally used to describe expected compressive strength levels. Nevertheless, it still acts as a useful baseline with which experimental observation and theoretical analyses can be compared.

In the earlier work on hybrid composites, it was considered that compressive properties of unidirectional laminates were similar to those in tension. The results of Dukes and Griffiths[60] in 1972 showed that the addition of carbon fibres to GRP causes the compressive modulus to be increased while having very little effect

on strength, an effect which was also observed in tension. When Kalnin[61] carried out tests on unidirectional S glass/graphite fibre interlayer hybrids, he too found that compressive strength and stiffness followed identical trends with respect to the relative carbon content to those he observed in tension, though actual values were lower in compression for both strength and stiffness. Kalnin's modulus results in hybrids did not obey the ROM. Addition of carbon fibres to GRP caused a greater increase in modulus than would be expected from simple averaging of properties. The stiffness, therefore, of glass-rich hybrids was high but the strengths recorded from the same lay-ups were very low. Addition of increasing amounts of GRP to CFRP composites caused progressively lower strengths to be recorded, even though the strength of the GRP monofibre material was greater than that of the CFRP. The presence of small amounts of carbon fibre therefore, greatly weakened the GRP material.

Kalnin[61] noted also that compressive failure was not catastrophic, but consisted of progressive interfacial debonding between the glass and graphite lamellae, followed by cumulative local buckling of the CFRP. He also observed from the stress vs strain curves that the initial modulus was constant only up to approximately 0.1 to 0.15% strain after which a progressively decreasing modulus occurred.

A significant contribution to the understanding of the compressive behaviour of hybrid composites was made by Piggott and Harris[62] in 1981, as a continuation of their work on compression of monofibre composites[53]. They used carbon/Kevlar, carbon/glass, Kevlar/glass, and HMS/HTS carbon fibre reinforcement in pultruded rod specimens and studied the effect on strength, modulus and failure mode of mixing the different fibre types. Their specimens contained intermingled tows or rovings of the different types of fibre but no

intimate mixing of individual fibres took place so that even by this method of manufacture, segregated regions of each type of reinforcement occurred. They compared the results obtained with rule-of-mixtures predictions which they defined as a simple average of the properties of the constituents in proportion to their volume fraction. (They used this definition for both modulus and strength).

In the Kevlar/glass hybrids, Piggott and Harris found that while strength properties roughly obeyed the ROM, modulus results fell below this expectation. The stress/strain curves of these specimens distinctly showed a secondary modulus which Piggott and Harris suggested was due to the GRP portions continuing to support load after the Kevlar had yielded. The CFRP was slightly stronger than the GRP, and in the carbon/glass hybrids strength did not obey the ROM but had a minimum value at a composition of about 20% carbon/80% glass. Modulus results also had a non-ROM relationship in which there were two linear regions which met at 40% carbon/60% glass composition, the deviations from the ROM again being negative. These results are shown in Figure 29. Carbon/Kevlar hybrids exhibited approximate ROM behaviour in their strength properties while their moduli fell below ROM, and the HMS/HTS carbon had approximately ROM strengths and non-ROM moduli.

By microscopic examination of polished sections, Piggott and Harris were able to analyse the effect of fibre mixing on the failure modes. They found that addition of glass fibres to carbon/glass hybrids progressively changed the mode of fracture from that of carbon to that of glass. There was a transition from the no-kinks, transverse fracture mode typical of their carbon composites to the kink-split mode typical of the GRP samples. The change of mode was observed at the glass-carbon interface. Piggott and Harris noted

that in these carbon/glass hybrids, though both types of fibre were brittle, cracks initiated more readily in the CFRP portions and the progress of these cracks through the laminate was inhibited by the GRP layers which favoured the kinking mode of failure. A transition from one type of composite failure to another was also apparent in the glass/Kevlar hybrids.

Summarising the important findings of Piggott and Harris[62] it was shown that in all hybrid types tested, the results of either strength or modulus deviated in some way from the rule-of-mixtures. Strength deviations tended to be favourable or positive while modulus deviations tended to be harmful or negative.

In the paper by Piggott[56] in 1981 on the compressive properties of aligned fibre composites, some explanation is given of the results obtained by Piggott and Harris[62] for the strengths of their hybrids. Specimens containing Kevlar/glass and Kevlar/carbon fibre reinforcement obeyed the ROM for strength. Piggott's explanation of this centred on the fact that Kevlar is a ductile fibre. It yields at approximately 0.4-0.5% strain so that as the strain in the compressive test continues to increase, the stress level in the Kevlar fibres remains constant. Failure will occur when the brittle fibre regions initiate failure. Thus the strength relationship for different hybrid fibre volume ratios of these composites will be a straight line from the yield stress of the KRP to the failure stress of the GRP (or CFRP). Each fibre, reasoned Piggott, makes the strength contribution indicated in the following equation:

$$\hat{\sigma}_c = V_{fK}\,\sigma_{fKy} + V_{fg}\,\hat{\sigma}_f + V_m\sigma_{ml} \qquad (2.35)$$

where σ_{fKy} = stress in Kevlar fibres when they yield

σ_{ml} = stress in resin at point of failure of the composite

In the glass/carbon hybrids however, neither fibre is ductile and at the point when the LE fibre regions initiate failure, the HE fibres are not carrying their maximum load because of the difference in failure strain and modulus. Negative hybrid effects from the ROM should therefore be expected, as observed by Piggott and Harris. The equation put forward by Piggott for this type of failure would be:

$$\hat{\sigma}_c = \hat{\sigma}_f \left(V_{fhi} + \frac{V_{flo} E_{flo}}{E_{fhi}} + \frac{V_m E_m}{E_{fhi}}\right) \qquad (2.36)$$

where the subscripts hi and lo refer to high modulus and low modulus fibres respectively.

Piggott and Harris' results for glass/carbon hybrids however did not fit equation 2.36. The strengths observed were greater than this so Piggott modified equation 2.36 to the following:

$$\hat{\sigma}_c = \hat{\sigma}_f \left(V_{fhi} + \frac{3V_{flo} E_{flo}}{E_{fhi}} + \frac{3V_m E_m}{E_{fhi}}\right) \qquad (2.37)$$

He reasoned that the actual failure stress was greater than the predicted stress of equation 2.36, "probably because the lower modulus fibres can assist the matrix in resisting the push of the higher modulus fibres." The multiplier 3 was required to account for the supporting lower modulus fibres once the higher modulus fibres reached $\hat{\sigma}_f$.

In the HMS/HTS carbon hybrid specimens of Piggott and Harris, a positive hybrid effect had been observed. Piggott's failure mechanisms could not account for this positive hybrid effect, and

the negative hybrid effect on modulus which they observed in all their hybrid systems could not be explained either. Clearly then, although some aspects of the properties of hybrid composites in compression had been identified by the work of Piggott and Harris[62] and clarified by Piggott[56], compressive failure mechanisms were still far from well understood.

The work done so far has helped to reveal something of the different trends which these hybrid materials seem to demonstrate but it has also revealed unexpected and still unexplained problems of mechanical behaviour interpretation. A key problem for example, is why the modulus behaviour of hybrids in compression does not obey the ROM, as it is now generally accepted that it does in tension. In some cases hybrid moduli have been higher than the ROM[60,61], and in others they have been lower[62]. While strengths may not be expected to obey the ROM, the difficulties in understanding stem from the fact that trends do not appear to be consistent, though in a more recent publication Piggott[57] stated that "In the case of compression strengths and moduli the hybrid effects are usually cohibitive" or less than ROM.

The more involved analyses of monofibre composites in compression have not yet been successfully applied to hybrids and the limited explanation of the observed hybrid results has so far been mainly of a qualitative nature. Explanation of compressive behaviour in terms of the mechanics of elastic deformation and failure would be a helpful development.

2.5 ELASTIC MODULUS VARIATION

A considerable amount of work has been carried out on the mechanical properties of unidirectionally reinforced fibre composites. However, elastic modulus behaviour is still not entirely understood. It is invariably the case that either the elastic modulus is considered to have a rule of mixtures value or that the secant modulus results from experimental tests are considered to represent the elastic modulus value for the particular composite in question. Consideration is not usually given to the fact that the elastic modulus may not be a constant value through the test. Even the more thorough practical investigations of composite material behaviour tend to consider the modulus value as a constant, while other work which is aimed at investigating the strain dependence of modulus tends to be lacking in relating the theory or single fibre results to composite material data.

In this work, some effort is made to relate the theory to the data obtained from tests on composite materials, albeit qualitatively at this stage. A review of the more important works on modulus variation is therefore presented.

Swift[63] considered how the tensile modulus of a composite is reduced by the presence of buckling in the fibre reinforcement. This buckling may have occurred for many practical reasons, as a result of the processing stages through which the composite has gone during manufacture. His model was based on that of Rosen[44] and he considered both the extensional and shear modes of deflecton. The buckled fibre geometry was defined as the sine wave:

$$y = a \sin \frac{2\pi x}{\lambda} \qquad (2.38)$$

where y = lateral displacement of a point on the axis of the fibre, distance x along the mean fibre axis, measured from an antinode position

a = wave amplitude

λ = wavelength

Assumptions in the analysis were that

$$\lambda = \text{const}$$

$$a \ll \lambda$$

and that the frequency, $V = L/\lambda = \text{const}$

where L = the length of specimen under consideration.

Swift considered the straining of the composite by dividing it into two steps: fibre straightening producing matrix strain followed by fibre extension. Matrix resistance to straightening was therefore considered to act in series with the resistance to fibre extension, the same stress being applied to each.

Then

$$E_f \text{ eff} = \frac{1}{\left(\frac{1}{E^*} + \frac{1}{E_f}\right)} \tag{2.39}$$

where E_f eff = effective Young's modulus of a buckled fibre

E^* = modulus provided by matrix resistance to fibre straightening

E_f = true Young's modulus of the fibre.

The following formulae were derived for E^*:

For short wavelengths:

$$E_{shear}^* = \frac{t\,\lambda^2 G_m}{\pi^3 r\, a^2} \tag{2.40}$$

$$E_{ext} = \frac{\lambda^4 E_m}{2\,\pi^5 r a^3} \tag{2.41}$$

For long wavelengths:

$$E_{shear}^{*} = \frac{\pi L^4 \, t \, G_m}{8\lambda^2 re^2} \tag{2.42}$$

$$E_{ext}^{*} = \frac{\pi L^6 \, E_m}{32 \, \lambda^2 re^3} \tag{2.43}$$

where t = separation of neighbouring fibres

r = fibre radius

e = maximum displacement of fibre axis (replaces a where $\lambda >> L$).

From equations 2.39 and 2.40-2.43, the effective Young's modulus of a buckled fibre can be established. The modulus of the composite is then simply obtained from:

$$\left.\begin{matrix} E_e) \\ ) \\ E_s) \end{matrix}\right. = V_f E_f eff + (1 - V_f) \, E_m \tag{2.44}$$

where E_e and E_s are the composite moduli for the extensional and shear modes respectively.

Swift went on to show that the initial rate of increase in modulus for the shear mode is 4/3 times that for the extensional mode, and he reasoned that shear mode deformations lead to a far greater reduction in modulus than extensional mode deformations. He discussed some of the causes of the different buckling modes and reasoned that non-uniform cooling and curing shrinkage is likely to cause extensional mode misalignment, while straightening out sheet or tape (such as prepreg) produced from a continuously wound cylinder may cause shear mode misalignment.

Piggott[56] took Swift's equation (2.41) for the effective fibre modulus in the extensional mode and for long specimens, with a length much greater than λ. He applied it to the compressive modulus in composites with buckled fibres. The equation he produced for effective fibre modulus was:

$$E_{f1} = \frac{\lambda^4 E_m}{\pi^5 a^3} \tag{2.45}$$

where λ and a are dimensionless parameters so that

λd = wavelength , and λa = amplitude

Piggott's composite modulus was then:

$$E_1 = \frac{V_f}{\left(\frac{1}{E_f} + \frac{1}{E_{f1}}\right)} + V_m E_m \tag{2.46}$$

He reported that experimental results[53] obeyed equations 2.45 and 2.46 for their moduli, unless the material was near or above the transition between matrix yielding controlled failure and failure by any other process. From the modulus and strength results[53], Piggott[56] was able to calculate values of a, λ and R. However these values could only be reconciled with the results of Martinez et al[55] if the value used for d (=2r) was many fibre diameters.

Curtis Milne and Reynolds[64] noted that an appreciable increase in modulus of carbon fibres occurred under tensile loading. They measured the dynamic modulus of single fibres by transmitting an ultrasonic pulse down the fibre and measuring the velocity with which the pulse was transmitted. The transmitter and receiver at each end of the fibre were solid exponential horn transformers, and tension was applied to each fibre by mounting these horns in the

jaws of a tensile machine. Curtis et al performed a series of these tests on both type I and type II carbon fibres. They found that in both cases, an increase in modulus of about 30% occurred between loads of 0.2 and 7g. The effect was completely reversible with no hysteresis. Below 2.5g loads the rate of change of modulus was rapid but decreasing, while above 2.5g the dependence was linear.

The linear region of the modulus variation curve Curtis et al associated with a change of crystallite orientation. The lower loads were associated with stronger acoustic attenuation, which gradually decreased as the load was increased, reaching a constant value at the onset of the linear modulus region. Curtis et al suggested that these low load effects were due to basal dislocations which became pinned to grain boundaries at moderate loads. The variation in modulus was therefore a result of the complex internal structure of carbon fibres[65,66].

Johnson[67] carried out some further work to investigate the non-linear stress vs strain behaviour of carbon fibres. He performed single fibre tensile tests on type III carbon fibres and on type III carbon fibre cured impregnated resin tows. In another series of tests, the results of single fibre tests on types I, II and III carbon fibres were compared with the results from deadweight loading tests on the same fibres. The purpose of these latter tests was to eliminate all machine effects. They were performed by adding weights in 0.5g increments to a cardboard pan suspended from one end of the fibre, while extension was measured by means of a travelling microscope.

In the first series of tests on type III fibres and fibre tows, the load/extension curves were non-linear, the Youngs modulus increasing

with load. Average moduli between loads of 2g and 10g were about 8% higher than those for loads up to about 5g. Comparison with a deadweight loading test confirmed that this was due to an intrinsic non-linearity in fibre behaviour and not a machine effect.

In the second series of tests, similar trends were observed in the results of all three types of carbon fibre, with the modulus increasing more rapidly at lower loads up to about 2g, but increasing at a constant rate thereafter. Johnson's results compared favourably with those of Curtis et al[64] for both types I and II fibres, though actual values were approximately 10-20% lower in both cases. Johnson suggested that some of the initial curvature in the modulus vs load curve could be accounted for in straightening out of initially non-straight fibres. This was supported by the fact that a similar initial curvature occurred in a test on a tungsten wire.

The results of Curtis et al[64] had been obtained from tests on single fibres. Johnson's[67] investigations took this a stage further as he had investigated the elastic modulus in impregnated carbon fibre tows. In working with CFRP prepreg laminates, Dootson[68] in 1973 noted that the elastic modulus increased with increasing tensile strain. He recorded that at failure the secant modulus was 10% higher than its initial value. It is apparent therefore that there is some relationship between results obtained from carbon fibres, and those from CFRP laminates.

From the above works, it is clear that the elastic modulus of a unidirectional fibre composite material may not be a constant parameter with respect to strain or load. Buckling of fibres will cause a reduced composite modulus which is dependent upon:

i) the wavelength

ii) the amplitude, and

iii) the mode (extensional or shear) of the buckling.

This buckling occurs as a result of many factors, including thermal contraction effects or simply applied compressive strain. It can be expected to occur in both GRP and CFRP composites.

A further cause of non-constant elastic modulus in CFRP is the non-linear stress vs strain response of the fibres, which will be directly reflected in the composite's behaviour. The described works investigate this by means of tensile tests on individual carbon fibres. Investigation of compressive behaviour on a similar basis would clearly prove to be very difficult.

It is apparent that further work is required for a more complete picture and explanation of the modulus behaviour of composites to be drawn. A key question may be to find out what proportion of the change in modulus is due to buckled fibres. This is a difficult quantity to determine since buckled fibre effects and non-linear fibre stress/strain response can produce similar results and therefore shroud each other. However, determination of this could give more insight into the nature of compressive failure mechanisms.

3. EXPERIMENTAL WORK

3.1 INTRODUCTION

3.2 MATERIALS

3.2.1 Glass Fibres

3.2.2 Carbon Fibres

3.2.3 Epoxy Resin Prepregs

3.2.4 Vinyl Ester Resins

3.3 EQUIPMENT

3.3.1 Laminate Manufacturing Equipment

3.3.2 Volume Fraction Analysis Equipment

3.3.3 The Celanese Compression Test Fixture

3.3.4 Mechanical Testing Equipment

3.4 TECHNIQUES

3.4.1 Manufacture of Composite Slabs

3.4.2 Preparation of Test Specimens

3.4.3 Volume Fraction Analysis

3.4.4 Environmental Conditioning

3.4.5 Strain Measurement

3.4.6 Mechanical Testing and Data Acquisition

3.4.7 Resin Density Measurement

3.4.8 Determination of Strain Gauge Requirement on Compressive Test Specimens

3.4.9 Poisson's Ratio Measurement

3.1 INTRODUCTION

Consideration is being given to the question of whether the type of matrix resin has any significant effect on the composite's properties, including mechanics of failure and the extent of the hybrid effect with different fibre lay-ups. One of the aims of the experimental testing was to provide data which would clarify the effect of the different resin matrices in their contribution to the hybrid effect in both tension and compression. The programme of tests was therefore planned with a view to investigating the nature of the hybrid effect and the effect of changing the matrix resin. Four main composite systems were studied, namely two Ciba-Geigy Fibredux epoxy resin prepreg systems 913 and 914, and two Derakane vinyl-ester resin wet lay-up systems, 411-45 and 470-36. (Prepreg is a sheet of fibre reinforced material already preimpregnated with the uncured resin matrix, and containing a latent curing agent which causes hardening to occur at at high temperature).

Every effort was made to keep the variable characteristics of these systems constant throughout so that valid comparisons could be made. Both the glass and carbon fibres used in the vinyl ester specimens were identical with those used by Ciba-Geigy in the manufacture of their epoxy prepregs.

When using a prepreg system, good quality laminates with fairly high fibre volume fractions (~ 0.65) can be repeatedly produced, but with a wet lay-up system this is much more difficult. For this reason, the method adopted for the vinyl esters involved using a predetermined amount of fibre in each laminate and also, fixing the

final laminate thickness by using spacers in the moulds. By so doing, the fibre volume fraction was maintained within a range of approximately ±0.05 V_f about the nominal value. In the prepreg systems an average fibre volume fraction of 0.67 was achieved, while with the wet lay-up technique the achieved average of 0.57 was a more practical figure for ease of repetition. This difference in mean volume fraction was considered acceptable for the purposes of the current work.

In order to obtain a complete picture of the behaviour of hybrid composites with different resin materials, various configurations of fibre content were laid up. These included GRP and CFRP and a range of combinations of glass and carbon fibre hybrids with varying volume ratio of the two constituents and also a varying number of plies of the two constituents. Different mechanical properties were plotted versus the ratio (V_{fc}/V_{ft}), so that each one of these lay-ups would represent a single point on each of these graphs. Clearly, to produce a result by means of tests on specimens which have all come from the same slab, would be unsatisfactory. It was therefore necessary to make two slabs of each lay-up configuration so that any weakness or defect in the lay-up would be evident and any abnormal result which occurred because of such a defect could not be interpreted as a material property. At least six specimens were tested for each lay-up configuration and therefore three were taken from each slab. However since both tensile and compressive tests were carried out on identical lay-ups, three specimens of each type were made from each laminated slab.

Since four resin matrices were selected for analysis, a complete series of tests was carried out for each of the four systems. No conclusions from one set of results were assumed to apply to the

other systems without the full back-up of experimental data. This was so that the effect of the resin matrix could be properly investigated. However, after carrying out tests on each of the parent composite materials and on hybrids containing equal volumes of glass and carbon, it became clear that a fuller investigation into composite behaviour with respect to hybrid fibre reinforcement volume ratio (V_{fc}/V_{ft}) was required. The 913 prepreg system was therefore selected to carry out a further experimental programme with the emphasis being placed on the variation of properties in terms of the hybrid fibre volume ratio (V_{fc}/V_{ft}). This enabled more complete graphs of the properties vs (V_{fc}/V_{ft}) to be plotted.

The series of fibre lay-ups for both tensile and compressive tests were as follows:

913	914	411-45	470-36
G_8/G_8	G_8/G_8	G_8/G_8	G_8/G_8
C_8/C_8	C_8/C_8	C_8/C_8	C_8/C_8
G_4C_4/C_4G_4	G_4C_4/C_4G_4	G_4C_4/C_4G_4	G_4C_4/C_4G_4
C_4G_4/G_4C_4	C_4G_4/G_4C_4	C_4G_4/G_4C_4	C_4G_4/G_4C_4
G_6C_2/C_2G_6	$G_2C_4G_2/G_2C_4G_2$	$G_2C_4G_2/G_2C_4G_2$	$G_2C_4G_2/G_2C_4G_2$
C_6G_2/G_2C_6	$C_2G_4C_2/C_2G_4C_2$	$C_2G_4C_2/C_2G_4C_2$	$C_2G_4C_2/C_2G_4C_2$
G_2C_6/C_6G_2			
C_2G_6/G_6C_2			
G_7C/CG_7			
CG_7/G_7C			
$G_2C_4G_2/G_2C_4G_2$			
$C_2G_4C_2/C_2G_4C_2$			

Further interlaminar shear tests, transverse tensile strength tests, and Poisson's Ratio measurements were made where this was considered necessary, to help in the interpretation of the uniaxial tensile and compressive test results.

3.2 MATERIALS

3.2.1 Glass Fibres

The glass fibre used in this work was Fibreglass Equerove 23/14. It was purchased on 10 kg cheeses and wound onto the laminate frames as required for impregnation with the vinyl ester resins. Equerove is an untwisted reinforcement roving which has been designed to give fast wet-out and good air-release properties. It is coated with a polyester/vinyl ester/epoxy compatible size, containing a silane coupling agent. Table 1 presents the details of this roving. The epoxy resin prepreg materials contained the identical glass fibre reinforcement. Further details are given in the manufacturers product sheet[69].

3.2.2 Carbon Fibres

The carbon fibre used was Courtaulds Grafil E/XA-S 10K. This is a high performance twist-free tow. The fibres are surface treated for good fibre-matrix bond properties and have an epoxy resin size to assist handling. Details of this roving are given in Table 2. The epoxy resin prepreg materials contained the identical carbon fibre reinforcement. Further details are given in the manufacturers data sheet[70].

3.2.3 Epoxy Resin Prepregs

The two epoxy prepreg materials used were the Ciba-Geigy Fibredux 913 and 914 systems. These materials consist of unidirectional fibres of glass or carbon, preimpregnated with a modified epoxy resin system. They contain a latent curing agent so that curing will only occur at elevated temperatures and they can be stored for long periods at -18°C ($\sim$ 1 year).

The structure of the 913 system is known to contain two epoxy resin constituents and a further additive, with dicyandiamide as a hardener. The two epoxies are MY-750 and MY-720, of which the former is in the greater proportion[9]. The cured composites exhibit exceptionally high resistance to water and high humidity environments[71]. In the 914 prepreg systems, MY-720 is the major constituent, and since this has better high temperature properties[9], it gives the cured 914 laminates high strength retention at a large range of operational temperatures (-60°C to + 180°C)[72]. The cure conditions used in the compression moulding processes of 913 and 914 are presented in Table 3.

3.2.4 Vinyl Ester Resins

The Derakane vinyl ester resins 411-45 and 470-36 were used in this work. Vinyl ester resins have the backbone structure of an epoxy but the reactive vinyl sites of a polyester. This enables the good mechanical properties of an epoxy resin to be combined with the more favourable curing processes which are characteristic of polyester resins using free-radical initiating catalysts. The difference between the 411 and 470 resins is the structure of the backbone of

the polymer molecule. While the 411 structure is based on the DGEBA epoxy resin, the 470 has an epoxy novolac structure giving it better thermal stability. These chemical structures and their related mechanical properties are discussed more fully in Section 2.2.3. Because these resins possessed good wet-out properties, high quality laminates could be made by a simple hand lay-up technique.

The curing system used in the vinyl ester composites consisted of methyl ethyl ketone peroxide, cobalt octoate and dimethyl anilene, as recommended by Dow Chemicals[16,73]. The proportions used are given in Table 4. This gave a gel time of approximately 40 minutes, enough time for complete wetting of fibres to be achieved. The "-45" and "-36" in the resin identification code indicates the amount of styrene diluent present (expressed as weight %). Even with the higher styrene content 411-45 is more viscous than 470-36, making it a little more difficult to handle. However, since it has a longer gel time than the 470, this effect is balanced out. The composites are allowed to cure for 24 hours at room temperature, followed by a further period of post-curing for two hours at 80°C. The post-curing ensures that the crosslinking processes are complete.

Properties of both the vinyl ester and epoxy cured resins are given in Table 5.

3.3 EQUIPMENT

3.3.1 Laminate Manufacturing Equipment

For making up the vinyl ester composites a filament winder was used. This wound the fibres from the cheeses onto steel frames. In order to maintain good alignment of fibres within the specimens, the filament winding machine was modified so that a low traverse speed

could be obtained. An auto-reverse mechanism enabled the traverse width to be pre-set to the required laminate size.

A leaky mould used for making the vinyl ester composites is shown in Figure 30. The thickness of the laminate produced by this type of mould is determined simply by the spacers used in the edges. The clamping force was provided by means of four G-cramps.

The uncured epoxy prepeg laminates were made by simply cutting up the sheets to size with a sharp guillotine and pressing them together with a hand mangle. This simple equipment produced very good quality laminates. Curing was carried out in a heated press under a pressure of 2000 kN/m^2.

Post-curing of the vinyl ester laminates and the 914 prepreg laminates was carried out in an air-recirculation oven, and a large desiccator cabinet was used for storing all laminates and specimens while not being processed.

Metallic objects with which resin came into contact during the laminating process were previously coated with a release agent. These included the leaky moulds and spacers, frames for both wet lay-up and prepreg forms of laminating and the steel plates between which the prepregs were cured. The type of release agent used in this work was Vydax* AR. This is a dispersion of a white, waxy, short-chain telomer of tetrafluoroethylene in Freon solvent. Metal surfaces coated with Vydax AR have a very low coefficient of friction and excellent release or anti-stick properties. It was applied by hand with a paint brush and, in order to improve

---

* Vydax is a registered trademark of the Du Pont Co.

adhesion, coated articles were heated to 300°C for ten minutes in accordance with the manufacturers' recommendations[74]. This caused the release agent to be fused onto the surface and enabled 20-30 releases to be achieved without any need for recoating of the articles.

3.3.2 Volume Fraction Analysis Equipment

In volume fraction analysis work, an accurate and precision balance is required which must be located on a firm base away from draughts and direct sunlight. The balance used in this work was a Stanton measuring to 0.0001g.

The resin burn-off tests required a furnace which was located in a fume cupboard. This ensured that the fumes expelled by the burning resins were not expelled into the laboratory. Several porcelain crucibles were used in which the samples were contained for burning off and for weighing.

The equipment used in the acid digestion tests is shown in Figure 31.

3.3.3 The Celanese Compression Test Fixture

This piece of equipment is designed to support a specimen of fibre reinforced plastic as it is loaded in uniaxial compression, and to prevent it from buckling. It was made in accordance with the ASTM Standard D3410[75] and is shown in Figure 32. The fixture consists of two sets of conical shaped collet grips which clamp onto the specimen by means of bolts. These grips fit into the tapered sleeves which in turn fit into the cylindrical shell. The shell

provides strong support to prevent lateral movement during the test, but is not a load bearing part of the jig. It is provided with windows through which the specimen failure can be observed and also through which wires can pass from the strain gauges. The specification of the fixture used differed from the American Standard in the following ways:

i) The jaws were removable from the collets and mounted on spacers. These spacers could be changed, to enable different thicknesses of specimen to be accepted
ii) The whole jig was made to a metric specification rather than the imperial one given in the standard, with 10 mm wide jaws.

When mounting a specimen, the two collet halves are initially located together on dowels, and then screwed up tightly gripping the specimen end tabs. Once mounted in the tapered sleeves and placed into the cylindrical shell, the whole unit is placed between the platens of the test machine, which bear on the sleeve ends. As the unit is loaded, the screws holding the collets together are relieved of their load and the jaws increase their grip from the load applied through the tapered sleeves. Experience in the use of this compression test fixture showed that keeping the tapered faces of the sleeves and collets clean was of primary importance. Trapped debris from previous specimen failures caused excessive and irregular loads to be recorded It was therefore cleaned regularly during each batch of tests and a special heavy duty grease was used on all the bearing surfaces. Also, if any damage occurred to the pins locating the two pairs of collet grips, they were replaced in order to ensure freedom from relative axial movement within the cylindrical shell. Observation of these precautions enabled many tests to be performed with very few problems.

3.3.4 Mechanical Testing Equipment

All tensile tests were carried out on the Dartec servohydraulic test machine shown in Plate 1. The specimen was gripped directly by hydraulically operated jaws. The maximum load capacity of the machine was 100 kN.

Compression testing was carried out on the Mand servo-screw test machine shown in Plate 2. Compressive load was applied by means of flat platens which pressed directly onto the tapered sleeves of the compression test jig. The maximum load capacity of this machine was also 100 kN.

Different test machines were employed for the different types of test for the simple convenience of using tensile test jaws on one machine while being able to keep the flat platens on the other. This avoided the necessity of changing jaws regularly.

Transverse tensile tests were performed on an ESH servohydraulic test machine, and interlaminar shear strength tests were performed on an Instron servomechanical test machine.

3.4 TECHNIQUES

3.4.1 Manufacture of Composite Slabs

Two different methods were employed for making up composite slabs from the fibre and resin raw materials. For the epoxy resin composites an elevated temperature compression moulding technique was carried out while for the vinyl ester resins, a wet lay-up technique at room temperature was used. The two procedures are

detailed as follows. The dimensions of the slabs produced are given in Figure 33, which also shows how the slabs were utilised.

a) Compression Moulding of Prepreg Epoxy Resin Laminates

The prepreg was cut up with a guillotine into sheets of the required size. Each laminate consisted of sixteen layers, or sixteen sheets of prepreg, which produced a cured composite slab with a nominal thickness of 2 mm. After removing the backing layer off each sheet, they were pressed together by running the laminate through a hand mangle. Each layer was added and pressed separately until the full thickness of sixteen layers had been made up. Because at this stage no curing had taken place, the laminate was flexible and careful handling was necessary. It was then placed in a steel frame and laid up in the porous and non-porous moulding materials, as shown in Figure 34. The sequence of material layers as used in the compression moulding process was as follows:

LAMINATE

layer 1: Tygavac TFG075P porous PTFE coated glass fabric

layer 2: Tygavac NW153 medium weight breather and absorption fabric

layer 3: glass fibre woven roving

layer 4: Tygavac TFG075 non-porous PTFE coated glass fabric

STEEL PLATE

These materials were used on both sides of the laminate to produce a symmetrical lay-up. Following this, the complete lay-up was placed in the press and the appropriate cure schedule as presented in Table 3 was carried out. The manufacturers recommendations for cure schedule were strictly adhered to as detailed in the material information literature for 913[71] and 914[72]. The 914 laminates required a post-curing period of four hours at 190°C, which was

carried out in the air recirculation oven. 913 does not require a post-cure.

b) Wet Lay-up of Vinyl Ester Resin Laminates

The fibre was wound from the cheese onto a thin steel frame as shown in Figure 35 using the filament winding machine. One of the chief aims when carrying out this process was to ensure that equal volumes of fibre were contained in each laminate. In order to achieve this, a predetermined number of "winds" of the glass or carbon fibre tow was applied during each traverse of the filament winder, and a total of eight passes (or sixteen layers, considering the symmetry about the central axis of the laminate) were used in each laminate. With the fibre used in this work, 26 turns per pass of carbon fibre and 50 turns per pass of glass fibre were found to be suitable. In total, therefore, each CFRP or GRP layer within a completed composite contained 26 or 50 tows of the respective fibre. Clearly the figures differ because of the difference in the volume of fibre per unit length of tow. Hybrids were made by stopping the machine and changing the cheese over before commencement of the next traverse. Symmetry of the laminates about their central axis was automatically maintained due to the nature of the winding process.

The curing agents were added to the resin which was thoroughly mixed and allowed to stand for five minutes while de-gassing took place. A vacuum was not used in the de-gassing process since this would have resulted in the loss of some of the styrene diluent. The usual safety precautions were taken during the preparation of the resin[76].

The fibre-wound frame was then placed in a leaky mould and impregnated with resin. A laminating roller was used to speed up the wetting process and ensure complete impregnation of the fibres by

the resin, as detailed by Dow Chemicals[77]. Only laminating rollers with circumferential fluting were used since it was found that the type with axial fluting caused excessive damage to the carbon fibre. The lid was placed on the mould, and G cramps were applied at each corner to provide the compressive force. Spacers which determined the thickness of the laminates were placed in the gaps along the edge of the mould, and excess resin was squeezed out of the ends, removing with it any air which may have still been present in the fibre lay-up. The resin was allowed to cure for 24 hours at room temperature followed by a two hour post-cure at 80°C in the air recirculation oven. The laminate could then be removed from the mould.

Using this method, and by keeping the fibre content and laminate thickness constant throughout, it was possible to repeatedly produce good quality flat laminates with extremely low void content. Every effort was made to keep the amount of fibre damage down to a minimum.

Specimen slabs made by both of the above methods of manufacture were sent away for C-scan tests to be carried out. These would reveal any internal defects which may have resulted from poor manufacturing techniques. The results indicated that the laminates were of good quality with no significant defects being apparent.

3.4.2 Preparation of Test Specimens

a) Tensile Test Specimens

Tensile test pieces were made from the composite slabs in accordance with BS 2782[78], method 320E. This is a straight sided specimen with aluminium end tabs as shown in Figure 36. A strip at least 10 mm

wide down each side of the slab was discarded in order to minimise any edge defects in the laminate as a result of fibre misalignment or build up from the laying up stage. The specimens were cut into 25 mm wide strips from the slabs using a diamond studded rotary wheel, and great care was taken to ensure accurate alignment in the fibre direction because even small deviations in fibre alignment from the longitudinal direction can have a considerable effect on strength[54]. Having cut the specimens the edges were smoothed on a linisher and then by hand with 240 grade silicon carbide paper. Aluminium alloy HS 30 end tabs were cut 25 mm x 45 mm on a guillotine from 16 gauge sheet and the edges of these also were smoothed on the linisher. After a 110 mm guage length had been marked on each test-piece, the surfaces of the end tabs and the composite specimen were roughened with a coarse grit paper on the linisher. The tabs were then bonded using Araldite MY750 epoxy resin containing a 1:10 ratio of HY951 hardener. A load was applied by means of a heavy weight and a curing period of 24 hours was allowed at room temperature.

b) Compressive Test Specimens

The standard compressive test adopted in this work was the ASTM D3410[75] specification, commonly known as the Celanese type specimen. (Note that the specimen dimensions adopted for this work were a modification of those specified in the ASTM standard). Production of test pieces followed the same procedure as that described above for tensile test specimens with the exception of the specimen dimensions. These are shown in Figure 37. Care was taken to ensure that a surplus amount of adhesive was forced out when bonding the end tabs, so that a smooth transition was formed by the glue between the gauge section and the end tab. This would help to eliminate excessive stresses at these points.

c) Inter-Laminar Shear Test Specimens

The method used for obtaining inter-laminar shear strength was the British Standard three point bend test method[79], but on a test rig with loading members of 3 mm diameter. Small specimens were cut from the slabs 10 mm in width x 12 mm long, with the fibres parallel with the long dimension. The edges were smoothed with 400 grit silicon carbide paper. Inter-laminar shear strength specimens were made from the GRP and CFRP slabs of both of the epoxy resin and both of the vinyl ester resin systems.

d) Transverse Tensile Test Specimens

Transverse tensile test specimens were made from the 913 and 914 GRP and CFRP laminates. The specimens used were 25 mm wide x 60 mm gauge length x 2 mm thickness (nominal). Aluminium end tabs 25 mm x 25 mm x 16 gauge were bonded to the specimens in the same way as the longitudinal test specimens. The total specimen length was 110 mm.

3.4.3 Volume Fraction Analysis

Small samples (~0.4-1g) were cut from each composite slab at a position which was considered to best represent the overall volume fraction of the slab (see Figure 33). The cutting process was carried out on a diamond studded wheel. After this, the edges of each specimen were smoothed using 240 grade silicon carbide paper. The specimens were then rinsed in cold water and dried immediately so that no increase in weight could occur through moisture uptake.

a) GRP Specimens

For laminates containing glass fibre reinforcement only, the resin burn-off procedure was carried out, in which the sample is placed in a furnace at 600°C for three hours. It was found that this

temperature and duration was adequate for eliminating all traces of the resin. After cooling for at least twelve hours in a desiccator the remaining glass fibres were weighed. The empty crucible weight was recorded after the burn off process so that any change in weight of the crucible would not affect the result. The fibre volume fraction was calculated by the following equation:

$$V_{fg} = \frac{1}{1 + \frac{\rho_g}{\rho_m}\left(\frac{c - f}{f}\right)} \qquad (3.1)$$

where c = weight of composite sample before burn off

f = weight of remaining fibre after burn off

ρ_g = density of glass

ρ_m = density of resin

b) CFRP Specimens

The laminates containing just carbon fibre reinforcement required the acid digestion technique for determination of fibre volume fraction. The method used was that of Haynes and Tolbert[80]. After being weighed, the sample was placed in beaker with 20 cm^3 concentrated sulphuric acid, and heated to fumes. After complete breakdown of the composite had occurred, a 50% solution of hydrogen peroxide was added dropwise until the solution was colourless, followed by the addition of a further 2 cm^3 to ensure complete decomposition of the polymer. After cooling the beaker in an ice bath, the fibres were filtered in a sintered glass crucible and washed with distilled water until the filtrate had a neutral pH value. An alcohol rinse then aided in the removal of surface moisture. The fibres were then dried for one hour at 100°C and cooled in a desiccator for at least twelve hours, after which time they were weighed. The fibre volume fraction was calculated by the following equation:

$$V_{fc} = \frac{1}{1 + \frac{\rho_c}{\rho_m}\left(\frac{c - f}{f}\right)} \qquad (3.2)$$

where c = weight of composite sample before acid digestion

f = weight of remaining fibre after acid digestion

ρ_c = density of carbon

ρ_m = density of resin

An experiment was carried out to compare the above two methods of volume fraction determination by carrying out further burn off and acid digestion tests on the same slabs of 470 and 411 GRP materials. It was found that the two methods generated results which agreed to within 1% fibre volume fraction, the burn off method giving the slightly higher fibre volume fraction in each case.

c) Hybrid Specimens

When hybrid fibre reinforcement was concerned, both of the above two methods of analysis were required. The resin burn off technique resulted in total oxidation of the carbon fibres so that glass content could be determined. The acid digestion technique, which was carried out on a separate sample, enabled the total content of glass and carbon fibre to be determined. By combining the results the volume fraction of each individual constituent could be calculated. Although Haynes and Tolbert[80] suggested that the concentrated sulphuric acid could cause some weight loss in the glass fibre, tests involving prolonged exposure to the hot acid showed that this was negligible. The method could therefore be justified for use with hybrids. The fibre volume fractions were calculated by the following equations:

$$V_{fg} = \frac{1}{1 + \frac{g}{c}\left(\frac{c_1 f_2}{c_2 f_1} - 1\right) + \frac{g}{r}\left[\frac{c_1}{f_1}\left(1 - \frac{f_2}{c_2}\right)\right]} \qquad (3.3)$$

and

$$V_{fc} = \frac{1}{1 + \frac{\rho_c}{\rho_g}\left[\frac{1}{\left(\frac{f_2 c_1}{f_1 c_2}\right) - 1}\right] + \frac{\rho_c}{\rho_r}\left[\frac{\left(\frac{c_2}{f_2}\right) - 1}{1 - \left(\frac{c_2 f_1}{c_1 f_2}\right)}\right]} \qquad (3.4)$$

where: <u>for the burn off sample</u>:

c_1 = weight of composite sample before burn off

f_1 = weight of remaining glass fibre after burn off

<u>and for the acid digestion sample</u>:

c_2 = weight of composite sample before acid digestion

f_2 = weight of remaining glass and carbon fibres after acid digestion

3.4.4 Environmental Conditioning

Composite materials made with "conventional" thermosetting resins such as the vinyl-ester and epoxy systems used in this work are not totally resistant to atmospheric moisture. The composite will absorb moisture from the surroundings until an equilibrium condition is reached, and this moisture content can adversely affect the mechanical properties of the material, in some cases to a considerable extent[81]. It is clear therefore, that when looking at mechanical properties which can be affected by moisture content, such as elastic modulus, tensile strength, compressive strength or interlaminar shear strength, for example, some standard conditioning process must be adopted which will enable comparison of results to be justifiable.

Immediately after manufacture, the laminates are in a "dry" condition. It was decided that the best conditioning exercise was

to maintain the dry condition by placing the laminates into a desiccator cabinet. An alternative conditioning procedure could have been to expose the materials to certain humid conditions for a standard period of time. However the advantage of using a dry condition was that since the laminates were already dry at manufacture, no long periods of time were involved in waiting for an equilibrium level to be attained. Also, since the absorbed water serves to weaken the composite, maintaining a dry condition would also result in better mechanical properties being observed than those of "wet" composites. In addition to this, a desiccator cabinet is more convenient than maintaining an environmental chamber at a fixed temperature and relative humidity. Since the specimens were being maintained at a dry equilibrium, the temperature of the environment did not need to be controlled and simply followed room temperature. (The relative humidity of the environment determines the amount of water that the composite will have absorbed to reach equilibrium, while the temperature will only affect the rate at which the equilibrium is approached[82]).

3.4.5 Strain Measurement

The following three techniques for direct strain measurement are in fairly common use:

i) strain measurement with a re-usable extensometer
ii) strain measurement by means of strain gauges
iii) modulus obtained from a plot of 1/apparent stiffness (where apparent stiffness = machine displacement/applied load) vs the specimen gauge length. The slope of this graph is 1/EA.

The apparent stiffness plot, method (iii), as used by Piggott and Harris[53] does not lend itself to specimens with end tabs since

successive shortening of the gauge length is required. Also, in composites where the elastic region is not necessarily linear it is important that actual strain is measured as an extension or compression within the gauge length of the specimen. For these reasons, method (iii) was considered inappropriate in this work.

In the tensile tests, strain was measured by means of an extensometer. The advantage of this over strain gauges was the speed with which it could be fitted to each specimen in turn when a large batch of tests were being performed. The extensometer was fitted onto the specimen by means of knife-edge jaws. As an extra precaution, small strips of double-sided tape were placed on the specimen onto which the jaws gripped. This resulted in the combined benefits of completely eliminating the possibility of the jaws slipping on the surface, and also of preventing any damage being caused to the surface layers of the composite from the extensometer jaws, which may have resulted in premature failure. The knife edge jaws were in two pairs - one on each side of the specimen, and the strain recorded was the average of the readings from the two sets of jaws. This eliminated errors which may have occurred as a result of bending strains.

For the compressive tests, due to the small size of the specimens and the limited space within the Celanese type fixture, the use of an extensometer was prevented. Instead strain gauges were employed for measuring extension through the test, and again one was bonded to each side of the specimen so that errors due to bending were eliminated. This was found to be necessary for the compressive tests. (See Section 3.4.8). Strain gauges were selected that were as large as could conveniently fit within the specimen gauge section because smaller gauges can result in greater errors as a result of

difficulties in installation[83]. The details of the gauges used are given in Table 6.

One of the most important factors when using the strain gauges was to ensure that a good and uniform bond was achieved between the gauge and the specimen. A thorough preparation of the surface of the composite was therefore required prior to bonding. The procedure followed was based on the recommendations of M-Line Measurements Group[84] and is detailed as follows:

1. Degreased with freon on clean cloth
2. Dry lapped with 240 grit silicon carbide paper
3. M-Prep Conditioner-A applied and wet lapped, keeping surface wet. Wiped with cloth and repeated with 400 grit.
4. Alignment marks drawn with a hard pencil.
5. Rewet with Conditioner-A. Scrubbed with cotton buds until one remained clean. Wiped dry with cloth.
6. M-Prep Neutralizer-5 applied liberally. Scrubbed with cotton buds keeping surface wet. Not allowed to evaporate, but wiped dry with clean cloth.
7. Strain gauge removed from acetate with tweezers and placed on a clean glass slide, bonding side down.
8. Terminal strips cut as required and aligned alongside strain gauge.
9. Cellophane tape stuck over gauge in one wiping action, and removed by lifting at 45° to the surface.
10. Tape with gauge and terminal strip positioned on specimen and lifted off so that the gauge and terminal were free but the remainder of the tape stuck. Gauge could then be instantly re-positioned on specimen.
11. Gauge and terminal coated with adhesive.

12. Gauge and terminal re-stuck using firm pressure.
13. Soft pad, backing plate and clamp applied.
14. Adhesive allowed to cure.

The adhesive used was M-Bond AE-10 which was prepared in accordance with the supplier's recommendations[84]. It was allowed to cure for two hours in an air recirculation oven at 50°C. Following this, the tape was removed, and the lead wires were soldered to the terminal strips. The wires from the strain gauge connector box containing the bridge circuit were soldered to the wires from the strain gauges after each specimen had been mounted in the compression test fixture. A specimen with attached strain gauges is shown in Figure 37.

The bridge circuit used for processing the strain gauge signals is shown in Figure 38 and is situated inside the strain gauge connector box (SGCB). It consists of four strain gauges, two of which are "active" and mounted on the specimen remote from the SGCB, while the other two are mounted on a dummy specimen inside the SGCB. This arrangement eliminates the effect of temperature changes since all the arms of the bridge are subject to the same variations, and the output signal remains unaffected. (It is assumed that the active gauges on the specimen and the dummy gauges inside the SGCB experience the same temperature fluctuations). Buckling or bending effects in the specimen are also eliminated from the strain readings because the circuit averages the strain measured by the two active gauges. The zero adjustment circuit enables the output signal to be zeroed before commencement of the test, while the specimen is not supporting load. (An off-zero signal can occur due to slight variations in the nominal gauge resistances and also due to residual strains occurring in the gauges during the bonding process). The

calibration circuit provides a 1% change in resistance of one of the strain gauges so that the output signal can be calibrated.

Two tensile specimens were fitted with strain gauges of the type used in the compressive tests. Strain readings from these were compared with similar readings taken by means of the extensometer as the specimens were subjected to tensile loading. The readings obtained by each of these methods agreed to within 0.5% of the reading, up to values of 2% strain. These tests confirmed that both methods of strain measurement were accurate.

3.4.6 Mechanical Testing and Data Acquisition

a) Tensile Tests

While strain in the tensile tests was measured by means of an LVDT extensometer, through an amplifier, load was measured directly through the load cell of the test machine. Both of these signals were fed to an XY plotter so that load vs extension curves were obtained for each specimen. After applying the appropriate scale factors, these are equivalent to stress vs strain curves. The tests were carried out at a constant rate of grip separation of 5 mm/min and each test was continued until the specimen was unable to support load. The wearing of safety spectacles was necessary during the testing operations.

b) Compressive Tests

Strain was measured by means of strain gauges via an amplifier in a bridge circuit and load was monitored directly via the load cell of the test machine. As in the tensile tests, both load and strain signals were fed to an XY plotter to produce stress vs strain curves for each specimen. It was found necessary to give each specimen an

initial preload of 5-10 KN which was then "unloaded" again before the test commenced. This reduced the initial irregular part of the stress vs strain relationship down to a minimal amount, allowing more accurate tangent modulus assessments to be made at lower loads than would have otherwise been possible. It is believed that the irregularity was due to non-uniform loading rates as the compression test piece clamping fixture (the Celanese jig) was initially compressed, and allowed slack to be taken up. A constant compression speed of 1.2 mm/min was used. In almost every specimen, initial failure resulted in total loss of compressive load bearing capacity and therefore concluded the test.

c) Interlaminar Shear Tests

The loading rate was 1 mm/min, and the maximum load sustained was read directly from the test machine's built in load/time plotter. After removal of the specimen, a check was made that failure had occurred by true interlaminar shear.

d) Transverse Tensile Tests

The loading rate used was 0.3 mm/min and the peak load was obtained directly from the test machine's digital read-out in "peak load" mode.

3.4.7 Resin Density Measurement

Cured resin density was determined using a 100 cm^3 density bottle, distilled water, and small clear cast specimens of the 411-45 and 470-36 vinyl ester resins. The technique involves measuring the weight of water displaced by the specimen so that its volume is determined because the density of the displaced water is known. It follows that its density can be calculated as shown:

weight of density bottle containing water only . . . . . W_{wo}
weight of density bottle containing specimen + water . . . . . W_{w+s}
weight of specimen . . . . . W_s

$$\text{specimen density} = \frac{W_s \, \rho_w}{W_{wo} + W_s - W_{w+s}}$$

where ρ_w = density of water (= 1.000 g/cm^3).

Care was taken during the procedure to ensure that no air bubbles were trapped on the surface of the specimen, that the bottle was always full when a weight reading was taken, and that it was dry on the outside. The process was repeated with ten different specimens of each of the vinyl ester resins and the resin density result was taken as the average of these. The results are presented in Table 7.

The densities of the cured resin in the prepreg materials were obtained from the manufacturers trade literature since clear resin specimens were not available and could not be easily made. Resin density was required in the volume fraction calculations (see Section 3.4.3).

3.4.8 Determination of Strain Gauge Requirement on Compressive Test Specimens

An experiment was carried out to determine the effect of using either one single strain gauge, or one on each side of the specimen in the compression tests. Four specimens were made from vinyl ester 411-45 resin and glass fibre reinforcement. GRP was used for these tests because the lower modulus specimens are more prone to buckling.

Once the specimens had been made, strain gauges and connector terminals were bonded to both sides. The normal procedure for compression testing each specimen was then carried out, but in each case the test was stopped when 10 kN compressive load was reached. This was performed three times for each of the four specimens. Each time, strain was measured in the following way:

i) first series of tests - strain measured using strain gauge on side A only
ii) second series of tests - strain measured using strain gauge on side B only
iii) third series of tests - strain measured using strain gauges on both sides A and B.

In the third series of tests, the strain was calculated from the two gauges as:

$$\varepsilon = \left(\frac{\varepsilon_A + \varepsilon_B}{2}\right)$$

The stress/strain curve obtained from each test was used to determine the secant modulus of the specimen from 1 kN to 10 kN load. This provided a convenient comparison of each form of strain measurement. The results are presented in Table 8 where average values and standard deviations have been calculated for each series of tests.

The results show that considerably less variation in the modulus occurs when the two gauge measurement technique is employed. The coefficient of variation is less than half that when only a single gauge is used. The apparently very high value of modulus measured on side A of specimen 2 is counteracted by the very low value measured

on side B of the same specimen. This is an indication of the occurrence of some bending, or a flexural component of strain.

Individual surface strains on the compressive specimens are therefore not necessarily equal and the conclusion of the observation is that some degree of specimen bending does occur. It is therefore necessary, when measuring compressive strain, to average the strain measured on both surfaces of the specimen. The two strain gauges used to do this were in opposite arms of the bridge circuit as described in Section 3.4.5.

3.4.9 Poisson's Ratio Measurement

The Poisson's Ratios of GRP and CFRP were measured in the following way using standard tensile test specimens.

Four strain gauges were bonded to each specimen; a longitudinally mounted and a transversely mounted one on each side. The test was carried out in two stages:

i) The strain measuring circuit was connected to the two longitudinally mounted strain gauges. The specimen was then loaded in tension, in increments, up to a value of approximately half of its failure load. Readings of longitudinal strain were taken at the regular load increments. The gradient:

$$y_1 = \frac{P}{\varepsilon_1} \text{ was established}$$

where P = load in specimen

ε_1 = longitudinal strain

ii) After unloading the specimen slowly, the strain measuring circuit was reconnected to the transverse strain gauges and a repeat exercise was performed.

The gradient:

$$y_2 = \frac{P}{\varepsilon_2} \text{ was established}$$

where ε_2 = transverse strain.

The Poisson's Ratio (ν) was calculated from the equation:

$$\nu = \frac{y_1}{y_2}$$

4. RESULTS

4.1 INTRODUCTION

4.2 TENSILE PROPERTIES

4.2.1 Observations from the Tensile Tests

4.2.2 Tensile Failure Strain

4.2.3 Ultimate Tensile Strength

4.3 COMPRESSIVE PROPERTIES

4.3.1 Observations from the Compressive Tests

4.3.2 Compressive Failure Strain

4.3.3 Ultimate Compressive Strength

4.4 ELASTIC MODULUS

4.4.1 Methods of Elastic Modulus Measurement

4.4.2 Secant Modulus Results

4.4.3 Tangent Modulus Results

4.5 OTHER PROPERTIES

4.5.1 Inter-Laminar Shear Strength

4.5.2 Transverse Tensile Strength

4.5.3 Poisson's Ratio

4.1 INTRODUCTION

The results of the tensile and compressive tests are listed numerically in Tables 9 to 32 and are also shown graphically in Figures 39 to 62. In order to obtain results with reasonable certainty six specimens were tested of each individual lay-up configuration. These were made from two separate composite slabs and therefore inevitably had slightly different glass:carbon volume fraction ratios. In the graphs where the material property is plotted against (V_{fc}/V_{ft}) as the base axis, the six individual specimen results did not represent one value of V_{fc}/V_{ft}. For this reason each point represents the result of three tests from one single composite slab.

All results have been normalised to a standard total fibre volume fraction of 60% by the following equations:

$$E_{60} = E \times \frac{0.6}{V_{ft}} \qquad (4.1)$$

$$\sigma_{60} = \sigma \times \frac{0.6}{V_{ft}} \qquad (4.2)$$

where E_{60} and σ_{60} = normalised modulus and stress

E and σ = measured modulus and stress

V_{ft} = total fibre content as volume fraction ($V_{ft}=V_{fc}+V_{fg}$)

In each of Figures 39 to 62, a dotted line has been drawn through the average value for the GRP results and the average value for the CFRP results. This represents the rule of mixtures relationship. It is included as a reference only and is not indicative that the rule of mixtures is observed, or even that it may be expected.

Although with 913 composites a complete range of hybrid fibre ratios has been analysed, in the case of 411, 470 and 914, the analysis of hybrids has been limited to those of approximately equal volumes of glass and carbon. Consequently in the figures where the properties are plotted vs V_{fc}/V_{ft}, the hybrid results appear bunched around the central point where $V_{fc}/V_{ft} = 0.5$. However presentation of the complete graph was considered to be of value.

Complete sets of results for individual specimens are given in Appendix 1.

4.2 TENSILE PROPERTIES

4.2.1 Observations from the Tensile Tests

The stress/strain curves obtained from the tensile test results consisted of an approximately linear elastic region followed by either sudden or progressive failure depending on the type of fibre lay-up. The initial part of the curve at very low loads (<5 kN) was nearly always non-linear.

During the tests, loud cracks were occasionally heard, and these were accompanied by small jumps in the stress/strain curves. These cracks were due to shear failure occurring through the resin matrix near the edges of the specimen and did not involve specimen tensile failure. In most cases however the cracks were either not evident or only occurred at high loads, approaching the UTS of the specimen (see discussion Section 5.3.4).

While in the CFRP, failure was sudden and catastrophic, in all other lay-ups of GRP and hybrids it tended to be progressive with some tensile failure beginning to occur before the peak load was reached.

The sequence of failure in hybrids was initiated in the CFRP layers since they fail at lower strains than do the GRP. This is defined as first or primary failure. In most hybrid lay-ups, the GRP layers retained some rigidity after primary failure, and another failure was observed at a much greater strain. This is known as secondary failure and finalises the test since the specimen is no longer able to carry load. The stress vs strain curves for a series of tensile specimens are shown in Figures 63-70.

The tensile failures of all the GRP specimens were characteristically brush-like, with much separation of fibres occurring throughout the gauge length. The vinyl ester GRP specimens were reduced to a notably finer fibre structure as a result of a significantly greater amount of debonding. Plates 3, 4 and 5 show typical GRP specimen failures observed in epoxy and vinyl ester 411-45 and 470-36 specimens respectively. It is apparent from Plates 4 and 5 that the debonding in 470-36 specimens is slightly more extensive than in 411-45 GRP specimens.

The failures of the CFRP specimens fell into two distinct categories: those of the epoxy prepregs which failed with very little debonding in clean transverse breaks and an occasional longitudinal crack, and those of the vinyl esters where significant debonding caused them to resemble the GRP failures. Examples of these types of failure are shown in Plates 6, 7 and 8. It can be seen from Plate 6 that the 913 CFRP failure contains very little debonding. In the 411-45 and 470-36 CFRP failure shown in Plates 7 and 8 respectively it is apparent that the debonding in the 470-36 composite is greater than that in 411-45.

The individual layers in hybrid specimens demonstrated the same failure characteristics as the respective parent material composites. An example of this is shown in Plate 9 where the clean failure of the CFRP outer plies of a 913 hybrid is in contrast to the GRP inner where much debonding and fibre pull out occurred.

4.2.2 Tensile Failure Strain

Due to the nature of the tensile stress-strain curves, the definition of primary failure strain can be unclear. It is defined as that strain beyond which a linear increase of load with strain no longer occurs (see Section 5.3.4). The shear cracks therefore, which cause the "jumps" in the stress-strain curves are ignored when determining the point of primary failure.

The primary failure strains recorded from the tensile tests are listed in Tables 9-12 and shown graphically in Figures 39-42. The lowest GRP failure strains were those of the 411 composites while for the CFRP the 914 specimens exhibited considerably lower strains than in composites of the other three resins. Failure strains in hybrid lay-ups in all cases were greater than those of the CFRP material. That is, a positive hybrid effect always occurred. The statistical significance of this hybrid effect is calculated in Appendix 2. There was no significant difference between the tensile failure strains of three ply hybrids and those of the five ply hybrids. However a significant difference was observed between hybrids with glass layers on the outside and those with carbon layers on the outside, those with external GRP layers being stronger. The hybrid effect was dependent on the ratio of glass:carbon fibre reinforcement. The hybrid specimens containing

the greater proportions of glass fibres demonstrated greater hybrid effects.

4.2.3 Ultimate Tensile Strength

Ultimate tensile strength is, by definition, measured from the point of greatest load supported by the specimen during the test. In GRP specimens and hybrids, it often did not occur at the same point to which primary failure strain was recorded since the limit of linear elastic behaviour (to which failure strain is measured) usually occurred before the peak load was reached.

The strengths observed are recorded in Tables 13-16 and their relationship with V_{fc}/V_{ft}, the fibre volume ratio, is shown in Figures 43-46.

The strengths of the GRP specimens were of the order of 1000-1400 MPa while those specimens containing only carbon fibre attained average strengths of about 1750 MPa, with the exception of 914 where only 1200 MPa was attained. Tensile strengths in the hybrid lay-ups fell above and below the value in the GRP material depending upon the lay-up configuration and the matrix resin.

The dotted line in Figures 43-46 labelled $\hat{\sigma}_H$, is the expected strength of the material if it were to fail at the tensile failure strain of CFRP. It is defined by equation 5.3.

4.3 COMPRESSIVE PROPERTIES

4.3.1 Observations from the Compressive Tests

The most significant difference between the compressive stress/strain behaviour compared with the tensile results, was that failure always occurred suddenly and catastrophically. Progressive failure, as observed in the tensile GRP and hybrid specimens, never occurred in compression. No further compressive load could be carried by the specimen after failure had occurred so primary failure in compression is total failure and no meaningful secondary failure occurs. In the compressive tests, an initial "settling down" or non-linear region of stress/strain behaviour sometimes occurred at very low load levels (< 5 kN). The compressive stress/strain curves of a GRP, CFRP and hybrid specimen are shown in Figures 71, 72 and 73 respectively.

The characteristics of failure in the compressive specimens were significantly more varied than those observed in tension. Four different types of failure were observed as follows:

i) Splitting occupying a major part of the gauge length. This was observed in both epoxy and vinyl ester GRP specimens. Typical examples are shown in Plates 10 and 11 of 913 and 470 specimens respectively.

ii) A kink band structure with a characteristic angle of 70° to the fibre axis. This occurred mainly in vinyl ester GRP specimens but was also observed in 913 epoxy GRP. A typical example is shown in Plate 12.

Fibre failure did not appear to occur in any significant proportion in either of the above two types of failure.

iii) A clean break at 45° to the fibre axis, but with much raggedness owing to the failure following the line of the end tab. This is shown in Plate 13. It was observed in all epoxy CFRP specimens. A high magnification SEM micrograph of the shear surface in this type of failure is shown in Plate 14.

iv) A clean break at 70°C to the fibre axis. In this type of failure also, there was often a ragged edge, where the line of failure propagation had followed the end tab. It occurred in the vinyl ester CFRP specimens. Plate 15 shows an example. A higher magnification SEM micrograph of part of the failure surface in Plate 16 reveals distinctively different characteristics from those of shear failure (Plate 14).

In hybrid compressive specimens, as with tensile failures, the characteristics of failure in the individual plies of the laminates resembled those of the respective parent composites.

4.3.2 Compressive Failure Strain

The compressive failure strains recorded are listed in Tables 17-20 and are shown graphically in Figures 47-50. While in the GRP lay-ups, failure strains were approximately 2.2% for all resin systems, in the CFRP specimens the epoxy composites failed at consistently higher strains than the vinyl ester composites. Average values were 1.18% and 0.72% for the two groups respectively. Failure strains of all the hybrid lay-ups were greater than for the respective CFRP materials in all the composite systems. This is a positive hybrid effect. The statistical significance of this increase in strain by hybridisation is calculated in Appendix 2. No significant difference was recorded between the failure strains of the 3 ply and 5 ply hybrids of equivalent fibre volume ratio (V_{fc}/V_{ft}). However

the sequence of hybrid lay-up was significant. Those specimens which contained glass fibre reinforcement in the outer layers were generally stronger than those with carbon fibre outer layers for the same overall volume fraction ratio. As shown in Figure 47 the compressive hybrid effect was dependent upon the ratio of glass:carbon fibre reinforcement. Those lay-ups with the greater amounts of glass demonstrated greater hybrid effects.

4.3.3 Ultimate Compressive Strength

The compressive strengths of the specimens tested are recorded in Tables 21-24 and shown in Figures 51-54 as a function of V_{fc}/V_{ft}.

Compressive strength in the GRP specimens was just over 1000 MPa though in the 411 composites a slightly higher average of 1075 MPa was recorded. This is equivalent to the lower end of the strength range in tension. In the CFRP specimens the vinyl ester 411 and 470 composites exhibited very poor results. An average strength of 835 MPa in these composites indicated that they were considerably weaker than the epoxy prepregs which averaged 1400 MPa. Only the 914 CFRP specimens exhibited better compressive strength than tensile.

The dotted line in Figures 51-54 labelled $\hat{\sigma}_H$, is the expected strength of the material if it were to fail at the compressive failure strain of CFRP. It is defined by equation 5.3.

4.4 ELASTIC MODULUS

4.4.1 Methods of Elastic Modulus Measurement

The analysis of the tensile and compressive elastic moduli of the composites under consideration was covered in two ways:

a) The secant modulus was considered. This is defined as the gradient of the line on the stress/strain curve which passes through the two points A and B, where:

A is a point on the curve, above zero load, just beyond the initial irregularity, and

B is a point on the curve at 75% of the maximum load.

(In the case of any discontinuity or obviously non-elastic variation in the stress/strain curve below 75% of the peak load, then point B immediately precedes this).

This secant modulus represents an approximation to the stress/strain relationship which for most comparison purposes is quite valid. Each specimen is said to have a characteristic tensile or compressive modulus which is representative of a 60% V_{ft} lay-up of the unidirectional fibre configuration in question. The adjustment for volume fraction is carried out by means of equation 4.1. The secant modulus is used for assessing differences in uniaxial stiffness between composites of different matrix resins or different fibre lay-ups.

b) The results have shown that in practice the elastic modulus of a composite does not remain constant throughout a displacement controlled test in either tension or compression. A determination of the material stiffness which was more accurate than secant modulus was therefore required. The tangent modulus of these materials has been studied. This is defined as the local gradient of the stress vs strain curve at any point on that curve. Because the stress/strain relationship is not a straight line, the tangent modulus varies through the test, and can therefore be described as a function of the applied strain. It is calculated from just beyond the initial irregularity in the curve and up to a point where the first obvious deviation

from elastic behaviour occurs (signs of failure). As with secant modulus, the results are normalised to reflect the value in a 60% V_{ft} lay-up of the composite in question by means of equation 4.1.

4.4.2 Secant Modulus Results

The tensile secant modulus results of the specimens analysed are given in Tables 25-28 and shown graphically in Figures 55-58. The compressive results are presented in Tables 29-32 and Figures 59-62. The GRP specimens had a tensile modulus of 45 GPa and a compressive value just a little higher. In the CFRP however, the difference between tensile and compressive values was much greater, the average results being 140 and 120 GPa respectively. There was very little variation between results for composites of the different matrix resins. Hybrid laminates all obeyed the rule of mixtures in both tension and compression, and no dependence on lay-up sequence or number of layers was observed.

4.4.3 Tangent Modulus Results

Certain composite lay-ups from the series of tests carried out in this work were selected for a more detailed analysis of modulus variation. For these specimens tangent modulus was measured and is expressed as a function of tensile or compressive strain. Figures 74-77 show the results of tangent modulus vs strain for each of the composite systems analysed. For these graphs, the best straight line fits through each set of points were calculated and these are detailed in Appendix 3. The results of a G_4C_4/C_4G_4 hybrid are compared with those of a C_4G_4/G_4C_4 hybrid in Figure 78.

From the results, the following observations were made:

- Tangent modulus is a function of tensile or compressive strain.
- This function is continuous through zero to include both tensile and compressive results, but the gradient is not necessarily the same in tension and compression.
- The tensile modulus at zero strain approximates to the compressive modulus at zero strain.
- The CFRP specimens' moduli exhibited greater strain dependence than did the GRP specimens.
- Because of the degree of this modulus variation, when the CFRP experiences high compressive strains ($\sim$ 1%), the modulus is considerably reduced ($\sim$ 30%).
- The tangent modulus in CFRP specimens increased with tensile strain and decreased with compressive strain, while in the GRP specimens there was a slight decrease with tensile strain and no significant variation in compression.
- In hybrid specimens containing equal volumes of glass fibre and carbon fibre the tangent modulus in both tension and compression was always half way between that for GRP and CFRP at the same strain. This could be described as a rule of mixtures effect.
- The modulus relationship in hybrids was independent of whether glass fibres or carbon fibres were in the outer layers.

4.5 OTHER PROPERTIES

4.5.1 Inter-Laminar Shear Strength

The inter-laminar shear strength results were calculated using the following equation (from ref. 79):

$$S = \frac{0.75F}{bd}$$

where S = apparent inter-laminar shear strength (MPa)

F = force of fracture (N)

b = width of test piece (mm)

d = thickness of test piece (mm)

Tests were carried out on GRP and CFRP lay-ups of each of the four composite systems under analysis and the results are presented in Tables 33 and 34. For each result, six specimens were tested and the inter-laminar shear strength was taken as the mean.

The epoxy composites had much better inter-laminar shear strengths than did the vinyl esters. This was true of both the GRP and CFRP laminates.

The results of these tests were used to aid in the interpretation of tensile failure mechanisms.

4.5.2 Transverse Tensile Strength

Transverse tensile strengths were measured for the GRP and CFRP lay-ups of the 913 and 914 composite systems. The results are presented in Tables 35 and 36. Five specimens were tested for each result, and the transverse strength was taken as the mean.

The GRP specimens had better transverse strengths than the CFRP. The poorest result was obtained from the 914 CFRP specimens.

These results were used in the consideration of uniaxial compressive failure mechanisms.

4.5.3 Poisson's Ratio

The Poisson's Ratio results measured for GRP and CFRP composites are given in Table 37. Two specimens were tested to obtain each result. These results were used, together with transverse tensile strength, in the consideration of uniaxial compressive failure mechanisms.

5. DISCUSSION

5.1 THE RULE OF MIXTURES AND HYBRID EFFECTS

5.2 THE VARIABLE ELASTIC MODULUS

5.2.1 Modulus Variation and the Rule of Mixtures

5.2.2 The Effect of a Composite Modulus which Varies with Strain

5.2.3 The Causes of the Variation in Modulus

5.3 TENSILE FAILURE

5.3.1 Tensile Failure and Bond Strength

5.3.2 Analysis of the UTS Results

5.3.3 A Model for Tensile Failure

5.3.4 Tensile Fracture of Hybrid Laminates

5.4 COMPRESSIVE FAILURE

5.4.1 Introduction to Compressive Failure Modes

5.4.2 Compressive Failure of Monofibre Composites

5.4.3 Compressive Failure of Hybrid Composites

5.4.4 An Assessment of the Celanese Compression Test Fixture and Specimen Geometry

5.5 RESIN EFFECTS

5.5.1 Introduction

5.5.2 Bond Strength

5.5.3 914 CFRP

5.5.4 Tensile Strength

5.5.5 Compressive Strength

5.5.6 Elastic Modulus

5.5.7 The Hybrid Effect

5.6 CHARACTERISATION OF THE HYBRID EFFECT

5.1 THE RULE OF MIXTURES AND HYBRID EFFECTS

The rule-of-mixtures (ROM) defines a variable property of the composite as being in proportion to the relative volumes of the constituents. Therefore if one of these mechanical properties is plotted on a graph vs the fibre volume ratio (V_{fc}/V_{ft}) the relationship described by the rule of mixtures would be a straight line passing through the value for GRP at one extreme and the value for CFRP at the other. It is a simple matter, therefore, to determine this relationship once the results from the monofibre composites have been obtained, and to compare with it the experimental data obtained from hybrids.

For the elastic modulus of hybrid composites it is easily shown that a ROM relationship is a reasonable expectation. Considering a undirectional composite containing glass and carbon fibres, if P is the axial load in the material:

$$P_c = P_{fg} + P_{fc} + P_m$$

or

$$\frac{P_c}{A_c} = \frac{P_{fg}}{A_{fg}}\frac{A_{fg}}{A_c} + \frac{P_{fc}}{A_{fc}}\frac{A_{fc}}{A_c} + \frac{P_m}{A_m}\frac{A_m}{A_c}$$

Therefore

$$\sigma_c = \sigma_{fg}V_{fg} + \sigma_{fc}V_{fc} + \sigma_m V_m$$

and assuming $\varepsilon_c = \varepsilon_{fg} = \varepsilon_{fc} = \varepsilon_m$

$$E_c = E_{fg}V_{fg} + E_{fc}V_{fc} + E_m V_m \qquad (5.1)$$

Equation 5.1 shows that each constituent of the composite contributes to the modulus in proportion to its own individual modulus and volume fraction. If we consider, as in Figures 39-62, only total fibre volume fractions of 60% (V_{ft} = 0.6) then equation 5.1 can be represented as shown in Figure 79.

The results of both tensile and compressive tests confirm that the elastic moduli of all the composites tested obey this simple mixtures rule. This means that the modulus of any hybrid specimen can be predicted from the moduli of the individual components (GRP and CFRP in this case), if the volume fractions of the individual components are known. Referring back to the results of previous authors it is now generally accepted that the tensile moduli of hybrids obey the ROM[35], although some have reported non-linear modulus behaviour with respect to volume fraction[61]. A considerably smaller amount of work has been done on the compressive properties of hybrids, but in general, non-ROM moduli have been reported[57,61,62]. This is clearly in contrast with the results of this work.

Up to this point, no distinction has been made in the ROM between tensile and compressive behaviour. The results imply that a ROM can be used to predict the moduli of hybrids in both modes of loading, but it is important that tensile and compressive moduli are treated separately This means that the tensile moduli of monofibre composites cannot be used to predict the compressive moduli of hybrids, and of course the converse is also true. For the sake of comparison purposes, the modulus results of the four resin systems are combined and presented in Table 38 as average GRP and CFRP tensile and compressive values. Expressing the results in this way shows that in GRP specimens, the stiffness in compression is 3%

higher than in tension while for the CFRP, it is 15% lower. There is some indication that complex processes are involved in the origin of the elastic modulus of the composite. In order to investigate this significant difference in modulus in tension and compression, and in an attempt to resolve the problem of the discrepancy between the results of some previous authors and the current work, the tangent modulus, and its variability must be examined. A discussion of this is given in Section 5.2.

It has been shown that the elastic modulus of a unidirectional hybrid composite can be determined from the moduli of the constituent monofibre composites and the hybrid fibre volume ratio (V_{fc}/V_{ft}). This principle can be applied to the characteristic stress/strain curve of a hybrid laminate. The discussion of the rule of mixtures with application to hybrid parameters has so far been confined to the elastic modulus, or the relationship between the stress and strain in the composite. In moving on to consider failure in the composite, a fixed point on the stress/stain curve is defined rather than a function or relationship between stress and strain. It is therefore important at this stage to reassess whether or not rule of mixtures behaviour can realistically be expected to occur in the strength or failure strain results.

Considering a theoretical stress-strain curve for a hybrid laminate containing equal volumes of glass and carbon fibres, as shown in Figure 80, the initial modulus is the average of that for CFRP and GRP. If a simple average ROM approach is applied to the failure strains, the hybrid laminate would be expected to fail at a strain half way between $\hat{\varepsilon}_G$ and $\hat{\varepsilon}_C$. This strain can be denoted $\hat{\varepsilon}_{ROM}$. If the material were to reach this strain before initial failure occurred, the average stress in the laminate would have reached a theoretical

value $\sigma_{\hat{\varepsilon}ROM}$ which is clearly greater than can be expected since it is higher than the strength of either the GRP or the CFRP. A direct rule of mixtures relationship for initial failure strain is therefore unlikely to occur in practice.

Similarly, if the strengths of GRP and CFRP are averaged a direct ROM strength prediction $\hat{\sigma}_{ROM}$ is obtained. The corresponding strain would be $\varepsilon_{\hat{\sigma}ROM}$ as shown in Figure 81. This is a totally arbitrary point on the stress/strain curve of the specimen. There is no good reason why failure should be expected at this point. However it is a possible solution. Ultimate strength and strain lie between those of the parent composites.

A more useful parameter for predicting the strength of hybrid laminates is the value $\hat{\sigma}_H$, the stress in the laminate when the strain reaches the failure strain of the LE monofibre composite, which in this case is CFRP. Using this as a failure criterion, the carbon fibre layers in the hybrid laminate are considered to fail at their characteristic failure strain, as if they are simply part of a monofibre composite. The value $\hat{\sigma}_H$ is therefore dependent upon the modulus of the composite (E_c) and upon the failure strain of the CFRP ($\hat{\varepsilon}_C$). Since E_c is a linear function of the hybrid fibre volume ratio (V_{fc}/V_{ft}) and $\hat{\varepsilon}_C$ is a constant, $\hat{\sigma}_H$ is also a linear function of the hybrid fibre volume ratio. It is shown in Figures 43-46 and 51-54 as a dotted line.

There are therefore two different basic failure criteria for the strength of hybrid laminates. The former $\hat{\sigma}_{ROM}$, is a true rule of mixtures average and is defined by the general equation:

$$\hat{\sigma}_{ROM} = \hat{\sigma}_A V_A + \hat{\sigma}_B V_B \qquad (5.2)$$

for a system consisting of two components A and B, with volume fractions V_A and V_B, and strengths $\hat{\sigma}_A$ and $\hat{\sigma}_B$ of the two materials. The latter strength criterion $\hat{\sigma}_H$, is defined by the equation:

$$\hat{\sigma}_H = \hat{\sigma}_A V_A + \sigma_{B1} V_B \tag{5.3}$$

where σ_{B1} is the stress in the B component of the material when the LE component A, fails.

Due to the format of equation 5.3, $\hat{\sigma}_H$ can also be described as a rule of mixtures strength.

In much of the tensile strength research on hybrid composites, rule of mixtures strength was defined as $\hat{\sigma}_H$ from which synergistic deviations were measured, and defined as hybrid effects. Many authors reported positive hybrid effects on this basis. Marom, Fischer, Tuler and Wagner[2], and in a follow-up paper, Fischer, Marom and Tuler[37] used $\hat{\sigma}_{ROM}$ as their rule of mixtures. They justified doing this[37] by reasoning that load sharing takes place. Negative hybrid effects on strength were reported for their glass-carbon hybrid materials. However even in more recent papers, such as that of Fukuda[39] in 1983, the definition of hybrid effect generally adopted is the increase in failure strain over that of the LE component. In contrast to this, examination of previous work on the compressive properties of hybrids indicates that the definition of hybrid effect in general use is the deviation in the strength from $\hat{\sigma}_{ROM}$. (In this case $\hat{\sigma}_{ROM}$ is based on the compressive strengths of the parent materials). Piggott[56] for example, reports negative hybrid effects on this basis.

In this work, the term hybrid effect is defined as a change in stress or strain from the value it would take if the LE component failed at its own characteristic failure strain. That is, a deviation from $\hat{\varepsilon}_C$ or from $\hat{\sigma}_H$.

The failure strains of the tensile specimens are presented in Figures 39-42. In all cases a positive hybrid effect has occurred since the results for hybrids lie above the horizontal line representing $\hat{\varepsilon}_C$. Appendix 2 details the mathematical approach used to statistically determine the significance of the difference in strain between the hybrids and the parent CFRP. The corresponding compressive failure strains are presented in Figures 47-50. Again a positive hybrid effect has occurred in all cases. In the tensile results, the occurrence of the hybrid effect is significant at the 90% confidence level, and in the compressive results, it is significant at the 95% level.

Due to the fact that carbon fibres have a coefficient of thermal expansion lower than that of glass fibre or the resin, after cooling from the cure temperature the carbon fibre is put into compression. This could result in an apparent hybrid effect occurring in a tensile test on a hybrid composite. In order to demonstrate the extent of the thermal effects, the expected increase in primary failure strains of hybrid 913 laminates are shown in Figure 82 in comparison with the real, observed failure strains. The thermal effects were calculated using equations 5.6 and 5.7 and are based on a temperature change of 115°C. It is clear from Figure 82 that the increase in primary failure strain due to thermal effects is very small in comparison with the observed hybrid effects. In compressive tests, thermal contraction would have the effect of reducing the primary failure strain. In agreement with Zweben[34]

therefore, thermal effects alone cannot account for the observed hybrid effects.

5.2 THE VARIABLE ELASTIC MODULUS

5.2.1 Modulus Variation and the Rule of Mixtures

In the majority of work published on the properties of composite materials, the elastic modulus is considered to be simply the gradient of the stress vs strain relationship of the material before any failure has occurred. Composites are usually said to have a characteristic elastic modulus, and very little attention has been paid to the fact that this property may not be a constant or fixed value throughout a test. Because the results of this work show that a considerable variation in modulus can occur, attention has been given to defining this variation in terms of its dependent variable, strain, and to considering its effect in the interpretation of the results.

The results have shown that the modulus of hybrid specimens obey the rule of mixtures in both tension and compression. The actual values however in the two modes of loading were not the same (as shown in Table 38). The term "modulus" which has been used to describe the elastic stiffness of the material in the tests has really been referring to a secant modulus of the material, calculated by taking a secant of the stress/strain curve, as described in Section 4.4.1. The tangent modulus is now considered.

The tangent modulus of CFRP varied considerably with strain as shown in Figures 74-77. Unloading and reloading of a CFRP specimen before failure occurred resulted in an identical stress/strain curve being traced out by the chart recorder, indicating that these materials

are elastic but non-linear up to a point where failure begins. Since the secant modulus is essentially an average value of the tangent modulus, it is clear that the differences in secant modulus results for tension and compression are a result of the continuous variation of tangent modulus from negative to positive strains. The GRP results showed only a small increase in the secant modulus in compression. Within the bounds of experimental scatter this was not very significant (<1 SD). However an explanation is put forward for this effect in Section 5.3.3. The CFRP, on average for the four resin systems tested, had a 15% lower secant modulus in compression compared with that in tension. This was a result of the steeply falling value of tangent modulus with increasing compressive strain. From a knowledge of the tangent modulus variation as shown in Figures 74-77, the observed differences in secant modulus should be naturally expected. These results are comparable with those of Kalnin[61] who observed an increase of approximately 9% in the compressive modulus of GRP over that in tension and a decrease of approximately 17% in that of CFRP.

In Figures 74 and 75, the best straight line fits through the hybrid tensile and compressive results are shown, together with the ROM lines based on the GRP and CRFP results. The two lines are very close and as a result it can be concluded that the tangent moduli of hybrid specimens obey the rule of mixtures. Because the tangent modulus of a hybrid specimen is a variable quantity with respect to strain, and is always an average value of the tangent moduli of the parent materials at the same strain, this can be described as ROM behaviour occurring throughout the strain range. The rule of mixtures does not take into consideration the order of the layers in the laminate, and as shown in Figure 78 the modulus results are independent of whether glass or carbon fibre layers are outermost.

This observation supports the conclusion that the ROM alone defines the elastic modulus of hybrids. When describing moduli of hybrid specimens and the occurrence of the rule of mixtures behaviour with respect to this property, it is usual to consider only a fixed value of modulus for each hybrid composition. These results show that not only is the rule of mixtures obeyed at a particular value of strain, but that it is obeyed throughout the strain range. Clearly, laminated hybrid composites are made up of alternating layers of the monofibre parent materials. There is therefore no immediately apparent reason why the modulus or stress per unit of applied strain of the hybrid composite should not be in direct proportion to the relative volumes of the constituents. However as described in the review of previous work, non ROM behaviour is reported in hybrids[61,62]. In view of the apparent contradiction between some of these authors' results and the aforementioned conclusion, consideration is now given to some of the factors which may cause this discrepancy.

5.2.2 The Effect of a Composite Modulus which Varies with Strain

If the tangent moduli of a series of fibre composite hybrid materials are reported without maintaining a constant reference strain for each test, a ROM relationship cannot be expected to result. It is necessary to define and maintain a specific strain at which modulus measurements are made. Initial modulus or tangent modulus at zero strain would given an unrealistic measure of the stiffness of the material, being an extreme value on the stress/strain curve. It is also the most inaccurate point from which to measure stiffness due to the initial irregularities in specimen behaviour for practical reasons. A value of strain other

than zero is therefore invariably used. Reporting modulus in GRP and CFRP at a fixed proportion of the maximum strain achieved in each particular specimen, or at a fixed load or stress may result in non ROM behaviour. Similarly if secant modulus is reported, a ROM cannot be expected unless a fixed value of strain is used as a reference on the stress/strain diagram to which the secant is drawn. As already stated, some previous workers have observed modulus results in their hybrid specimens which do not obey the rule of mixtures. In some cases the authors do not report how they measured modulus, and the above suggestion may be a possible explanation for their materials' apparent behaviour.

The method of compression modulus measurement employed by Piggott and Harris[62] was to repeatedly reduce the length of the test specimen rod and to re-load it again, each time measuring the apparent stiffness by means of load applied and machine displacement. The modulus of the specimen was then obtained from the slope of the graph in which the reciprocal of the apparent stiffness was plotted vs the specimen length, as shown in Figure 83. In their previous paper[53], Piggott and Harris indicated that the stiffnesses were obtained by measuring the force required to produce a constant displacement of the test machine. For the shorter lengths of specimen, a much higher load would have been required to produce the same amount of deflection. It is apparent therefore that the specimen strain for each of Piggott and Harris' stiffness readings was not constant. If the modulus of the composite were constant with strain, this would not matter. However in the case of CFRP which has a signifantly decreasing modulus with compressive strain, a high value of modulus would be obtained by this method. Inaccuracies such as this in the modulus measurement could result in an apparent hybrid effect being reported when it did not really

occur. Piggott and Harris[62] reported negative hybrid effects in their hybrid composites.

Examination of Figures 74-77 reveals that the gradients of the tangent modulus vs strain curves of CFRP are greater in compression than in tension for all four composite systems. It is perhaps relevant to note in relation to this fact, that it is generally compressive moduli which are reported as non-ROM.

5.2.3 The Causes of the Variation in Modulus

It has been established that the rule of mixtures accurately predicts the modulus of a hybrid composite but that this modulus may vary as a function of the applied strain. The causes of this variation are now considered.

The elastic modulus of a composite is dependent upon:

i) the volume fractions of the constituents
ii) the elastic modulus of the resin matrix
iii) the elastic modulus of the fibre reinforcement
iv) the internal geometry of the composite e.g. fibre alignment, buckling etc.

a) <u>The Volume Fraction of the Laminate</u>

The volume fractions of the constituents are clearly fixed parameters in each particular laminate. They cannot vary with applied strain unless some of the fibres become ineffective as contributors to the overall modulus, changing the effective volume fraction. This could be the situation if either debonding or fibre failure had occurred which would result in an irreversible change in

modulus. Since only elastic changes are being considered at this stage, the discussion is restricted to the other parameters. There is some evidence that debonding during the tensile testing of GRP laminates may be causing an effectively reduced volume fraction. This is discussed in Section 5.3.3.

b) The Non-Linear Stress vs Strain Response of the Resin

Because the elastic modulus of the composite is the sum of the moduli of individual components, a proportion of the composite modulus is contributed by the resin. Thermosetting resins do not have perfectly linear stress vs strain curves and this could be considered as a factor which may contribute to the variation in the modulus of the composite. In the case of CFRP, the contribution of the resin modulus is such a small proportion ($\approx$ 1%) of the composite modulus that any direct influence of resin modulus variation on composite modulus would be insignificant. In the GRP, the resin modulus accounts for approximately 3% of the modulus of the composite in a 60% V_f laminate. A 50% fall in resin modulus would directly affect the composite modulus by less than 1 GPa. It is clear then, that the magnitude of any change in composite modulus due solely to a change in resin modulus would be very small. The effect of resin modulus contribution is therefore ruled out as being of no significance.

c) The Non-Linear Stress vs Strain Response of the Fibres

It is very often convenient to consider the stress vs strain response of a brittle material to be a linear relationship. Modulus variation of reinforcing fibres is usually overlooked but is considered here in terms of the contribution to the variation in modulus of the composite. The work of previous authors in this area has been considered.

The variation in dynamic modulus of carbon fibres reported by Curtis, Milne and Reynolds[64] was the result of an analysis on individual fibres. The amount of variation Curtis et al reported (approximately 30% increase in modulus for an increase in load from 0.2 to 7.0 g/fibre) would cause significant modulus variation in the CFRP laminate. In fact, neglecting misalignment effects, the composite modulus would almost be in direct proportion to the fibre modulus at any particular load, because the resin, having a very much lower modulus, supports only a very small proportion of the load.

The modulus results of Curtis et al[64] would, at the higher stresses, give a relationship of approximately 16 GPa increase in modulus for a 1 GPa increase in tensile stress in a CFRP laminate of 60% V_f. The observed increase in modulus in 913 CFRP laminates was approximately 14 GPa/GPa. The observed trend is therefore very similar to that predicted by Curtis et al's results. The gradient of the curve representing the 913 data would correspond to the straight line portion of their data, but the non-linear region described by Curtis et al at low stresses where modulus rises rapidly with respect to stress was not observed in the 913 composite. At such low stresses, there is a high probability that experimental error could shroud the relationship. However, if the extra compressive stress in the carbon fibres due to thermal contraction effects is taken into consideration, the real stress in the carbon fibres can be shown to be less than the apparent tensile stress of the specimen (see Section 5.2.3(d)). This rapid change of modulus would therefore occur at an apparently greater specimen tensile stress than that reported by Curtis et al for a single fibre. The thermal effects would therefore make this "non-linear" region of modulus behaviour easier to identify, but even so it is

not evident in the results. Even at negative stress values (by consideration of the compressive tangent modulus results) there is no sudden decrease in the modulus. This leads to the conclusion that it does not occur in the composites tested. The linear modulus relationship which Curtis et al observed at the higher stresses can therefore be considered to be continuous down to zero strain in the composites tested in this work. It is even continuous into the region of compressive stress. The very low modulus values which Curtis et al measured at low fibre stresses were probably a result of the dynamic method of modulus measurement which they employed.

Johnson's results[67] confirm the observed trend by showing that an increase in the Young's modulus of carbon fibres occurs with increasing tensile strain. He considered the modulus results of type III carbon fibres to fall into two distinct regions. At lower loads a lower modulus was recorded than that at higher tensile loads. Johnson's figures for the tensile modulus of single type II carbon fibres have been translated into those representing the expected modulus in a 60% V_f laminate. This has enabled a comparison to be made with the modulus results obtained from the CFRP composite tensile tests. Table 39 presents this comparison giving (a) Johnson's results for individual fibres, (b) Johnson's results applied to a 60% V_f composite, (c) 913 data for a 60% V_f CFRP composite.

Johnson's increase in modulus at higher stress levels is reflected in the results for 913 CFRP composite specimens. Since the increase in the 913 modulus is of a similar magnitude (4% average but 12% over the whole range) to that observed by Johnson (8%) over the stress range considered, this indicates that the major cause of the variation in modulus of the CFRP is the non-linear stress vs strain

response of the fibres. Other factors which may make some contribution must therefore be of lesser significance at the range of stresses considered.

Both Johnson[67] and Curtis et al[64] observed an initially much steeper modulus vs stress relationship at low loads, which Johnson suggested may be partially due to the straightening of fibres. This explanation goes some way to accounting for the fact that it does not appear to happen in composites. As the resin cures, it forms a bond around the fibres in their initial non-straight form, and then resists their straightening out as the tensile load is applied.

Comparing the results of either Johnson or Curtis et al with those from CFRP composites is effectively a comparison of fibre modulus with composite modulus. Matching data would indicate that no "laminating effect" occurs in the modulus results i.e any effect which alters the modulus of a composite due to the fibre reinforcement having been made up into a composite laminate (with the obvious exception of volume fraction difference which is accounted for by normalising all results to $V_f = 0.6$). In the case of Curtis et al, a dynamic rather than static modulus was measured and direct comparison may not be valid. However, consideration of the results of Johnson leads to the conclusion that the only significant laminating effect on modulus is that the initial, steep portion of the modulus vs stress curve of the fibre does not occur in the composite. This observation adds weight to Johnson's suggestion that it may be related to a fibre straightening mechanism.

d) Buckling of Fibre Reinforcement Under Thermally Induced Strain

Thermal stresses exist in these materials as a result of shrinkage from the cure temperature. If the constituents with higher and lower coefficients of thermal expansion (α) are referred to by subscripts 1 and 2 respectively; then for an equilibrium of forces

$$\sigma_1 A_1 = -\sigma_2 A_2 \tag{5.4}$$

and since $\varepsilon = \alpha \Delta T$:

$$\frac{\sigma_1}{E_1} - \frac{\sigma_2}{E_2} = (\alpha_1 - \alpha_2)\Delta T$$

substituting equation (5.4)

$$-\frac{\sigma_2 A_2}{A_1 E_1} - \frac{\sigma_2}{E_2} = (\alpha_1 - \alpha_2)\,\Delta T$$

and since

$$\frac{A_2}{A_1} = \frac{A_2}{V_1}: \quad \sigma_2 \left(\frac{V_2}{V_1 E_1} + \frac{1}{E_2}\right) = (\alpha_2 - \alpha_1)\Delta T$$

$$\sigma_2 = \frac{(\alpha_2 - \alpha_1)\ \Delta T\ V_1 E_2}{\left(\frac{V_2 E_2}{E_1} + V_1\right)} \tag{5.5}$$

σ_1 can then be found from equation (5.4).

The strain in the (2) component is: $\varepsilon_2 = \frac{\sigma_2}{E_2}$

$$\varepsilon_2 = \frac{(\alpha_2 - \alpha_1)\ \Delta T\ V_1}{\left(\frac{V_2 E_2}{E_1} + V_1\right)} \tag{5.6}$$

The coefficient of thermal expansion of the composite can be calculated from:

$$\alpha_c = \frac{\alpha_1 E_1 V_1 + \alpha_2 E_2 V_2}{E_1 V_1 + E_2 V_2} \tag{5.7}$$

The thermal stresses and strains which result from cooling from the cure temperature are presented in Figure 84 for 913 composites as a function of V_{fc}/V_{ft}. The fibres in both the glass and carbon fibre parent composites experience compressive stresses due to thermal contraction because in each case the coefficient of thermal expansion is lower than that of the resin. However it is clear from Figure 84 that these initial stress levels are very low. The greatest stresses due to thermal contraction are those in the carbon fibres of laminates with very low carbon fibre content. Even in this extreme case, the stresses are less than 200 MPa and are still very small compared with the applied stress during the test. Thermal contraction alone is not significant in causing buckling which may reduce the modulus. These thermal contraction effects can be considered as a displacement of the stress or strain scale and added to the applied strain.

e) Buckling of the Fibre Reinforcement Under Applied Compressive Strain

The basis of Rosen's compressive strength model[44] for unidirectional fibre composite materials was that microbuckling of fibres occurs throughout the composite. If this could begin to occur before failure, then the modulus of the composite would certainly be affected. Buckled fibres would result in a lower composite modulus than straight fibres. It could be possible to interpret the non-linear elastic behaviour of the CFRP composites as due to the effect

of microbuckling. However it appears that this is not so for the following reasons:

i) While microbuckling would cause a significant decrease of modulus with compressive strain, the rising modulus with tensile strain would be difficult to account for by the same mechanism. A totally different mechanism is unlikely when the modulus vs strain relationship is a continuous curve through zero strain (see Figures 74-77).

ii) If microbuckling was the only cause of the change in modulus of CFRP there would be some evidence of a similar effect occuring in the GRP. This is not the case.

iii) It has already been shown that a major proportion of the variation in elastic modulus of the composite is due to the non-linear stress/strain response of the carbon fibres. If this is the case the effect of microbuckling on the composite's stiffness can only be small.

iv) While the above suggestions reason that microbuckling is not the sole cause of the reduction in modulus of the CFRP under compressive strain, SEM micrographs of the CFRP compressive failure surfaces show evidence that internal microbuckling of fibres can occur at some stage during the test. As discussed in Sections 5.4.2 (c and d), when failure occurs in the vinyl ester CFRP specimens it is due to a fibre microbuckling mechanism. However in the epoxy laminates the failure is one of shear, and microbuckling does not appear to be involved. There is no clear distinction between the compressive modulus variation in the vinyl esters with that in the epoxies even though it is only in the vinyl ester composites that evidence of buckling is seen.

v) The maximum amount of buckling which occurs in the vinyl ester CFRP composites is at the point of failure. Assuming that the fibre geometry can then be described by the sine wave of equation 2.38

$$y = a \sin \left(\frac{2\pi x}{\lambda}\right)$$

where ad = wave amplitude

λd = wavelength

the dimensionless parameters a and λ have been calculated for the point of failure of an individual carbon fibre (see Section 5.4.2(d)).

Thus at failure of the carbon fibre $\lambda = 11.5$

$a = 0.069$

Using these parameters the reduction in effective fibre modulus at the point of failure is now considered:

From Piggott[56]

The effective fibre modulus is $\dfrac{1}{\left(\frac{1}{E_f} + \frac{1}{E_{f1}}\right)}$ (5.8)

where $$E_{f1} = \frac{\lambda^4 E_m}{\pi^5 a^3} \quad (5.9)$$

so that for 411-45 CFRP: $E_{f1} = 598{,}000$.

This has the effect of changing the effective fibre modulus from 170 MPa to 169.95 MPa, a difference of less than 0.03%.

It is therefore concluded that the reduction in the elastic modulus of CFRP with compressive strain is not caused by the buckling of the fibre reinforcement. It is due solely to the non linear stress vs strain response of the carbon fibres themselves.

5.3 TENSILE FAILURE

5.3.1 Tensile Failure and Bond Strength

Unlike compressive failure, tensile failure does not have the complication of many totally different competing mechanisms. Though fibre failure plays a key role in the tensile failure of unidirectional composites, the main parameters which have an influencing effect are:

i) fibre tensile strength
ii) resin tensile strength
iii) fibre-resin bond strength.

Therefore even though there may only be one main mechanism involved in tensile failure, depending upon the above variables, the characteristics of failure can be totally different.

In all the GRP specimens tested the considerable amount of debonding which occurred throughout the gauge length was evidence of a weak interface bond. This brush-like failure is typical of unidirectional GRP tensile failure and has been observed by many other workers[9,82,85]. There was no significant difference between any of the specimen failures with the exception that the resulting "bristles" were slightly coarser in the 913 and 914 epoxy GRP materials than in the 411 and 470 vinyl ester laminates. This indicated that the extent of the debonding in the vinyl esters was greater than in the epoxies because the bond they formed with the fibres was not as good as that formed by the epoxies. It is generally known that vinyl esters form poorer bonds with glass fibres than do epoxy resins[14]. The GRP fibres from the two types of vinyl esters showed some evidence that the 470 forms slightly poorer

bonds with the fibre than does the 411. This is evident from the finer fibre separation which occurs in the 470 failures, as shown in Plates 4 and 5.

Analysis of the ultimate tensile strength results shown in Tables 13-16 shows that this reduction in bond strength in the vinyl esters does not result in poorer ultimate strengths being recorded. There was no significant difference between the UTS results of the epoxy GRP specimens and those of the vinyl ester GRP specimens, even though the former group showed a distinctly more "clumped" failure.

The appearance of the failures of the epoxy CFRP specimens was indicative of the better bond which carbon fibres form with the matrix compared with glass fibres. It was clear from the (roughly) straight fracture surfaces that failure had propagated transversely across the specimen with very little debonding or fibre pull-out. Again, this is characteristic of other workers' observations[9,85]. The clumpy, brush-like failure appearance of the vinyl ester CFRP specimens however (which much more resembled GRP than that of the epoxy CFRP) was an indication that the bonding of the vinyl esters to carbon fibres was poor. As with GRP, this was not reflected in the UTS results which showed that the 913 is comparable with both of the vinyl ester resin CFRP composite systems. Also as in GRP, the tensile failures indicated that 470 vinyl ester resin forms better bonds with carbon fibres than does the 411 resin. This is apparent in Plates 7 and 8.

The results of the interlaminar shear tests in Tables 33 and 34 confirm these observations. In GRP, the two vinyl esters had interlaminar shear strengths approximately 20% lower than those of the epoxies. This offers some explanation of why the debonding in

the vinyl ester failures was more extensive than that in the epoxies. Similarly, for the case of CFRP, the interlaminar shear strengths of the vinyl ester composites were approximately 35% lower than those of the epoxies. This demonstrates the reason why the debonding in the vinyl ester CFRP specimens was considerably greater than the epoxy CFRP.

SEM micrographs of the fibres from the inter-laminar shear failures also show that bonding in the epoxy resin specimens is stronger than in the vinyl esters. Plates 17 and 18 show 913 GRP and CFRP inter-laminar shear failures at high magnification. In both cases there is evidence of resin remaining adhered to the fibres. While glass fibres form relatively poor bonds, Plate 17 shows that in some regions glass fibres retained a resin coating. This was not evident in any of the vinyl esters. Plates 19 and 20 show 411-45 GRP and CFRP inter-laminar shear failures respectively. The fibres are very much cleaner than those in epoxy inter-laminar shear failures because of the weaker bonds formed.

From an analysis of the tensile failures of the various fibre/resin systems used in this work, together with a comparative consideration of the interlaminar shear strength results, the relative strengths of the fibre-matrix bonding have been ascertained. While glass fibres form weaker bonds than carbon fibres, it is also clear that the vinyl ester resins produce composites with weaker bonds than do the epoxies with respect to the fibre systems used in this work. However the poorer bonding formed by the vinyl ester resins does not result in weaker composites. It can be concluded therefore, that the UTS of the material is not directly or proportionally related to the fibre-resin bond strength. It appears to be true that the UTS remains unaffected even when the mechanism of failure propagation

through the material is considerably altered. This is important when considering practical design criteria. In composites where a debonding mechanism occurs, internal damage is occurring well before the ultimate load is reached. This could be critical in circumstances where the component is part of a chemical plant or pressure vessel. There would be the possibility of leakage occurring, even when the material is mechanically sound.

5.3.2 Analysis of the UTS Results

In Fukuda and Kawata's analysis of tensile properties[29] of undirectional composites, their strength predictions were a little lower than the ROM equation (equation 2.6) would predict. For this reason they suggested that if the ROM is to be used the strength equation should be modified to include some multiplication factor attached to the fibre strength $\hat{\sigma}_f$. Mascia[86] applies a similar multiplication factor to $\hat{\sigma}_f$. He states that the rule of mixtures (equation 2.6) only refers to the case of a perfect bond between the fibres and resin. The case of imperfect interface bonding is therefore accounted for by this modified ROM equation and the strength is defined by:

$$\hat{\sigma}_c = K\,\hat{\sigma}_f V_f + \sigma_{ml}\,(1 - V_f) \qquad (5.10)$$

Mascia describes K as the "adhesion factor, or fibre utilisation efficiency factor". For simplicity, the term "K factor" is used in this work.

It is quite clear that it is not only the interface bond strength which can affect the efficiency of the fibres' load bearing characteristics. Other imperfections in the laminate can have a

serious adverse effect. The K factor is therefore used more generally to account for any imperfections which may cause the maximum fibre stress to be limited. These may include:

i) broken or damaged fibres
ii) debonded fibres
iii) local or general misalignment of fibres
iv) voids
v) poor interface adhesion.

All of these factors will have the effect of reducing the reinforcing fibres' general load bearing capabilities in the composite and could therefore be represented by the value of K being less than unity. Although perhaps not so in the theoretical sense, it is impossible in practice to produce a laminate without any of the above defects. The ROM (equation 2.6) which effectively incorporates a K factor of one is therefore an unreasonably high expectation of any composite's strength performance.

Fibre manufacturers often quote more than one value for $\hat{\sigma}_f$. These may be the virgin filament strength and another, lower figure which is often the result of impregnated tow tests. The latter figure is lower than the virgin filament strength because of the limited adhesion and perhaps the presence of surface defects on the fibre. The difference between these figures is a simple demonstration of how the full potential of the fibres is never used. In the case of laminated composites the strength is lower still, and an effective utilisation of only 60% of the fibres' full load bearing capacity may not be an unrepresentative figure for some composite systems.

In order to assess the load bearing efficiency of the fibres used in this work, K factors were calculated using the following equation:

$$K = \frac{\hat{\sigma}_c}{\hat{\sigma}_f \left[V_f + \frac{E_m}{E_f}(1 - V_f)\right]} \qquad (5.11)$$

where: $\hat{\sigma}_c$ = the composite UTS measured experimentally

$\hat{\sigma}_f$ = the fibre's virgin filament strength (obtained from manufacturers data)

This was done for the GRP and CFRP composites made with each of the four resins, and the results are presented in Table 40. Hybrids are not considered here because the presence of multiple types of fibre over-complicates the analysis and the occurrence of synergistic effects makes the interpretation of the results unclear.

From Table 40 it is clearly seen that the K factors of CFRP composites are much better than those of GRP composites. This might initially be expected as a result of the other evidence for carbon fibres forming a stronger bond with the matrix than glass fibres. With the exception of the 914 laminates, all CFRP composites had K factors of approximately 0.8 while those of GRP were generally less than 0.6 and exhibited greater variation. It is believed that the very low value obtained with 914 CFRP was a result of defective material and is not a true representation of the normal behaviour of 914 CFRP. This problem is discussed further in Section 5.5.3 and in the proceeding discussion 914 is excluded from the consideration of the CFRP K values.

It has already been shown (in Section 5.3.1) that the fibre-resin bond formed by carbon fibres is better than that of glass fibres, but also that in both cases laminates made with vinyl ester resins result in poorer bond strengths than those made with epoxies. This latter effect is clearly not reflected in the K factor in Table 40. As already discussed, the K factor is not only a measure of bond strength but of the fibres' load bearing potential in the composite, which is affected by various defects. The K values were obtained by measurement of the ultimate tensile strengths, yet it has been demonstrated that UTS is not directly affected by bond strength. On that basis therefore, the K factor does not reflect the weakness in bonding of the composite, and by the same reasoning the lower K factors obtained in GRP composites, compared with CFRP, is not a result of poorer bonding, but rather of the reduction in fibre strength due to other defects.

Having determined that the initiation of tensile failure of the material is more directly related to fibre defects than to the fibre-matrix bond, this in turn indicates that the glass fibres appear to be more subject to fibre damage than do the carbon fibres. The K factors show that while the glass fibres have lost about 40% of their load bearing potential, the carbon fibres have lost only 15%. In addition to this, it is also apparent that the method of production of the laminate does not directly affect the result. The figures for the vinyl esters made by the hand lay-up technique were not significantly different from those of the epoxies which were made from prepreg.

In the consideration of compressive failure (see Section 5.4.2(d)) the conclusion is arrived at, that defects such as fibre misalignments which cause stress raising effects in the <u>composite</u>

were greatest in the vinyl-ester CFRP laminates. The weakening of the actual fibres however due to surface defects is apparently greater in glass fibres.

5.3.3 A Model for Tensile Failure

In a recent study by Moghisi[85] of tensile failure using acoustic emission techniques, it was found that during the early stages of GRP failure lower amplitude level acoustic emissions were produced which were associated with debonding. These were followed by higher amplitude level acoustic emissions associated with fibre failure and fibre-matrix splitting. Moghisi concluded that in GRP a general debonding mechanism precedes fibre failure. When results from the vinyl esters were compared with those from the epoxy resin prepregs, it was found that the lower amplitude emissions occurred earlier in the vinyl esters. The debonding was therefore occurring earlier on in specimens which exhibited a weaker bond strength. Similar tests carried out on 913 CFRP specimens revealed no evidence of this debonding mechanism. Because no debonding is seen in the failed 913 CFRP specimens this observation reinforced the interpretation of the results. After consideration of the results of Moghisi, together with the previously described observations, a simple model is proposed which describes the process of tensile failure. The models for GRP and CFRP are shown in Figures 85 and 86 respectively.

It has been shown that the ultimate tensile strength of unidirectional continuous fibre composites does not vary in direct relation to the bond strength formed by the resin and the fibres. This does not in any way imply that debonding does not occur before a significant amount of fibre failure occurs. Indeed as already described, the results of Moghisi indicate that debonding occurs in

tensile GRP specimens very early on in the failure process. Some of his specimens started to give significant amounts of acoustic emission at strains only a little over 50% of the failure strain. This debonding is shown in Figure 85(b). It must be emphasised that this is not composite failure which is occurring. It is not the destructive longitudinal splitting which characterises the tensile failure of GRP. That process begins at higher loads. The debonding described can only be relatively slight, because when the tensile tests are performed the observer is not aware of its occurrence.

In a long, defect free specimen with perfectly straight fibres, there would be no shear stress between the fibres and the resin and therefore no tendency for debonding to occur. However in real composites, defects do exist and it is at these points where the debonding will be initiated. Defects such as voids, fibre breaks, or fibre misalignments cause local three-dimensional stress intensities. Once local debonding has occurred, the absence of the local stress intensity, together with the local ineffectiveness of the fibre, reduces the composite stress to a very small extent. The accumulation of many regions of slight local debonding would then result in a lower composite modulus. Reference to Figures 74-77 indicates that in GRP, the modulus does indeed decrease with tensile strain. In addition to this, the more weakly bonded vinyl ester resin specimens, in which Moghisi recorded the occurrence of debonding at an earlier stage, show a greater reduction in tensile modulus with strain than do the epoxy specimens. The tangent modulus results therefore add a great deal of weight to this debonding model.

As the load in the GRP specimen increases further, fibre failures begin to occur. The amount of debonding will increase more rapidly as a result of fibre failure (Figure 85(c)). The propagation of a tensile fracture will therefore be prevented from running transversely through the composite as it will be halted by the debonded regions. Ultimate failure of the composite involves tensile failure of the fibres and any resin regions left intact, and vast amounts of longitudinal splitting (Figure 85(d)).

The process of failure in the carbon fibre reinforced specimens appears to be simpler. The early process of debonding does not occur (in the epoxy specimens) so that at the onset of fibre failure, very little debonding has occurred (Figure 86(b)). Fibre failure is likely to cause small amounts of debonding, evidenced in the fact that the failure surface is not an absolutely flat plane, but forms a rough edge (Figure 86(c)).

The work of Fuwa, Bunsell and Harris[28] showed that internal crack propagation mechanisms in CFRP can occur by means of related adjacent fibre breakage, but that this is limited to small sub-bundles of fibres within the specimens. The small bundle failures, according to Fuwa et al, are then linked together by shear failure in the fibre direction. The appearance of the tensile fracture surfaces of CFRP specimens confirms this.

It is therefore believed that certain amounts of fibre failure do occur in the CFRP composite before final catastrophic failure, amounting to many small group failures which then link up at the point of catastrophic failure. If all fibre failures were to occur at the point of, and as a result of catastrophic crack propagation through the composite, the failure surface would be a much smoother,

plane surface. This is not the case. Plate 6 shows a typical tensile failure from a 913 epoxy CFRP specimen and Plate 17 shows the type of failure which was typical of the 914 CFRP specimens. Although in the 914 the failure was "cleaner" than in the 913 it is evident that propagation did not occur by a single crack running through fibres and resin.

By the nature of the fractures in the vinyl ester CFRP specimens, it is apparent that they fall into a category somewhere between the two models of failure described. While transverse crack propagation is active there is also a considerable amount of the longitudinal splitting/debonding behaviour associated normally with GRP.

By this model, it is clear how the bond strength between fibre and resin, affects the final fracture of the specimen. The debonding which occurs before final failure influences the way that the failure propagates through the specimen. The greater the amount of debonding, the more individually the fibres will be separated when final failure occurs.

5.3.4 Tensile Fracture of Hybrid Laminates

a) Failure Mechanisms

The characteristic features of the hybrid specimen failures were identical to those observed in the parent materials. This was especially noticeable in the epoxy specimens in which the failure of the CFRP plies consisted of straight, transverse cracks, while the GRP plies exhibited a great deal of debonding with much longitudinal splitting. The small amount of longitudinal cracks in the carbon plies were limited both in quantity and extent. Failures of the carbon plies were very often adjacent indicating that there was some

means of propagation of the failure through the GRP plies. It is likely that this was due to the shock wave passing through the specimen as a carbon ply failed. The great similarity in nature between the failures of the plies in hybrid laminates and the failures of the parent materials indicated that mechanisms of failure in hybrids do not differ from those in single fibre type composites. This appears to be true even though the strain levels at which initial failure occurs are greater than those observed in the CFRP alone.

b) Hybrid Stress vs Strain Curves

In interpreting the stress/strain curves from individual tensile tests, difficulties were occasionally encountered establishing the true strain to first failure. A stress/strain curve of a CFRP specimen is shown in Figure 64. It was apparent from some of these stress/strain curves that sudden small load drops were occurring during the test. These are labelled "A", "B" and "C" in Figure 64. During the tests, it was observed that these "jumps" were associated with a cracking noise and with longitudinal cracks which appeared in the test piece close to the edges. The apparent slight increase in strain at these points was interpreted as a true effect since extensometer slippage had been eliminated by sinking the knife edge jaws into double sided tape. It was apparent from observing the tests, that these small jumps in the initial loading curve represented shear failure along the direction of the fibres. Since matrix shear strength is very much lower than fibre tensile strength, uneven loading from the end tabs could be a cause of the longitudinal split in the matrix between fibres. In addition to this, it is believed that a small fibre misalignment, angle ϕ to the specimen axis may cause a similar effect as a result of fibres coming to an end at the edge of the specimen within the gauge

length. Both of these effects could have caused the shear failures observed, but it was difficult to determine the exact cause due to the close proximity of the splits to the edge of the specimen, and because they often occurred very near to specimen failure.

It is clear that the point on the stress/strain curve at which this occurs cannot be used to represent the strain to first failure since actual tensile failure had not taken place. The problem of interpreting the curves to obtain failure strain values was sometimes made more difficult by the fact that several jumps could occur at the higher strain levels. For all the tests performed, strain to first failure is therefore defined as that strain, during the testing of the material, after which the stress-strain curve no longer shows linearity. In Figure 64, the first of the jumps is labelled point "A". In this particular specimen it occurred at a relatively low strain compared with tensile failure strain. In the curve shown, the failure strain coincides with the UTS. However that was not always the case when hybrids or GRP failures were being analysed.

The series of stress/strain curves for 913 GRP, CFRP, and various hybrid fibre configurations, shown in Figures 63 to 70, have some interesting features which were common to all the series of tensile specimens tested in this work.

The GRP specimens (Figure 63) often showed indications of failure before the ultimate load was reached. The drops in load which often appeared to progressively increase in frequency were the result of fibre failure and longitudinal splitting. The CFRP specimen (Figure 64) in contrast to the GRP does not give any indication of tensile failure before it occurs. The jumps in the curve, labelled "A", "B"

and "C" have already been described as due to shear failure. It is clear from the sharply pointed stress/strain curve that in CFRP, failure is sudden and catastrophic.

The stress/strain curves shown in Figures 65-68 were obtained from a series of 913 hybrids, each with GRP in the outer layers, and of increasing proportion of glass fibres. In the specimen with only a small amount of glass (G_2C_6/C_6G_2 can be described as 25% GRP), once the carbon fails the remaining glass fibres, which are unable to support the load, also fail (Figure 65). In the specimen containing 50% GRP (Figure 66), the glass did not fail immediately after the carbon but carried some load, which often increased as the test proceeded. The load in the specimen is very much lower at this point because its cross sectional area has been reduced by about a half and also because the modulus of GRP is lower than that of the hybrid. In the specimen containing 75% GRP (Figure 67) the secondary modulus was much better defined because the GRP had not been as badly damaged relatively, as the thinner GRP plies in the other specimens. That with the greatest proportion of glass (Figure 68) showed that sometimes the remaining GRP will sustain loads greater than those in the specimen just prior to failure of the CFRP. This is the point at which the ROM equation for very low carbon content defines the material strength:

$$\hat{\sigma}_C = V_G \hat{\sigma}_G \qquad (5.12)$$

where V_G = the volume fraction of GRP in the composite

$\hat{\sigma}_G$ = the ultimate tensile strength of the GRP plies.

Figure 69 shows the stress/strain curve from a hybrid specimen in which the CFRP plies were in the outer layers. It contains the same proportions of constituents as the specimen whose stress/strain curve is shown in Figure 66. The main difference between the two is that no secondary modulus was observed in the specimen with CFRP outer plies. This was true of all the hybrids tested because the extensometer, which measured strain in the test was rendered ineffective after failure of the outer plies onto which it was fixed. In this, and similar specimens, peak load was obtained directly from the digital display on the test machine, rather than from the stress/strain plot obtained.

Stress/strain curves obtained from the 5 ply hybrids (Figure 70) were not significantly different from those of the 3 ply hybrids (Figure 66).

5.4 COMPRESSIVE FAILURE

5.4.1 Introduction to Compressive Failure Modes

One of the most significant developments in the understanding of compressive failure mechanisms has been due to the work done by Piggott[56] in 1981. He discussed how compressive failure is controlled by several different mechanisms. The one which determines the failure of the composite is the one which predicts the lowest stress level at failure. The current work supports the idea that different mechanisms can occur. However Piggott's discussion of six independent failure mechanisms would perhaps be more useful as a guide to composite strength prediction if it were simplified. Some modes of failure which Piggott discussed can be dismissed as inappropriate to the composites under consideration.

For example, the fibre yielding mode of failure is unlikely to occur in glass or carbon fibre composites. Kevlar fibres which have a very low yield strength in compression do give composites with a low compressive strength. In the absence of Kevlar, although this particular mode is not considered, the failure mode of carbon fibre/epoxy composites in shear is very similar, and the same rule of mixtures equation applies which would have been appropriate to the Kevlar composite yield strength. Also, Piggott considered the action of soft matrices by testing composites in various states of cure. The resins used in this work all have yield strains greater than those of the fibres so matrix yielding is not considered to be a failure mode appropriate to the composites in question.

Close examination of the various composite systems used in this work revealed four specific failure mechanisms. These are considered individually as follows:

5.4.2 Compressive Failure of Monofibre Composites

a) <u>The Transverse Tensile Failure Mechanism</u>

Compressive strain in the axial (or y) direction results in the x and z directions experiencing a tensile strain due to Poisson's expansion.

Since the transverse tensile strength of the composite is considerably lower than the axial strength, it is possible for compressive failure to occur by means of transverse splitting. This splitting as a result of Poisson's expansion is now considered as a mechanism of failure initiation:

If ε_1 = axial strain

ε_2 = transverse strain

$$\varepsilon_1 = \frac{\varepsilon_2}{\nu} \quad \text{by definition of Poisson's Ratio}$$

$$\frac{\sigma_1}{E_1} = \frac{\sigma_2}{\nu E_2}$$

$$\sigma_1 = \frac{\sigma_2 E_1}{\nu E_2} \tag{5.13}$$

If axial compressive failure is considered to be defined by the limiting transverse tensile strength of the composite, it occurs when

$$\sigma_2 = \hat{\sigma}_2$$

Therefore

$$\sigma_1^* = \frac{\hat{\sigma}_2 E_1}{\nu E_2} \tag{5.14}$$

where σ_1^* = the expected compressive strength of the composite due to transverse tensile failure.

The two elastic moduli E_1 and E_2 in equation 5.14 can be defined by the two ROM equations[86]:

$$E_1 = E_f V_f + E_m V_m$$

$$E_2 = \frac{1}{V_f/E_f + V_m/E_m} \tag{5.15}$$

Substituting equations 5.15 into 5.14, an expression for σ_1^* is obtained:

$$\sigma_1^* = \frac{\hat{\sigma}_2}{\nu} (E_f V_f + E_m V_m) \left(\frac{V_f}{E_f} + \frac{V_m}{E_m}\right)$$

or

$$\sigma_1^* = \frac{\hat{\sigma}_2}{\nu} \left[V_f^2 + V_m^2 + V_m V_f \left(\frac{E_m}{E_f} + \frac{E_f}{E_m}\right)\right] \qquad (5.16)$$

Transverse tensile strength ($\hat{\sigma}_2$) and Poissons Ratio (ν) have been measured experimentally for both GRP and CFRP materials. From the results (presented in Tables 35-37) and substituting into equation 5.16 a compressive strength prediction (σ_1^*) is obtained. The values of σ_1^* calculated from equation 5.16 are presented in Table 41.

From Table 41, it is apparent that in both the 913 and 914 GRP specimens failure took place at the predicted stress level if this were the controlling failure mechanism. Though in the 914 GRP specimens, σ_1^* is approximately 10% lower than the observed strength, it is within one standard deviation of the mean level.

Observation of the failed GRP specimens confirmed that transverse tensile stress was a cause of failure. Plates 10 and 11 show that longitudinal splitting has occurred in both the epoxy specimens (Plate 10) and in the vinyl ester specimens (Plate 11). A considerable amount of debonding and separation of fibres results within the gauge length of the specimen. Some "splaying out" of the fibres also occurred as the compliance of the test machine caused further displacement of the platens when the specimen no longer supported load. (The test was always stopped immediately after failure, but this extra displacement was instantaneous and

cf Table p. 170

unavoidable). Although in the table, the σ_1^* value for 914 is below its actual compressive strength, this was not the failure mode observed. Since the splitting failures in epoxy and vinyl-ester specimens appeared very similar, and occurred at similar load, it was concluded that the mechanism of failure did not differ between these two types of composite systems.

Piggott[56] recognised that transverse tensile stresses are present in the specimens under compression but he did not consider them to be of great enough magnitude to cause failure directly. He quoted an expression for the fibre-matrix interface stress as:

$$\sigma_r = \sigma_{1m} (\nu_m - \nu_f) (0.48 + 0.52 V_f - 0.12 V_f^2) \qquad (5.17)$$

where σ_r = maximum interface stress

σ_{1m} = applied axial compressive stress

By applying equation 5.17 to a glass-polyester composite with $\hat{\sigma}_f$ = 1.3 GPa, he determined that σ_r would be only 5.2 MPa. Piggott reasoned that fibre curvature was contributing to creating the greater transverse tensile stresses, making it a parameter dependent not only on bond strength, but also on the amount of buckling or fibre misalignments. The vinyl ester-GRP specimens tested in this work, due to the different method of manufacture, contained a greater degree of fibre misalignment defects than the epoxy-GRP specimens (though perhaps the difference was not as great as in the CFRP laminates) but there was no difference in compressive strength. It seems also that, while bond strength must play a very significant role in the transverse tensile strength, the difference between the epoxies and vinyl esters was not significant enough to affect the longitudinal compressive strength.

High magnification SEM micrographs of typical epoxy GRP transverse tensile failures are shown in Plates 22 and 23 for 913 and 914 specimens respectively. The clean fibre surfaces verify that fibre-matrix bond failure occurs in these transverse tensile tests. However no difference in strength between GRP matrix systems was apparent in either transvere tension or longitudinal compression.

b) Kink-Band Mechanism of Compressive Failure

The series of GRP specimen failures revealed two distinct types of fracture pattern. Although the most commonly observed result was the longitudinal splitting, as previously described, a kink-band pattern was also regularly seen in the GRP specimen failures. An example of this kinking pattern of compressive failure is shown in Plate 12 for a vinyl-ester GRP laminate. Kink-bands have been observed and described in some detail by various authors[52,53,59,87]. It was notable that both longitudinal splitting and kink-band types of failure occurred at the high and low ends of the scatter in the strength results. Neither mechanism could be associated with either higher or lower strengths.

The only factor which was observed to be significantly associated with the difference in failure mode was the point of failure initiation. While the longitudinal splitting was simply restricted to within the specimen gauge length, the kink bands always occurred beneath the end tabs and rarely occupied any of the gauge section. From these observations, it can be concluded that the particular type of failure likely to occur will be governed by the location of the point of failure initiation within the specimen.

The end tabs on a specimen serve to transfer the applied load from the grips of the test fixture to the laminate. They do this by applying a shear load through the adhesive along the length of the tab. This results in the compressive load in the laminate building up gradually from zero at the end of the specimen, to its maximum value at the gauge section, as shown in Figure 87. Clearly, the compressive stress in the laminate just underneath the end of the tab is near to its maximum value. There is no reason why an imperfection in this region could not cause a higher stress concentration than that resulting from any imperfections within the gauge length. Failure therefore is easily initiated underneath the end tab. If the critical imperfection is internal there is no reason to assume that it must occur within the gauge section. However it is unlikely for failure to occur near the extreme ends of the specimen since the compressive stress in these regions is very low.

For these reasons, it is believed that the occurrence of two distinct types of failure is simply the result of the fact that the initial failure can originate from within the tabs or in the open gauge section. The restriction imposed by the tabs prevents lateral splaying of the fibres in the z direction and a neat kink band occurs. In the open gauge section however, in the case of splitting type failures, lateral spread occurs once failure has started and the debonded region extends.

The formation of a kink-band is therefore not simultaneous across the width of the specimen. Chaplin[52] demonstrated how these kink-bands occur by means of the debonding propagating laterally across the specimen in a progressive manner. He explained that defects, acting as stress concentrators initiate the start of the kink-band,

and it is of course impossible to manufacture a specimen which is totally free of defects. The problem of determining actual stress levels he put down to the classical fracture mechanics problems of determining the extent to which a defect decreases the material's load bearing capacity.

While it may be true that it is not easy to determine quantitatively the amount by which a defect influences the local strength of a material, because the defects can be considered to be distributed throughout its volume in significant numbers, the overall effect of them can be determined. The strength prediction σ_1^*, was based on determining the transverse tensile strength of the material from experimental tests on samples. The strength value obtained by this means therefore incorporates a "defect factor".

The 70° plane of the kink band fracture appears to be a characteristic of this type of failure. In all specimens, which exhibited kink bands, the angle at which they occurred was the same. This type of kink band failure has been observed in carbon fibre reinforced PEEK materials[88], in which the angle of the kink bands, as with the GRP materials used in this work, was 70°. It is concluded therefore that the 70° direction of kink band propagation is not a function of fibre or matrix parameters, but is a characteristic of this type of failure. In the vinyl ester CFRP materials also, in which compression failure occurred by a fibre microbuckling process (see Section 5.4.2(d)) the angle of the failure surface was 70° to the longitudinal axis. This observation suggests the possibility that the two processes are related but on a very different scale. While the kink bands of GRP contained a considerable amount of debonding, in contrast with the CFRP microbuckling failures this was probably due to the weaker bond

strength formed by the glass fibres, and the excessive amounts of deformation involved.

c) Fibre and Matrix Shear Failure

In the epoxy CFRP compressive specimens tested, the compressive failure surface was fairly well broken up due to the high energy released upon failure. However the intact regions of the failure surface lay at an angle of 45° to the fibre axis, revealing that shear failure had taken place through the fibres and the matrix. This contrasts with the GRP failures in the respect that very little debonding occurred.

Shear is an active mechanism by which compressive failure occurs in many materials. It defines the limiting compressive strength of the fibres and therefore of the composite also because the matrix material cannot sustain load after fibre failure. This shear type of compressive failure of CFRP has been observed by other authors[49,51].

Hancox's linear variation of strength with fibre volume fraction[51] is easily explained if the cause of failure is directly related to fibre strength, as would be the case if fibre and resin shear failure were occurring. The fibres carry the majority of the load since they have a much greater modulus than the resin matrix. Increasing volume fraction therefore enables the composite to carry proportinally higher loads before failing. This is very similar to the linear strength vs volume fraction relationship which is observed in tension, again because composite failure is brought on by fibre failures. Ewins and Ham[49] discussed the fact that not only is there a linear relationship in both tension and compression, but also that actual strength values are very similar in both tension

and compression for various unidirectional composite materials, This, they suggested is because tensile failure of the fibre material is also governed by the same shearing mechanism. The maximum shear stress, governed by the equation:

$$\hat{\tau} = \frac{1}{2}(\sigma_y - \sigma_x) \qquad (5.18)$$

on a plane at 45° to the fibre axis, reasoned Ewins and Ham, is equally applicable to axial tensile and compressive stresses. (This reasoning is taken a step further in Section 5.4.4 as the correlation between tensile and compressive values is used to give some indication of the efficiency of the compression test fixture and specimen configuration).

From the linear strength vs volume fraction dependence of other workers together with the appearance of fracture in the CFRP-epoxy specimens, it has become clear that fibre compressive failure, or shear failure is an active failure mechanism in unidirectional composites. However as this work has shown, it is not the only mechanism by which CFRP can fail at room temperatures. The same linear strength vs volume fraction relationship cannot necessarily be expected to occur where totally different mechanisms of failure predominate. In GRP for example, resin tensile strength and interface bond strength play more active roles. The work of Martinez, Piggott, Bainbridge and Harris[55] showed that in GRP, HM-S carbon and HT-S carbon fibre composites, the strength/volume fraction relationships were only linear up to about $V_f = 0.4$, indicating a possible change of failure mode at this volume fraction. They also found that within the linear part of the relationship, the compressive strength was insensitive to fibre strength, suggesting that the mode of failure in their glass fibre

and carbon fibre polyester composites was not one of fibre failure. This is reinforced by the fact that the highest strengths they achieved in HT-S carbon fibre composites were well below 600 MPa at V_f = 0.5. (This is less than half the strength achieved in the epoxy CFRP laminates in this work, even after accounting for a linear volume fraction correction. The linear strength vs volume fraction relationship obtained by Piggott and Harris[53] in GRP broke down for volume fractions greater than 0.3.

An analysis of the relationship between compressive strength and volume fraction is beyond the scope of this work. However it is believed that further work carried out in this field of study with an emphasis on relating the results to the observed failure mechanisms would generate helpful information for understanding compressive failure processes.

d) The Fibre Microbuckling Failure Mechanism

In both sets of vinyl ester CFRP specimens tested, the fracture surface appeared to be a "clean" failure along a plane inclined at approximately 70° to the axis of loading. A typical example of such a failure is shown in Plate 15. SEM micrographs of the fracture surface, which are shown in Plates 24 and 25, supplied clear evidence of fibre microbuckling. In Plate 25, separate regions of tensile and compressive failure are visible on the fracture surface of an individual fibre indicating that a sharp buckling had been the cause of failure.

The lower magnification SEM micrographs revealed steps in the fracture surface (Plate 24). Clearly several planes of fracture are formed and the transmission of this type of failure through the

cross section takes place at an angle to the specimen's cross sectional plane. Assuming a regular sinsuoidal type of buckling, the steps in the fracture surface enable an estimate of the buckling wavelength (λd) to be established. The steps are always the same "height" and it is therefore reasoned that each one represents one half of a buckling wavelength:

$$\text{visible step height} = \frac{1}{2}\lambda d \qquad (5.19)$$

where, if d = fibre diameter, λ is a dimensionless parameter.

If multiple wavelengths were to occur between each step of the fracture, they would vary in height depending upon the number of wavelengths included. Also, by the nature of this model it is clearly not possible for failure planes to occur at spacing of less than half a wavelength. Since the step height was not only constant at different parts of the specimen, but also between different specimens in the batch, and even in samples of both the 411 and 470 resin matrix material, it was concluded that this did represent the natural buckling wavelength of the carbon fibres in this type of resin matrix material.

Thus, by application of equation 5.19 to the SEM micrographs:

$\lambda d = 0.083$ mm

$d = 7.2\ \mu m$ from the manufacturer's specification[70]

therefore $\lambda = 11.5$

Having established a value of λ which appears to be a constant value in the CFRP materials, the microbuckling is partially quantified. This is helpful in consideration of this failure mode.

There is some reason to believe that the failure of a fibre in tension or compression is due essentially to shear failure[49]. For this reason, in the following analysis, the strength of the carbon fibre material (in tension or compression) in a laminated composite is obtained from the compressive strength results of the epoxy CFRP specimens, which failed in shear. The rule of mixtures is applied so that

$$\hat{\sigma}_c = \hat{\sigma}_f V_f + \hat{\sigma}_f \cdot \frac{E_m}{E_f} \cdot V_m \qquad (5.20)$$

The fibre strength obtained is 2.3 GPa. This is probably a fairly realistic value to use in the following analysis, since it represents the compressive strength of the carbon fibre after having been made up into a laminate. It incorporates any factors which affect strength such as damage, defects etc.

For microbuckling fibre failure to occur, a carbon fibre is considered in a sinusoidally buckled state such that the bending stresses at the outer edge of the fibre are equal to $\hat{\sigma}_f$. Plate 25 shows that the fracture surface of a fibre which has broken in this manner exhibits approximately equal regions of tensile and compressive fracture. For this reason, bending stresses only are considered, with no overall resultant compressive stress.

By simple bending mechanics, the bending stresses are:

$$\sigma_b = \frac{Ey}{R} \qquad (5.21)$$

where y = the distance from the neutral axis (r in this case because the fibre surface is the point of highest stress)

R = the radius of curvature of the fibre at the antinode of the buckling.

Substituting σ_b = 2.3 GPa ($\hat{\sigma}_f$) gives:

$$R = 0.352 \text{ mm}$$

This is the minimum radius of curvature that a carbon fibre within a composite laminate can tolerate before breaking in flexure. Manual handling of carbon fibres has revealed that they can generally be bent to radii smaller than 0.35 mm. This would be expected since the strength of a fibre is always greater than its effective strength in a composite structure.

Assuming sinusoidal buckling of the form

$$y = a \sin \left(\frac{2\pi x}{\lambda}\right) \tag{5.22}$$

as defined by Piggott[56], the equation is used (from ref. 56) which relates the minimum value of R (i.e.at the antinode) to the sine wave geometry parameters, a and λ:

$$R = \frac{d\lambda^2}{4\pi^2 a} \tag{5.23}$$

where R = minimum radius of curvature of fibre

$d\lambda$ = wavelength of buckling

da = amplitude of buckling

d = diameter of fibre

(Both a and λ are dimensionless parameters).

Substitution for R, λ and d gives

$$a = 0.069$$

This means that in a CFRP composite, if fibre failure is to be initiated by means of the fibre microbuckling mode described above, it could occur when the amplitude of the buckling displacement amounts to only 7% of the fibre diameter (assuming sinusoidal buckling at the specified wavelength). Therefore, although a quantitative analysis of the microbuckling model in unidirectional laminates is still very limited, it can be concluded at this stage that the amount of buckling in carbon fibres which would initiate failure is very small.

The principle of the Rosen model[44] of fibre buckling was to compare the strain energy contained in the composite in the initially compressed, but unbuckled state with that in the buckled configuration. He equated the difference in these two energies with the work done by the fibre loads in the buckling process. The fibre do not buckle gradually or progressively in the elastic region of the compressive test because this would require a greater amount of energy than the elastic shortening of the fibres. Effectively, Rosen's failure criterion was the point where there was enough energy in the composite to enable buckling to occur. For the case of higher volume fraction laminates, this criterion was defined by equation 2.24

$$\hat{\sigma}_c = \frac{G_m}{(1 - V_f)}$$

We can apply this criterion to the vinyl ester 411-45 CFRP laminates tested. The value of G_m obtained by Richmond[89] for 411-45 vinyl ester resin was:

$$G_m = 2.15 \text{ MPa}$$

Substitution into equation 2.24 together with the average measured volume fraction of 411-45 CFRP (V_f = 0.599) gives:

$$\hat{\sigma}_c = 5.36 \text{ GPa}$$

The actual compressive strength of the 411-45 CFRP material was only 828 MPa. This is clearly well below the strength predicted by the Rosen model and confirms the observations of others that the Rosen buckling strength does not realistically represent the buckling strength of real composite materials.

The epoxy resin CFRP materials failed in a shear mode. There was no evidence from the failures that any form of microbuckling had occurred, and as a result, they exhibited much higher strengths. However both vinyl ester-CFRP materials did demonstrate microbuckling together with low strength, and they did not obey Rosen's prediction of composite strength. Ewins and Ham[49] observed a change in failure mode from one of shear to one of microbuckling by raising the temperature of the CFRP material over 100°C thereby reducing the matrix shear modulus. The microbuckling failures observed in the vinyl ester specimens in this work however occurred at room temperature. It is clear that there is some characteristic of the vinyl ester CFRP materials which causes microbuckling that is not present in the epoxies. There are several differences between the composites in question which must be considered in the explanation.

i) The properties of the resin matrix:

The main difference in resin matrix properties which may cause microbuckling as Ewins and Ham showed, is the shear modulus. The specific values of shear moduli of the epoxy resins used

are not known and since clear cast resin samples were not available, they could not be measured. Ciba Geigy were unable to provide the required information so direct comparison with vinyl esters was not possible. The 411-45 shear modulus is known to be 2.15 GPa. This is comparable with that of a typical epoxy resin so it is not believed that the microbuckling is the result of a particularly low shear modulus.

ii) The fibre-resin bond strength:

While it has been shown that the bond which the vinyl esters form with the matrix is weaker than that of the epoxies (see Section 5.3.1) neither microbuckling nor shear failure involves debonding to any significant extent, and this factor can be dismissed.

iii) The fibre volume fraction:

The average fibre volume fraction in the epoxy-CFRP laminates was 0.664, while that in the vinyl esters was 0.580. It is possible that this difference may have had some influence on the change in failure mode. As already suggested, a full investigation of the effect of volume fraction on compressive strength in relation to different failure modes, would be helpful in developing the theory further.

iv) Method of manufacture of laminate:

The method of preparation of the epoxy prepreg materials caused very little misalignment of fibre. However in the case of the vinyl esters the manual winding process and impregnation with resin resulted in a certain amount of fibre breakage and misalignment, especially in the outer layers.

Though every attempt was made to keep this to a minimum it was inevitable that more defects would result than in a prepreg system of lay-up. The reason why the Rosen[44] prediction of strength appears to be so high is because it considers the composite to be made up of perfectly straight, aligned fibres. The effect of fibre misalignments was Hull's suggestion[54] why compressive strengths are much lower than the microbuckling model of Rosen.

After consideration of the above four factors, the effect of lower volume fraction and of fibre misalignments are thought to be the main ones which contribute to the change in failure mode from shear to microbuckling. However even for lower volume fractions Rosen's prediction of strength is extremely high. It is therefore concluded that the most significant cause of microbuckling failure in the vinyl ester CFRP material is the presence of defects in the laminate. Probably the most notable of these is fibre misalignment. In addition to this, the lower volume fraction may be playing a contributory role so that the combined effect is enough to change the failure mode. Initiation of failure as a result of composite defects would create a great amount of scatter in the results. Reference to Tables 23 and 24 reveals that the coefficients of variation of the vinyl ester CFRP composite strengths are very large. They are higher than the coefficients of variation of the other parent material strengths. This confirms the conclusion that failure is initiated at a lower level as a result of composite defects.

In summary, the microbuckling model which was first introduced by Rosen considered the energy required to transform a unidirectonal composite from one that is unbuckled to one that is buckled.

However this is a very high strength prediction because it assumes perfectly straight fibres, and a great deal of energy would be required to deform them to an unstable buckled state. A real composite could not be made with such perfect linearity.

In real composites there are many defects which include misalignment of fibres. These defects would have the tendency of lowering the required buckling stress considerably. The effect of misalignment and other defects in the stressed composite are such that local 3-D stress systems are set up. Combining already present deformations in the fibres with the extra deformations as a result of the local 3-D stress systems enables buckling to be initiated. It has been shown that only very small deformations cause the fibre buckling mode of failure observed. Once buckling has been initiated at one point, it will be transmitted throught the material in a similar way to the larger scale kink-bands observed in GRP.

e) A Comparison of Compressive Failure Modes

It has been demonstrated that different mechanisms of failure do occur in the compression of unidirectional fibre composites. In the composite systems used in this work, four were identified. In the following table, these are identified in relation to the composite materials in which they occurred.

Longitudinal splitting (caused by transverse tension (Poisson effect)) cf. P.

	COMPRESSIVE FAILURE MODE			
~~Longitud~~	Splitting due to Transverse ~~Splitting~~ stress	Kink-Bands	Fibre and Matrix Shear	Fibre Microbuckling
913 GRP	✓	✓		
914 GRP	✓	✓		
411-45 GRP	✓	✓		
470-36 GRP	✓	✓		
913 CFRP			✓	
914 CFRP			✓	
411-45 CFRP				✓
470-36 CFRP				✓

The difference in bond strength between the GRP and CFRP laminates made itself very evident from the failures. While the first two modes consisted of much debonding, in the latter two it occurred only to a very limited extent.

The upper limit on compressive strength is determined by fibre failure in the shear mode and it has been shown that "prepregged" epoxy resin CFRP composites can achieve this "best" failure criterion, with strengths of up to 1700 MPa being recorded in some specimens (before V_f correction). However even in the shear mode of failure, stress intensity effects probably due mainly to the influence of the end tabs, limit the strength so that it is below that observed in tension. (Tensile strengths of over 1900 MPa have been recorded in some specimens before V_f correction).

Due to the presence of defects such as fibre misalignments, or as other authors[49] have observed, low resin shear modulus, fibre microbuckling failure can prevent the maximum shear stress from being achieved. Carbon fibre reinforced vinyl ester composites have demonstrated this type of failure, their strengths being approximately 40% lower than those of the epoxy resin composites. Since the same fibres are used in each of these systems, improvements in the laminating methods of making the vinyl ester composites should cause improvements in their compressive strengths until the shear mode of failure predominates, forming the upper bound to compressive strength.

In GRP specimens, the weaker bond strength has a considerable influence on compressive failure, and the modes observed included a considerable amount of debonding. Failure consisted of longitudinal splitting occurring throughout the gauge length of the specimen as a result of Poisson's expansion in the z direction. However in cases where failure initiation occurred underneath the end tabs, z direction displacement was limited and a kink-band formation resulted. In the results obtained from the GRP specimens, the particular mode of failure which occurred had no influence on the ultimate compressive strength. In addition to this, the apparent difference in bond strength between the epoxy and vinyl ester specimens had no apparent effect on the compressive strengths attained. In all composite systems the average GRP strength was just over 1000 MPa. Notably, this was higher than the vinyl ester CFRP specimens which failed by means of fibre microbuckling.

The strongest CFRP specimens which failed in shear exhibited the characteristic 45° shear plane. The CFRP microbuckling failures and the GRP kink-bands however, all demonstrated that failure

propagation had occurred at an angle of 70° to the fibre axis. It appears that this angle is characteristic of these types of buckling failures, irrespective of fibre/matrix properties.

Rosen's buckling model[44] predicts strengths which are far in excess of those measured in real composites because its basis is a perfect set of aligned fibres in a 2-D format with no defects. Real composites are far removed from this situation and therefore fail at much lower values. However if a perfect composite could be made, shear failure would prevent the Rosen buckling strength expectation from being fulfilled. The reason why linear strength vs volume fraction relationships have been observed, contrary to this theory, is because other failure modes have predominated. Nevertheless, in a qualitative sense it has been shown that fibre microbuckling does occur and that, in contrast to Hancox' comments[51], it does occur at room temperature. For this reason alone, the theory cannot be dismissed.

Piggott's discussion of several failure modes[56] with the active one depending on the variable composite parameters, is a good representation of true composite behaviour. Piggott however did not consider fibre failure other than the low strength yielding of Kevlar fibres and neither did he consider transverse tensile failure to be an active mechanism. It is acknowledged that a considerable amount of further work is required to study the mechanics of compressive failure in order to satisfactorily explain all the observed trends and fracture characteristics. While the complexity of tensile failure appears to be the statistical nature of fibre breakage, compressive failure interpretation is proving be equally complex because of the number of different mechanisms involved.

5.4.3 Compressive Failure of Hybrid Composites

a) Failure Mechanisms

The compressive failures in the hybrid specimens appeared very similar to those in corresponding parent materials. The failed CFRP layers in hybrids exhibited the characteristics typical of CFRP monofibre specimen failures, while the GRP layers similarly exhibited typical GRP specimen failure characteristics.

A considerable amount of debonding occurred in the GRP layers but very little fibre failure. As with single fibre type composites these failures could be divided into two groups; those where general debonding and general spread of fibres in the transverse direction was occurring, and those in which a neat kink band was formed beneath the end tabs. Hybrid specimens demonstrating both these types of fracture are shown in Plates 26 and 27. They can be compared with the failures of GRP specimens in Plates 11 and 12.

The CFRP layer fracture surfaces were much "cleaner" than those of GRP with relatively little debonding and a relatively small number of axial cracks. As in the monofibre composites, the failure surface took the nature of an oblique fracture, though in most cases it was very poorly defined. Due to the CFRP layers being thinner in hybrids than in the parent material, the end tabs had a greater influence on failure. In nearly every case, failure was initiated at or very near to the end of the tab and the oblique angle of the fracture plane was very often hidden by the raggedness of the failure as it followed the line of the tab. Plate 28 shows this effect. In single fibre type composites, it was suggested that the strength of CFRP material was apparently affected by the fact that failure was often initiated at the tabs. In the hybrids this was

again demonstrated by the fact that the presence of GRP in the outer layers did offer some improvement to the strengths achieved in the reverse lay-ups. It protected the CFRP somewhat from the more extreme stresses immediately next to the end of the aluminium tab. There was a greater amount of fibre failure in the GRP layers when they were internal, as shown in Plate 28.

Even in the more complex lay-ups containing five individual layers of GRP or CFRP, the failures of individual layers were adjacent. This is evidence of the fact that failure starts at one point and travels through the specimen. Because carbon fibres are the LE component of the reinforcement, the initiation of failure occurs within a CFRP layer and travels through that layer. Due to the sudden release of energy, adjacent CFRP layers fail and this is immediately followed by the failure of the GRP, which is due to the sudden extra compressive load to which it is subjected.

In the 913 lay-ups containing the smallest amount of glass fibres, there was a considerable proportion of glass fibre breakage. This was because of the high energy released as the carbon fibre failed, and the large load suddenly subjected to relatively few glass fibres, causing complete fracture of the GRP layers.

b) <u>The Hybrid Effect</u>

The failure mechanism observed in the stronger, epoxy CFRP specimens is governed by fibre compressive strength because it is fibre failure which initiates composite failure. Under normal circumstances, the material from which the fibre is made can be said to have a characteristic failure strain. The stress in the fibre at failure is governed by this and the material's modulus such that

$$\sigma = E.\varepsilon$$

This is the reason why strength may be expected to show proportionality to volume fraction in composites where fibre failure is a governing mechanism. If failure strain is fixed by the material, the stress in each fibre is constant at failure (assuming the modulus is the same) and the strength of the composite will simply be a linear function the number of fibres. Effectively, a linear strength vs V_f relationship is indicative of a constant failure strain which is independent of volume fraction. This is important when considering the hybrid effect, as the parameter under analysis is the failure strain of the fibres in the composite.

The theory of Rosen[44] predicted a non-linear strength vs volume fraction relationship. Taking Rosen's shear mode buckling strength prediction which is for the higher V_f composites; equation 2.24

$$\hat{\sigma}_c = \frac{G_m}{(1-V_f)}$$

Therefore

$$E_c\hat{\varepsilon}_c = \frac{G_m}{(1-V_f)} \qquad (5.24)$$

But $E_c = E_fV_f + E_mV_m$.

So that equation 5.24, after substitution for E_c becomes:

$$\hat{\varepsilon}_c = \frac{G_m}{E_f[V_f(1-V_f)] + E_m[1-V_f]^2} \qquad (5.25)$$

Equation 5.25 defines an increasing failure strain with increasing fibre volume fraction. This means that, by Rosen's theory, hybrid effects could be explained by possible increases in volume fraction of the LE fibre layers. With the presence of glass fibres in the CFRP laminates (i.e. hybrids), the flow of the resin around the different types of fibre during cure, together with the difference

in fibre diameter, could quite easily account for the carbon fibre layers being of higher volume fraction than they would be in the parent material, or indeed than the average for the whole laminate. Increased fibre volume fraction in the carbon fibre together with reduced volume fraction in the glass fibre layers would result in positive hybrid effects as the results show. Table 42 gives examples of the hybrid effect which would occur if equation 5.25 were obeyed. Assuming a CFRP parent material V_f of 0.6, a hybrid laminate in which the CFRP layers were of V_f = 0.7 would exhibit a positive hybrid effect of 15%. This is quite a realistic figure.

This theory also offers some explanation for the fact that the hybrid effect is dependent on the volume ratio of the two types of fibre present. A higher proportion of glass fibre would have a greater influence on the carbon fibre layer volume fractions, which in turn affects the measured failure strains. While Rosen's microbuckling model is not entirely satisfactory for composite strength prediction, the vinyl-ester CFRP specimens did demonstrate a microbuckling mechanism of failure, and it has been shown in the above analysis that some explanation of the hybrid effect can be incorporated into Rosen's strength predictions. The main difficulties with this theory are that CFRP has demonstrated a linear strength vs V_f relationship[51], and that the strength values that it predicts are too high.

In contrast with Rosen's theory, Hancox[51] showed that in CFRP composites the strength is directly proportional to the volume fraction, this indicated that the failure strain could be independent of the volume fraction. It would mean that the hybrid effect can only be a result of the different types of fibres present in the laminate rather than a volume fraction or packing density

effect. It is therefore apparent that a better understanding of the failure processes in monofibre composites is required before significant advances in hybrid theory are made. Even with the problems in the buckling theories, until the alternatives can be proved to a greater degree by backing up with experimental strengths and fracture appearance, Rosen's theory cannot be abandoned.

The parent composite materials each have their own average characteristic compressive failure strains. Since the hybrid lay-ups consist of laminations of the parent composites, there is no clear reason why individual layers in a hybrid do not fail at their own characteristic strain. The increase in compressive strain of the LE carbon fibres which is observed in hybrids is dependent on the ratio V_{fc}/V_{ft} and can be as great as 80% in the lay-ups containing only a small amount of carbon. In terms of simple mechanics this hybrid effect is difficult to explain. The fact that increases in strain occur in the hybrids in both tension and compression shows that it cannot be put down to residual strains in the individual layers of the composite. The effects of differential thermal contraction, while serving to enhance the tensile hybrid effect (albeit to a very small extent - see Figure 82) can only reduce the compressive hybrid effect. For the purposes of explaining the large increases in strain, thermal effects are considered negligible.

Piggott stated that in his compressive specimen, the actual maximum stress achieved in the CFRP layers can be greater than the expected carbon fibre strength, "probably because the lower modulus fibres can assist the matrix in resisting the push of the higher modulus fibres".[56] He accounted for this mathematically by applying a "multiplier 3" factor to glass and resin terms in the strength equation so that the simple ROM relationship becomes:

$$\hat{\sigma}_c = \hat{\sigma}_f \left(V_{fc} + \frac{3V_{fG}E_{fG}}{E_{fc}} + \frac{3V_m E_m}{E_{fc}}\right) \qquad (5.26)$$

While Piggott's results for glass/carbon hybrids fitted this equation well it is not clear exactly how the glass fibres provide the supporting effect.

It was apparent from the analysis of monofibre composites that the end tabs have a stress raising effect. The difference in strength between laminates of similar lay-up but containing carbon fibres in the outer layers rather than glass is also due to the influence of the end tabs. Since failure is initiated at the CFRP layers a lower strength results when these are immediately adjacent to the end tabs. Instead of laminates with GRP in the outer layers exhibiting a greater hybrid effect, it is more correct to describe those with CFRP in the outer layers as having a reduced hybrid effect. These results show that the stress raising effects of the end tabs are not so great in the inner layers of the laminate as they are on the surface.

5.4.4 An Assessment of the Celanese Compression Test Fixture and Specimen Geometry

Compressive failure of the epoxy-CFRP specimens was initiated by fibre failure and the mechanism was shear along a plane at 45° to the fibre axis. As discussed by Ewins and Ham[49], this limiting shear strength must be common to both tensile and compressive failure of the fibre reinforcement. This means that if shear is identified as the mechanism which causes compressive failure, the corresponding tensile strength would not be expected to exceed the compression strength. (The compressive strength of the fibres is clearly a

difficult property to measure. However Hawthorne and Teghtsoonian[90] have described a method).

Reference to Table 43 shows that in all the CFRP composite systems (except 914) the tensile strengths recorded were significantly higher than the compressive shear failure strengths of the epoxy CFRP specimens. There could be several possible explanations for this, as follows:

i) The compressive failures were not true fibre shear failures
ii) The quality of the specimens used in the tests were not comparable
iii) Compressive composite failure is initiated by a smaller number of individual fibre breaks than tensile composite failure
iv) The difference in test specimen geometry and fixture was such that extra stress raising effects occurred in the compressive tests.

If compressive failure in the epoxy-CFRP specimens did not occur by a mechanism of true shear failure, the characteristic 45° fracture plane would be difficult to explain. In the case of the materials under consideration, both tensile and compressive specimens were cut from the same laminate slabs. This means that untrue shear failure and the difference in specimen quality can both be ruled out as causes. There is a possibility that composite compressive failure could be initiated by a lower number of individual fibre breaks than tensile failure requires. However observation of the fracture surface of a round composite rod broken in flexure reveals equal areas of tensile and compressive failure[49]. This indicates that the stress required to initiate tensile or compressive failure is approximately equal. It is therefore concluded that the lower

strengths in compression compared with those observed in tension are due to some inefficiency in test specimen geometry and fixture.

The difficulties in measuring the compressive strength of CFRP were recognised by Woolstencroft et al[43], who carried out a comparison study of different test techniques commonly employed for compression testing fibre composite materials. In that study, using 914-XAS CFRP material, the best result was obtained from the RAE type specimen. That from the Celanese compression fixture was much poorer. However the results obtained from this work on the 914-XAS CFRP material show a distinct improvement over those obtained from the same material by Woolstencroft et al[43] and by Lee[88] using the Celanese compression fixture. In Table 44, a comparison of these results is presented. The improvement in the strength of the 914 CFRP over that recorded by these other authors is thought to be due to the increased specimen width in the current work. It is concluded therefore, that increasing the width of the specimen can be beneficial for obtaining better (more representative) compressive strength values. It follows that if comparisons are to be made between different materials, a fixed specimen geometry must be employed in the tests.

Even though compressive strengths are lower than the measured tensile strengths, they compare favourably with those of other peoples work. The "low" values produced are not peculiar to this piece of work. Compression test methods generate results which are not as truly representative of material strength as tensile test methods. The reduction in strength of the material in compression compared with the tensile value is interpreted as a stress intensity effect from the specimen geometry and test fixture.

It is estimated from the following equation

$$\text{Stress intensity factor } Z = \frac{\text{tensile strength}}{\text{compressive strength (shear failure)}} \tag{5.27}$$

From the results obtained, by substitution into equation 5.27

$$Z = 1.26$$

Therefore at the failure load of CFRP there is an increased local stress intensity of 26% as a result of the specimen geometry and test fixture. This conclusion is supported by the fact that compressive failures in CFRP were always initiated at the end tabs, and in the case of the epoxy specimens, followed the line of the end tabs.

5.5 RESIN EFFECTS

5.5.1 Introduction

The analysis of the mechanical properties of both hybrid and non-hybrid composites has been presented without any particular consideration of the effect of using different types of resin matrix. The use of epoxy resin prepregs is now fairly widespread and it is important, if different resins are to be employed, that contrasting effects resulting from their different properties are understood and assessed in some form of quantitative manner. The reason why vinyl esters were used in this work was to analyse the performance of their composites in comparison with the epoxy resin prepregs which are more familiar. The characteristics of the different resin effects are now considered.

In order to make valid comparisons between resin systems, the identical fibres to those which Ciba-Geigy put into their prepregs were purchased for the vinyl ester hand lay-up systems. While this eliminated any effects from fibre differences, it was possible that the difference in the method of manufacture of the laminate slabs could have had a noticeable effect on the acquired results. The most likely effect would be the presence of a greater amount of defects in the vinyl ester resin composites as a result of the resin impregnation process. This had to be taken into consideration in the comparisons.

5.5.2 Bond Strength

As discussed in Section 5.3.1 it is clear from the tensile failures that in both GRP and CFRP composites the vinyl esters form a poorer bond with the fibres than the epoxy resins. This conclusion was made from the observation that in the vinyl ester specimens the extent of debonding was much greater than in the epoxies. Coupling agents have been developed which give very good results with vinyl-ester resins[91].

5.5.3 914 CFRP

One of the most significant matrix effects observed in the tests carried out was the very low tensile strength of the 914 CFRP material. The average UTS of 914 CFRP was 1200 MPa while that of the CFRP composites made with the three other resins was approximately 1750 MPa. This was the result of very low strains at which the 914 failed (0.9%). The modulus of the material was "normal". Since the appearance of failure in the 914 specimens was very similar to that in the 913, there was no apparent reason why such a low strength was

recorded. The manufacturers' product information bulletin[72] specifies a tensile strength of 1650 MPa.

The low strengths were consistent. Out of six parent CFRP material specimens tested, the CV was only 4.4%. These specimens were made from two completely independently manufactured slabs of prepreg. However all the 914 CFRP used in this work was from a single batch of the material from the supplier. The following observations were made with regard to the 914 CFRP in comparison with 913 CFRP.

914 CFRP defective material properties:

axial tensile strength	LOW
axial tensile modulus	NORMAL
axial compressive strength	NORMAL
axial compressive modulus	NORMAL
transverse tensile strength	LOW
bond strength	NORMAL

The inter-laminar shear strength, though lower than that of the 913 system was much higher than those of both the vinyl ester resin CFRP systems.

It is apparent, from the above information, that the material was defective. The longitudinal and transverse tensile strengths were the only basic properties however which were severely affected. As shown above, the others were normal. Since tensile strength is particularly sensitive to the presence of voids, this may be the explanation of the poor results. The inter-laminar shear strength, which is also a void sensitive property[92], was reduced by approximately 10% from that of the 913 CFRP.

Comparison of the tensile failures of 913 and 914 CFRP materials in plates 29 and 30 indicates that the defectiveness in the 914 laminate had aided crack propagation. The failure was smoother, with less pull out. In communication with Ciba-Geigy, it was suggested that improvement of the curing cycle may be the solution.

This meant that information about the effect of the resin matrix material could not be obtained from the 914 CFRP or hybrid specimen results with any degree of confidence. However an important fact has been made clear with these findings: it has been proven that the mechanical properties of these materials can occasionally fall considerably short of the manufacturer's specification, even when proper and careful techniques have been used in their processing. When used in production, therefore, tests should be carried out to ensure that the material's properties are up to the required specification.

5.5.4 Tensile Strength

Even though the vinyl ester resins form a weaker bond with the fibres than the epoxies, the ultimate tensile strength of their composites is not impaired. Reference to Table 43 shows that the tensile strengths of the vinyl ester GRP specimens were not significantly different from those of the 913 and 914 composites, even though a much greater amount of debonding was occurring in the specimens to produce these results.

The reason for this is that UTS is a fibre dominated property. While a certain amount of debonding occurs in GRP specimens before fibre failure, it is apparently not enough to cause the effectiveness of the composite to be reduced to the extent where

failure will occur at a lower stress level. Ultimate tensile strength is still dependent on the tensile failure of the fibres. The debonding does not cause fibres to fail early and it is not extensive enough to reduce them to a state of total ineffectiveness. Its primary influence is therefore on the way the failure propagates through the material rather than the stress at which the failure is initiated.

The tensile strength comparisons have been made from the series of specimens which were made by the two different techniques described in Section 3.4.1. As a result of different techniques of manufacture, the vinyl esters had an average fibre volume fraction of 0.55 while that of the epoxies was 0.65. In the comparison of results, all strength values have been normalised to represent a constant fibre volume fraction of 0.6. It is true therefore that the actual strengths measured in the vinyl esters were lower than in the epoxies. Failure strains however were the same so the real difference in strength is not interpreted as being of any significance.

5.5.5 Compressive Strength

Due to the different mechanisms of failure involved and the dependence of these on matrix properties, compressive tests provide more information about differences between composite systems than do tensile tests. While in tension the systems used were closely comparable, in compression the inferiority of the vinyl ester composite systems was clearly evident. (While the 914 CFRP was weaker than the others in tension, this has been diagnosed as due to defective laminates. Under similar circumstances, any one of the composite systems may have demonstrated poor tensile properties).

The compressive strengths of each of the monofibre composite systems are presented in Table 43.

The low compressive strengths of the vinyl ester CFRP specimens, when compared with the epoxies, reveals that a different mode of failure is occurring. Microscopic examination of the fracture surface has confirmed this. As has already been discussed (see Section 5.4.2) microbuckling failure, which the vinyl esters exhibit, does not enable full utilisation of the fibre strength to be achieved, indicating why the strengths are not as high as those of the epoxies. It was concluded that, while several factors could be involved in the cause of the transformation from one mode of failure to another, in the composites used in this work, the main factor was the greater amount of fibre misalignment defects in the vinyl ester composites. This therefore is not the result of a different resin material being used, but rather of the different method of lamination by which the composite slabs were made. Volume fraction is also thought to be an influencing factor which may interact with the effect of the defects. On the basis of these conclusions, the compressive strengths of the vinyl ester CFRP laminates could probably be increased by improving the laminating process to incorporate less fibre misalignment defects and a higher fibre volume fraction. If the shear mode of failure could then be achieved, the strength should be comparable with that of the epoxy CFRP materials. Perhaps the most obvious suggestion along these lines might be to develop a prepreg system of vinyl ester composite. However the differences in the curing chemistry would present serious difficulties.

The GRP laminates did not demonstrate any matrix dependence in their compression strengths. While debonding plays an important role in GRP compression failure, the difference in bond strength between the vinyl ester and epoxy resins with the glass fibres did not have any significant effect. As already discussed (see Section 5.4.2(a)) the mechanism of failure in the GRP laminates is transverse tensile fracture due to Poisson's expansion. The transverse tensile strength of a laminate approximates to the strength of the matrix if the interface bond is perfect. A reduced bond strength would result in a reduced transverse tensile strength. However in the case of imperfect bonding, reduced volume fraction of fibres improves the tensile strength. Therefore the reduced bond strength in the vinyl esters is counteracted by the fact that they also have a lower volume fraction than the epoxy laminates. Similar strength results are obtained.

While the CFRP laminates showed great sensitivity to defects, making the vinyl ester composites much weaker, in the case of glass fibre reinforcement this was not evident for the following reasons:

i) While the glass fibres are prone to surface damage, they are not as brittle as the carbon fibres. Therefore the hand laminating process applied to GRP does not result in the same quantity of broken and stray fibres as for CFRP.

ii) The mechanism of failure which predominates in GRP, that of transverse tensile failure, is not as sensitive to fibre misalignment effects as is the carbon fibre microbuckling mechanism.

5.5.6 Elastic Modulus

There was no significant difference in the secant modulus results of composites of the different resins when equivalent fibre lay-ups were compared. In each case the elastic moduli obeyed the rule of mixtures predictions, and since the resin moduli were so low in comparison with the fibre moduli, slight differences between resins were insignificant.

A closer examination of the results by consideration of the tangent modulus variation indicated that the modulus appeared to decrease at a greater rate with respect to compressive strain in the 470-36 CFRP system (Figure 77) than it did in the other CFRP systems (Figures 74, 75, 76). This however was interpreted as an experimental effect rather than a real one for the following reasons:

i) The variation in modulus of the CFRP has been shown to be due to the fibres' non-linear stress vs strain relationship, and not to the internal geometry of the specimen or any other mechanism such as buckling. It is unlikely therefore that the use of a different resin could change this relationship.

ii) Any effect additional to the variation in fibre modulus, such as buckling, would result in a lower compressive strength than that of the 411-45 CFRP system. This was not recorded.

iii) The compressive moduli of hybrid lay-ups of the 470 resin system had average values a little above the rule of mixtures (see Figure 62). This indicated that the measured values of the CFRP modulus were likely to be a little low.

iv) The points which indicate this steeper gradient of the modulus vs strain relationship in Figure 77 have a very low degree of correlation.

5.5.7 The Hybrid Effect

The four composite systems are now compared in terms of the amount of hybrid effect which they exhibit. This analysis is carried out for hybrids containing equal volumes of glass and carbon fibres.

It has already been made clear that every hybrid composite system tested demonstrated a synergistic increase in the failure strain over that of the corresponding parent CFRP material, in both the tensile and the compressive modes of loading. The amount by which strain increased for each fibre lay-up is given in Table 45 for the tensile failure strains and in Table 46 for the corresponding compressive failure strains. After having already found that the 914 CFRP material used was defective, it was not considered helpful to use these hybrid effect results for serious comparisons and as Tables 45 and 46 show, 914 was the system which demonstrated the smallest hybrid effects, especially in compression.

The poor compressive failure strains of the vinyl ester CFRP specimens has been associated with internal defects, caused during the laminating stage. This damage will be greatest in the outer layers of the composite. The vinyl ester hybrid composites with GRP in the outer layers therefore exhibited the largest hybrid effects because failure was initiated within the stress-raising effect of the end tabs. Increases in strain of 60% of the parent material value showed that the glass fibres in the outer layers had a very significant protecting effect (see Table 46). However the hybrids with carbon fibre in the outer layers did also have failure strains considerably greater than the CFRP (Table 46) so the extent of this explanation of the compressive hybrid effect is limited. While the

epoxy resin systems demonstrated smaller hybrid effects, their actual failure strains were greater than those of the vinyl esters.

In tension hybrid effects on average were smaller than those in compression, but again, the vinyl esters demonstrated greater strain increases than did the epoxies, in this case in spite of the fact that the actual failure strains were higher than those of the epoxies, too.

In order to summarize the comparison of hybrid performance of the four resin systems, Figure 88 shows the strengths represented in bar form. Since both tensile and compressive strengths are represented together, this gives an indication of the working stress range of each composite system. Results of both 3 ply and 5 ply laminates were combined in Figure 88 for simplicity of presentation. It is apparent that under the conditions of testing carried out in this work, the 913 hybrid system exhibited the best stress range, though generally the mechanical properties of each of the composite systems were comparable. There were two really significant weaknesses which this work has revealed. These were:

i) the poor tensile strength of 914 CFRP.
ii) the poor compressive strengths of both 411 and 470 CFRP.
Both of the above factors affected hybrid performance.

In general, the vinyl esters performed well in a detailed comparison of their mechanical behaviour with epoxy resins. With the very significant bonus of excellent chemical resistance which other authors have reported on[12,13,14] vinyl esters will almost certainly occupy an important share of the thermosetting resin market, especially if the method of laminating can be improved upon.

5.6 CHARACTERISATION OF THE HYBRID EFFECT

It has been pointed out (see Section 5.1), that the rule of mixtures strength can be defined as either $\hat{\sigma}_{ROM}$ or $\hat{\sigma}_H$, where each is defined by equations 5.2 and 5.3 respectively. $\hat{\sigma}_{ROM}$ is an arbitrary relationship and there is no apparent reason why a hybrid laminate should be expected to fail with an ultimate strength value of $\hat{\sigma}_{ROM}$. However, reference to Figures 43-46 and 51-54 shows that they very often do! $\hat{\sigma}_H$ defines the strength of the hybrid such that initial failure would occur at the failure strain of CFRP. Clearly this is the strength at which the hybrid is expected to fail, neglecting synergistic effects. Because all the hybrid specimens exhibited a positive hybrid effect and failed at strains greater than that of the CFRP, this has caused all the hybrid strength results to lie above the $\hat{\sigma}_H$ line (see Figures 43-46 and 51-54). Clearly, if positive hybrid effects are a characteristic of the material, which the results verify is indeed the case, then $\hat{\sigma}_H$ will always lie below the real strengths. It can be considered as a lower bound to the ultimate strength value in a hybrid ($\hat{\sigma}_{ROM}$ is not an upper bound since in several lay-ups, strengths greater than this were recorded). Neither of these parameters is totally satisfactory for hybrid strength prediction.

Using the experimental data, an attempt to quantitatively characterise the actual failure strains and strengths of the hybrid laminates is possible. This has been undertaken for the 913 system.

In the analysis of the hybrid effect, it is important to consider not only the ratio of carbon fibre to total fibre reinforcement (V_{fc}/V_{ft}), but also the order of the lay-up. The results have demonstrated that the failure strains of laminates with glass fibres

in the outer layers (GO.laminates) are greater than those of lay-ups with carbon fibre reinforcement in the outer layers (CO.laminates).

In order to quantify this effect, the difference in failure strain between GO.laminates and CO.laminates has been plotted vs the ratio V_{fc}/V_{ft}. The results of this exercise are shown in Figure 89(a) for tensile failure strains, and in Figure 89(b) for compressive failure strains. Several conclusions can be drawn from these results:

i) The order of the individual plies within the laminate does have a significant effect on its strength even if the volume fraction ratio of glass:carbon fibre is the same.

ii) Laminates with glass fibres in the outer layers are stronger than those with carbon fibre reinforcement in the outer layers.

iii) A similar effect occurs in both tension and compression.

iv) The actual differences of strain observed in the tensile and compressive modes are of approximately the same magnitude at equivalent glass:carbon fibre reinforcement ratios.

v) This difference in failure strain can be approximately represented by a simple exponential relationship of the form

$$y = Ae^{Bx}$$

where the y variable = strain (%)

and the x variable = V_{fc}/V_{ft}.

For the tensile failure strain results A = 0.45 (%)

and B = -4

While for the compressive failure strain results A = 0.55 (%)

and B = -4

vi) The results at high ratios of V_{fc}/V_{ft} appear to disobey the above simple relationship. This discrepancy is greater in the compressive strain results than in the tensile ones.

By extrapolating back to $V_{fc}/V_{ft} = 0$, the constant A is determined. This is denoted $\Delta\hat{\varepsilon}_o$. It is used in the following analysis to obtain the theoretical value $\hat{\varepsilon}_{GRP-CO}$ (see Figure 89)

where $$\hat{\varepsilon}_{GRP-CO} = \hat{\varepsilon}_{GRP} - \Delta\hat{\varepsilon}_o \qquad (5.28)$$

The failure strain results of both GO and CO 913 hybrid specimens are presented in Figures 39 and 47 plotted vs the ratio of V_{fc}/V_{ft}. It is clear, simply by observation that to fit a curve to these results, an exponential function is required, of the form

$$y = Ae^{Bx}$$

The failure strains at the CFRP extreme of this graph do not level off but continue decreasing up to the point where $V_{fc}/V_{ft} = 1.0$. That is, the gradient does not decay to zero. An extra term is therefore required to account for the continuing gradient, plus a constant since it does not go through 0, A:

$$y = Cx + D$$

and the general equation becomes

$$y = Ae^{Bx} + Cx + D \qquad (5.29)$$

The constants A, B, C and D are selected so that the equation best describes the experimental data. Although there are four unknown variables, they are easily selected using the following equations:

$$\text{i)} \quad C = \left[\frac{d(\hat{\varepsilon}_c)}{d(V_{fc}/V_{ft})}\right]_{V_{fc}/V_{ft}=1.0} \tag{5.30}$$

$$\text{ii)} \quad D = \hat{\varepsilon}_{CFRP} - C \tag{5.31}$$

$$\text{iii)} \quad A = \hat{\varepsilon}_{GRP} - D \tag{5.32}$$

$$\text{iv)} \quad B = \frac{\left[\frac{d(\hat{\varepsilon}_c)}{d(V_{fc}/V_{ft})}\right]_{V_{fc}/V_{ft}=0} - C}{A} \tag{5.33}$$

In order to simplify equation 5.30 above, the function described by equation 5.29 is assumed to be a close approximation to a straight line between V_{fc}/V_{ft} = 0.5 and V_{fc}/V_{ft} = 1.0, of gradient C.

Equation 5.30 can therefore be re-written:

$$C = \frac{[\hat{\varepsilon}_c]V_{fc}/V_{ft}=1.0 - [\hat{\varepsilon}_c]V_{fc}/V_{ft}=0.5}{0.5}$$

or

$$C = 2[\hat{\varepsilon}_{CFRP} - (\hat{\varepsilon}_c)_{V_{fc}/V_{ft}=0.5}] \tag{5.34}$$

Equation 5.34 is used to replace equation 5.30 and the constants C, D and A are respectively calculated using equations 5.34, 5.31 and 5.32. The constant B is calculated by estimating the slope of the

curve at $V_{fc}/V_{ft} = 0$ and substituting this value into the equation 5.33.

Using data from the 913 tensile tests on specimens with GRP in the outer plies, the constants were calculated as:

$$A = 1.10$$
$$B = -10$$
$$C = -0.38$$
$$D = 1.71$$

Therefore the general equation for the failure strain of 913 hybrids with GRP outer plies is:

$$\hat{\varepsilon}_c = 1.1\ e^{(-10x)} - 0.38x + 1.71 \qquad (5.35)$$

where x = the variable V_{fc}/V_{ft}.

Equation 5.35 is shown in Figure 90(a) in comparison with the experimental data.

The variation of composite modulus with respect to the fibre volume ratio V_{fc}/V_{ft} is a straight line (ROM) relationship. The equation for this relationship can be written as:

$$E_c = (E_{CFRP} - E_{GRP})x + E_{GRP} \qquad (5.36)$$

where the x variable = the ratio of V_{fc}/V_{ft}.

Multiplying the right hand sides of equations 5.35 and 5.36 together results in an expression for the composite's strength in terms of

the fibre volume ratio. It strictly defines the stress at the point of first failure, but this is nearly always very close to the ultimate strength and is considered coincident for these purposes. Figure 90(b) shows how the resultant expression for composite strength matches the results obtained. The agreement is good.

A similar analysis was carried out for the tensile failure strain results of laminates containing CFRP in the outer plies. Figure 39 shows that at small fibre volume ratios (V_{fc}/V_{ft} approaching zero) the composite strain does not tend towards $\hat{\varepsilon}_{GRP}$, but towards the lower value $\hat{\varepsilon}_{GRP-CO}$, which is defined by equation 5.28. The parameter $\hat{\varepsilon}_{GRP}$ is therefore replaced by $\hat{\varepsilon}_{GRP-CO}$ in the analysis.

The same method of characterisation was applied to the compressive failure strain results. It has been shown (by comparison of Figures 89(a) and (b)) that there is a similar difference in failure strain expectation between GO and CO laminates at values of V_{fc}/V_{ft} approaching zero. This difference in strain defined by the compressive value of $\Delta\hat{\varepsilon}_o$ which (from Figure 89(b)) is 0.55. This means that at V_{fc}/V_{ft} approaching 0, the GO.laminates have an expected failure strain 0.55% (strain) greater than the CO.laminates. Using the same method as that applied to the tensile results it was found that in order to obtain a good agreement with the data, the CO laminates must be considered to approach $\hat{\varepsilon}_{GRP}$ at $V_{fc}/V_{ft} = 0$, while the GO.laminates tend towards the higher value, $\hat{\varepsilon}_{GRP-GO}$. This is defined by the equation:

$$\hat{\varepsilon}_{GRP-GO} = \hat{\varepsilon}_{GRP} + \Delta\hat{\varepsilon}_o$$

The different terms used are clarified in Table 47 which lists the data used to obtain the constants A, B, C and D in each case.

Figures 90-93 show how the generated functions compare with the experimental data.

Because the results from G0.laminates appear to be approaching strains greater than $\hat{\varepsilon}_{GRP}$, some consideration is required of whether this is a practical possibility. It would mean that the CFRP inner layers would be causing a synergistic increase in the failure strain of the GRP layers! The following observations are made concerning this possibility:

i) At the lowest values of V_{fc}/V_{ft} tested, the compressive hybrid effect was so large that failure of some hybrid specimens did occur at strains greater than the average GRP failure strain.
ii) The transverse tensile stresses, which initiated failure in the GRP specimens, are greatest in the centre of the laminate. This is the region occupied by the CFRP layer.

GRP and CFRP layers fail by totally different mechanisms. It is possible that the interaction of different properties in the different layers, causes an inhibition of failure initiation in both the GRP and the CFRP. The results indicate that the addition of a small amount of carbon fibre in the centre of a GRP laminate may improve compressive failure strain, as well as strength and modulus.

It has been shown that it is possible to characterise the failure strain of a hybrid composite system using a relatively small amount of experimental data. The relationships obtained have given some indication of the way the interaction of different properties between layers affects the failure strains. This is a basis from which to develop a deeper understanding of how the hybrid effect works. Suggested future work in this area is described in Section 7.

6. CONCLUSIONS

6.1 COMPOSITE MODULUS

6.2 TENSILE FAILURE

6.3 COMPRESSIVE FAILURE

6.4 THE HYBRID EFFECT

6.5 RESIN EFFECTS

The following conclusions can be drawn from the results of the tests, under the conditions and with the materials described in this work.

6.1 COMPOSITE MODULUS

The secant moduli of the composites under consideration differ in the tensile and compressive modes of loading. While the GRP moduli were, on average, 3% higher in compression than in in tension, CFRP moduli were 15% lower. The secant moduli of hybrids do obey the rule of mixtures as long as the tensile ROM is defined by the tensile moduli of GRP and CFRP, and similarly for the compressive ROM.

The tangent modulus of CFRP increases considerably with tensile strain, while that of GRP decreases slightly. The tangent modulus of CFRP decreases considerably with compressive strain while that of GRP shows no appreciable change. The relationships defining the variation in tangent modulus are continuous from negative (compressive) strains through zero to positive (tensile) strains. Contrary to some reports, the results show that not only does modulus obey the ROM but that it obeys it throughout the strain range. The modulus of a hybrid specimen can be considered to be an average of the moduli of the GRP constituents <u>at the same strain</u>. It is likely that the non-ROM moduli have been reported because the variation in modulus with respect to strain has not been considered, causing some confusion in the results.

The variation in the CFRP elastic modulus is a result of the variation in the fibre modulus with respect to strain. This is due to the fibres' complex internal structure. The decreasing modulus of GRP with respect to tensile strain is the result of local debonding.

(This is an irreversible process and cannot strictly be defined as a variation in modulus).

6.2 TENSILE FAILURE

Glass fibres form weaker bonds with both the epoxy and vinyl ester resins used in this work than do the carbon fibres. In addition to this, the fibre-resin bonds formed by both of the vinyl ester resins are poorer than those of the epoxies in both GRP and CFRP laminates. The weaker bond formed by the vinyl-ester composites does not adversely affect the ultimate tensile strength.

The weaker bonds in the GRP laminates cause some initial, pre-failure debonding. The extent of this debonding affects the mechanism of failure propagation through the composite. This internal debonding before ultimate failure is an important consideration as a design criterion, for damage may be occurring at low loads even though the UTS is unaffected. A model for tensile failure is presented in which the bond strength determines the extent of the pre-failure debonding.

The ROM describes the tensile strength of monofibre composites if the fibre strength value is adjusted by a K factor. This K factor is effectively a measure of fibre surface damage. For the composite systems analysed the K factors have been calculated:

In CFRP $K = 0.85$

In GRP $K \leqslant 0.6$

The GRP K factor exhibited greater variability than that of CFRP.

Tensile failure mechanisms in hybrid composites resemble those in the parent materials. Individual layers in hybrids fail in a

similar manner to the respective monofibre composites. This is true even though the strains at which failure occurs are greater than those of CFRP alone.

6.3 COMPRESSIVE FAILURE

Many different mechanisms of failure can occur in the compression of undirectional fibre composites. In the GRP and CFRP systems studied four different mechanisms of compressive failure have been identified:

i) splitting due to Poisson expansion (GRP - vinyl ester and epoxy)
ii) kink-bands due to restriction of transverse expansion (GRP - vinyl ester and epoxy)
iii) fibre and matrix shear failure (CFRP - epoxy)
iv) fibre microbuckling (CFRP - vinyl ester).

The "best" compressive strengths are exhibited by the CFRP epoxy laminates in which shear failure occurs. In this mode strength is limited only by defects within the fibres.

The microbuckling mode of failure in the vinyl-ester CFRP composites occurs, even at room temperature, because fibre misalignment defects cause buckling instabilities at stresses below the shear strength. In the systems analysed, this resulted in a 40% reduction in strength from that of the epoxy CFRP and a greater amount of scatter. They were the lowest strengths recorded in either tension or compression. The buckling wavelength is constant, characteristic of the CFRP materials. It can be estimated from the height of steps visible in the fracture surface. In the vinyl-ester CFRP, the

microbuckling wavelength was estimated to be 0.08 mm. Because this mode of failure is initiated by misalignment defects, the measured strengths are very much lower than the Rosen[44] theory.

The tensile failure results show that glass fibres are more susceptible to surface damage than carbon fibres, making them weaker and thus directly affecting the composite UTS to a greater extent. The compressive failure study however, shows that fibre misalignment defects have the most significant effect in the vinyl ester CFRP composites, reducing compressive strength considerably.

Weaker fibre-resin bond strength results in a significant amount of debonding in both failure modes active in GRP specimens. The compressive strength of GRP is limited by its transverse tensile strength. Failure occurs in this mode due to Poisson's expansion. In cases where lateral displacement is restricted (such as failure initiation between the end tabs) failure propagation occurs by means of kink-bands rather than the splitting which is usually observed. The compressive strength has no dependence on whether the kink-band formation or splitting failure mode occurs. The transverse tensile strength criterion of failure therefore holds true for all GRP specimens.

Glass fibre kink-bands and carbon fibre microbuckling failures always occur at an angle of 70° to the fibre axis, suggesting that this angle is not a function of fibre/matrix parameters, but that it is a characteristic of buckling failure due to axial compressive load.

Increasing the width of the Celanese compressive specimens to 10 mm results in better compressive strengths being observed. Compressive

strengths however are lower than tensile strengths even when the fibre and matrix shear mode of compressive failure occurs. This is a result of stress intensities of approximately 1.26 occurring in the compressive specimens as a function of specimen geometry and test fixture.

Compressive failure mechanisms in hybrid laminates closely resemble those in the respective monofibre composites. Individual layers fail in a similar manner to the parent materials even though the strains are greater than those of CFRP alone.

6.4 THE HYBRID EFFECT

It has been confirmed that in unidirectional glass/carbon hybrid composites tested in tension a positive hybrid effect occurs. The results show that a similar effect occurs in compression, with compressive failure strains of hybrids exceeding those of CFRP. The hybrid effect in both tension and compression is dependent upon:

i) the ratio V_{fc}/V_{ft}
ii) the order in which the individual plies occur in the laminate (whether GRP or CFRP occurs in the outer layers)

The compressive hybrid effect is also dependent upon a third factor:
iii) the nature of the matrix/composite system into which the fibres are laid up when different mechanisms of CFRP failure result from different resin matrices.

The greatest hybrid effects occurred in the vinyl ester composites in compression. The results did not indicate that the hybrid effect has any dependence upon the number of plies in the laminate.

The difference in failure strain between laminates with GRP outer layers and those of the same V_{fc}/V_{ft} ratio with CFRP outer layers, can be quantified by the equation:

statistical analysis? experimental response?

$$y = Ae^{Bx}$$

where y = difference in failure strain between laminates with GRP outer layers and those with CFRP outer layers

x = variable ratio V_{fc}/V_{ft}

A,B are constants

For the 913 composites analysed:

A = 0.45 (% strain) in tension

0.55 (% strain) in compression

B = -4

The failure strains of hybrid composites can be characterised in terms of the ratio V_{fc}/V_{ft} by the equation

$$y = Ae^{Bx} + Cx + D$$

where y = failure strain difference ?

x = variable-ratio V_{fc}/V_{ft}

A,B,C,D are constants

P.T.O.

This has been done for the 913 composite system for both tensile and compressive failure, and individually for laminates with GRP outer layers and those with CFRP outer layers. If the modulus is similarly defined by the equation

$$y = Ex + F$$

where y = elastic modulus

x = variable ratio V_{fc}/V_{ft}

E,F are constants

then the product

$$z = (Ae^{Bx} + Cx + D)\ (Ex + F)$$

approximately defines the strength of the hybrid system.

6.5 RESIN EFFECTS

The performances of 411-45 and 470-36 vinyl ester resin glass/carbon composites have been assessed in comparison with 913 and 914 epoxy resin composites with similar reinforcement.

While the vinyl-esters form poorer bonds with the fibres than do the epoxies, this does not affect performance because:

i) in tension composite strength is dominated mainly by fibre strength

ii) in CFRP compressive properties debonding does not play a major role

iii) in GRP compressive properties resin failure dictates the transverse tensile strength criterion.

The most significant difference between the composite systems under analysis is that the vinyl esters demonstrate poor CFRP compressive strength, with a different mode of failure from that of the epoxy CFRP occurring. In the specimens used in this work, this was due mainly to the difference in method of manufacture of the composite

laminates. The hybrid effect has not been shown to be affected by the actual resin type except where a different type of composite system results in a different mode of failure. The change in CFRP compressive failure mode from shear in the epoxies to microbuckling in the vinyl-esters results in lower empirical values of failure strain but greater hybrid effects.

The use of either epoxy or vinyl-ester resin as a matrix material has no significant effect on the composite's elastic modulus.

The use of vinyl esters as a matrix for glass/carbon fibre reinforcement is an effective replacement for epoxy resin matrices. The quality of laminates produced is however a very important consideration especially if compressive properties are to be exploited. The method of preparation of the vinyl ester laminates requires some improvement before their performance will fully match that of the epoxies. The poor vinyl-ester CFRP compressive strength must be weighed against other considerations such as improved chemical resistance for appropriate decisions to be made regarding the most suitable matrix material in design considerations.

CHAPTER 7

FURTHER WORK

To continue the study of tensile failure it is suggested that a close examination of the various stages of tensile failure during the test be carried out. This would be helpful in gaining understanding of the mechanisms involved. It would involve stopping some of the tests before final fracture in order to assess the internal damage. A greater amount of information could be gained using techniques such as acoustic emission, electronic speckle pattern interferometry, or sound image analysis.

It is clear that different mechanisms of failure occur in compression. Rosen's microbuckling theory of compressive strength[44] did not predict a linear variation of strength with volume fraction. While a microbuckling mode of failure has been identified, a linear strength relationship with V_f is usually reported. It is suggested that a programme of study investigating the relationship between compressive strength and fibre volume fraction for different composite systems and mechanisms of failure would give helpful insight into the parameters which control the failure mechanisms observed. Martinez et al's[55] linear strength vs volume fraction relationship broke down at $V_f = 0.4$ suggesting a possible change of failure mode. It is therefore believed that the results must be related to the observed failure mechanisms to be of any value.

The more extensive analysis of hybrids of various V_{fc}/V_{ft} ratios is limited in this work to the 913 system because time did not allow tests on all V_{fc}/V_{ft} ratios to be carried out with all four matrix material systems. Further tests using different matrix materials and

a whole range of glass:carbon ratios would give a more complete picture.

If a 16 layer laminate is to remain symmetrical, the lowest nominal V_{fc}/V_{ft} ratio that can be obtained is 0.125. Increasing the number of layers to 17 would enable a symmetrical laminate to be made with a V_{fc}/V_{ft} ratio of 0.06. Tests carried out using such a lay-up would reveal a clearer picture of the hybrid effect since it is at the very low values of V_{fc}/V_{ft} that the synergistic increases in strain are the greatest. Particular emphasis should be paid to the study of compressive failure in laminates of very low carbon content with the CFRP layer in the centre, for which the current results indicate a trend towards failure strains even greater than that of pure GRP.

Merrall and Stolton[93] carried out a series of tensile, compressive and inter-laminar shear strength tests on composites with a wide range of resin properties, and concluded that these simple test methods generated only a narrow range of results. They suggested that more searching tests, such as compressive or fatigue, be employed to provide results which may better distinguish between the resin systems. The compressive tests carried out have indeed shown a significant difference in performance between vinyl ester and epoxy matrices albeit probably only a result of different manufacturing techniques. It is suggested that the continuation of this work may include some controlled variation in environmental conditions. The results must constantly be related to the observed failure mechanisms.

A method of characterising failure strain in hybrids has been introduced in which failure properties are defined using four mathematical constants for each composite system. Suggested further work may involve relating changes of failure mode to the mathematical constants. Hybrid performance of different composite systems may then be easily defined and predicted from a rudimentary knowledge of the failure mechanisms which may be expected to occur.

REFERENCES

1. Phillips, L.N.
   The Hybrid Effect - Does it Exist? Composites, January 1976, pp 7-8.

2. Marom, G., Fischer, S., Tuler, F.R. and Wagner, H.D.
   Hybrid Effects in Composites: Conditions for Positive or Negative Effects Versus Rule of Mixtures Behaviour. Journal of Materials Science 13 (1978) pp 1419-1426.

3. Parkyn B.
   Chemistry of Polyester Resins. Composites Jan/Feb 1972, pp 29-33.

4. Parker, D.B.V.
   Polymer Chemistry. Applied Science Publishers Ltd (1974).

5. Driver, W.E.
   Plastics, Chemistry and Technology. Publ. Van Nostrand Reinhold Company (1979).

6. Pritchard, G.
   Developments in Reinforced Plastic - 1. Applied Science Publishers (1980).

7. Garnish, E.W.
   Chemistry and Properties of Epoxide Resins. Composites, May 1972, pp 104-111.

8. Moore, W.R.
   An Introduction to Polymer Chemistry. University of London Press Ltd (1963).

9. Rhoades, G.
The Development and Mechanical Testing of Both Hybridised and Non-Hybridised Fibre Composites for Helicopter Applications. Progress Report, Dept. Materials Eng. and Design, Loughborough University, Nov. 1984.

10. Scola, D.A.
Novel Curing Agents for Epoxy Resins. Developments in Reinforced Plastics - 4. Ed. by Pritchard, G. Elsevier Applied Science Publishers (1984), Chapter 5, pp 225-241.

11. Ciba-Geigy Bonded Structures Div.
Personal communication, Aug. 1987.

12. Varco, P. and Seamark, M.J.
Vinyl Ester Resins. RPG Conference, Sept. 1973, Paper 3.

13. Vinyl Ester Resins for Chemical Plant and Pipes.
Reinforced Plastics, April 1973, pp 106-107.

14. Vetters, C.M.
Derakane Vinyl Ester Resins Show Improved Chemical Resistance for Corrosion Control. 25th Ann. Tech. Conf. 1970. RP/Comp. Div, the Society of the Plastics Industry, Inc.

15. Phillips, L.N. and Murphy, D.J.
Vinyl Esters as a Matrix for Carbon Fibre Laminates. RAE Tech. Memo MAT 201, 1974.

16. Derakane Vinyl Ester Resins.
General Bulletin. Dow Chemical Co. (UK) Information Bulletin EU 3633-E-876-R.

17. Kelly, A.
Strong Solids. Clarendon Press, Oxford (1966), Chapter 2, pp 121-166.

18. Flinn, R.A. and Trojan, P.K.
Engineering Materials and their Applications. Publ. by Houghton Mifflin Co. Boston (1986) Chapter 11.

19. Design Data - Fibreglass Composites.
Fibreglass Ltd, Reinforcements Div. St Helens.

20. Parratt, N.J.
Defects in Glass Fibres and their Effect on the Strength of Plastic Mouldings. Rubber Plastics Age, March 1960, pp 263-266.

21. Rosen, B.W.
Tensile Failure of Fibrous Composites. Journal of the American Institute of Aeronautics and Astronautics 2 (1964) pp 1985-1991.

22. Rosen, B.W.
Mechanics of Composite Strengthening - Tensile Strength. Fibre Composite Materials. Sem. of the American Soc. for Metals (1964) pp 37-58.

23. Zweben, C.
Tensile Failure of Fibre Composites. AIAA Journal Vol. 6 (1968) No. 12, pp 2325-2331.

24. Zweben, C. and Rosen, B.W.
A Statistical Theory of Material Strength with Application to Composite Materials. Journal of Mech. Phys. Solids 18 (1970) pp 189-206.

25. Gücer, D.E. and Gurland, J.
Comparison of the Statistics of Two Fracture Modes. Journal of Mech. Phys. Solids 10 (1962) pp 365-373.

26. Hedgepeth, J.M. and Van Dyke, P.
Local Stress Concentrations in Imperfect Filamentary Composite Materials. Journal of Composite Materials 1 (1967) pp 294-309.

27. Harris, B.
The Strength of Fibre Composites. Composites 3 (1972) pp 152-167.

28. Fuwa, M., Bunsell, A.R. and Harris, B.
Tensile Failure Mechanisms in Carbon Fibre Reinforced Plastics. Journal of Materials Science 10 (1975) pp 2062-2070.

29. Fukuda, H. and Kawata, K.
On the Strength Distribution of Unidirectional Fibre Composites. Fibre Science and Technology 10 (1977) pp 53-63.

30. Barry, P.W.
The Longitudinal Tensile Strength of Unidirectional Fibrous Composites. Journal of Materials Science 13 (1978) pp 2177-2187.

31. Hayashi, T.
On the Improvement of Mechanical Properties of Composites by Hybrid Composition. Proc. of 8th Int. RP Group Conf. 1972 pp 149-152.

32. Bunsell, A.R. and Harris, B.
Hybrid Carbon and Glass Fibre Composites. Composites, July 1974, pp 157-164.

33. Aveston, J. and Sillwood, J.M.
Synergistic Fibre Strengthening in Hybrid Composites. Journal of Materials Science 11 (1976) pp 1877-1883.

34. Zweben, C.
Tensile Strength of Hybrid Composites. Journal of Materials Science 12 (1977) pp 1325-13

35. Lovell, D.R.
Hybrid Laminates of Glass/Carbon Fibres - 1. Reinforced Plastics, July 1978, pp 216-221.

36. Summerscales J. and Short, D.
Carbon Fibre and Glass Fibre Hybrid Reinforced Plastics. Composites, July 1978, pp 157-166.

37. Fischer, S., Marom, G. and Tuler, F.R.
Hybrid Effects in Composites: A Comparison Between Interlaminar and Translaminar Configurations. Journal of Materials Science 14 (1979) pp 863-868.

38. Xing, J., Hsiao, G.C. and Chou, T-W.
A Dynamic Explanation of the Hybrid Effect. Journal of Composite Materials 15 (1981) pp 443-461.

39. Fukuda, H.
An Advanced Theory of the Strength of Hybrid Composites. Journal of Materials Science 19 (1983) pp 974-982.

40. Richardson, M.O.W. and Richmond, K.M.
Vinyl Ester Hybrid Composites. 39th Ann RP/Comp Inst. Conf. January 1984, Session 16-E.

41. Phillips, M.G.
Composition Parameters for Hybrid Composite Materials. Composites, April 1981, pp 113-116.

42. Phillips, M.G.
On Composition Parameters for Hybrid Composite Materials. In reply to a letter by Wagner, H.D. and Marom, G. Composites, January 1982, pp 18-20.

43. Woolstencroft, D.H., Curtis, A.R. and Haresceugh, R.I.
A Comparison of Test Techniques Used for the Evaluation of the Unidirectional Compressive Strength of Carbon Fibre Reinforced Plastic. Composites, October 1981, pp 275-280.

44. Rosen, B.W.
Mechanics of Composite Strengthening - Compressive Strength. Fibre Composite Materials. Sem of the American Soc. for Metals (1964) pp 58-65.

45. Foye, R.L.
Compression Strength of Unidirectional Composites. AIAA Third Aerospace Sciences Mtg, NY, USA (1966) Paper 66-143.

46. Hayashi, T.
Compression Strength of Unidirectionally Fibre Reinforced Composite Materials. 7th Int. RP Conf. Brighton, UK (1970) Paper 11.

47. Hayashi, T. and Koyama, K.
Theory and Experiments of Compressive Strength of Unidirectionally Fibre-Reinforced Composite Materials. Proc. of Int. Conf. on Mechanical Behaviour of Materials (1971) Vol. V.

48. Argon, A.S.
Fracture of Composites. Treatise on Materials Science and Technology, ed. by Herman, H. Academic Press, 1972, pp 79-114.

49. Ewins, P.D. and Ham, A.C.
The Nature of Compressive Failure in Unidirectional Carbon Fibre Reinforced Plastics. RAE Tech. Report 73057 (1973).

50. Greszczuk, L.B.
Compressive Strength and Failure Modes of Unidirectional Composites. Analysis of the Test Methods for High Modulus Fibres and Composites. ASTM STP 521 (1973) pp 192-217.

51. Hancox, N.L.
The Compression Strength of Undirectional Carbon Fibre Reinforced Plastic. Journal of Materials Science 10 (1975) pp 234-242.

52. Chaplin, C.R.
Compressive Fracture in Unidirectional Glass Reinforced Plastics. Journal of Materials Science 12 (1977) pp 347-352.

53. Piggott, M.R. and Harris, B.
Compression Strength of Carbon, Glass and Kevlar-49 Fibre Reinforced Polyester Resins. Journal of Materials Science 15 (1980) pp 2523-2538.

54. Hull, D.
An Introduction to Composite Materials. Cambridge University Press (1981). Chapter 7.

55. Martinez, G.M., Piggott, M.R., Bainbridge, D.M.R. and Harris B.
The Compression Strength of Composites with Kinked, Misaligned and Poorly Adhering Fibres. Journal of Materials Science 16 (1981) pp 2831-2836.

56. Piggott, M.R.
A Theoretical Framework for the Compressive Properties of Aligned Fibre Composites. Journal of Materials Science 16 (1981) pp 2837-2845.

57. Piggott, M.R.
Compressive Properties of Resins and Composites. Developments in Reinforced Plastics - 4 ed. by Pritchard, G. Elsevier Applied Science Publishers (1984) Chapter 4, pp 131-163.

58. Parry, T.V. and Wronski, A.S.
Kinking and Tensile, Compressive and Interlaminar Shear Failure in Carbon-Fibre-Reinforced Plastic Beams Tested in Flexure. Journal of Materials Science 16 (1981) pp 439-450.

59. Parry, T.V. and Wronski, A.S.
Kinking and Compressive Failure in Uniaxially Aligned Carbon Fibre Composites Tested Under Superposed Hydrostatic Pressure. Journal of Materials Science 17 (1982) pp 893-900.

60. Dukes, R. and Griffiths, D.L.
Marine Aspects of Carbon-Fibre and Glass-Fibre/Carbon Fibre Composites. Proc. Int. Conf. on Carbon Fibres, the Plastics Inst., London (1971) Paper No. 28.

61. Kalnin, I.L.
Evaluation of Unidirectional Glass-Graphite Fibre/Epoxy Resin Composites. Composite Materials - Testing and Design (2nd Conf) ASTM STP 497 (Feb. 1972) pp 551-563.

62. Piggott, M.R. and Harris, B.
Compression Strength of Hybrid Fibre Reinforced Plastics. Journal of Materials Science 16 (1981) pp 687-693.

63. Swift, D.G.
Elastic Moduli of Fibrous Composites Containing Misaligned Fibres. Journal of Phys. D 8 (1975) pp 223-240.

64. Curtis, G.J., Milne, J.M.and Reynolds, W.N.
Non-Hookean Behaviour of Strong Carbon Fibres. Nature 220 (1968) pp 1024-1025.

65. Johnson, D.J.
The Microstructure of Various Carbon Fibres. Proc. Int. Conf. on Carbon Fibres, The Plastics Inst. London (1971) Paper 8.

66. Fourdeux, A., Perret, R. and Ruland, W.
General Structural Features of Carbon Fibres Proc. Int. Conf. on Carbon Fibres, The Plastics Inst. London (1971) Paper 9.

67. Johnson, W.
On the Measurement of the Youngs Modulus of Carbon Fibres. RAE Tech. Memo. MAT 332, April 1980.

68. Dootson, M.
The Development of Unidirectional CFRP Test Specimens. British Aircraft Corporation Report SOR (P)88. December 1973.

69. Fibreglass Weaving, Winding, Pultrusion Rovings.
Fibreglass Ltd, Reinforcements Div. Product Sheet FPL 420.

70. Continuous Fibres Grafil XA-S.
Courtaulds ltd, Carbon Fibres Div. Data Sheet FC 13/XA 1.

71. Fibredux 913.
Ciba Geigy Information Sheet FTA 46d (May 1983).

72. Fibredux 914.
Ciba Geigy Information Sheet FTA 49c (Sept. 1979).

73. Derakane 470 Vinyl Ester Resins.
Dow Chemical Co. (UK) Information Bulletin EU 3616-E-881.

74. Vydax Fluorotelomer Dispersions.
E.I. Du Pont de Nemours and Co (Inc) Product Information Bulletin.

75. Standard Test Method for Compressive Properties of Unidirectional or Crossply Fibre-Resin Composites. ASTM D 3410-75.

76. Storage and Handling of Derakane Vinyl Ester Resins. Dow Chemical Co. (UK) Information Bulletin EU 3634-E-679.

77. Derakane Resins Fabricating Tips. Dow Chemical Co. (UK) Information Bulletin. Form No. 296-315-781.

78. Tensile Strength, Elongation and Elastic Modulus. BS 2782: Part 3: Method 320E: 1976.

79. Determination of Apparent Interlaminar Shear Strength of Reinforced Plastics. BS 2782: Part 3: Method 341A: 1977.

80. Haynes, W.M. and Tolbert, T.L. Determination of Graphite Fibre Content of Plastic Composites. Journal of Composite Materials 3 (Oct. 1969) pp 709-712.

81. Harper, J.F. and Naeem, M. The Effect of Temperature and Humidity on Glass Fibre Reinforced Vinyl Ester Resin. Proc. of the BPF RP Group 14th RP Congress, Brighton (Nov. 1984) Paper 38.

82. Naeem, M. The Resistance of Glass Reinforced Thermosetting Polymers to Thermohumid Conditions. PhD Thesis, Loughborough University (1985).

83. Kühl, H. Strain Gauges Theory and Handling. Philips Elektronik Industrie GmbH - Hamburg, MMA Department. Chapter 4.

84. Strain Gauge Applications with M-Bond AE-10/15 and M-Bond GA-2 Adhesive Systems. M-Line Accessories, Micro Measurements Div. Instruction Bulletin B-137-11.

85. Moghisi, M.
Acoustic Emission and Sound Imaging Analysis of Hybrid Composites. Progress Report. Dept. of Materials Engineering and Design, Loughborough University, April 1987.

86. Mascia, L.
The Role of Additives in Plastics. Publ. by Arnold (1974) Chapter 3.

87. Weaver, C.W. and Williams, J.G.
Deformation of a Carbon-Epoxy Composite Under Hydrostatic Pressure. Journal of Materials Science 10 (1975) pp 1323-1333.

88. Lee, R.J.
Compression Strength of Aligned Carbon Fibre-Reinforced Thermoplastic Laminates. Composites 18 (Jan. 1987) pp 35-39.

89. Richmond, K.M.
The Characterisation and Mechanical Properties of a Series of Fibrous Hybrid Composites. PhD Thesis, Loughborough University (1983).

90. Hawthorne, H.M. and Teghtsoonian, E.
Axial Compression Fracture in Carbon Fibres. Journal of Materials Science 10 (1975) pp 41-51.

91. Richardson, M.O.W. and Saidpour, S.H.
Mechanical Properties of Vinyl Ester Composites - the Role of E-Glass Treatment. BPF RP Congress, Nottingham (Sept. 1986) Paper 30.

92. Harris, B.
Engineering Composite Materials. Publ. by The Institute of Metals, 1986. Chapter 3.

93. Merrall, G.T. and Stolton, R.E.
The Influence of Epoxy Resin Matrix Properties on the Performance of Carbon-Fibre Composites. 1st Conf. on Carbon Fibres, The Plastics Inst. London (1971) Paper 22.

94. Chatfield, C.
Statistics for Technology. Publ. by Chapman and Hall, 1970. pp 140-146.

TABLES

TABLE 1: PROPERTIES OF THE GLASS FIBRES

Type of glass fibre	E
Density (kgm^{-3})	2.55×10^3
Filament diameter (μm)	13
Modulus of elasticity (GPa)	71
Tensile strength - virgin filament (GPa)	3.4
Tensile strength - roving (GPa)	2.4
Elongation (%)	3.37
Coefficient of thermal expansion (K^{-1})	5×10^{-6}
Mass/unit length of tow (mgm^{-1})	600

TABLE 2: PROPERTIES OF THE CARBON FIBRES

Type of carbon fibre	XA-S
Density (kgm^{-3})	1.81×10^3
Filament diameter (μm)	7.2
Tensile modulus (GPa)	225
Tensile strength - virgin filament (GPa)	3.43
Tensile strength - roving (GPa)	2.90
Elongation (%)	1.44
Coefficient of thermal expansion (K^{-1})	-1.0×10^{-6}
Mass/unit length of tow (mgm^{-1})	730

TABLE 3: THE EPOXY RESIN PREPREG COMPRESSION MOULDING CURE CONDITIONS

			913	914
Cure conditions:	temperature	(^{o}C)	140	175
	pressure	(kNm^{-2})	2000	2000
	duration	(min)	20	60
Post-cure:	temperature	(^{o}C)	-	190
	duration	(min)	-	240

TABLE 4: THE VINYL ESTER RESIN CURING SYSTEM

		411-45	470-36
Resin	(g)	100	100
MEKP 50%	(cm^3)	1.67	1.67
Cobalt Octoate 6%	(cm^3)	0.267	0.267
Dimethyl Anilene 10%	(cm^3)	0.05	0.05
Gel time - approx	(cm^3)	45	35
Cure conditions		24 hrs, RT	24 hrs, RT
Post-cure		2 hrs, $80^{o}C$	2 hrs, $80^{o}C$

TABLE 5: PROPERTIES OF THE CURED RESINS

	913	914	411-45	470-36
Density (kg/m^3)	1.23×10^3	1.3×10^3	1.14×10^3	1.17×10^3
Tensile modulus (GPa)	3.39	3.3	3.37	3.53
Tensile strength (MPa)	65.5		81.4	73.6
Elongation (%)			5	3-4

TABLE 6: DETAILS OF THE STRAIN GAUGES USED IN THE COMPRESSIVE TESTS

Type	Metal foil
Suppliers description	FLA-3-11
Gauge length (mm)	3
Gauge resistance (Ω)	120 ± 0.3
Gauge factor	2.12
Supplier	Techni Measure

TABLE 7: RESULTS OF RESIN DENSITY MEASUREMENT

Resin		411-45	470-36
Density measured:	1	1.1354	1.1720
(x 10^3 kgm^{-3})	2	1.1347	1.1783
	3	1.1391	1.1798
	4	1.1427	1.1680
	5	1.1345	1.1664
	6	1.1367	1.1774
	7	1.1348	1.1822
	8	1.1441	1.1725
	9	1.1403	1.1704
	10	1.1332	1.1750
	Average	1.138	1.174
	SD	0.00378	0.00521
	CV (%)	0.33	0.44

TABLE 8: SECANT MODULUS RESULTS DEMONSTRATING THE EFFECT OF USING EITHER ONE OR TWO STRAIN GAUGES ON EACH COMPRESSIVE SPECIMEN

	Specimen	Secant Modulus (GPa)	Average	~~SD~~	~~CV (%)~~
	1	40.21			
Single	2	55.49	46.44	~~7.20~~	~~15.5~~
Gauge	3	41.10			
Side A	4	48.97			
	1	48.86			
Single	2	37.88	46.31	~~5.67~~	~~12.2~~
Gauge	3	50.11			
Side B	4	48.39			
Two	1	41.47			
Gauges	2	41.67	43.52	~~2.60~~	~~6.0~~
Sides	3	47.07			
A and B	4	43.86			

TABLE 9: PRIMARY TENSILE FAILURE STRAIN RESULTS, 913 MATRIX

Lay-up	V_{fg}	V_{fc}	V_m	Strain (%)	CV (%)
G_8/G_8	68.1	0	31.9	2.81	15.1
C_8/C_8	0	63.9	36.1	1.33	9.4
G_4C_4/C_4G_4	31.1	33.6	35.3	1.55	4.6
C_4G_4/G_4C_4	30.6	34.6	34.8	1.49	3.7
G_6C_2/C_2G_6	50.0	16.7	33.3	1.65	1.7
C_6G_2/G_2C_6	16.2	49.2	34.6	1.49	4.7
G_2C_6/C_6G_2	15.8	49.1	37.1	1.54	5.6
C_2G_6/G_6C_2	47.5	17.5	35.0	1.47	8.9
G_7C/CG_7	57.6	8.3	34.1	1.92	7.2
CG_7/G_7C	59.9	8.8	31.3	1.65	5.1
$G_2C_4G_2/G_2C_4G_2$	30.9	34.9	34.2	1.49	9.9
$C_2G_4C_2/C_2G_4C_2$	30.8	34.4	34.8	1.42	9.6

TABLE 10: PRIMARY TENSILE FAILURE STRAIN RESULTS, 914 MATRIX

Lay-up	V_{fg}	V_{fc}	V_m	Strain (%)	CV (%)
G_8/G_8	71.0	0	29.0	2.62	5.2
C_8/C_8	0	69.0	31.0	0.90	5.1
G_4C_4/C_4G_4	36.1	34.5	29.4	0.94	5.3
C_4G_4/G_4C_4	35.9	35.0	29.1	1.00	12.9
$G_2C_4G_2/G_2C_4G_2$	35.3	35.9	28.8	1.03	9.9
$C_2G_4C_2/C_2G_4C_2$	35.5	35.1	29.4	0.95	9.9

TABLE 11: PRIMARY TENSILE FAILURE STRAIN RESULTS, 411-45 MATRIX

Lay-up	V_{fg}	V_{fc}	V_m	Strain (%)	CV (%)
G_8/G_8	58.9	0	41.1	2.28	8.0
C_8/C_8	0	54.7	45.3	1.28	8.3
G_4C_4/C_4G_4	27.1	26.7	46.2	1.44	11.0
C_4G_4/G_4C_4	28.3	27.3	44.4	1.46	15.1
$G_2C_4G_2/G_2C_4G_2$	28.3	27.1	44.6	1.61	11.1
$C_2G_4C_2/C_2G_4C_2$	28.3	26.1	45.6	1.50	10.7

TABLE 12: PRIMARY TENSILE FAILURE STRAIN RESULTS, 470-36 MATRIX

Lay-up	V_{fg}	V_{fc}	Vm	Strain (%)	CV (%)
G_8/G_8	56.1	0	43.9	2.80	10.5
C_8/C_8	0	55.4	44.6	1.33	11.8
G_4C_4/C_4G_4	29.7	27.4	42.9	1.42	15.0
C_4G_4/G_4C_4	30.2	27.2	42.6	1.52	14.3
$G_2C_4G_2/G_2C_4G_2$	28.0	27.8	44.2	1.59	15.3
$C_2G_4C_2/C_2G_4C_2$	29.5	27.6	42.9	1.48	9.2

TABLE 13: ULTIMATE TENSILE STRENGTH RESULTS, 913 MATRIX

Lay-up	V_{fg}	V_{fc}	Vm	UTS (MPa)	CV (%)
G_8/G_8	68.1	0	31.9	1257	13.5
C_8/C_8	0	63.9	36.1	1779	7.5
G_4C_4/C_4G_4	31.1	33.6	35.3	1506	4.4
C_4G_4/G_4C_4	30.6	34.6	34.8	1362	5.2
G_6C_2/C_2G_6	50.0	16.7	33.3	1120	4.0
C_6G_2/G_2C_6	16.2	49.2	34.6	1524	4.8
G_2C_6/C_6G_2	15.8	47.1	37.1	1495	3.7
C_2G_6/G_6C_2	47.5	17.5	35.0	1037	4.6
G_7C/CG_7	57.6	8.3	34.1	979	2.3
CG_7/G_7C	59.9	8.8	31.3	874	2.2
$G_2C_4G_2/G_2C_4G_2$	30.9	34.9	34.2	1364	10.8
$C_2G_4C_2/C_2G_4C_2$	30.8	34.4	34.8	1311	11.7

TABLE 14: ULTIMATE TENSILE STRENGTH RESULTS, 914 MATRIX

Lay-up	V_{fg}	V_{fc}	Vm	UTS (MPa)	CV (%)
G_8/G_8	71.0	0	29.0	1135	3.9
C_8/C_8	0	69.0	31.0	1204	4.4
G_4C_4/C_4G_4	36.1	34.5	29.4	828	6.6
C_4G_4/G_4C_4	35.9	35.0	29.1	982	6.6
$G_2C_4G_2/G_2C_4G_2$	35.3	35.9	28.8	956	2.6
$C_2G_4C_2/C_2G_4C_2$	35.5	35.1	29.4	935	7.8

TABLE 15: ULTIMATE TENSILE STRENGTH RESULTS, 411-45 MATRIX

Lay-up	V_{fg}	V_{fc}	Vm	UTS (MPa)	CV (%)
G_8/G_8	58.9	0	41.1	1094	7.6
C_8/C_8	0	54.7	45.3	1740	8.0
G_4C_4/C_4G_4	27.1	26.7	46.2	1528	8.9
C_4G_4/G_4C_4	28.3	27.3	44.4	1359	8.9
$G_2C_4G_2/G_2C_4G_2$	28.3	27.1	44.6	1537	6.7
$C_2G_4C_2/C_2G_4C_2$	28.3	26.1	45.6	1385	8.8

TABLE 16: ULTIMATE TENSILE STRENGTH RESULTS, 470-36 MATRIX

Lay-up	V_{fg}	V_{fc}	V_m	UTS (MPa)	CV (%)
G_8/G_8	56.1	0	43.9	1313	7.8
C_8/C_8	0	55.4	44.6	1768	6.9
G_4C_4/C_4G_4	29.7	27.4	42.9	1457	5.9
C_4G_4/G_4C_4	30.2	27.2	42.6	1370	10.3
$G_2C_4G_2/G_2C_4G_2$	28.0	27.8	44.2	1521	4.7
$C_2G_4C_2/C_2G_4C_2$	29.5	27.6	42.9	1272	8.9

TABLE 17: COMPRESSIVE FAILURE STRAIN RESULTS, 913 MATRIX

Lay-up	V_{fg}	V_{fc}	V_m	Strain (%)	CV (%)
G_8/G_8	68.1	0	31.9	2.15	8.5
C_8/C_8	0	63.9	36.1	1.13	15.0
G_4C_4/C_4G_4	31.1	33.6	35.3	1.49	4.9
C_4G_4/G_4C_4	30.6	34.6	34.8	1.40	11.9
G_6C_2/C_2G_6	50.0	16.7	33.3	1.77	10.1
C_6G_2/G_2C_6	16.2	49.2	34.6	1.29	13.3
G_2C_6/C_6G_2	15.8	47.1	37.1	1.43	11.1
C_2G_6/G_6C_2	47.5	17.5	35.0	1.58	7.6
G_7C/CG_7	57.6	8.3	34.1	2.12	7.7
CG_7/G_7C	59.9	8.8	31.3	1.81	7.7
$G_2C_4G_2/G_2C_4G_2$	30.9	34.9	34.2	1.57	4.5
$C_2G_4C_2/C_2G_4C_2$	30.8	34.4	34.8	1.58	10.4

TABLE 18: COMPRESSIVE FAILURE STRAIN RESULTS, 914 MATRIX

Lay-up	V_{fg}	V_{fc}	V_m	Strain (%)	CV (%)
G_8/G_8	71.0	0	29.0	2.26	11.5
C_8/C_8	0	69.0	31.0	1.22	13.3
G_4C_4/C_4G_4	36.1	34.5	29.4	1.41	13.0
C_4G_4/G_4C_4	35.9	35.0	29.1	1.36	4.9
$G_2C_4G_2/G_2C_4G_4$	35.3	35.9	28.8	1.48	15.6
$C_2G_4C_2/C_2G_4C_2$	35.5	35.1	29.4	1.52	5.2

TABLE 19: COMPRESSIVE FAILURE STRAIN RESULTS, 411-45 MATRIX

Lay-up	V_{fg}	V_{fc}	V_m	Strain (%)	CV (%)
G_8/G_8	55.4	0	44.6	2.15	19.3
C_8/C_8	0	59.9	40.1	0.71	32.9
G_4C_4/C_4G_4	28.5	29.6	41.9	1.12	18.3
C_4G_4/G_4C_4	28.8	26.2	45.0	1.09	11.8
$G_2C_4G_2/G_2C_4G_2$	30.5	27.1	42.4	1.11	14.2
$C_2G_4C_2/C_2G_4C_2$	28.6	27.9	43.5	1.07	17.1

TABLE 20: COMPRESSIVE FAILURE STRAIN RESULTS, 470-36 MATRIX

Lay-up	V_{fg}	V_{fc}	V_m	Strain (%)	CV (%)
G_8/G_8	62.3	0	37.7	2.23	12.7
C_8/C_8	0	56.0	44.0	0.73	28.2
G_4C_4/C_4G_4	29.3	27.5	43.2	1.17	15.6
C_4G_4/G_4C_4	31.1	26.5	42.4	0.96	19.5
$G_2C_4G_2/G_2C_4G_2$	30.1	26.4	43.5	1.24	17.0
$C_2G_4C_2/C_2G_4C_2$	31.3	27.5	41.2	1.04	21.3

TABLE 21: COMPRESSIVE STRENGTH RESULTS, 913 MATRIX

Lay-up	V_{fg}	V_{fc}	V_m	Comp.Strength (MPa)	CV (%)
G_8/G_8	68.1	0	31.9	1010	8.4
C_8/C_8	0	63.9	36.1	1332	14.2
G_4C_4/C_4G_4	31.1	33.6	35.3	1178	2.8
C_4G_4/G_4C_4	30.6	34.6	34.8	1147	9.6
G_6C_2/C_2G_6	50.0	16.7	33.3	1149	12.4
C_6G_2/G_2C_6	16.2	49.2	34.6	1345	8.4
G_2C_6/C_6G_2	15.8	47.1	37.1	1291	10.4
C_2G_6/G_6C_2	47.5	17.5	35.0	1022	9.8
G_7C/CG_7	57.6	8.3	34.1	1144	11.7
CG_7/G_7C	59.9	8.8	31.3	1003	9.5
$G_2C_4G_2/G_2C_4G_2$	30.9	34.9	34.2	1188	3.8
$C_2G_4C_2/C_2G_4C_2$	30.8	34.4	34.8	1163	6.4

TABLE 22: COMPRESSIVE STRENGTH RESULTS, 914 MATRIX

Lay-up	V_{fg}	V_{fc}	V_m	Comp.Strength (MPa)	CV (%)
G_8/G_8	71.0	0	29.0	1016	11.2
C_8/C_8	0	69.0	31.0	1476	6.8
G_4C_4/C_4G_4	36.1	34.5	29.4	1111	11.8
C_4G_4/G_4C_4	35.9	35.0	29.1	1102	4.7
$G_2C_4G_2/G_2C_4G_2$	35.3	35.9	28.8	1154	14.0
$C_2G_4C_2/C_2G_4C_2$	35.5	35.1	29.4	1184	7.9

TABLE 23: COMPRESSIVE STRENGTH RESULTS, 411-45 MATRIX

Lay-up	V_{fg}	V_{fc}	V_m	Comp.Strength (MPa)	CV (%)
G_8/G_8	55.4	0	44.6	1074	12.0
C_8/C_8	0	59.9	40.1	851	29.5
G_4C_4/C_4G_4	28.5	29.6	41.9	946	15.4
C_4G_4/G_4C_4	28.8	26.2	45.0	813	22.2
$G_2C_4G_2/G_2C_4G_2$	30.5	27.1	42.4	870	14.6
$C_2G_4C_2/C_2G_4C_2$	28.6	27.9	43.5	921	10.8

TABLE 24: COMPRESSIVE STRENGTH RESULTS, 470-36 MATRIX

Lay-up	V_{fg}	V_{fc}	V_m	Comp.Strength (MPa)	CV (%)
G_8/G_8	62.3	0	37.7	1015	14.6
C_8/C_8	0	56.0	44.0	815	20.7
G_4C_4/C_4G_4	29.3	27.5	43.2	1009	16.1
C_4G_4/G_4C_4	31.1	26.5	42.4	837	19.2
$G_2C_4G_2/G_2C_4G_2$	30.1	26.4	43.5	972	14.9
$C_2G_4C_2/C_2G_4C_2$	31.3	27.5	41.2	827	22.2

TABLE 25: TENSILE SECANT MODULUS RESULTS, 913 MATRIX

Lay-up	V_{fg}	V_{fc}	V_m	Modulus (GPa)	CV (%)
G_8/G_8	68.1	0	31.9	45.9	6.2
C_8/C_8	0	63.9	36.1	137.3	2.7
G_4C_4/C_4G_4	31.1	33.6	35.3	96.6	3.8
C_4G_4/G_4C_4	30.6	34.6	34.8	92.5	3.9
G_6C_2/C_2G_6	50.0	16.7	33.3	67.7	3.4
C_6G_2/G_2C_6	16.2	49.2	34.6	110.9	3.1
G_2C_6/C_6G_2	15.8	47.1	37.1	112.1	4.2
C_2G_6/G_6C_2	47.5	17.5	35.0	68.4	3.6
G_7C/CG_7	57.6	8.3	34.1	51.5	5.7
CG_7/G_7C	59.9	8.8	31.3	53.1	4.2
$G_2C_4G_2/G_2C_4G_2$	30.9	34.9	34.2	91.3	5.1
$C_2G_4C_2/C_2G_4C_2$	30.8	34.4	34.8	91.8	3.1

TABLE 26: TENSILE SECANT MODULUS RESULTS, 914 MATRIX

Lay-up	V_{fg}	V_{fc}	V_m	Modulus (GPa)	CV (%)
G_8/G_8	71.0	0	29.0	42.8	6.2
C_8/C_8	0	69.0	31.0	134.5	3.2
G_4C_4/C_4G_4	36.1	34.5	29.4	87.5	4.2
C_4G_4/G_4C_4	35.9	35.0	29.1	92.7	15.9
$G_2C_4G_2/G_2C_4G_2$	35.3	35.9	28.8	93.1	8.1
$C_2G_4C_2/C_2G_4C_2$	35.5	35.1	29.4	93.2	7.8

TABLE 27: TENSILE SECANT MODULUS RESULTS, 411-45 MATRIX

Lay-up	V_{fg}	V_{fc}	V_m	Modulus (GPa)	CV (%)
G_8/G_8	58.9	0	41.1	47.8	4.0
C_8/C_8	0	54.7	45.3	143.0	3.4
G_4C_4/C_4G_4	27.1	26.7	46.2	101.8	9.2
C_4G_4/G_4C_4	28.3	27.3	44.4	96.4	2.5
$G_2C_4G_2/G_2C_4G_2$	28.3	27.1	44.6	98.2	5.1
$C_2G_4C_2/C_2G_4C_2$	28.3	26.1	45.6	96.7	5.8

TABLE 28: TENSILE SECANT MODULUS RESULTS, 470-36 MATRIX

Lay-up	V_{fg}	V_{fc}	V_m	Modulus (GPa)	CV (%)
G_8/G_8	56.1	0	43.9	46.9	4.5
C_8/C_8	0	55.4	44.6	152.6	11.8
G_4C_4/C_4G_4	29.7	27.4	42.9	98.0	1.1
C_4G_4/G_4C_4	30.2	27.2	42.6	93.4	3.5
$G_2C_4G_2/G_2C_4G_2$	28.0	27.8	44.2	96.5	3.2
$C_2G_4C_2/C_2G_4C_2$	29.5	27.6	42.9	88.8	3.9

TABLE 29: COMPRESSIVE SECANT MODULUS RESULTS, 913 MATRIX

Lay-up	V_{fg}	V_{fc}	V_m	Modulus (GPa)	CV (%)
G_8/G_8	68.1	0	31.9	46.7	3.4
C_8/C_8	0	63.9	36.1	121.7	5.4
G_4C_4/C_5G_4	31.1	33.6	35.3	81.1	2.2
C_4G_4/G_4C_4	30.6	34.6	34.8	83.9	1.4
G_6C_2/C_2G_6	50.0	16.7	33.3	65.1	8.56
C_6G_2/G_2C_6	16.2	49.2	34.6	107.9	7.9
G_2C_6/C_6G_2	15.8	47.1	37.1	92.7	4.4
C_2G_6/G_6C_2	47.5	17.5	35.0	65.1	8.3
G_7C/CG_7	57.6	8.3	34.1	55.4	6.9
CG_7/G_7C	59.9	8.8	31.3	56.2	4.4
$G_2C_4G_2/G_2C_4G_2$	30.9	34.9	34.2	77.5	5.0
$C_2G_4C_2/C_2G_4C_2$	30.8	34.4	34.8	76.2	2.5

TABLE 30: COMPRESSIVE SECANT MODULUS RESULTS, 914 MATRIX

Lay-up	V_{fg}	V_{fc}	V_m	Modulus (GPa)	CV (%)
G_8/G_8	71.0	0	29.0	45.0	2.3
C_8/C_8	0	69.0	31.0	129.1	12.4
G_4C_4/C_4G_4	36.1	34.5	29.4	80.8	3.3
C_4G_4/G_4C_4	35.9	35.0	29.1	83.1	6.6
$G_2C_4G_2/G_2C_4G_2$	35.3	35.9	28.8	81.9	3.7
$C_2G_4C_2/C_2G_4C_2$	35.5	35.1	29.4	79.2	7.5

TABLE 31: COMPRESSIVE SECANT MODULUS RESULTS, 411-45 MATRIX

Lay-up	V_{fg}	V_{fc}	V_m	Modulus (GPa)	CV (%)
G_8/G_8	55.4	0	44.6	50.4	8.5
C_8/C_8	0	59.9	40.1	114.6	4.4
G_4C_4/C_4G_4	28.5	29.6	41.9	87.8	14.6
C_4G_4/G_4C_4	28.8	26.2	45.0	86.1	12.3
$G_2C_4G_2/G_2C_4G_2$	30.5	27.1	42.4	80.7	5.2
$C_2G_4C_2/C_2G_4C_2$	28.6	27.9	43.5	85.6	7.7

TABLE 32: COMPRESSIVE SECANT MODULUS RESULTS, 470-36 MATRIX

Lay-up	V_{fg}	V_{fc}	V_m	Modulus (GPa)	CV (%)
G_8/G_8	62.3	0	37.7	47.5	7.2
C_8/C_8	0	56.0	44.0	117.4	10.1
G_4C_4/C_4G_4	29.3	27.5	43.2	92.5	17.2
C_4G_4/G_4C_4	31.1	26.5	42.4	89.5	14.9
$G_2C_4G_2/G_2C_4G_2$	30.1	26.4	43.5	79.8	1.7
$C_2G_4C_2/C_2G_4C_2$	31.3	27.5	41.2	80.3	6.6

TABLE 33: INTER-LAMINAR SHEAR STRENGTH RESULTS FROM VINYL ESTER AND EPOXY-GRP MATERIALS

Resin Matrix	Inter-Laminar Shear Strength (MPa)	CV (%)	V_f
913	90.3	3.0	0.681
914	86.9	8.3	0.710
411-45	69.0	2.4	0.558
470-36	73.5	3.1	0.570

TABLE 34: INTER-LAMINAR SHEAR STRENGTH RESULTS FROM VINYL ESTER AND EPOXY-CFRP MATERIALS

Resin Matrix	Inter-Laminar Shear Strength (MPa)	CV (%)	V_f
913	89.1	8.7	0.639
914	80.3	5.1	0.690
411-45	57.3	2.3	0.547
470-36	53.2	2.7	0.554

TABLE 35: TRANSVERSE TENSILE STRENGTH RESULTS FROM EPOXY-GRP MATERIALS

Resin Matrix	Transverse Tensile Strength (MPa)	CV (%)	V_f
913	62.7	15.6	0.681
914	62.0	14.9	0.704

TABLE 36: TRANSVERSE TENSILE STRENGTH RESULTS FROM EPOXY-CFRP MATERIALS

Resin Matrix	Transverse Tensile Strength (MPa)	CV (%)	V_f
913	54.3	12.7	0.646
914	34.0	13.0	0.686

TABLE 37: POISSON'S RATIO RESULTS FROM 913 GRP AND CFRP MATERIAL

	Poisson's Ratio	CV (%)
GRP	-0.272	2.4
CFRP	-0.314	9.8

TABLE 38: AVERAGE TENSILE AND COMPRESSIVE MODULUS RESULTS FROM GRP AND CFRP COMPOSITES OF THE FOUR RESIN SYSTEMS EMPLOYED

	GRP	(SD)	CFRP	(SD)
Tensile Modulus (GPa)	45.9	(2.2)	141.9	(8.0)
Compressive Modulus (GPa)	47.4	(2.3)	120.7	(6.3)
Ratio $\frac{\text{Compressive Modulus}}{\text{Tensile Modulus}}$	1.03	(0.022)	0.85	(0.086)

TABLE 39: A COMPARISON OF THE SINGLE CARBON FIBRE MODULUS RESULTS OF JOHNSON (from Ref.67) NORMALISED TO REPRESENT A 60% V_f CFRP LAMINATE, WITH THOSE OF 913 CFRP LAMINATES

				Increase
Johnson's results for type II carbon	Load range (g)	0-5	2-10	
	Young's mod (GPa)	227	246	8%
Johnson's results representing a 60% V_f laminate	Equivalent stress range (MPa)	0-540	200-1100	
	Average mod (GPa)	136	148	8%
Observed results 913 60% V_f CFRP	Stress range (MPa)	0-540	200-1100	
	Young's mod (GPa)	128-135	130- 143	4% ave 12% max

TABLE 40: THE K FACTORS OF THE GRP AND CFRP LAMINATES CALCULATED FROM THE TENSILE STRENGTH RESULTS

Laminate Description	K Factor
913 GRP	0.60
914 GRP	0.55
411 GRP	0.52
470 GRP	0.62
913 CFRP	0.86
914 CFRP	0.58
411 CFRP	0.83
470 CFRP	0.85

TABLE 41: EXPECTED VALUES OF LONGITUDINAL COMPRESSIVE STRENGTH OF GRP AND CFRP COMPOSITES USING TRANSVERSE TENSILE STRENGTH AS THE FAILURE CRITERION (STRENGTHS ARE NOT NORMALISED TO REPRESENT 60% FIBRE VOLUME FRACTION)

Material	Predicted Compressive Strength σ_1* (MPa)	Actual Compressive Strength Measured (MPa)	SD
913 GRP	1147	1145	89.7
914 GRP	1097	1202	137.9
913 CFRP	2638	1417	190.4
914 CFRP	1562	1697	115.1

TABLE 42: THE HYBRID EFFECT RESULTING FROM AN INCREASE IN FIBRE VOLUME FRACTION OF CFRP, FROM EQUATION 5.25 BASED ON THE ROSEN THEORY[44] OF FIBRE BUCKLING IN THE SHEAR MODE

Fibre Volume Fraction of CFRP	Expected Hybrid Effect (% increase in failure strain)
0.6	0
0.62	1.95%
0.65	5.70%
0.7	14.71%
0.75	28.70%
0.8	50.97%

TABLE 43: A SUMMARY COMPARISON OF UNIAXIAL STRENGTH RESULTS OBTAINED FROM THE PARENT MATERIAL COMPOSITES

a) Tensile Strengths (MPa)

Matrix Resin	GRP (CV)		CFRP (CV)	
913	1257	(13.5%)	1779	(7.5%)
914	1135	(3.9%)	1204	(4.4%)
411-45	1094	(7.6%)	1740	(8.0%)
470-36	1313	(7.8%)	1768	(6.9%)

b) Compressive Strengths (MPa)

Matrix Resin	GRP (CV)		CFRP (CV)	
913	1010	(8.4%)	1332	(14.2%)
914	1016	(11.2%)	1476	(6.8%)
411-45	1074	(12.0%)	851	(29.5%)
470-36	1015	(14.6%)	815	(20.7%)

TABLE 44: A COMPARISON OF THE EPOXY-CFRP COMPRESSIVE STRENGH DATA WITH THAT OF OTHER WORKERS

Ref. No	Material Used	Specimen Type	Strength (MPa)	CV (%)
43	914C-XAS	RAE	1400	2.1
43	914C-XAS	Celanese	1266	10.1
88	914C-XAS	Celanese	1120	5.9
This work	913C-XAS	Celanese (10 mm width)	1332	14.2
This work	914C-XAS	Celanese (10 mm width)	1476	6.8

TABLE 45: A COMPARISON OF THE TENSILE HYBRID EFFECTS IN EACH OF THE FOUR COMPOSITE SYSTEMS STUDIED

Tensile Failure	913	914	411	470
CFRP failure strain	1.33	0.90	1.28	1.33
G_4C_4/C_4G_4 failure strain	1.55	0.94	1.44	1.42
increase	(+16.5%)	(+4.4%)	(+12.5%)	(+6.8%)
C_4G_4/G_4C_4 failure strain	1.49	1.00	1.46	1.52
increase	(+12.0%)	(+11.1%)	(+14.1%)	(+14.3%)
$G_2C_4G_2/G_2C_4G_2$ f.strain	1.49	1.03	1.61	1.59
increase	(+12.0%)	(+14.4%)	(+25.8%)	(+19.5%)
$C_2G_4C_2/C_2G_4C_2$ f.strain	1.42	0.95	1.50	1.48
increase	(+6.8%)	(+5.6%)	(+17.2%)	(+11.3%)

TABLE 46: A COMPARISON OF THE COMPRESSIVE HYBRID EFFECTS IN EACH OF THE FOUR COMPOSITE SYSTEMS STUDIED

Compressive Failure	913	914	411	470
CFRP failure strain	1.13	1.22	0.71	0.73
G_4C_4/C_4G_4 failure strain	1.49	1.41	1.12	1.17
increase	(+31.9%)	(+15.6%)	(+57.7%)	(+60.3%)
C_4G_4/G_4C_4 failure strain	1.40	1.36	1.09	0.96
increase	(+23.9%)	(+11.5%)	(+53.5%)	(+31.5%)
$G_2C_4G_2/G_2C_4G_2$ f.strain	1.57	1.48	1.11	1.24
increase	(+38.9%)	(+21.3%)	(+56.3%)	(+69.9%)
$C_2G_4C_2/C_2G_4C_2$ f.strain	1.58	1.52	1.07	1.04
increase	(+39.8%)	(+24.6%)	(+50.7%)	(+42.4%)

TABLE 47: THE DATA USED FOR CALCULATION OF THE CONSTANTS A, B, C AND D IN FAILURE STRAIN CHARACTERISATION ($x = V_{fc}/V_{ft}$)

	Tensile		Compressive	
	Glass Outer	Carbon Outer	Glass Outer	Carbon Outer
$\hat{\varepsilon}_{CFRP}$	1.33	1.33	1.13	1.13
$[\hat{\varepsilon}_c]_{x=0.5}$	1.52	1.455	1.53	1.49
$\hat{\varepsilon}_{GRP-GO}$			2.70	
$\hat{\varepsilon}_{GRP}$	2.81			2.15
$\hat{\varepsilon}_{GRP-CO}$		2.36		
$\frac{d}{dx}[\hat{\varepsilon}_c]_{x=0}$	$\frac{-2.81}{0.245}$	$\frac{-2.36}{0.245}$	$\frac{-2.70}{0.5}$	$\frac{-2.15}{0.5}$
A	1.1	0.78	0.77	0.3
B	-10	-12	-6	-12
C	-0.38	-0.25	-0.8	-0.72
D	1.71	1.58	1.93	1.85

F I G U R E S

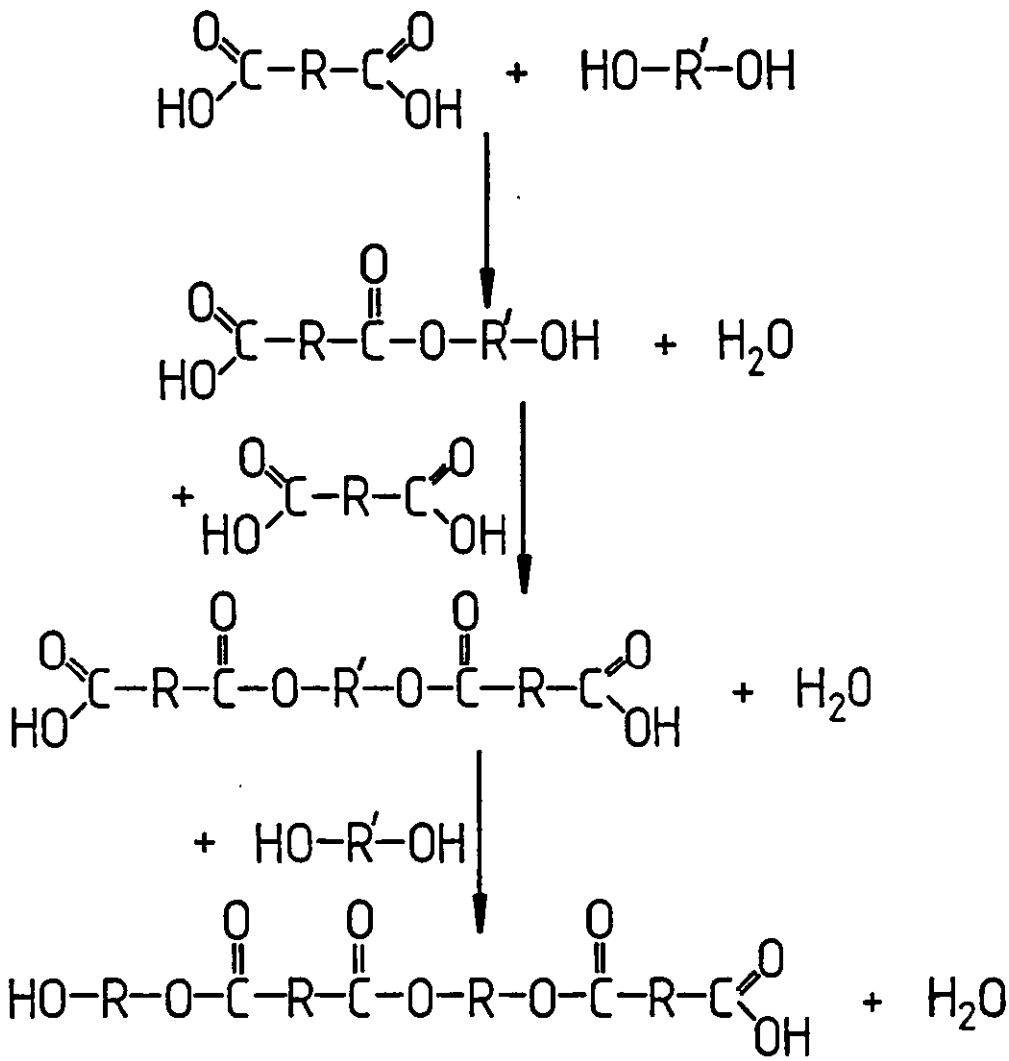

FIGURE 1: SYNTHESIS OF A POLYESTER RESIN FROM A DIBASIC ACID AND A DIOL

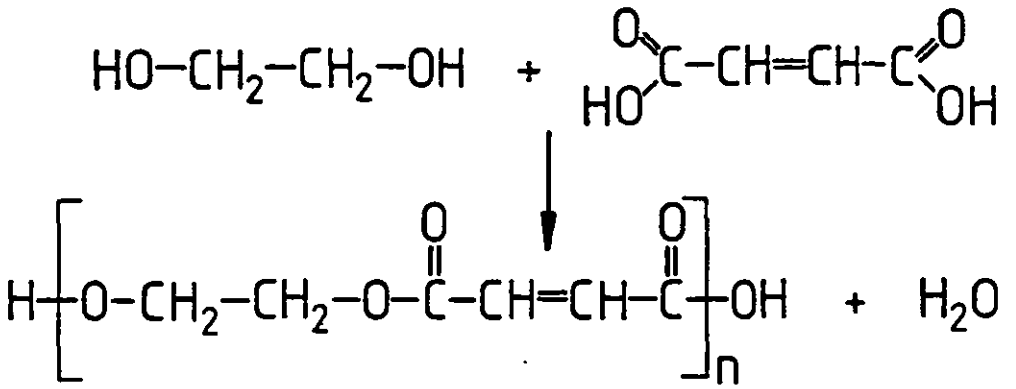

FIGURE 2: PRODUCTION OF A SIMPLE LINEAR POLYESTER FROM ETHYLENE GLYCOL AND MALEIC ACID

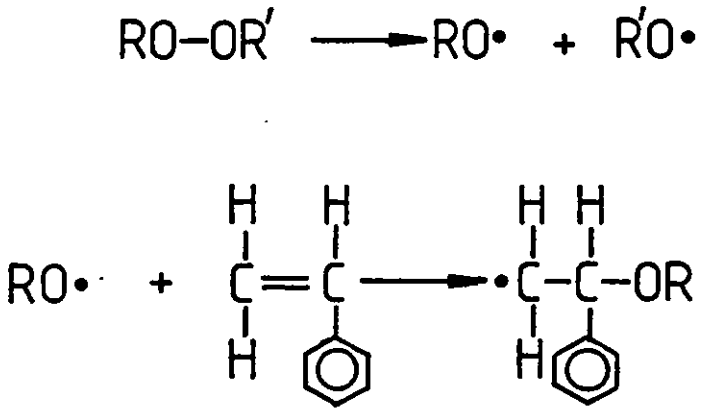

FIGURE 3: THE ACTION OF THE PEROXIDE FREE RADICALS WITH STYRENE

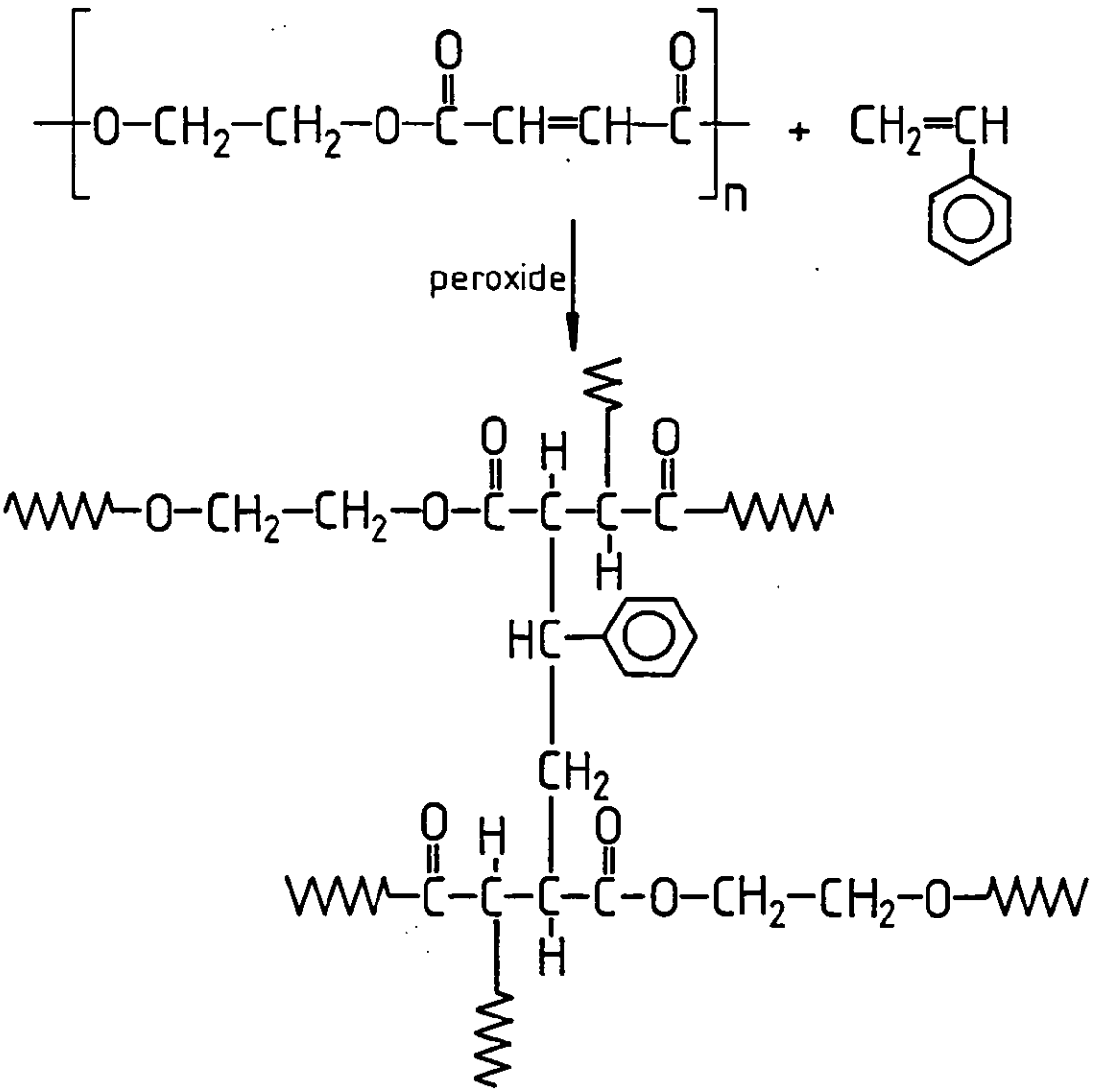

FIGURE 4: THE CROSSLINKING ACTION OF A SIMPLE POLYESTER RESIN WITH STYRENE

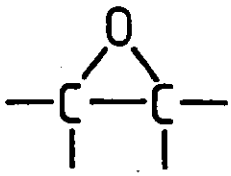

FIGURE 5: THE MOLECULAR STRUCTURE OF THE EPOXIDE GROUP

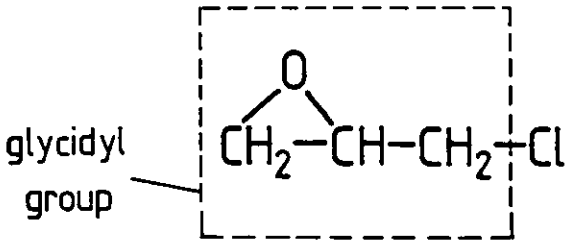

FIGURE 6: THE MOLECULAR STRUCTURE OF EPICHLOROHYDRIN

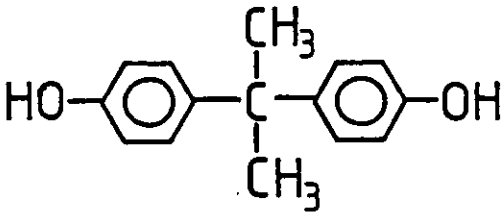

FIGURE 7: THE MOLECULAR STRUCTURE OF BISPHENOL-A

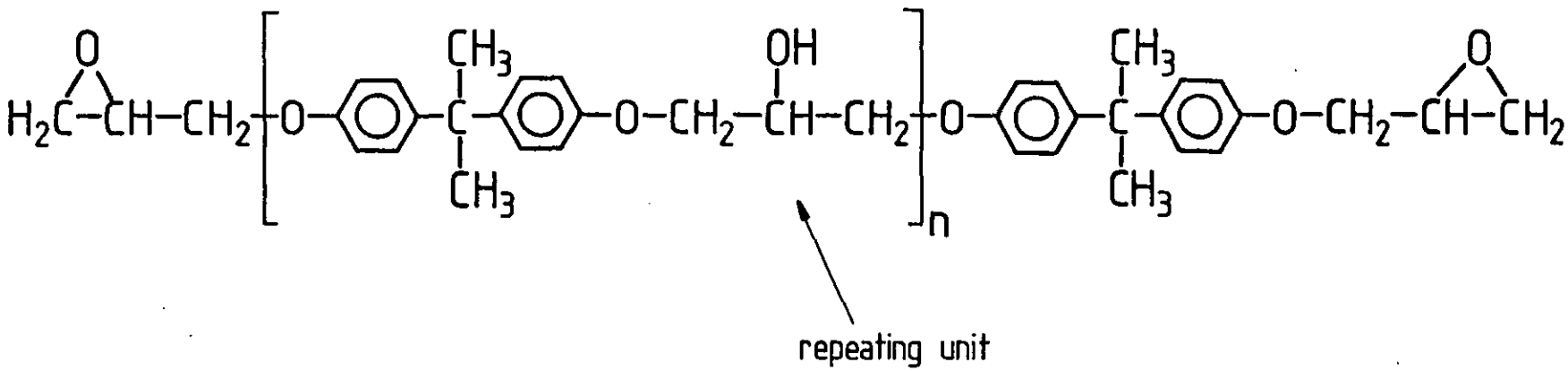

FIGURE 8: THE BISPHENOL-A/EPICHLOROHYDRIN EPOXY (OTHERWISE KNOWN AS DGEBA OR MY-750)

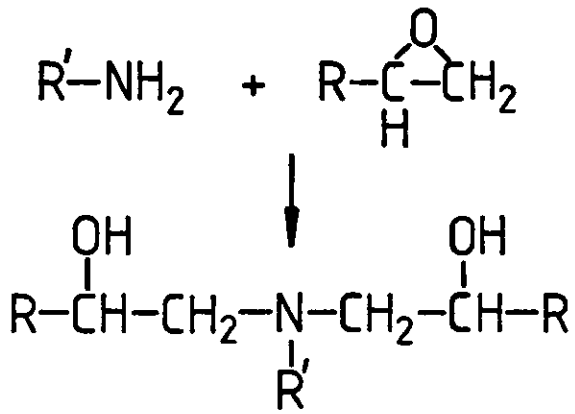

FIGURE 9: THE CROSSLINKING ACTION OF A PRIMARY AMINE WITH AN EPOXY RESIN

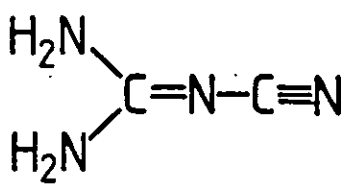

FIGURE 10: DICYANDIAMIDE, A LATENT CURING AGENT USED IN EPOXY RESINS

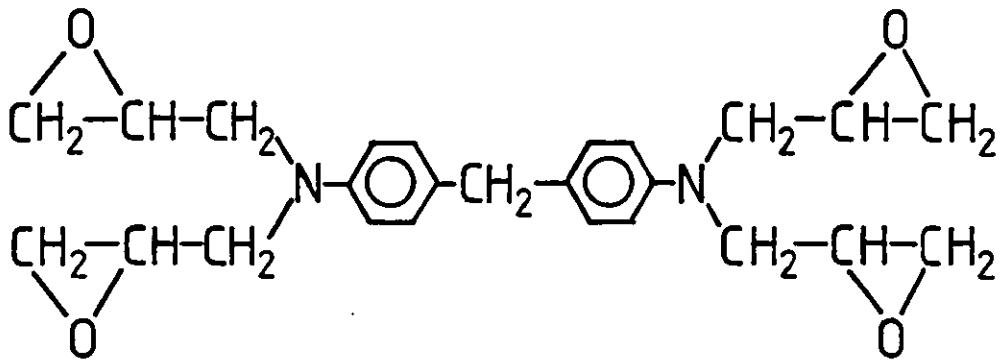

FIGURE 11: THE MOLECULAR STRUCTURE OF MY-720 EPOXY RESIN

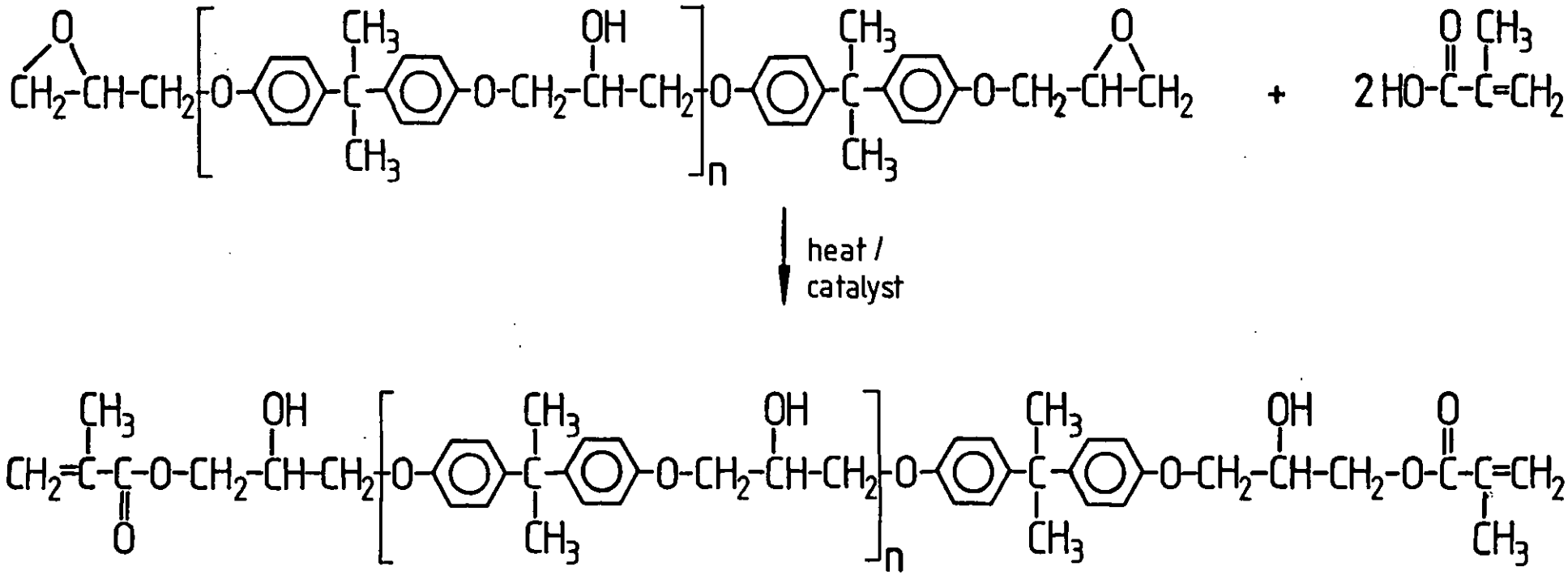

FIGURE 12: THE REACTION OF METHACRYLIC ACID WITH DGEBA TO PRODUCE THE DERAKANE 411 VINYL-ESTER RESIN

Bisphenol-A-Fumaric Acid Polyester

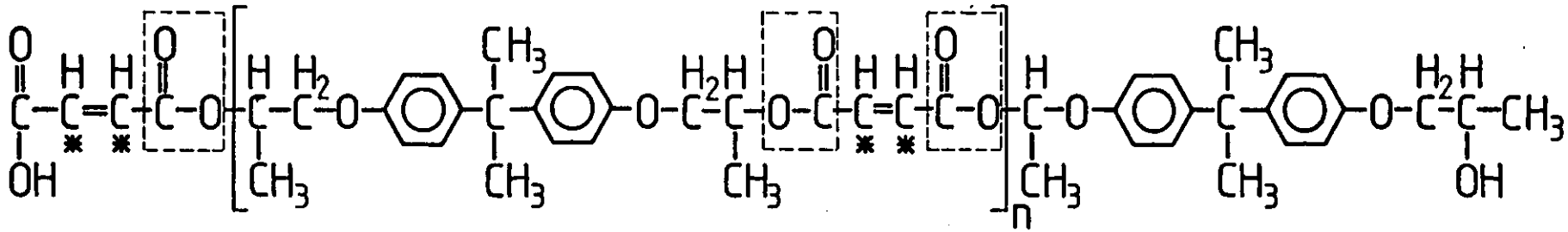

Derakane 411 Vinyl Ester

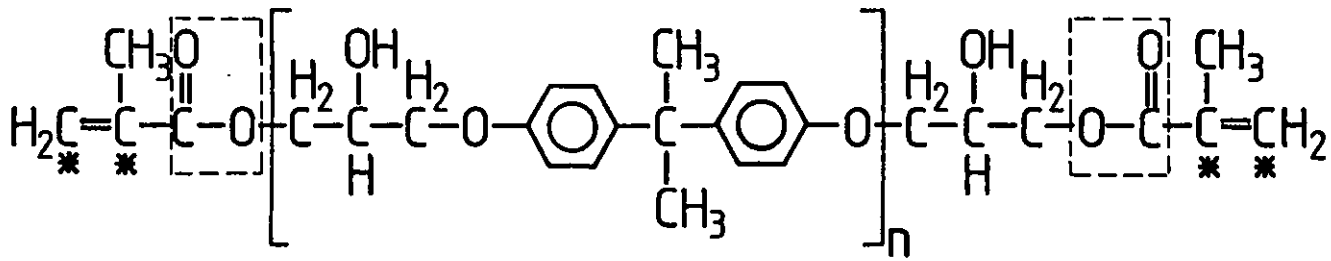

ester group

✱ reactive sites

FIGURE 13: COMPARISON OF THE STRUCTURES OF A POLYESTER AND A VINYL-ESTER RESIN

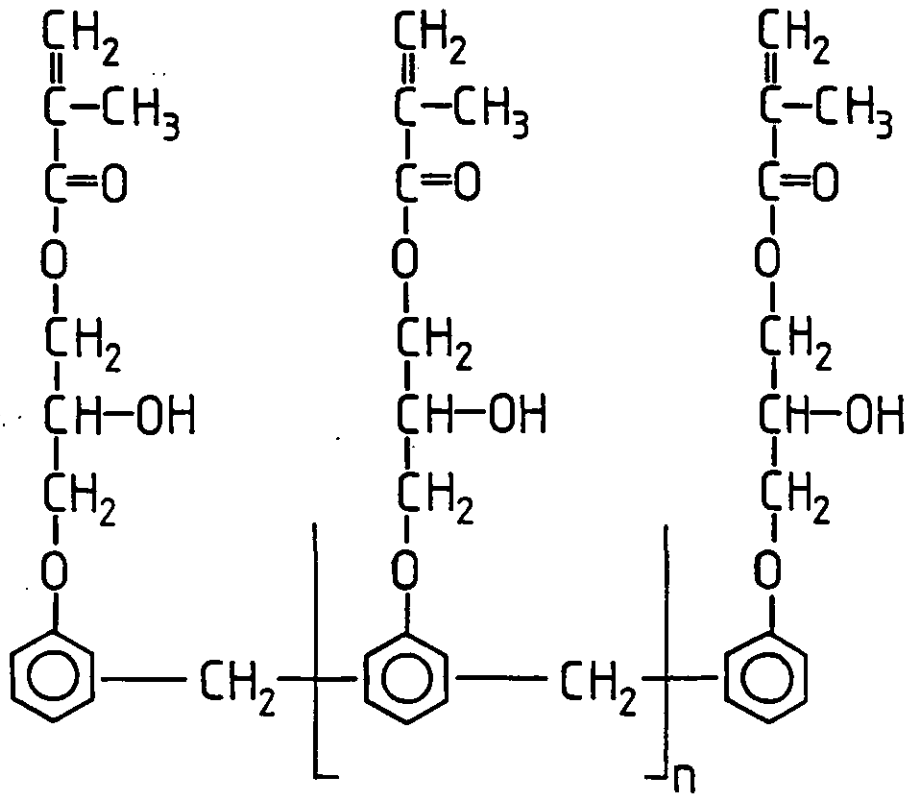

FIGURE 14: THE MOLECULAR STRUCTURE OF THE DERAKANE 470 VINYL ESTER RESIN, BASED ON THE EPOXY NOVOLAK STRUCTURE

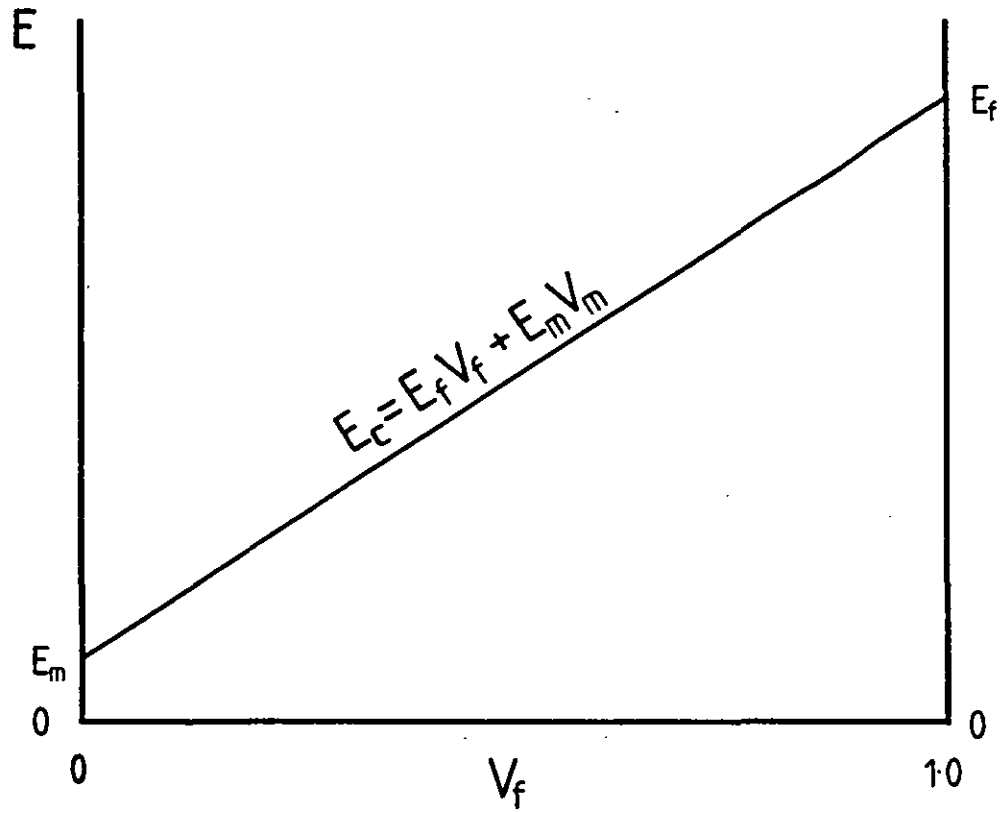

FIGURE 15: THE RULE OF MIXTURES RELATIONSHIP: MODULUS VS FIBRE VOLUME FRACTION

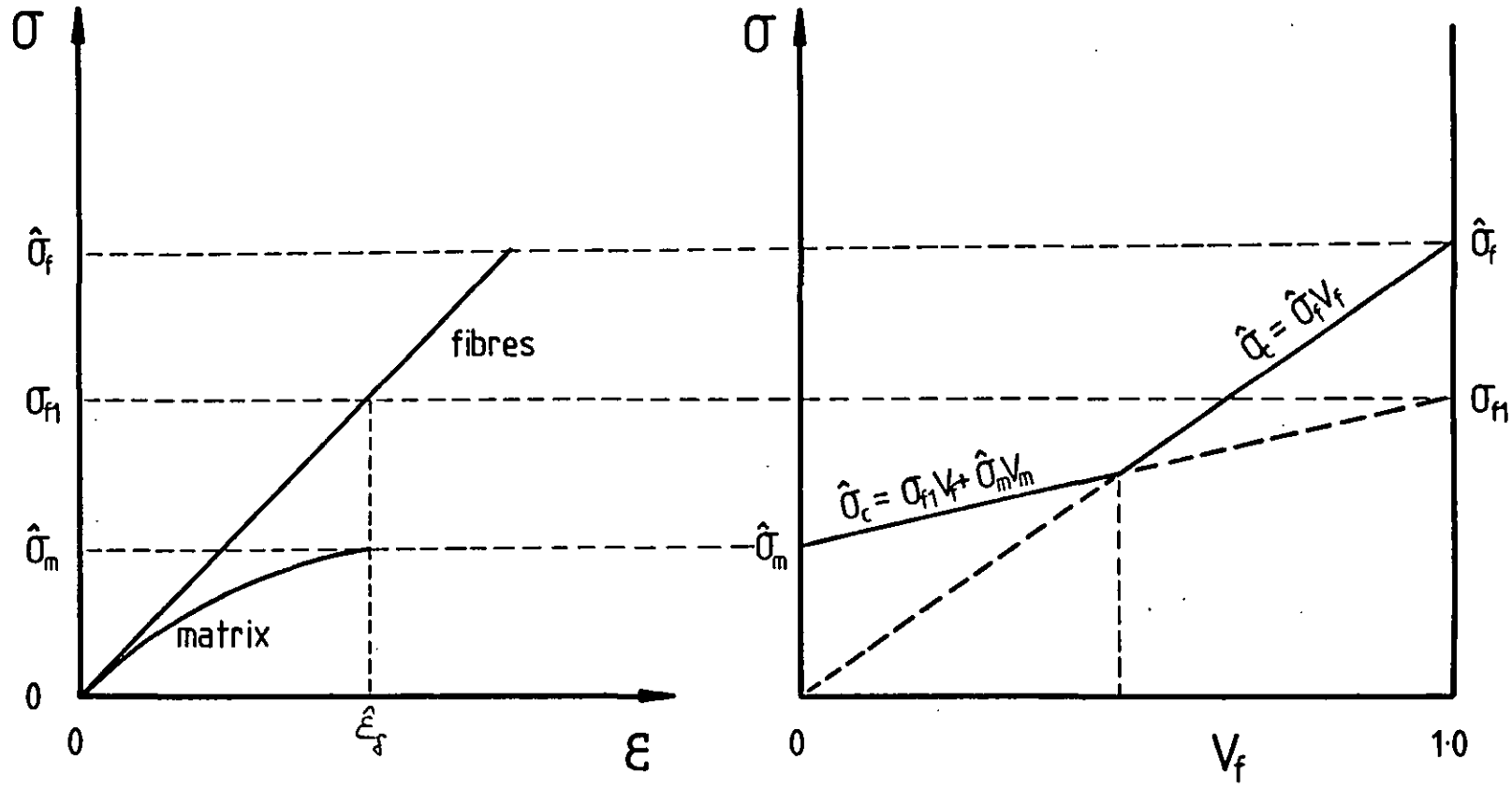

FIGURE 16: THE RULE OF MIXTURES RELATIONSHIP FOR THE STRENGTH OF UNIDIRECTIONAL COMPOSITES IN WHICH $\hat{\varepsilon}_f > \hat{\varepsilon}_m$

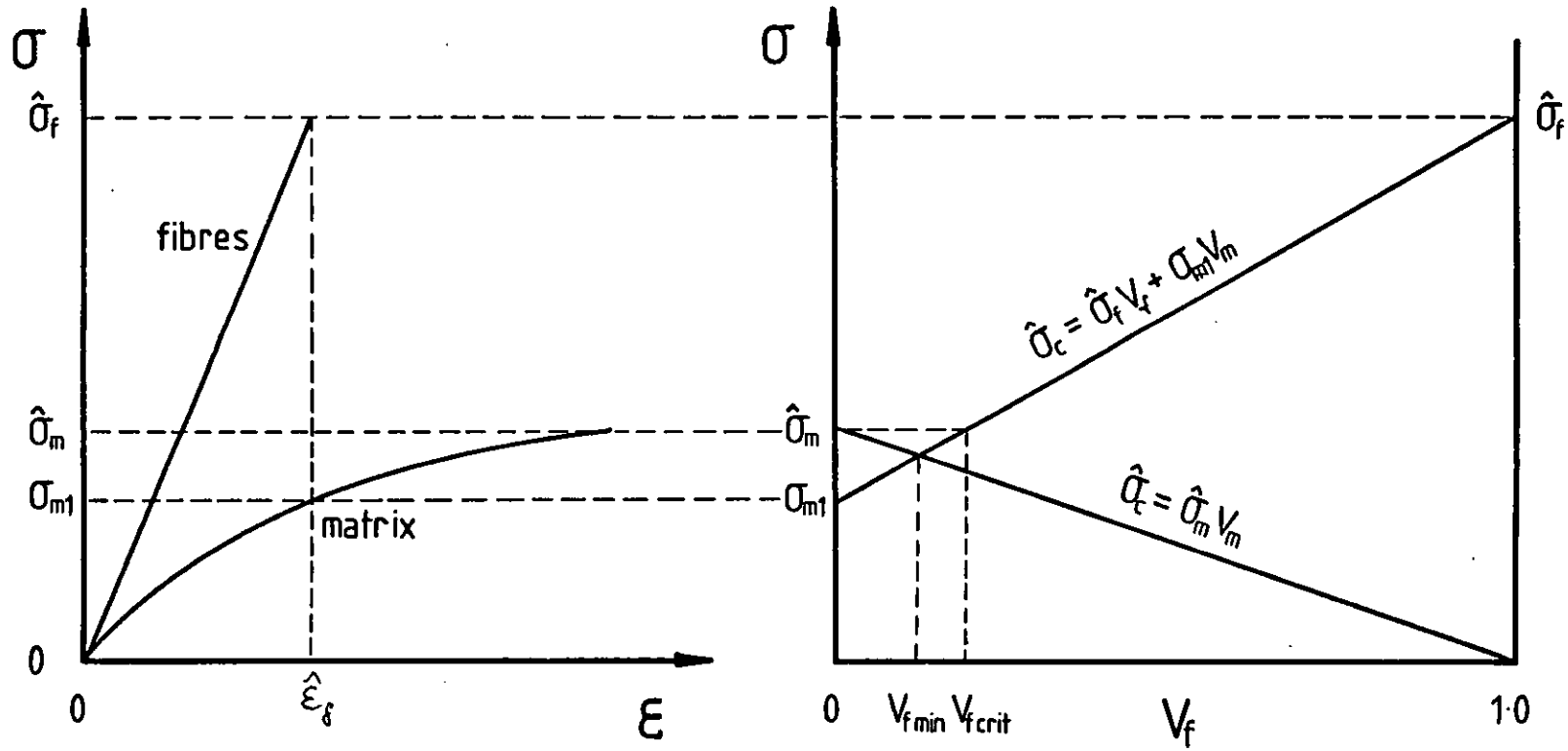

FIGURE 17: THE RULE OF MIXTURES RELATIONSHIP FOR THE STRENGTH OF UNIDIRECTIONAL COMPOSITES IN WHICH $\hat{\varepsilon}_m > \hat{\varepsilon}_f$

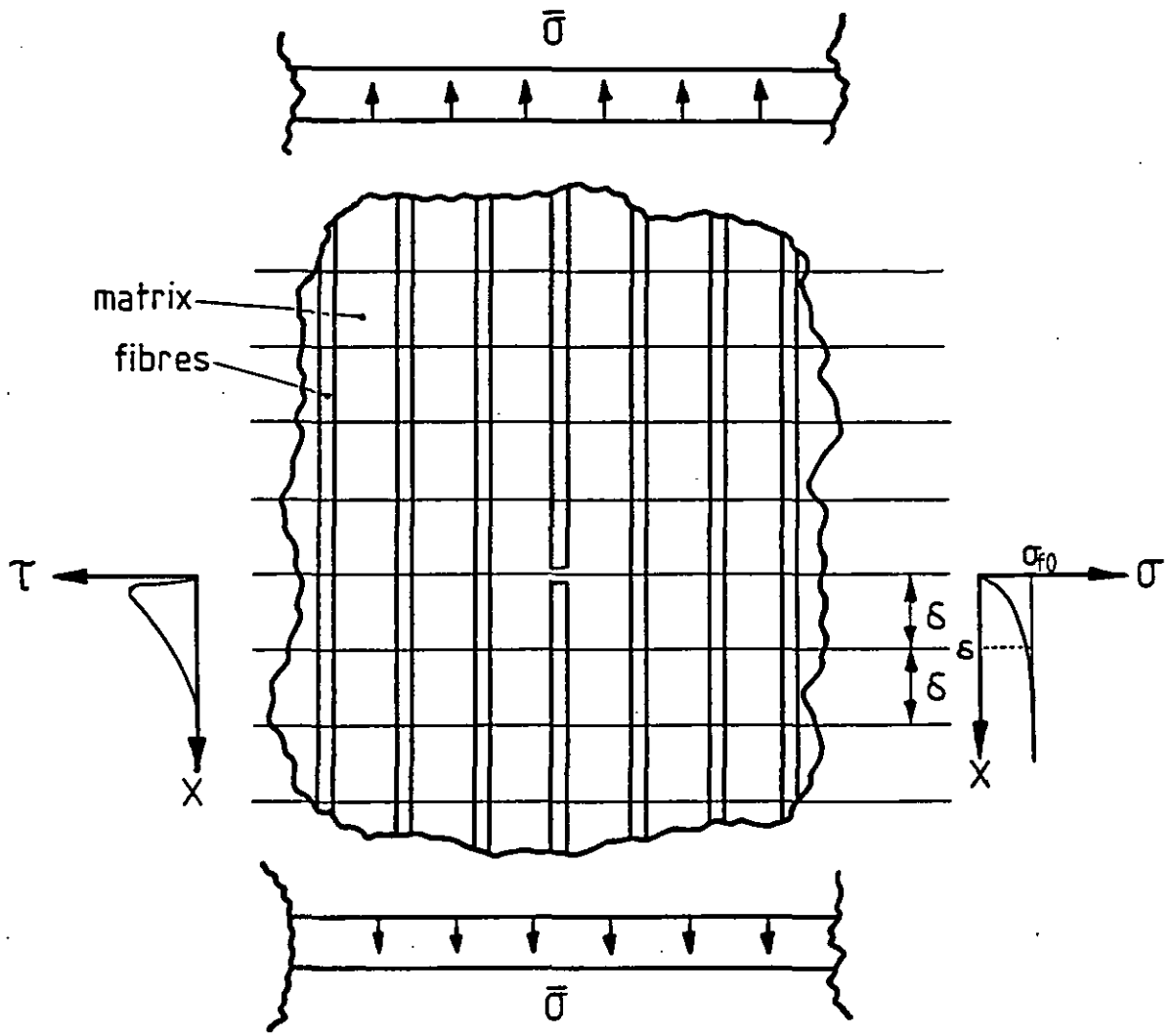

FIGURE 18: ROSEN'S MODEL FOR THE ANALYSIS OF TENSILE STRENGTH IN MONOFIBRE COMPOSITES (From Ref 22)

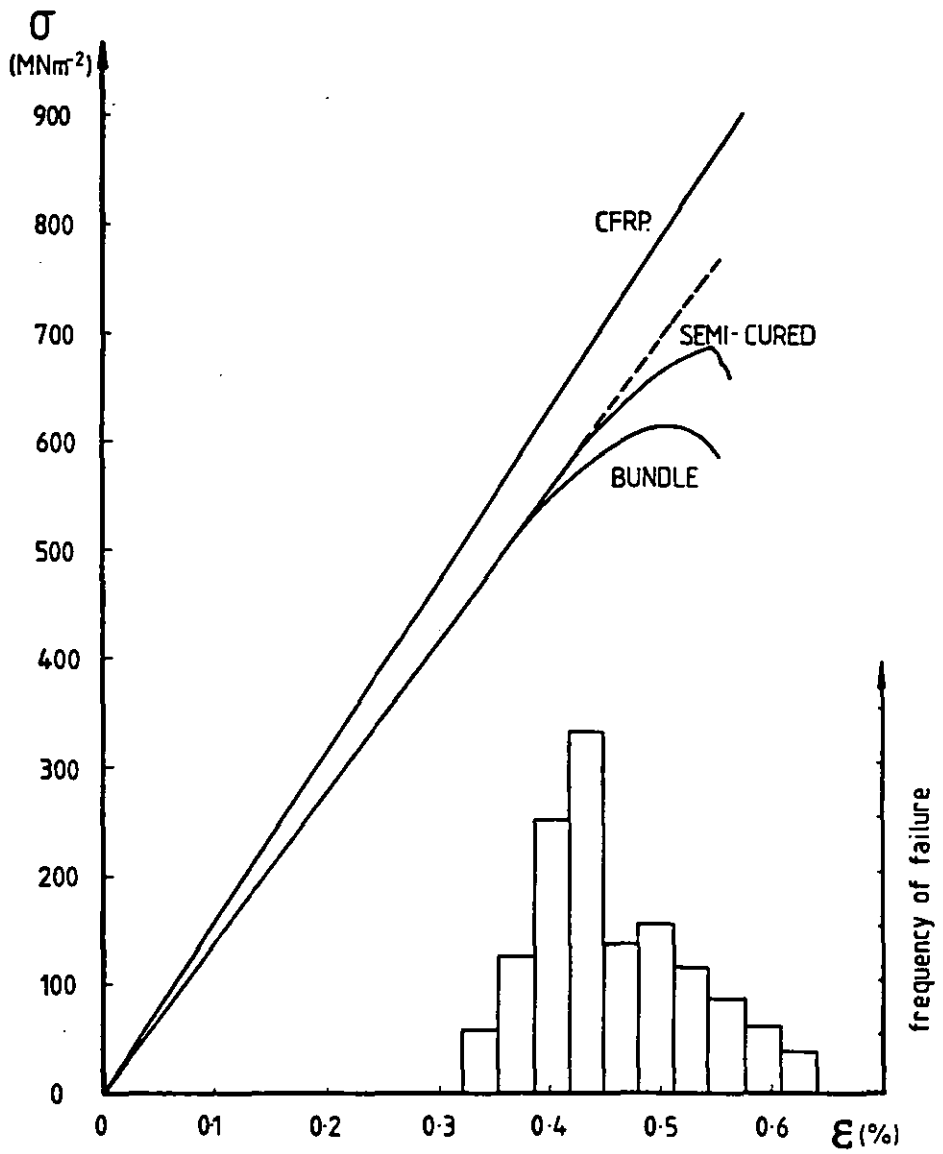

FIGURE 19: THE STRESS/STRAIN CURVES OF CURED AND SEMI-CURED CFRP AND FIBRE BUNDLES OBTAINED BY FUWA ET AL (From Ref 28). THE FREQUENCY DISTRIBUTION OF THEIR CURED CFRP FAILURE STRAINS IS SHOWN

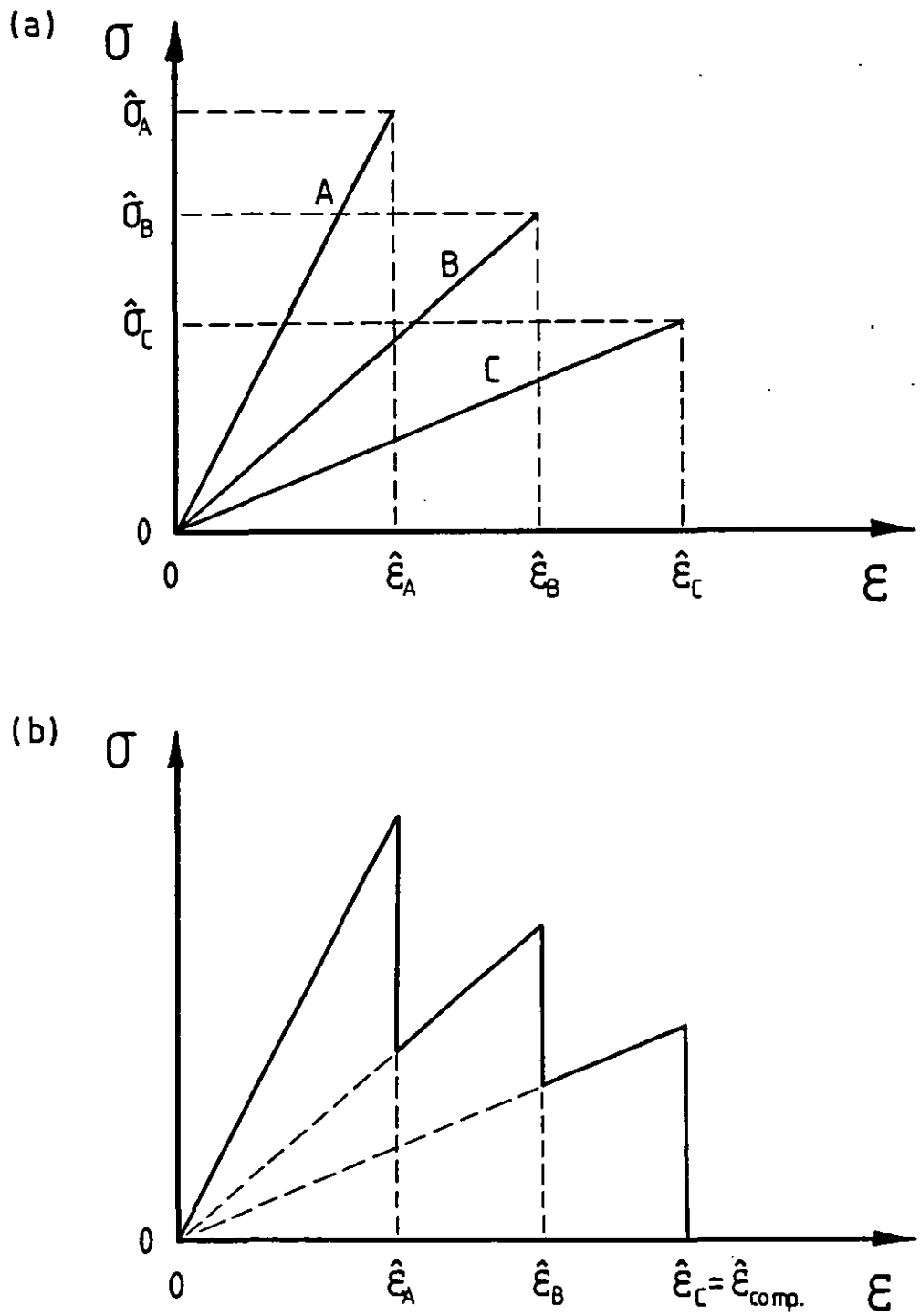

FIGURE 20: HAYASHI'S MODEL FOR A HYBRID COMPOSITE SYSTEM (From Ref 31)

a) STRESS/STRAIN PROPERTIES OF THE THREE COMPOSITE MATERIALS

b) STRESS/STRAIN RESPONSE OF THE RESULTING HYBRID

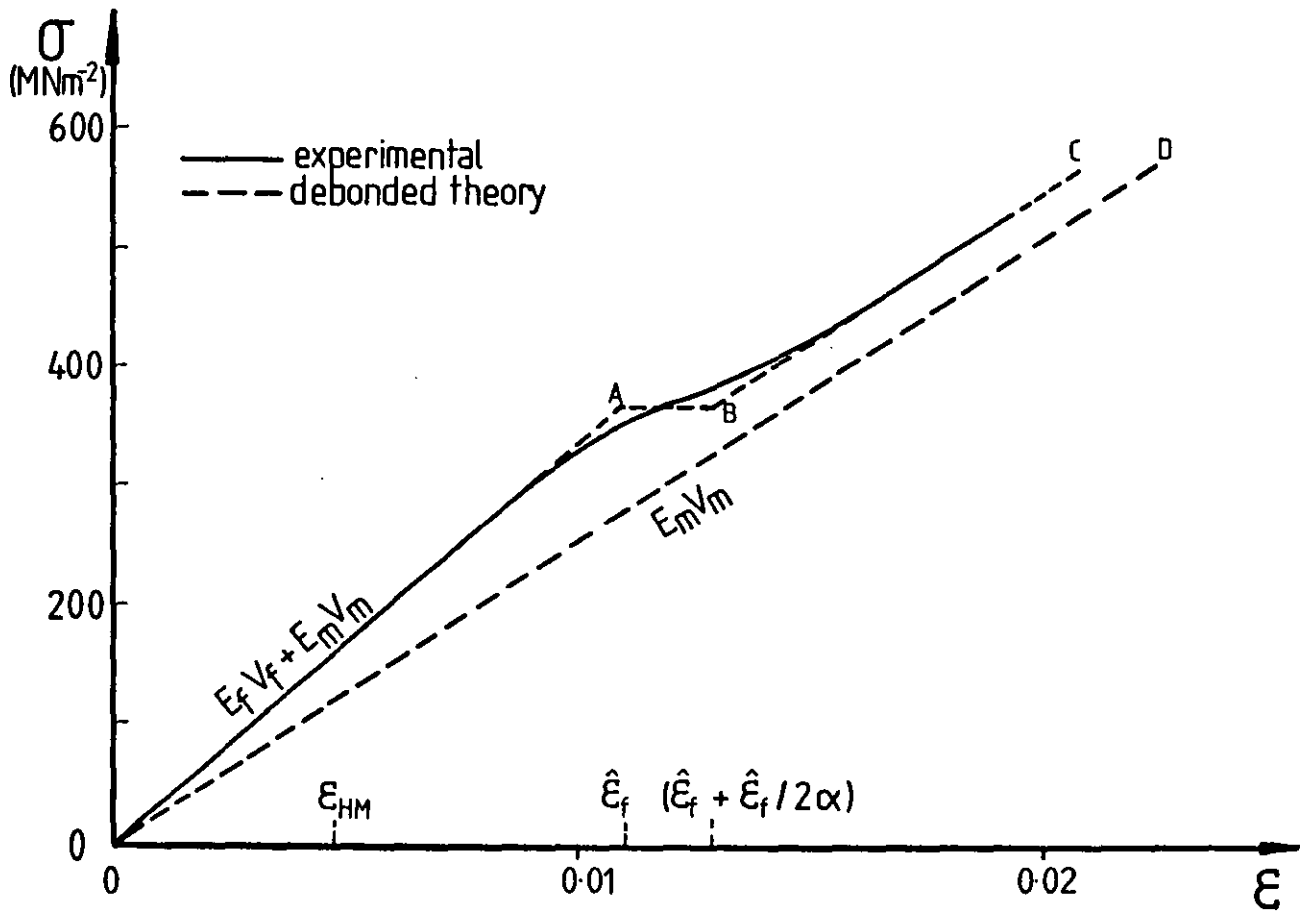

FIGURE 21: THE TENSILE STRESS/STRAIN DIAGRAM OF A HYBRID CARBON GLASS-EPOXY COMPOSITE OF AVESTON AND SILLWOOD, IN COMPARISON WITH THEIR DEBONDED THEORY (From Ref 33)

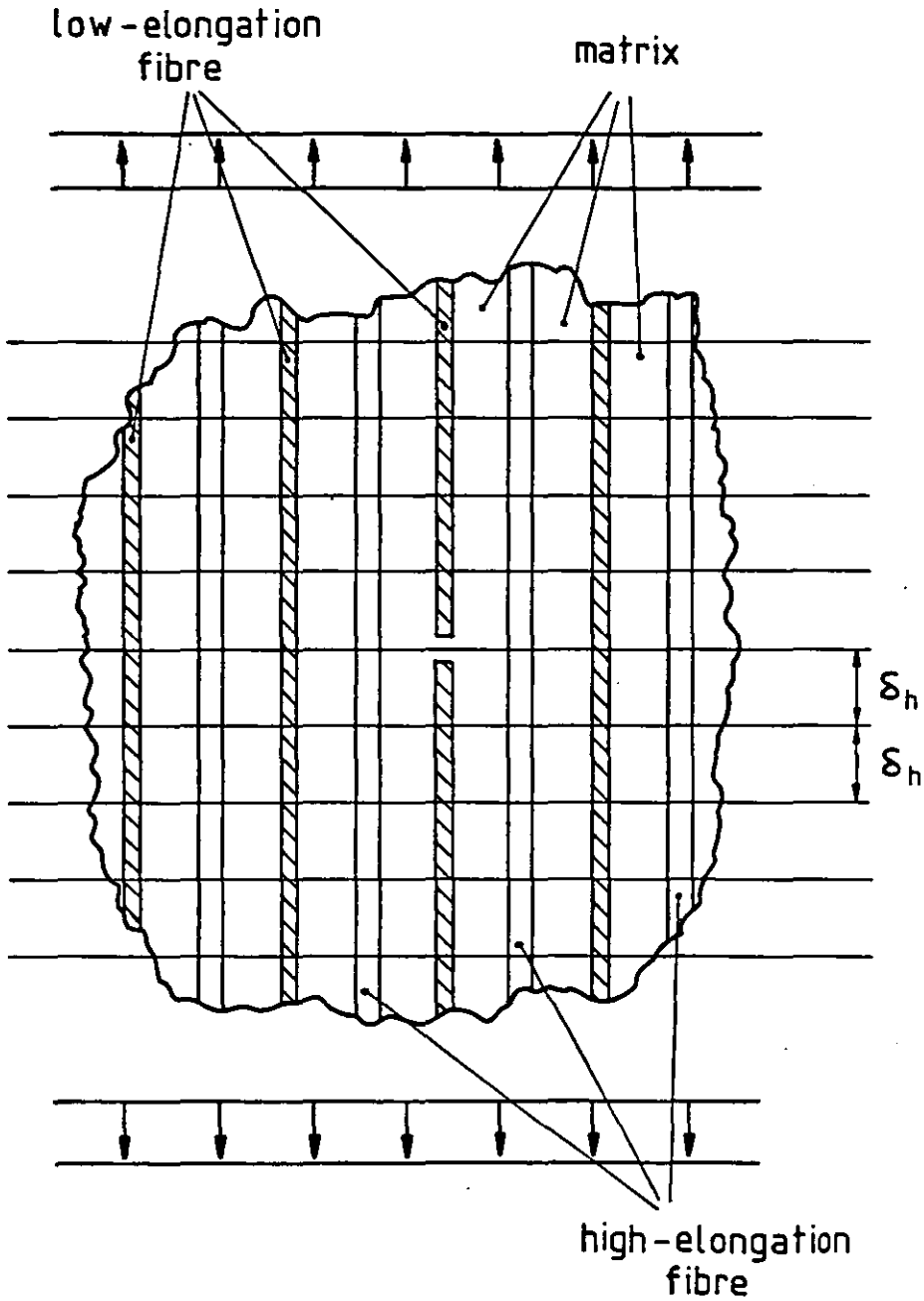

FIGURE 22: ZWEBEN'S MODEL FOR THE ANALYSIS OF TENSILE STRENGTH IN HYBRID COMPOSITES (From Ref 34)

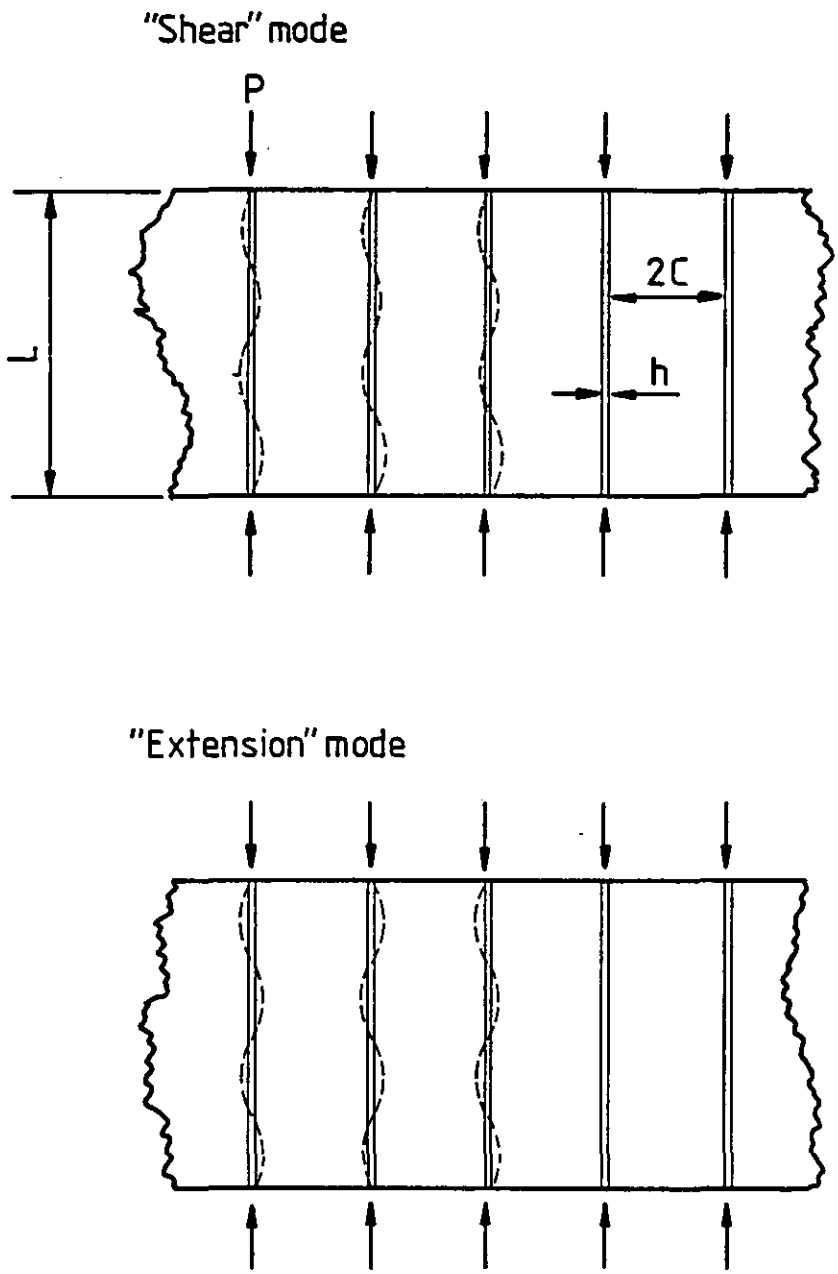

FIGURE 23: ROSEN'S ANALYTICAL MODEL FOR THE COMPRESSIVE STRENGTH OF UNIDIRECTIONALLY REINFORCED FIBRE COMPOSITES INVOLVING FIBRE MICROBUCKLING (From Ref 44)

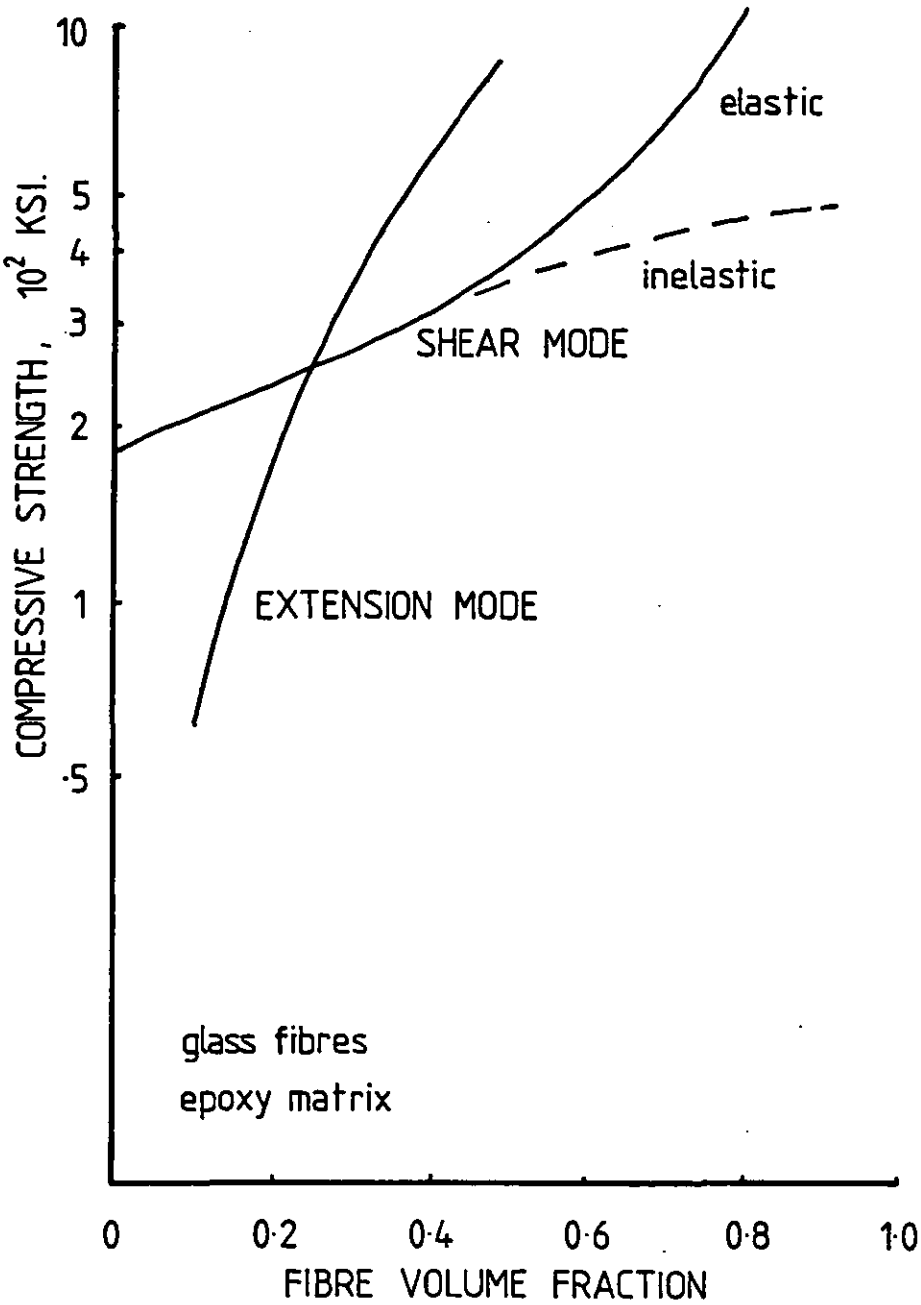

FIGURE 24: THE COMPRESSIVE STRENGTH OF GLASS REINFORCED EPOXY COMPOSITES AS PREDICTED BY THE ROSEN BUCKLING MODEL (From Ref 44)

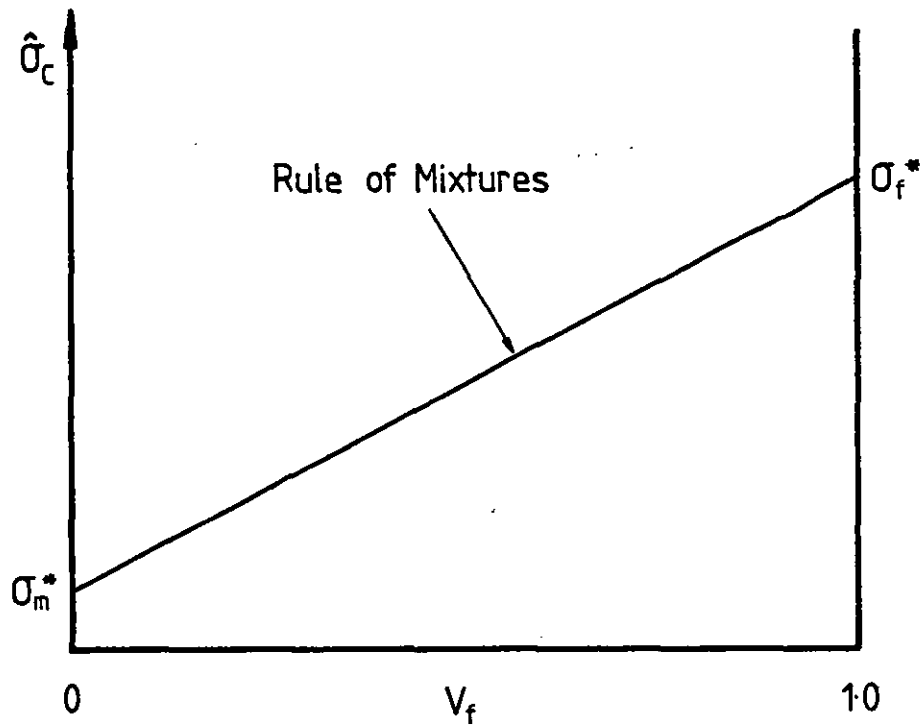

FIGURE 25: HAYASHI'S RULE OF MIXTURES RELATIONSHIP FOR THE COMPRESSIVE STRENGTH OF UNIDIRECTIONALLY REINFORCED FIBRE COMPOSITES (From Ref 46)

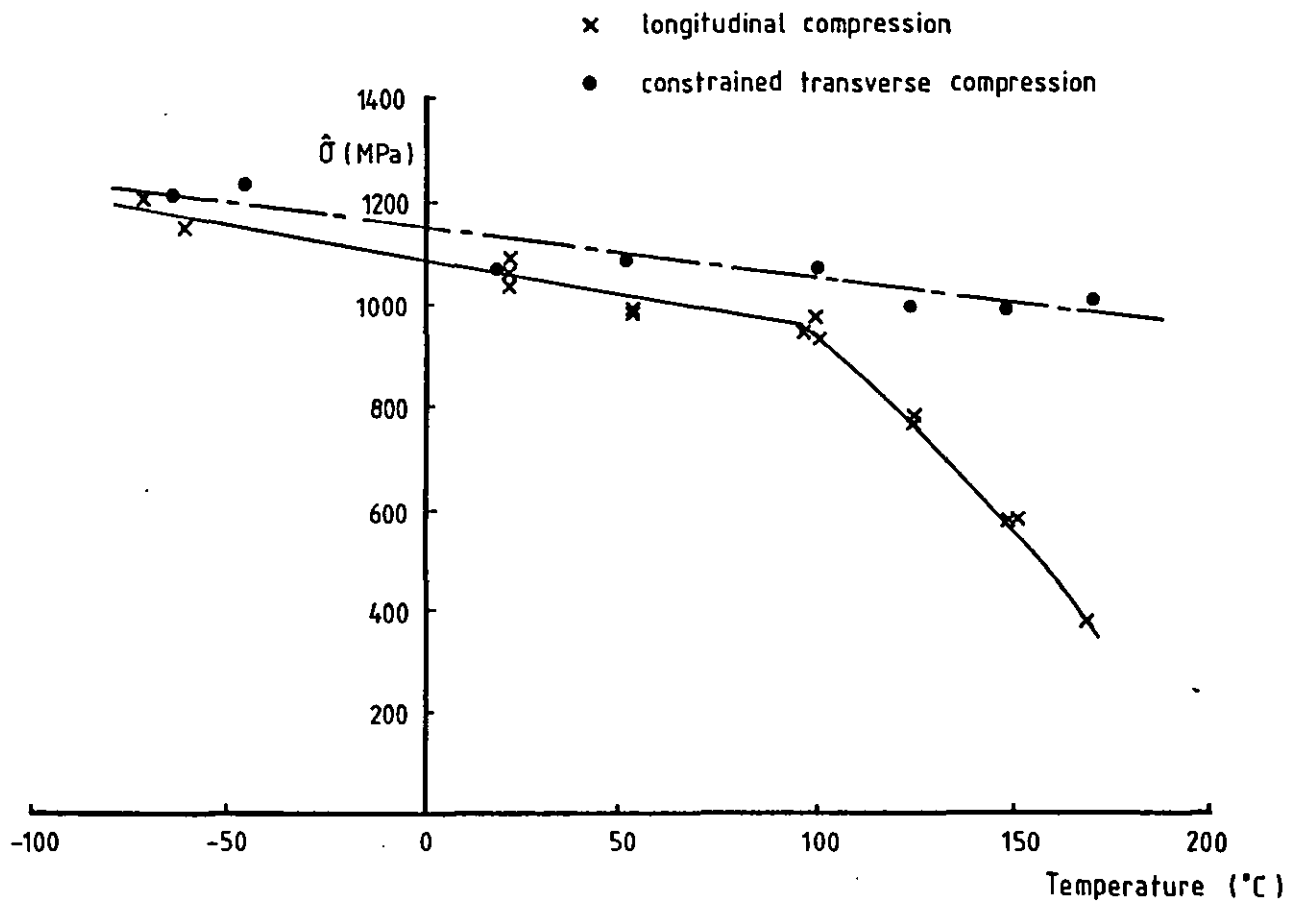

FIGURE 26: THE VARIATION OF LONGITUDINAL AND CONSTRAINED TRANSVERSE COMPRESSIVE STRENGTH OF HT-S CFRP WITH TEMPERATURE, OBSERVED BY EWINS AND HAM (From Ref 49)

ALAN WALKER

Tendering care

The long-awaited Griffiths report on community care is due out soon. In reality, it may mark another milestone in the decline of public provision of decent social services

Sir Roy Griffiths' report on community care has still not appeared; but already it is possible to make an intelligent guess at what he will recommend. Among the ideas for community care he is likely to adopt are: the concept of "lead" responsibility for community care (local authorities in the case of mental handicap services and health authorities for mental illness services); a joint board to cover services for the elderly with a single manager responsible for buying in services; and an increase in formal contracts between clients and those who serve them.

It would be very surprising if Sir Roy's proposed reorganisation did not include further reductions in the role of local authorities as service *providers* (although this might be coupled with an increased managerial role). It would be surprising if he did not recommend an expanding role for the private sector together with some additional expectations for the growth of the voluntary sector. Equally surprising would be the omission of a strong managerial bias in the proposals and the absence of real concern with the issues of how services are to be financed.

As we mark the twentieth anniversary of the Seebohm report, it is worth noting that it had only two paragraphs out of 706 devoted to finance—because everyone assumed that the money the services needed would be found. The tide began to turn for the personal social services soon after the election of the Conservative government. Patrick Jenkin, the social services secretary, immediately reduced the central grant for these services by 9 per cent.

> ***'A reduced role in the provision of services could be replaced by an increased regulatory role. But this overlooks the ideological driving force behind the expansion of the market. What the government wants is expanded private provision, but it is distinctly reluctant to regulate.'***

The impact was not immediate, for these were the days before the introduction of the block grant and rate capping. Some authorities were at first able to counter the cuts by making up the difference from the rates, but increased financial controls on local authorities has closed that avenue.

Over the same period, a series of what seemed as they occurred to be separate policy developments may now be seen as part of the Conservative government's strategy towards the social services. The aim was to turn local authority social services from the main providers of services into something far more limited: the provider of those residual services which no one else could or would take on.

In 1980, in a speech to directors of social services, Jenkin spoke of a supportive and decidedly residual role for the social services. They would be, he said, "a long-stop for the very special needs going beyond the range of voluntary services." In 1981 the white paper on services for the elderly, *Growing Older*, contained the now famous phrase: "care *in* the community must increasingly mean care *by* the community." But it was Jenkin's successor's speech to the 1985 Joint Social Services Conference in Buxton that contained the clearest and most detailed outline of the new residual role proposed for social services. Norman Fowler argued that social services departments should stop regarding themselves primarily as service providers and promote the participation of all other available sources of care.

The Audit Commission report, *Making a Reality of Community Care* (1986), came to the same conclusion as countless previous independent studies: "Community care policy is in some disarray." The remedy proposed was organisational: the establishment of lead responsibility in the care of the mentally handicapped and mentally ill, and a manager with control of a single budget, to run services for the elderly.

Meanwhile, Fowler had been promising, for two years, a green paper on the personal social services. This did not materialise. Instead, in response to the debate following the Audit Commission report, Griffiths was appointed in March 1987. His remit was to examine problems in the arrangements for community care between the NHS and local authorities and to explore the option of putting the whole service for elderly people "under the control of a manager who will purchase from whichever public or private agency is appropriate."

Sir Roy was the obvious candidate for the job. He had conducted a similar inquiry into the management of the NHS in 1983 which had resulted in the appointment of general managers. That made clear his centralising views of management. In social services he might be expected to go further, since there is much less support for social workers' professional autonomy than for that of doctors.

Together, these policy developments amount to a strategy which might be called residualisation, which the Griffiths report may be expected to provide further impetus.

There are three main dimensions to this strategy. First, the provision of community care is being deliberately fragmented. This is partly to break the dominant position of local authorities. Sir Kenneth Stowe, the former permanent secretary of the DHSS, described the new approach as "letting a hundred flowers bloom."

Back in 1980 Patrick Jenkin had argued that it was reasonable to cut the social services while protecting

Alan Walker is Professor of Social Policy at Sheffield University.

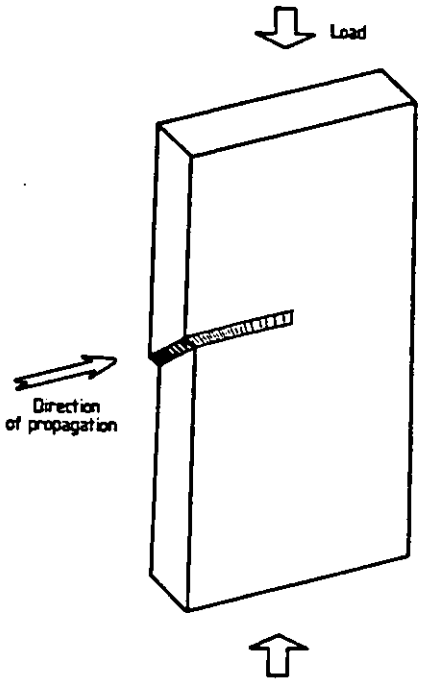

FIGURE 27: AN ARRESTED COMPRESSIVE FAILURE SPECIMEN OF CHAPLIN, SHOWING PROPAGATION OF THE KINK-BAND (From Ref 52)

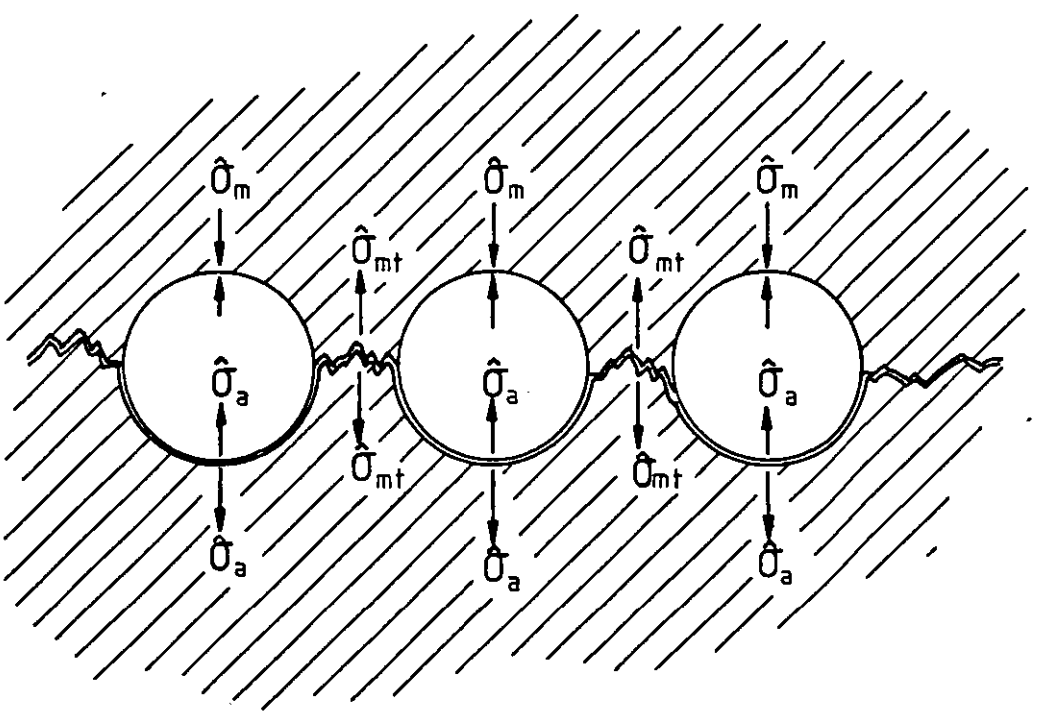

FIGURE 28: PIGGOTT'S CONSIDERATION OF INTERFACE AND MATRIX FAILURE AS A RESULT OF SINUSOIDALLY BUCKLED FIBRES (From Ref 57)

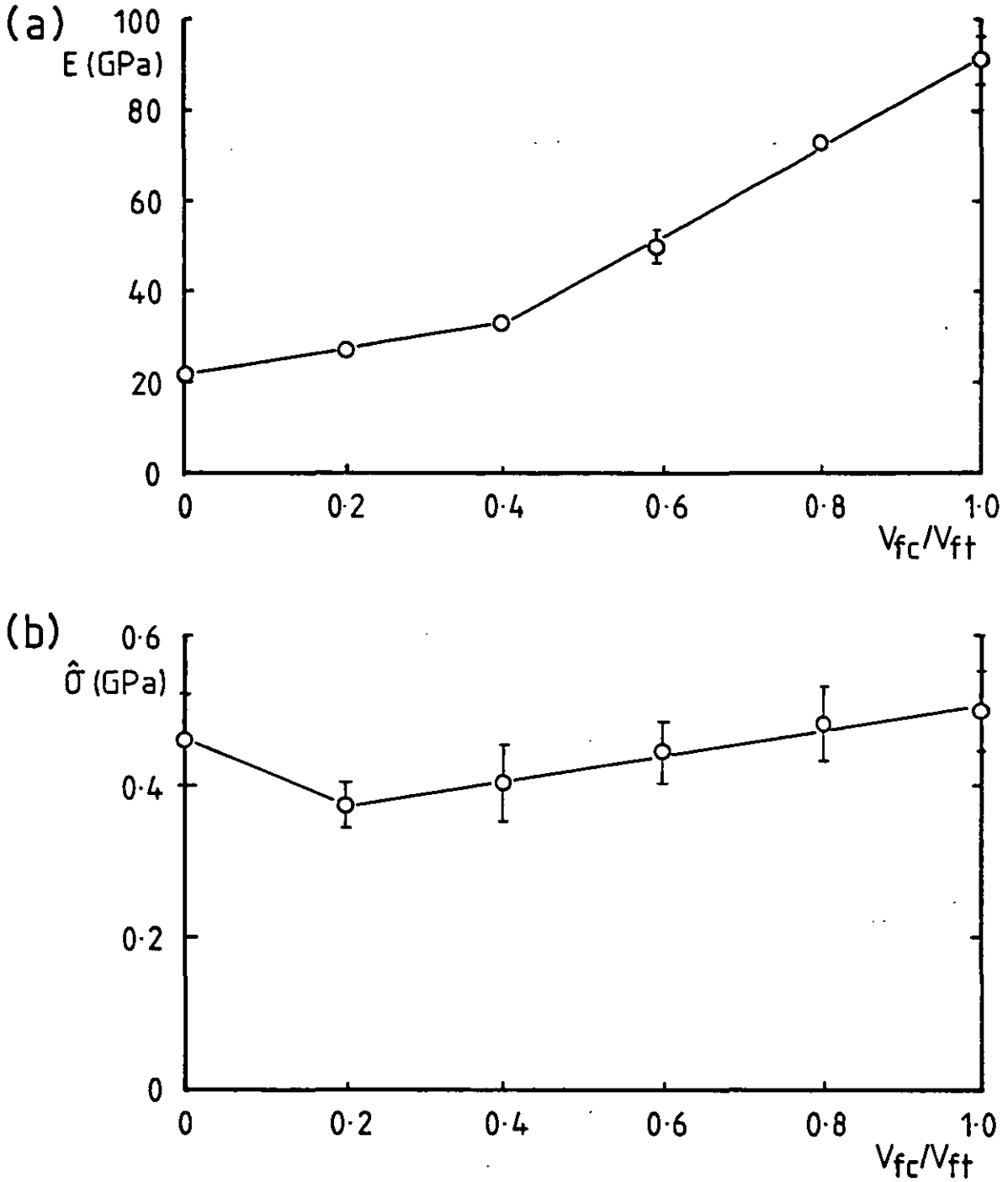

FIGURE 29: NON RULE OF MIXTURES RESULTS OBTAINED BY PIGGOTT AND HARRIS WITH HM-S CARBON/GLASS HYBRIDS (From Ref 62) FOR
a) COMPRESSIVE MODULUS
b) COMPRESSIVE STRENGTH

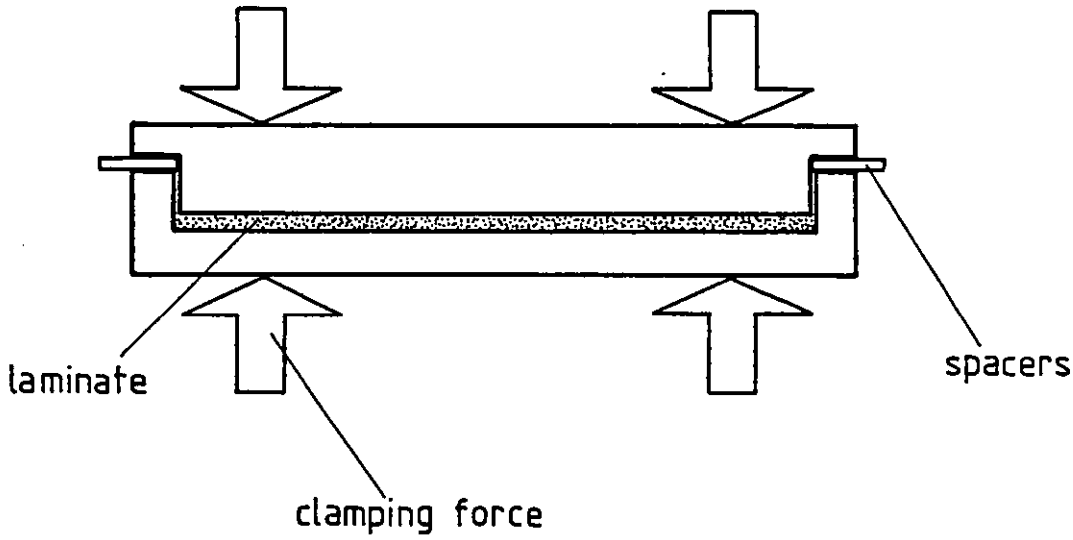

FIGURE 30: CROSS SECTION OF A LEAKY MOULD USED IN THE WET LAY-UP OF VINYL ESTER COMPOSITES

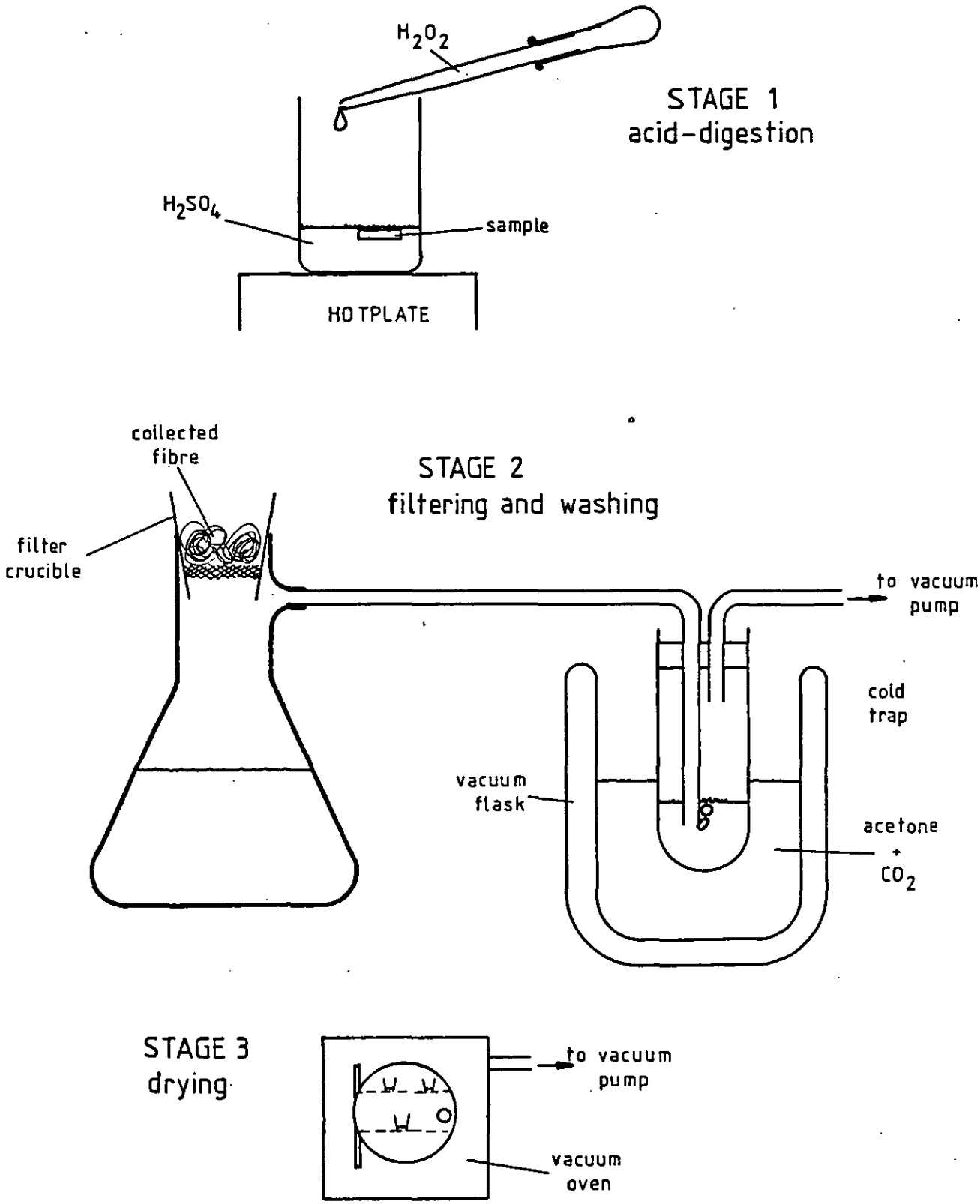

FIGURE 31: THE ACID DIGESTION PROCESS OF VOLUME FRACTION MEASUREMENT

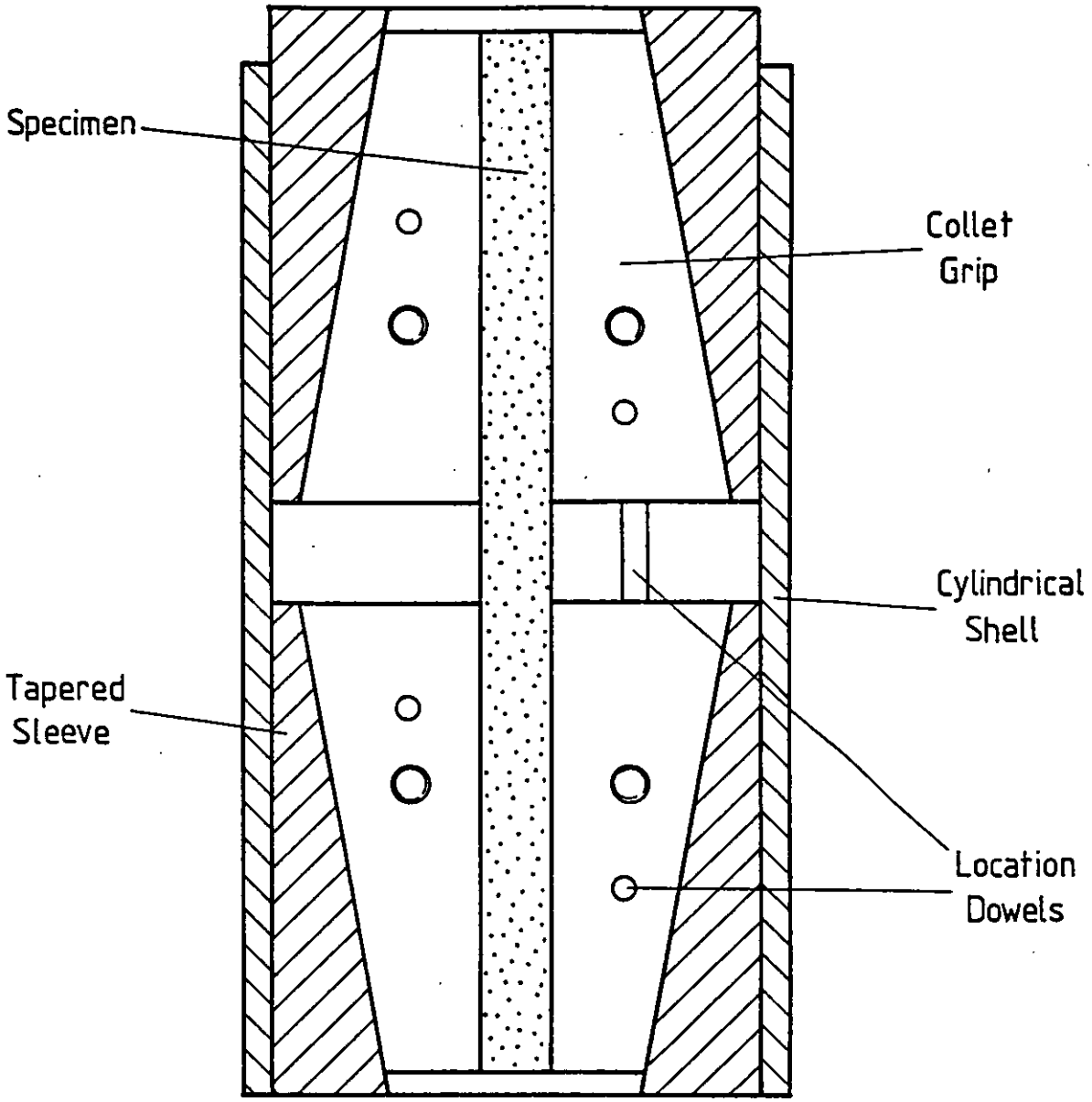

FIGURE 32: CROSS SECTION OF THE CELANESE COMPRESSION TEST FIXTURE

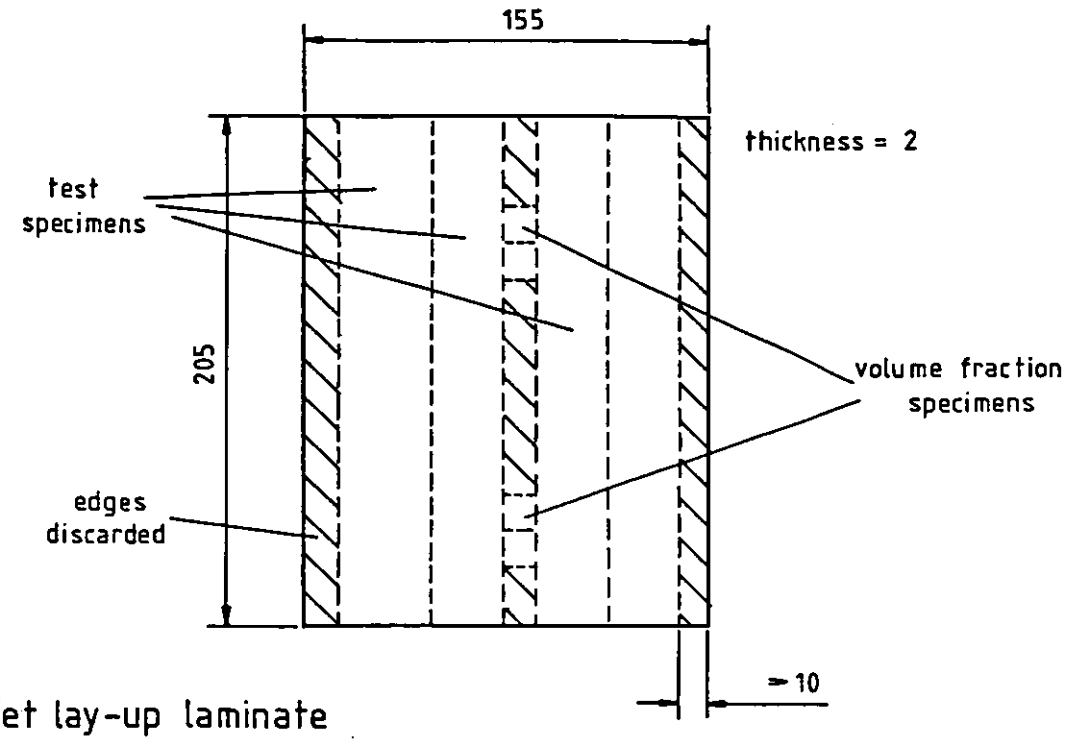

(a) Wet lay-up laminate

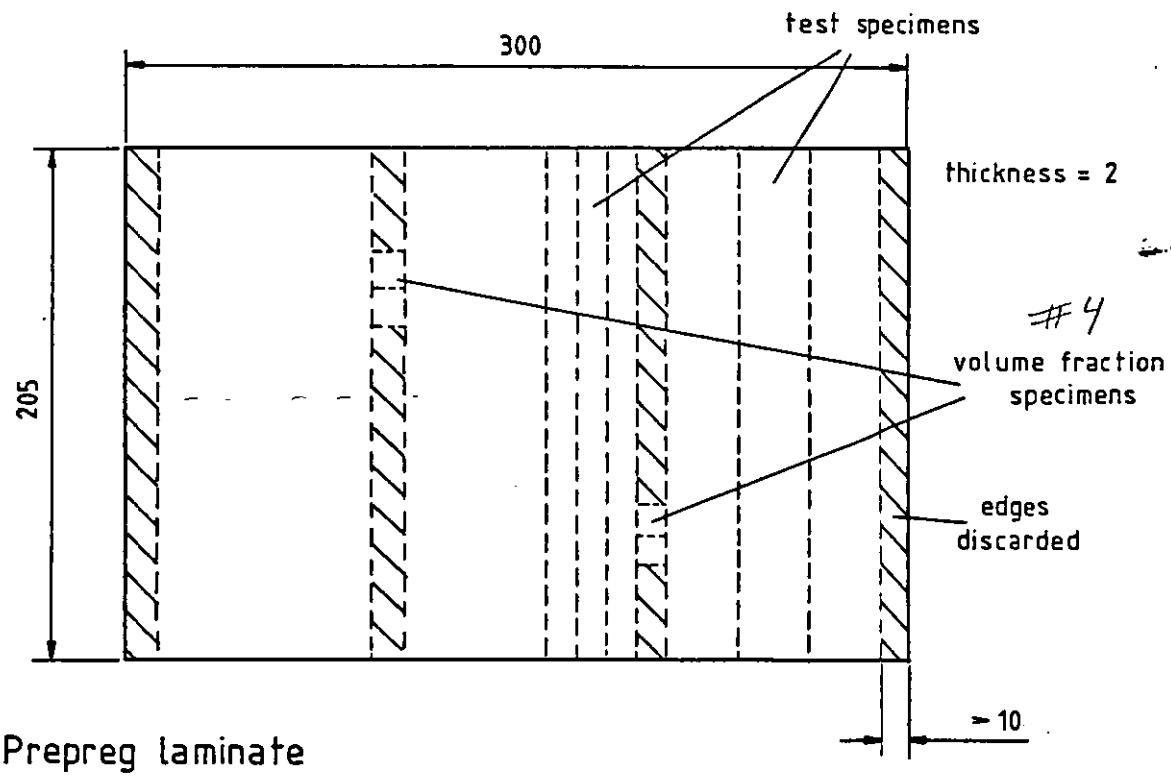

(b) Prepreg laminate

FIGURE 33: COMPOSITE LAMINATES MADE BY:
a) WET LAY-UP TECHNIQUE FOR VINYL ESTER LAMINATES
b) PREPREG COMPRESSION MOULDING TECHNIQUE FOR EPOXY LAMINATES (DIMENSIONS IN mm)

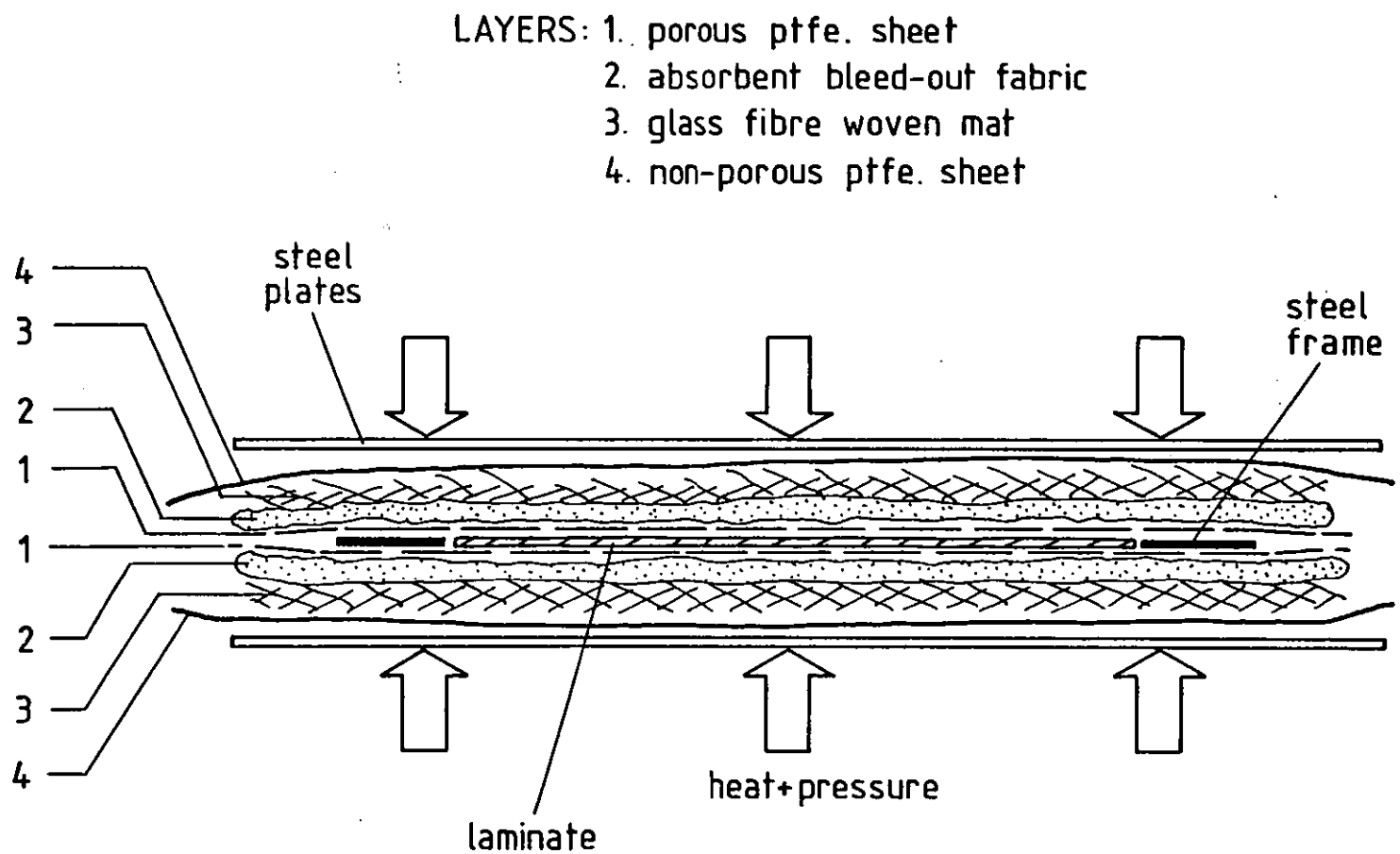

FIGURE 34: THE LAY-UP OF A PREPREG LAMINATE IN THE COMPRESSION MOULDING PROCESS

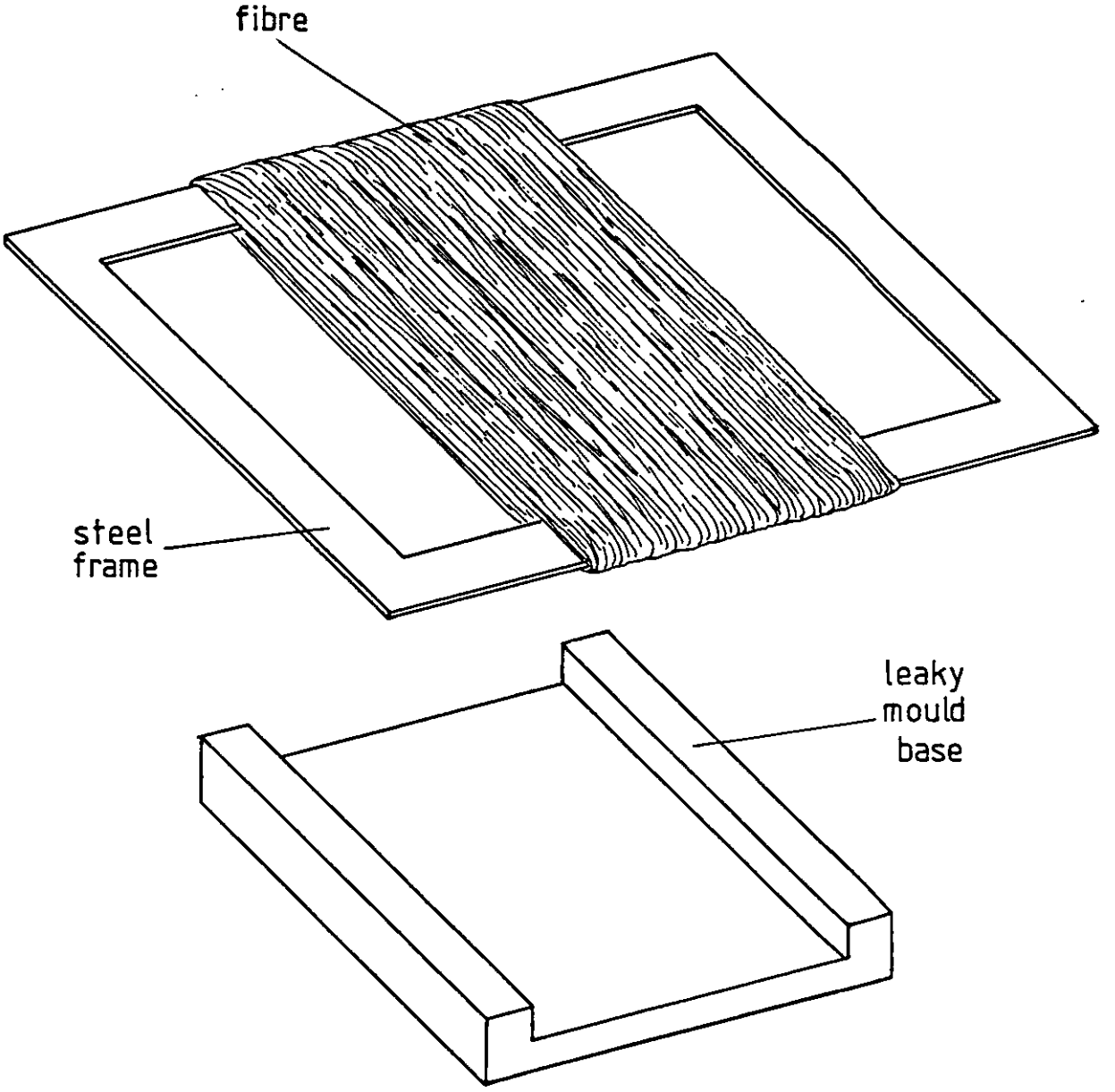

FIGURE 35: A FIBRE WOUND STEEL FRAME READY FOR RESIN IMPREGNATION BY THE WET LAY-UP TECHNIQUE

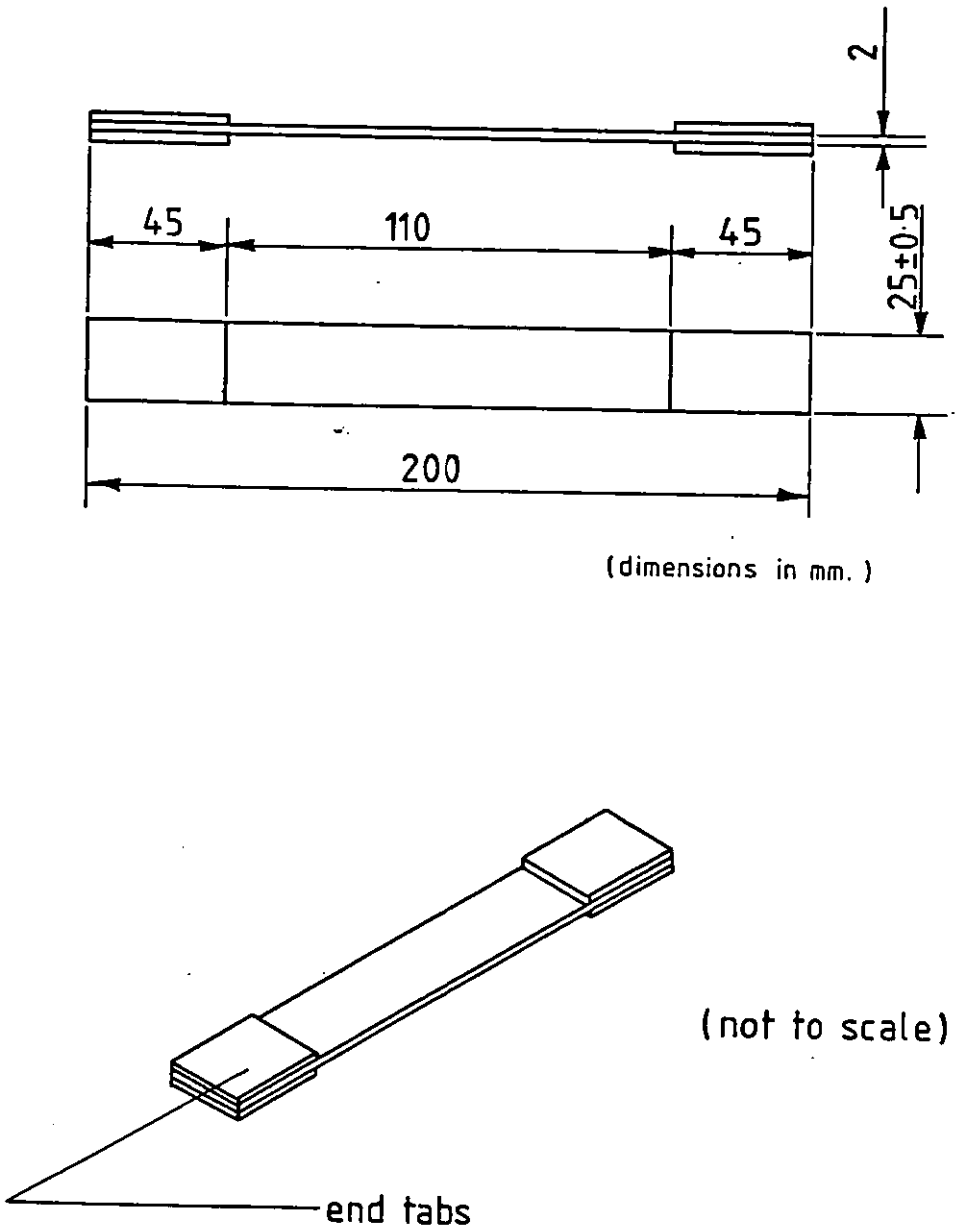

FIGURE 36: THE TENSILE TEST SPECIMEN

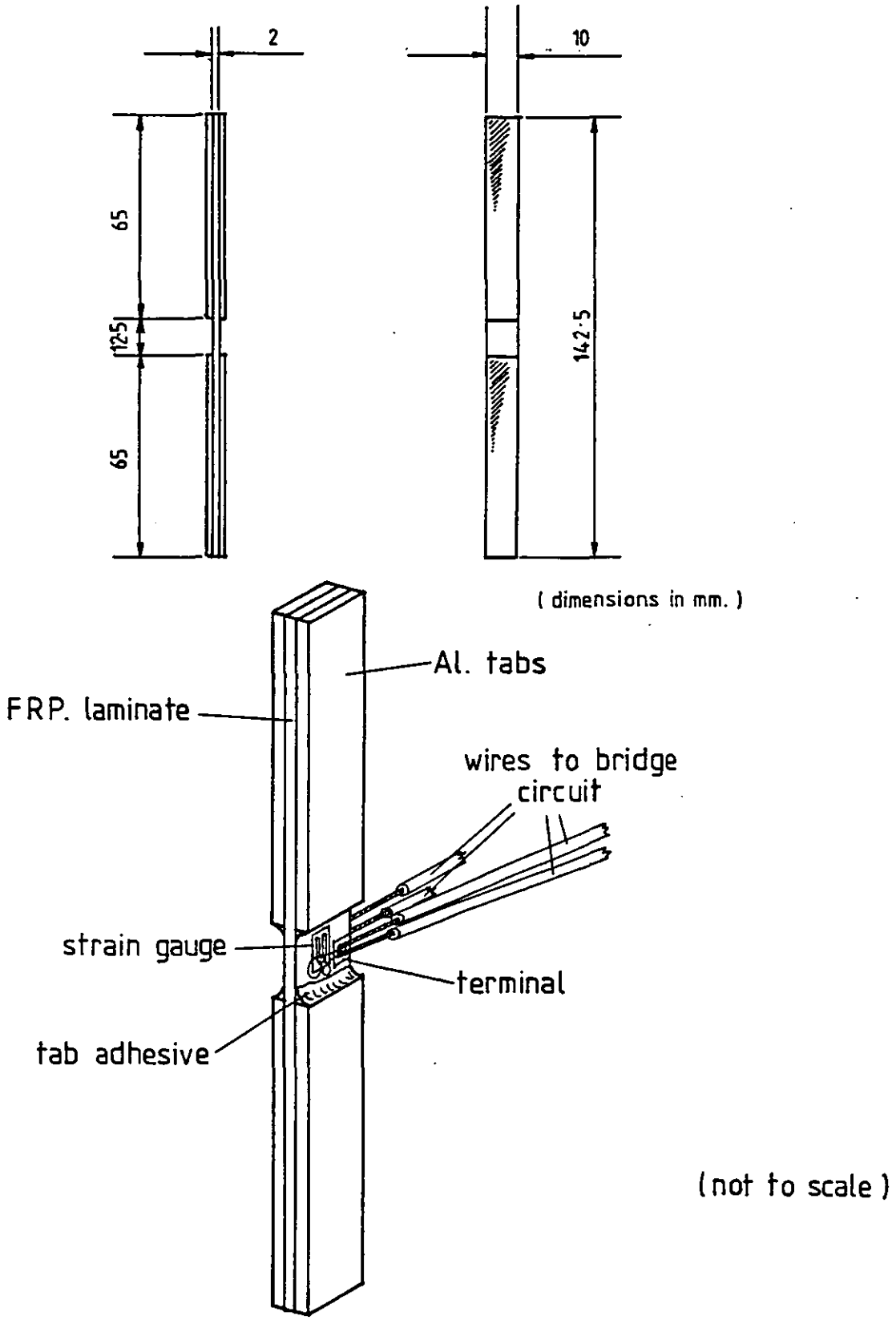

FIGURE 37: THE COMPRESSIVE TEST SPECIMEN

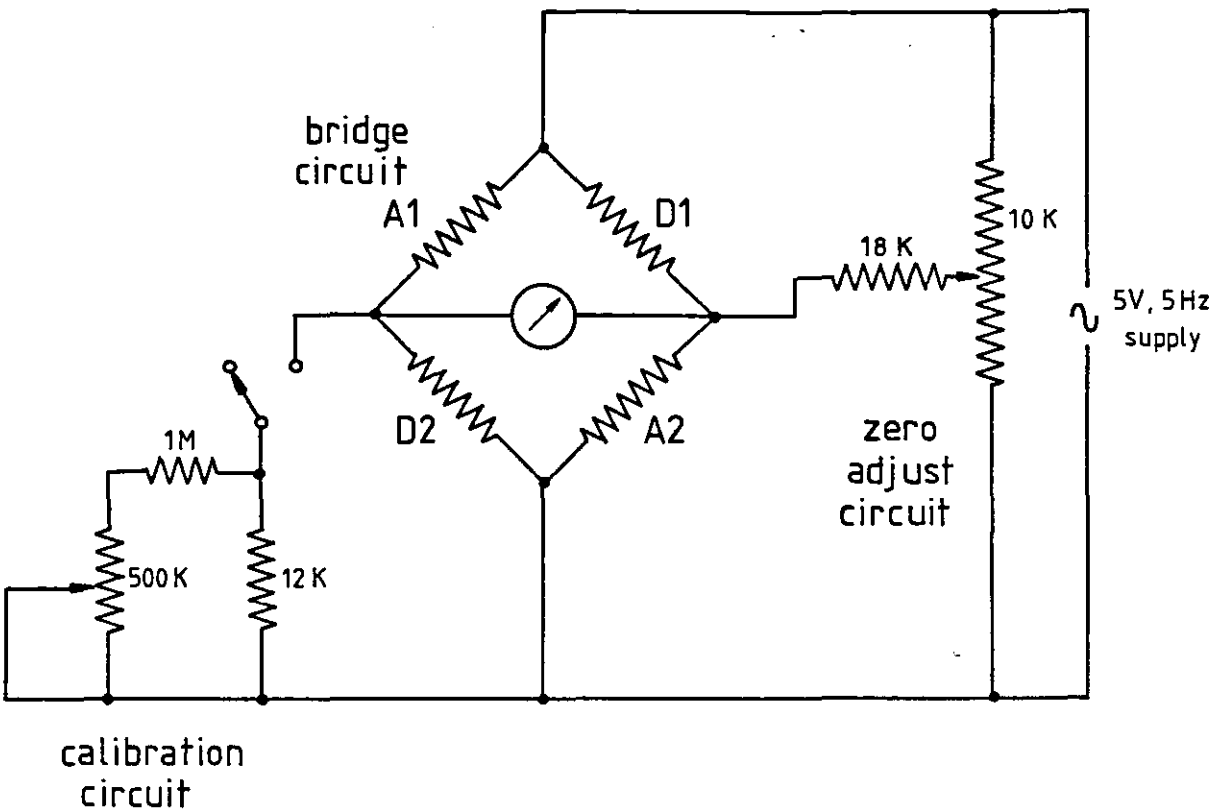

A1, A2 } active 120Ω strain gauges

D1, D2 } dummy 120Ω strain gauges (mounted inside SGCB)

FIGURE 38: THE STRAIN GAUGE BRIDGE CIRCUIT

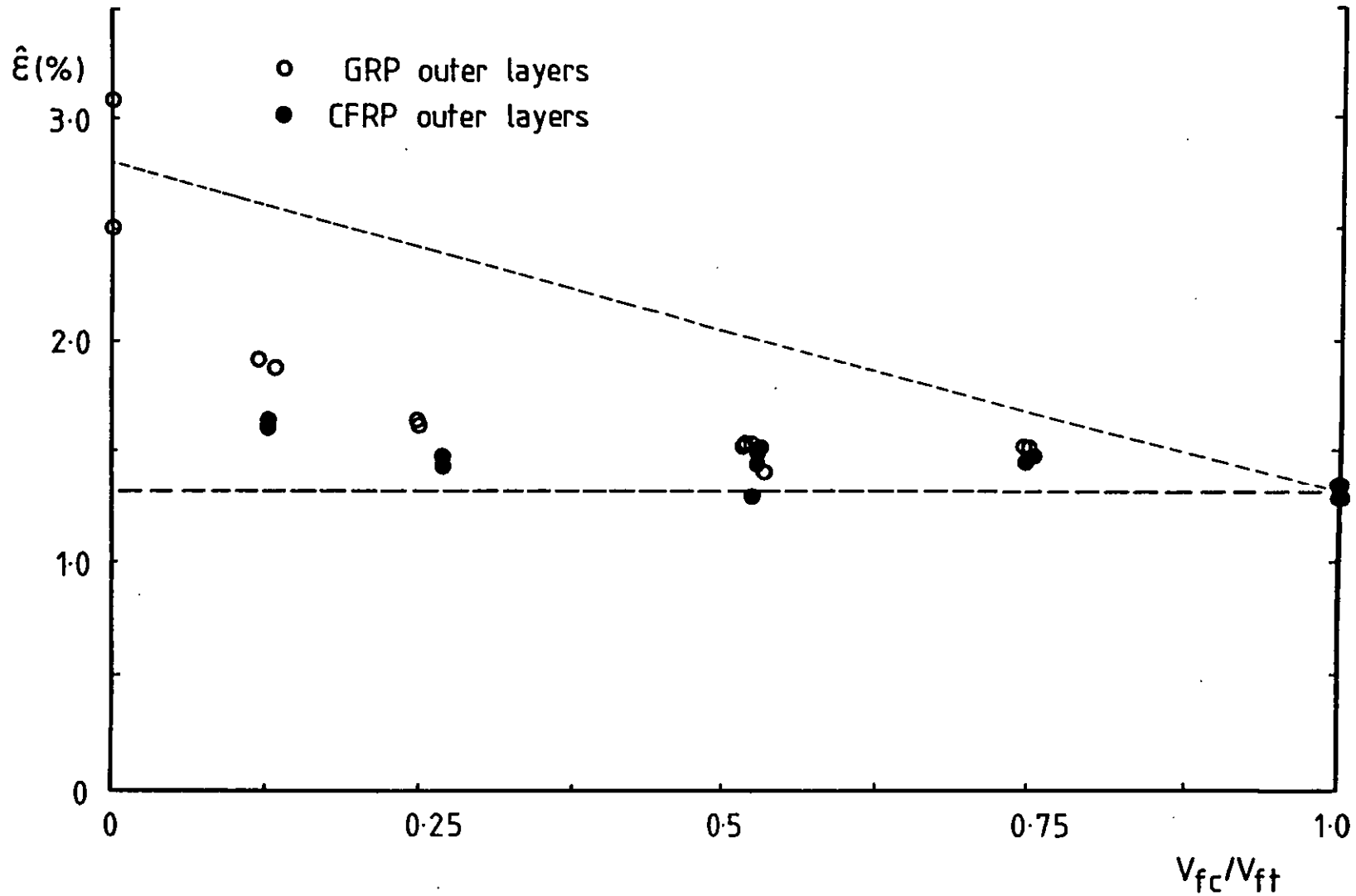

FIGURE 39: PRIMARY TENSILE FAILURE STRAIN RESULTS AS A FUNCTION OF V_{fc}/V_{ft}, 913 MATRIX

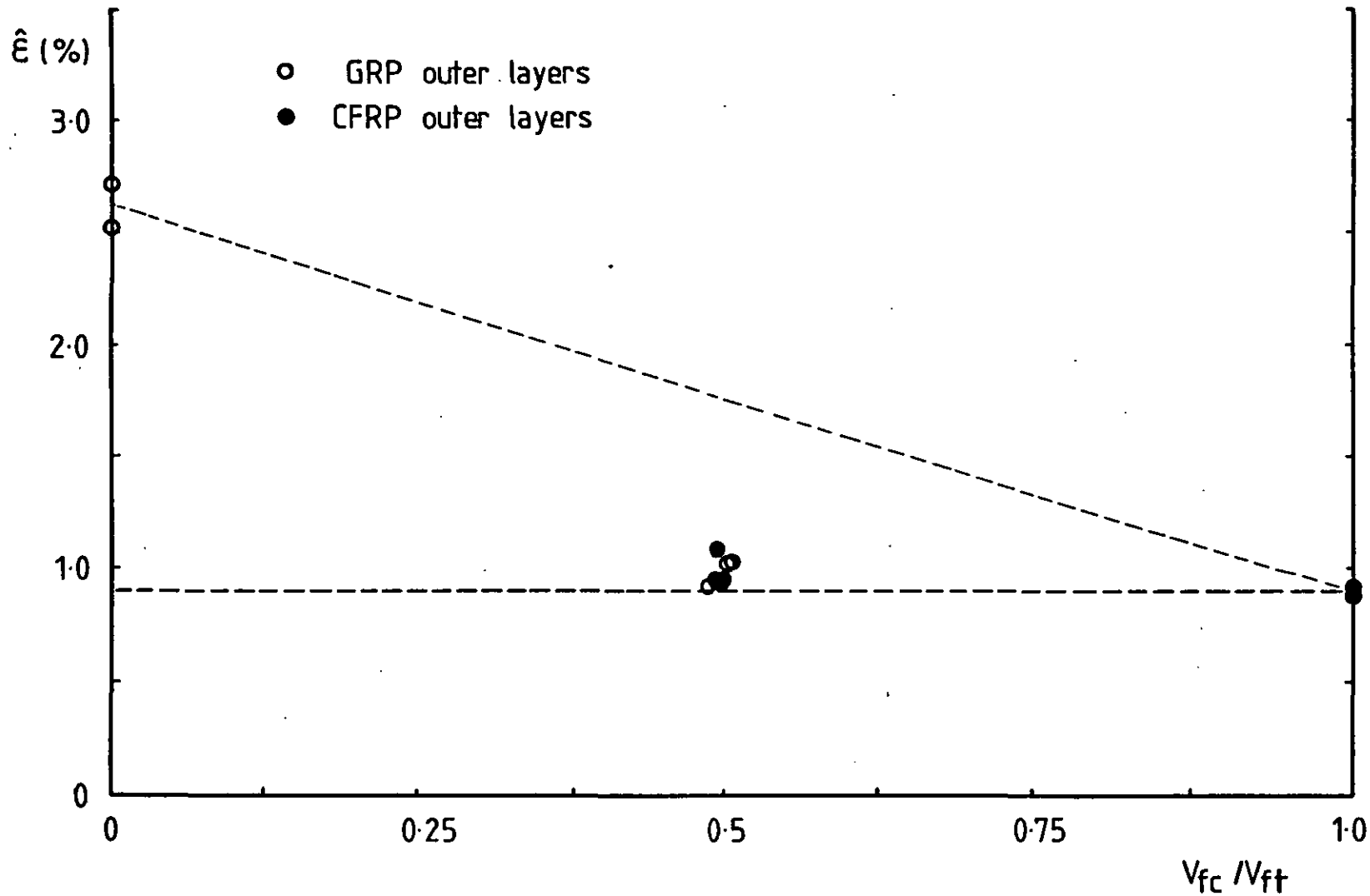

FIGURE 40: PRIMARY TENSILE FAILURE STRAIN RESULTS AS A FUNCTION OF V_{ft}/V_{ft}, 914 MATRIX

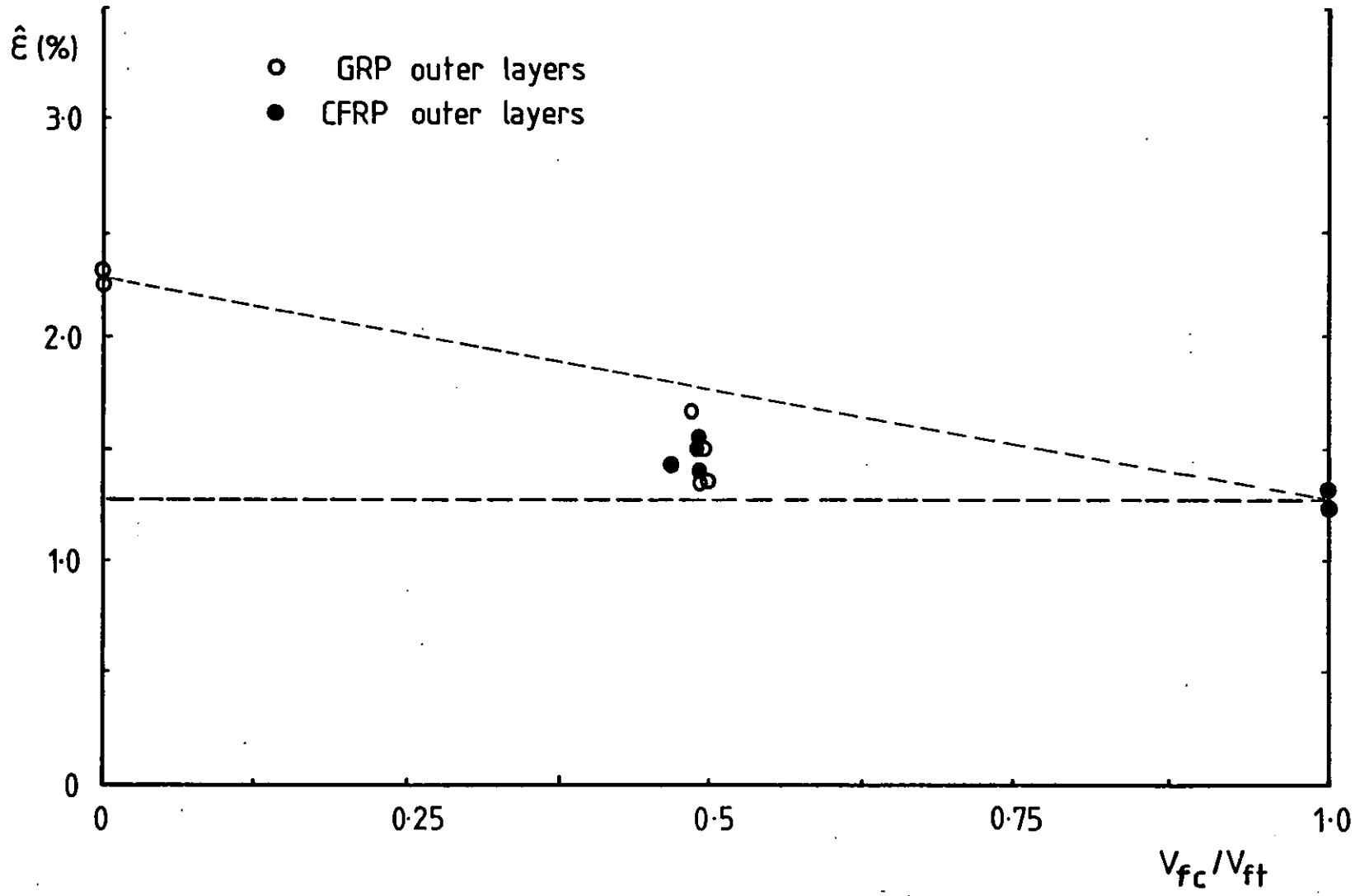

FIGURE 41: PRIMARY TENSILE FAILURE STRAIN RESULTS AS A FUNCTION OF V_{ft}/V_{ft}, 411-45 MATRIX

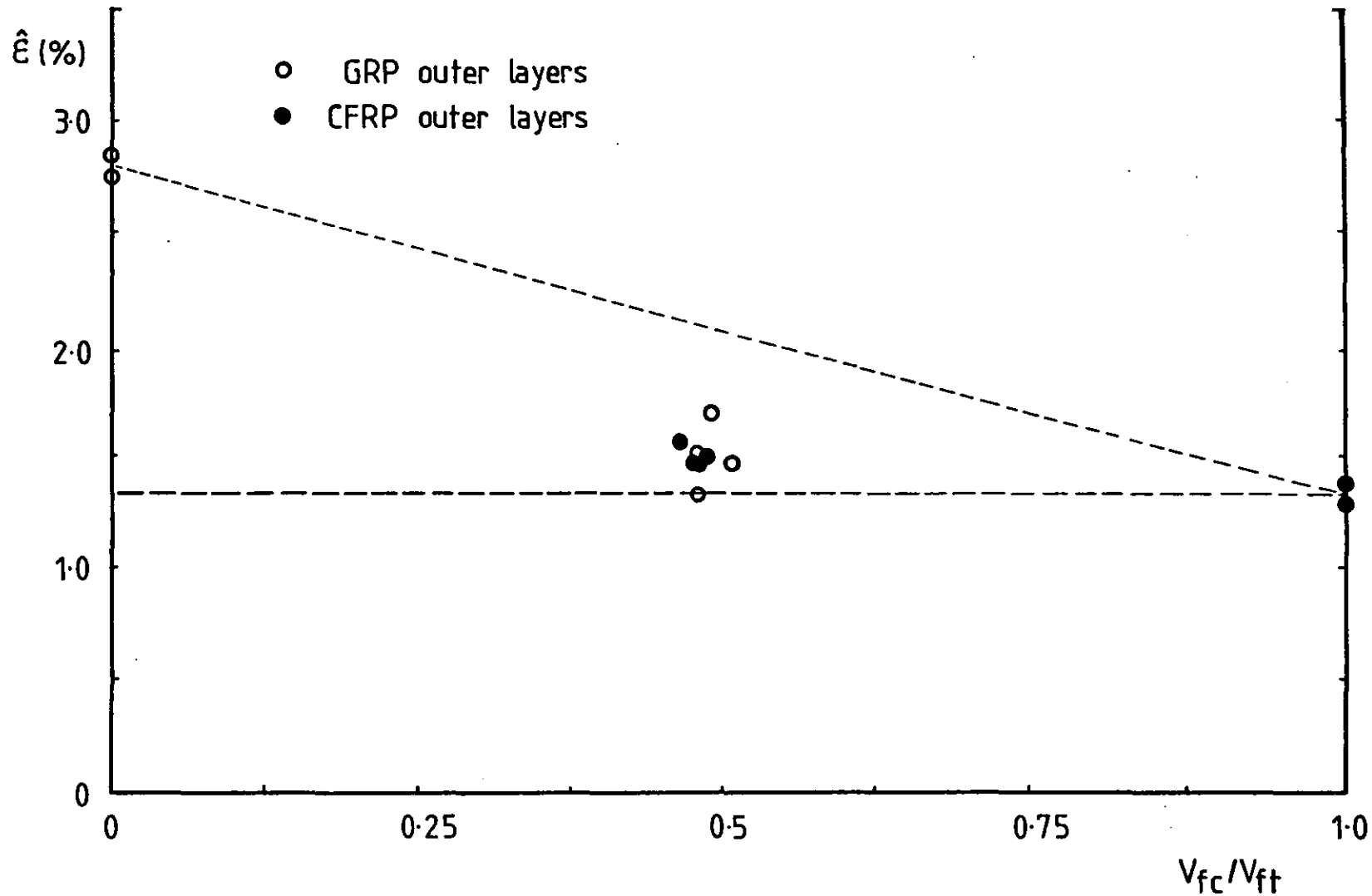

FIGURE 42: PRIMARY TENSILE FAILURE STRAIN RESULTS AS A FUNCTION OF V_{fc}/V_{ft}, 470-36 MATRIX

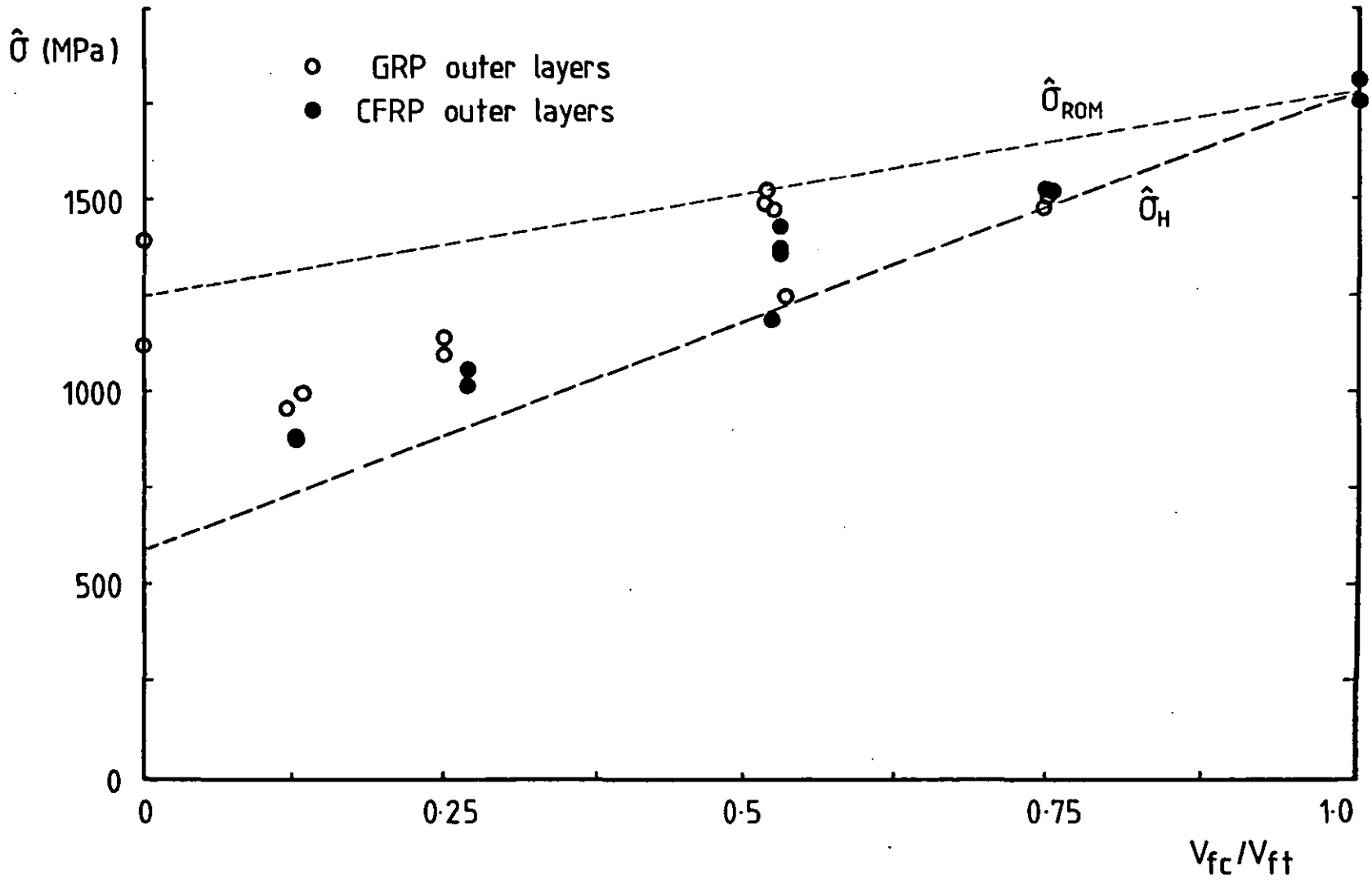

FIGURE 43: ULTIMATE TENSILE STRENGTH RESULTS AS A FUNCTION OF V_{ft}/V_{ft}, 913 MATRIX

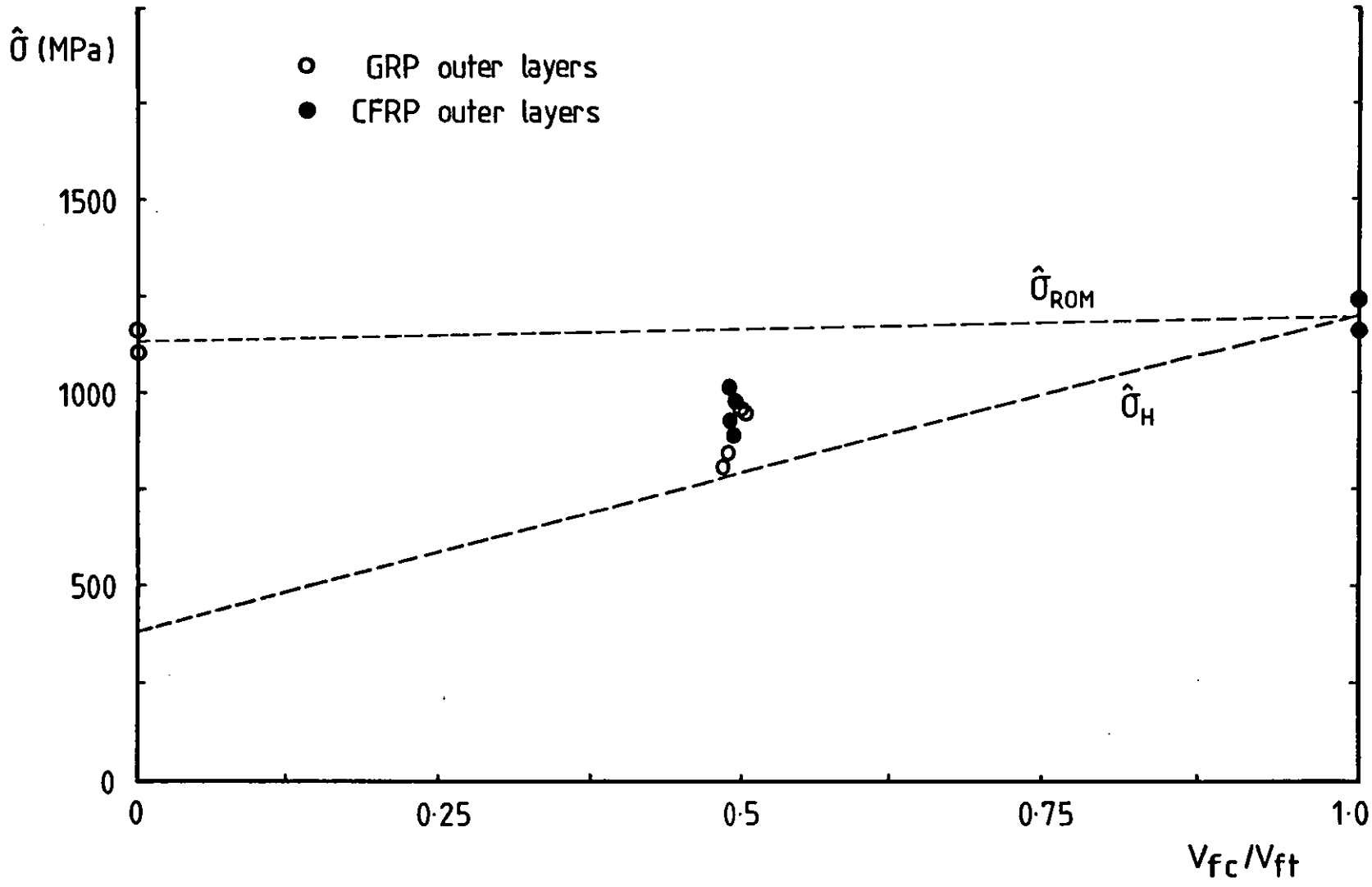

FIGURE 44: ULTIMATE TENSILE STRENGTH RESULTS AS A FUNCTION OF V_{fc}/V_{ft}, 914 MATRIX

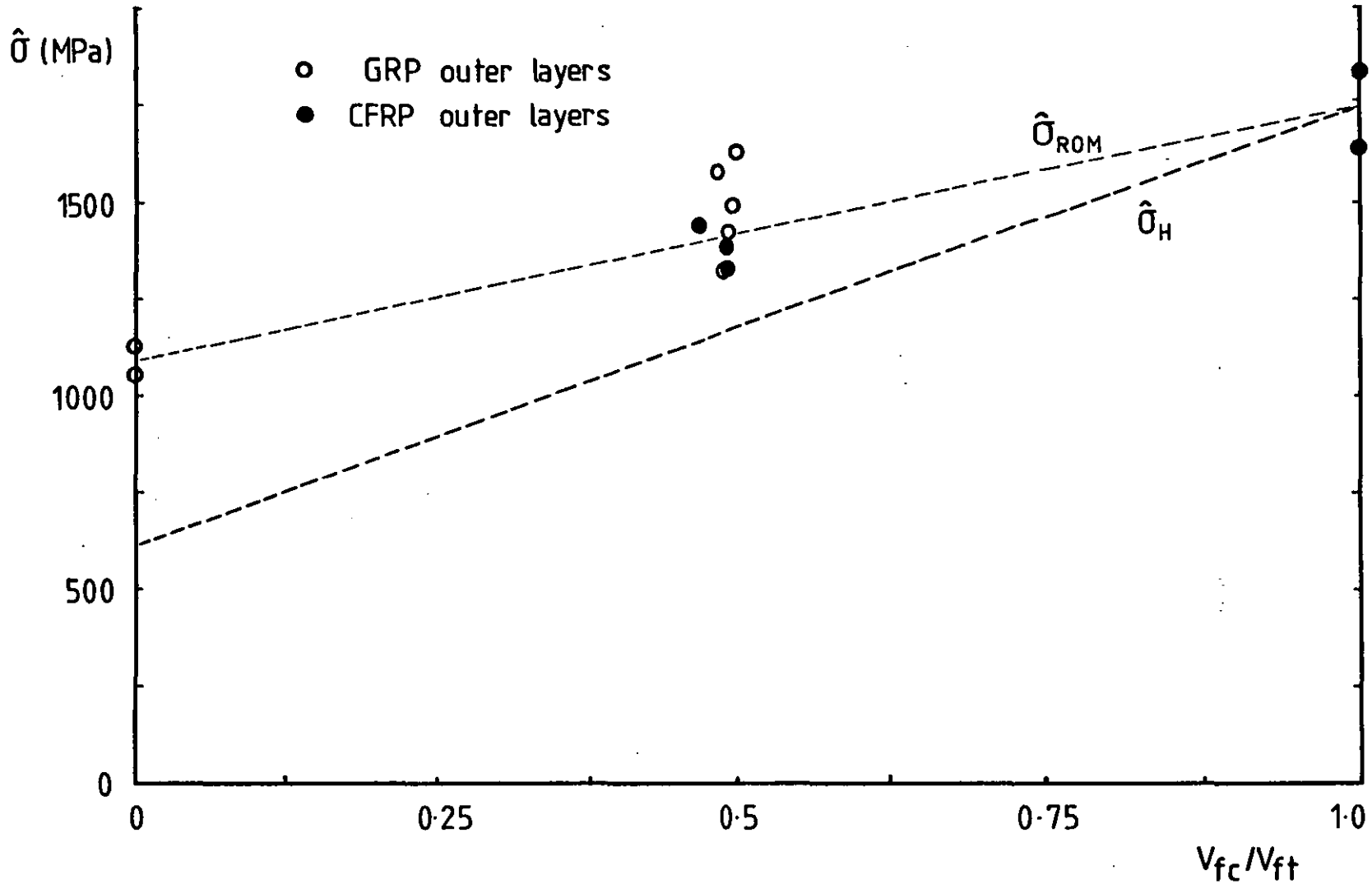

FIGURE 45: ULTIMATE TENSILE STRENGTH RESULTS AS A FUNCTION OF V_{fc}/V_{ft}, 411-45 MATRIX

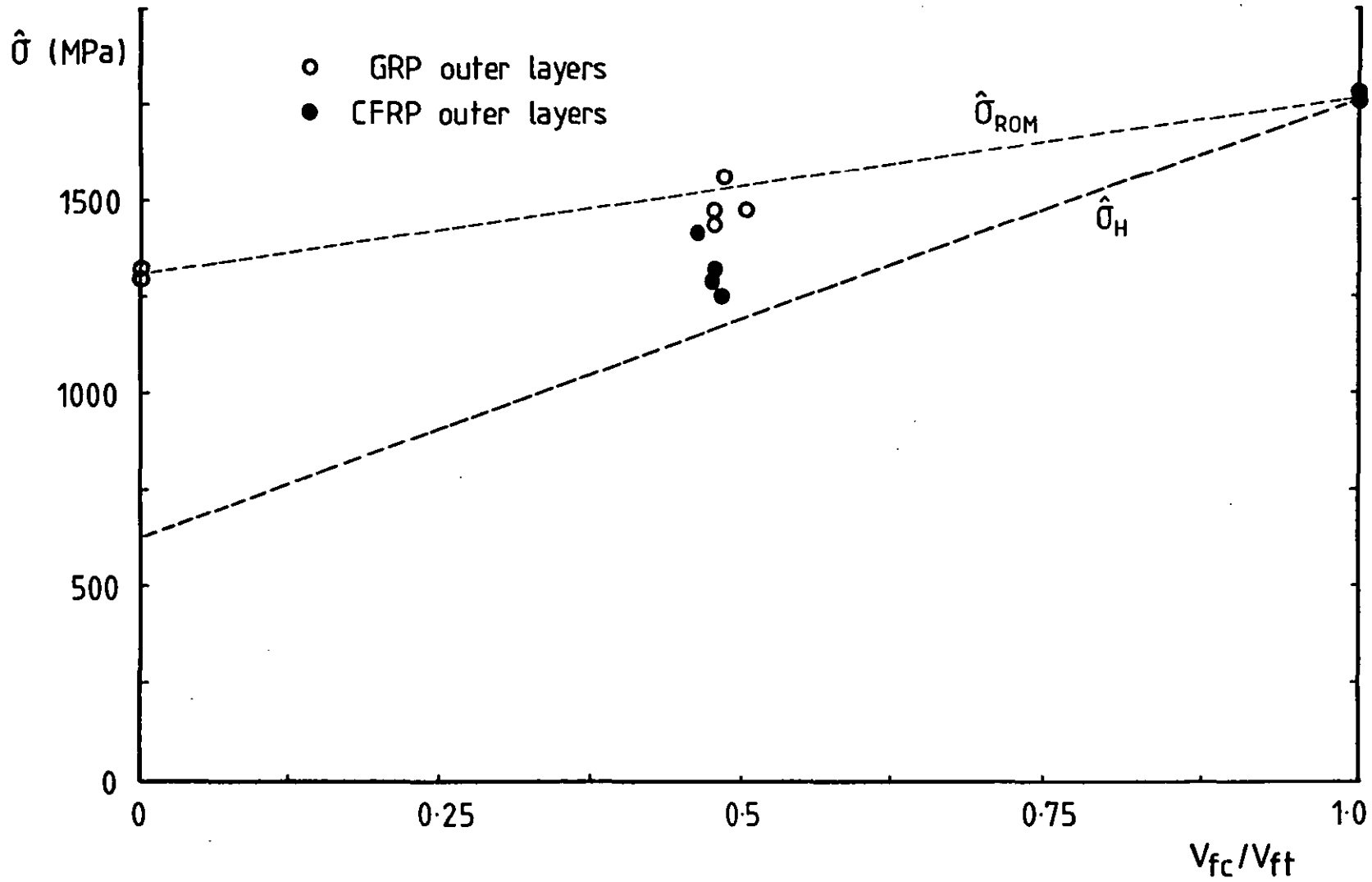

FIGURE 46: ULTIMATE TENSILE STRENGTH RESULTS AS A FUNCTION OF V_{fc}/V_{ft}, 470-36 MATRIX

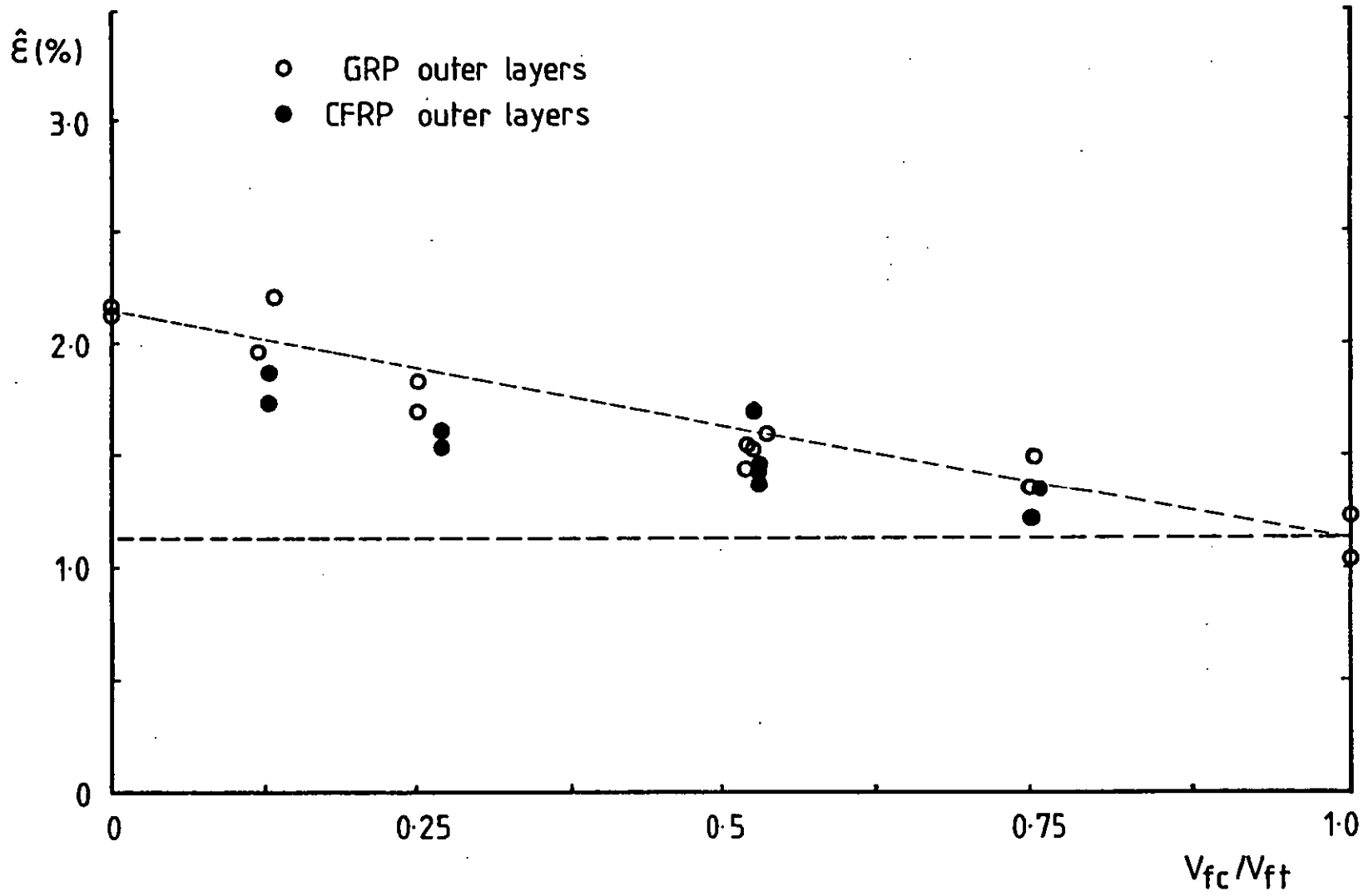

FIGURE 47: COMPRESSIVE FAILURE STRAIN RESULTS AS A FUNCTION OF V_{fc}/V_{ft}, 913 MATRIX

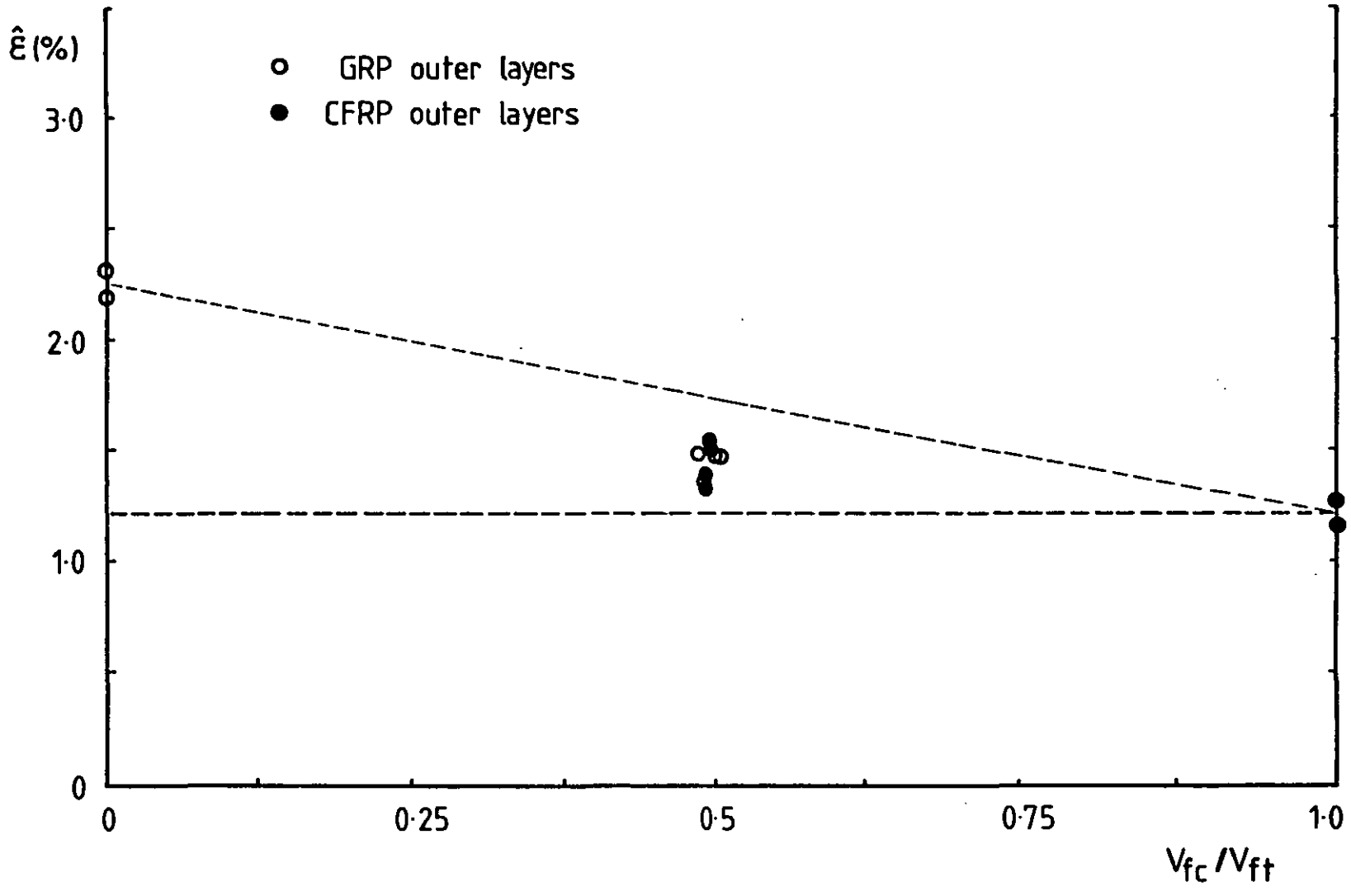

FIGURE 48: COMPRESSIVE FAILURE STRAIN RESULTS AS A FUNCTION OF V_{fc}/V_{ft}, 914 MATRIX

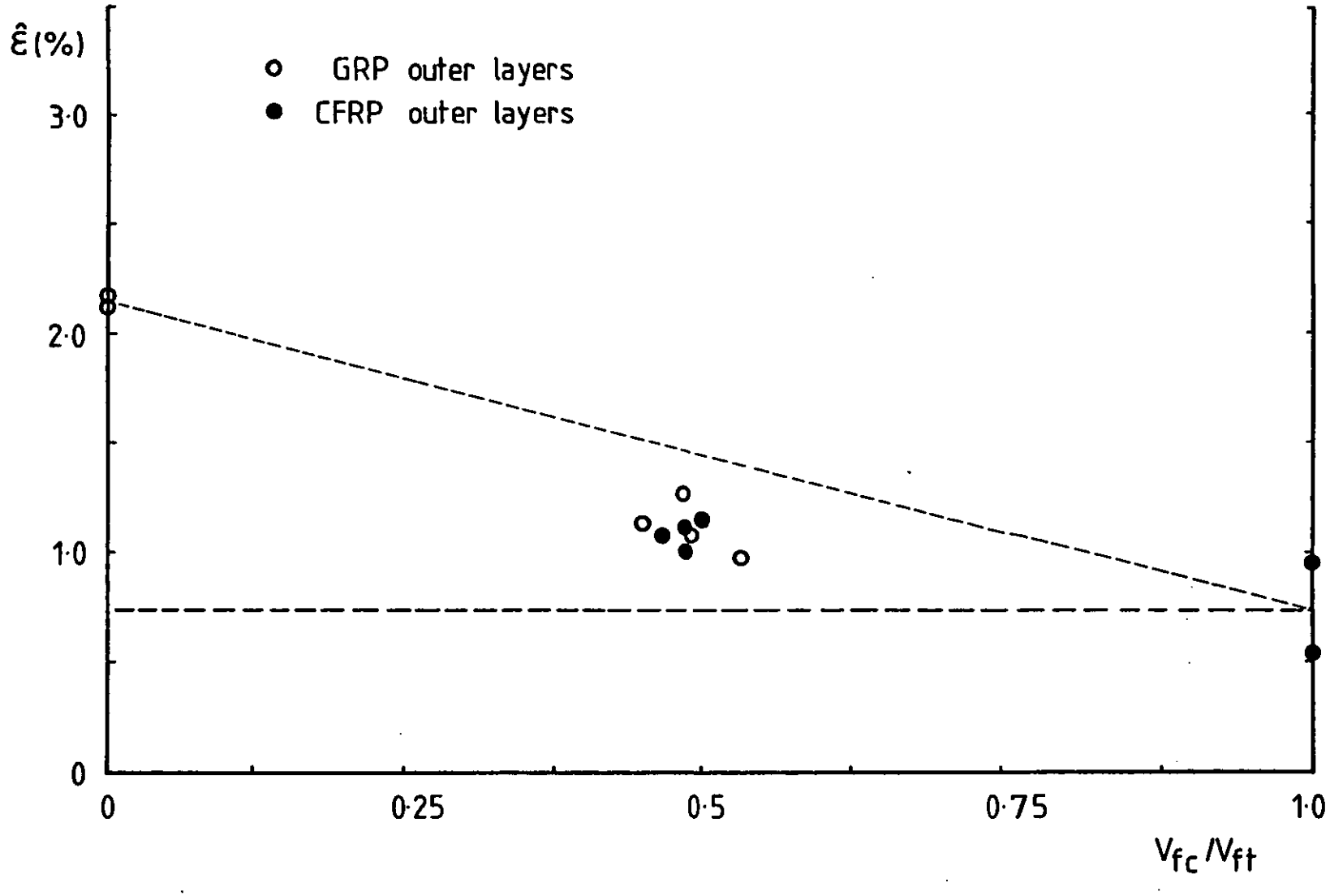

FIGURE 49: COMPRESSIVE FAILURE STRAIN RESULTS AS A FUNCTION OF V_{fc}/V_{ft}, 411-45 MATRIX

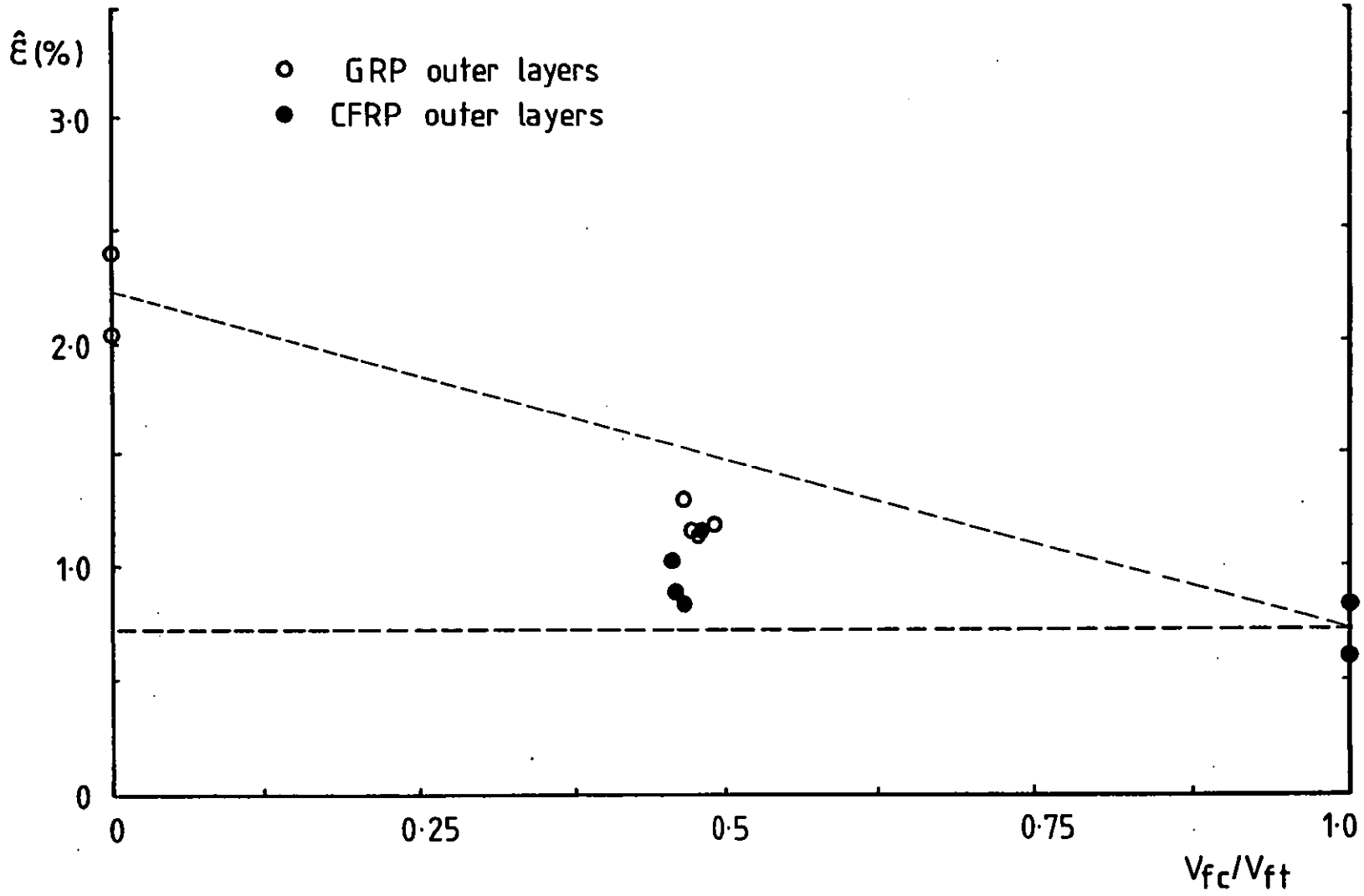

FIGURE 50: COMPRESSIVE FAILURE STRAIN RESULTS AS A FUNCTION OF V_{fc}/V_{ft}, 470-36 MATRIX

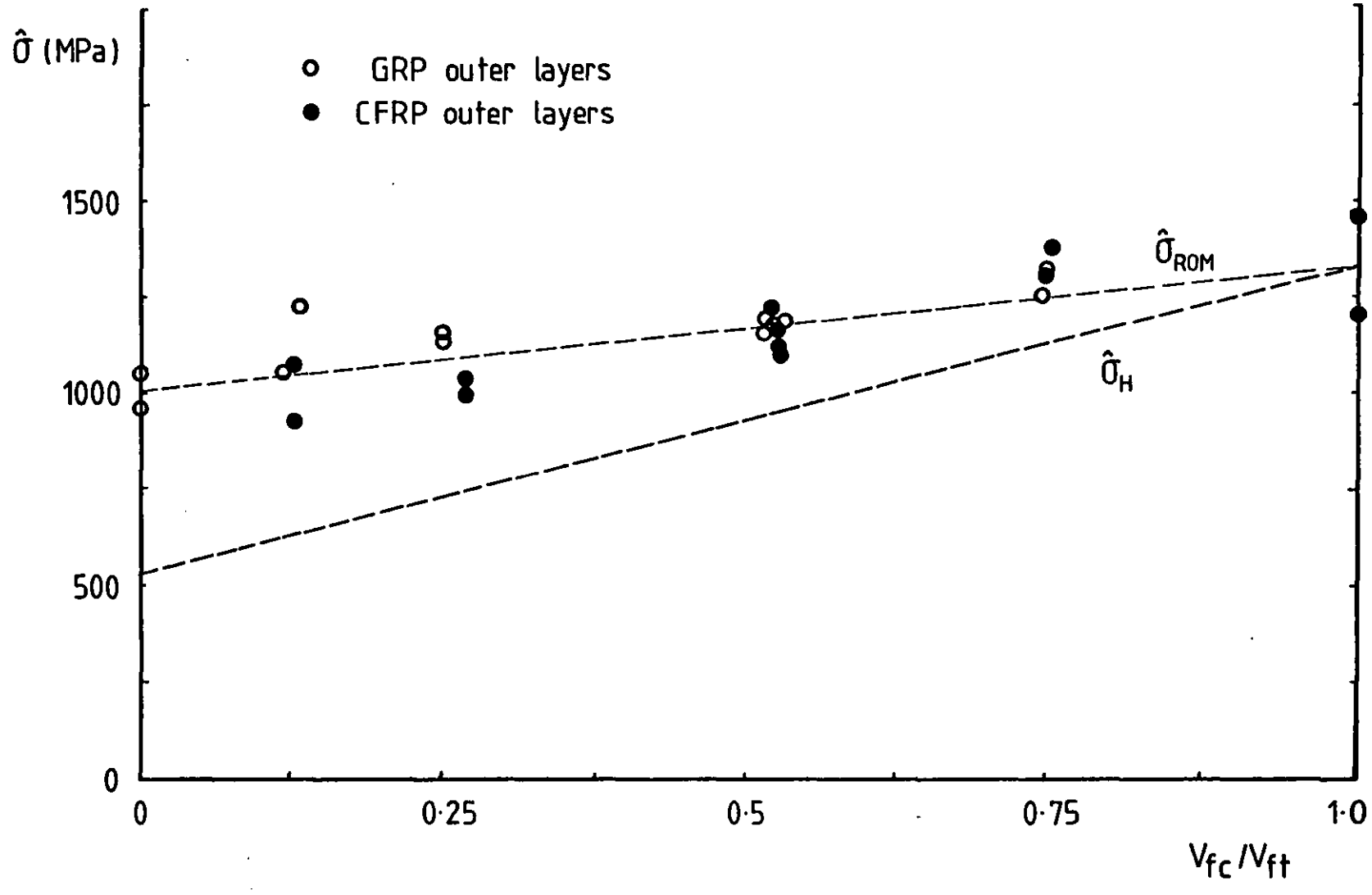

FIGURE 51: COMPRESSIVE STRENGTH RESULTS AS A FUNCTION OF V_{fc}/V_{ft}, 913 MATRIX

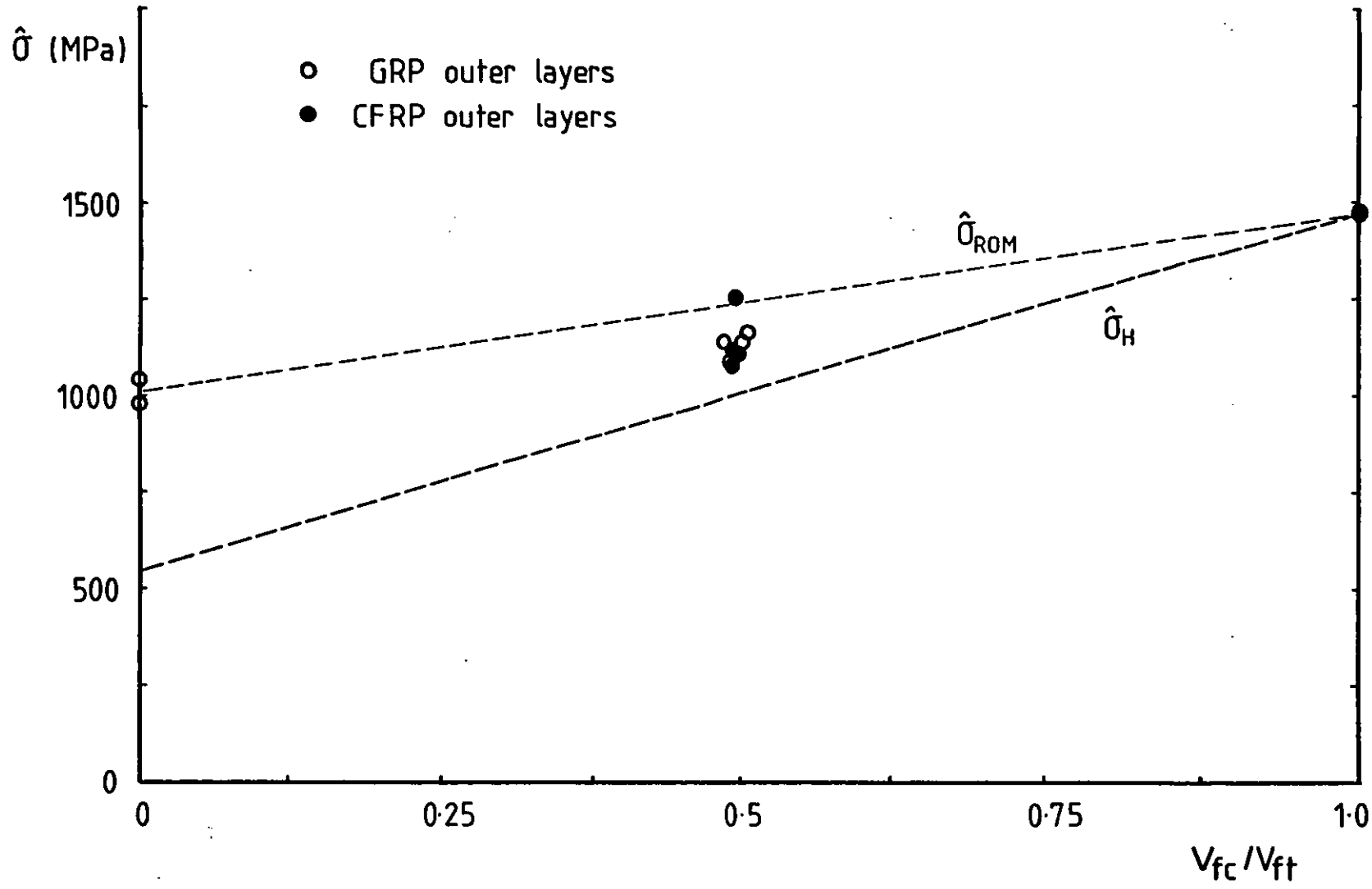

FIGURE 52: COMPRESSIVE STRENGTH RESULTS AS A FUNCTION OF V_{fc}/V_{ft}, 914 MATRIX

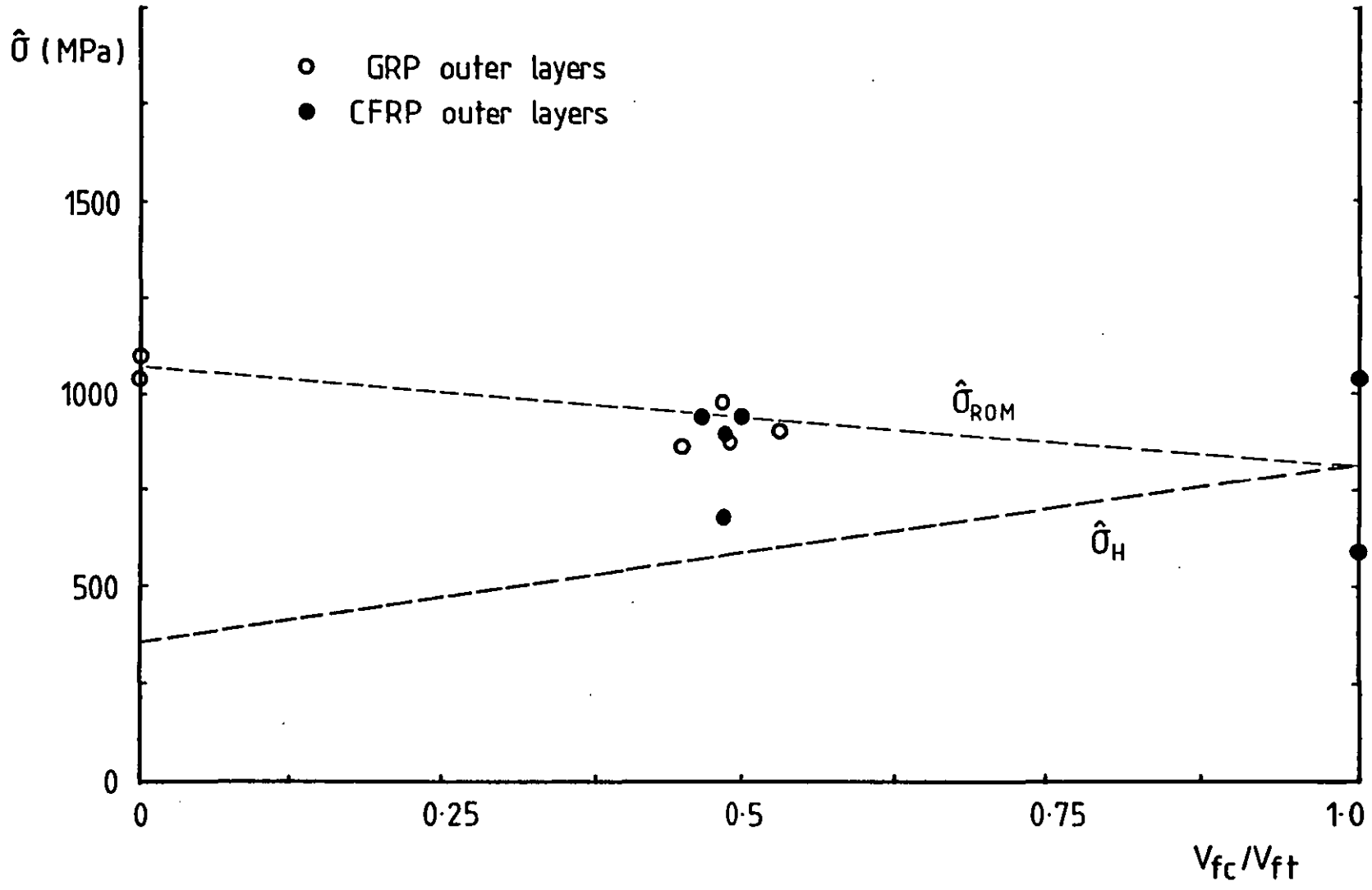

FIGURE 53: COMPRESSIVE STRENGTH RESULTS AS A FUNCTION OF V_{fc}/V_{ft}, 411-45 MATRIX

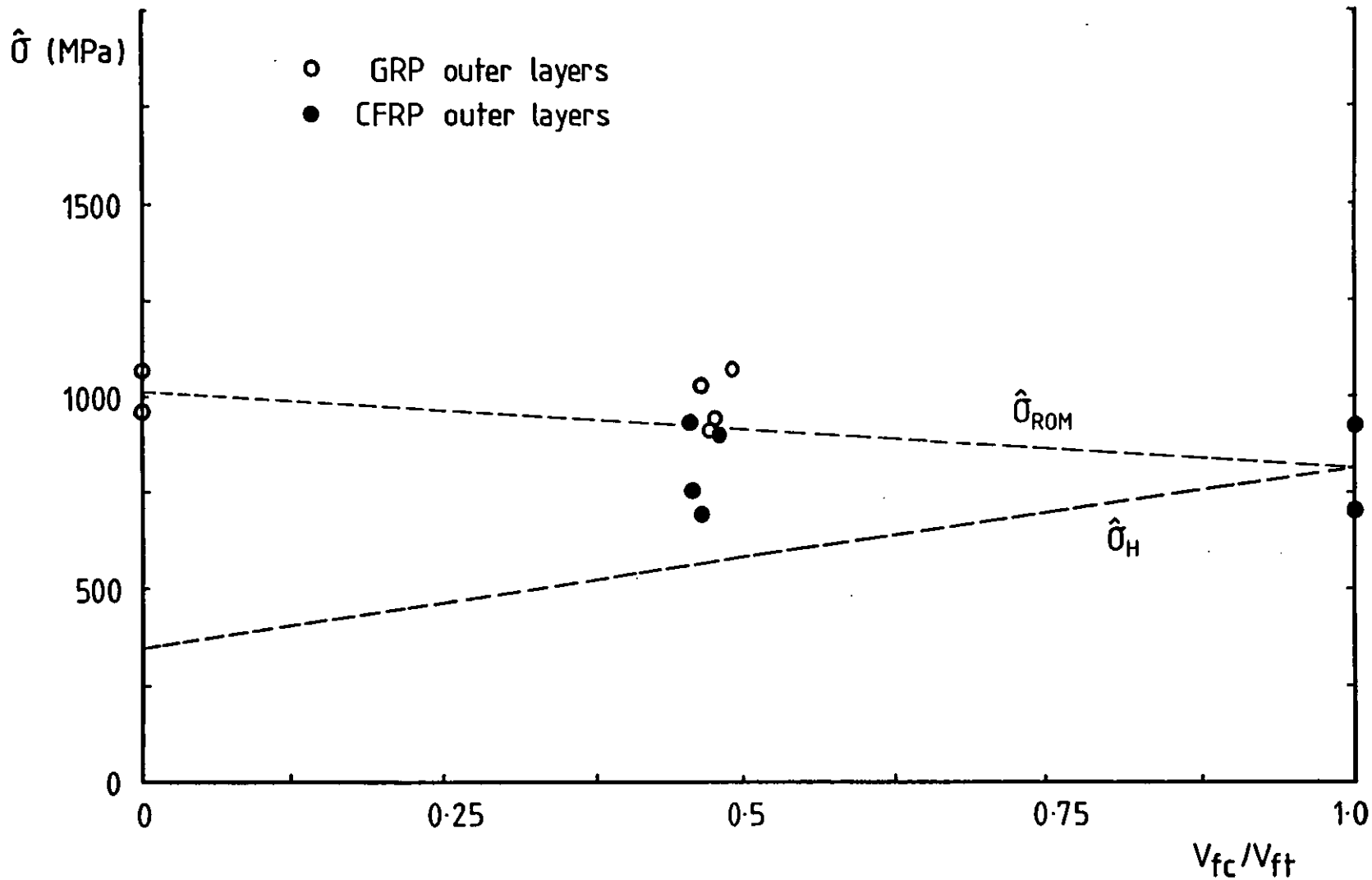

FIGURE 54: COMPRESSIVE STRENGTH RESULTS AS A FUNCTION OF V_{fc}/V_{ft}, 470-36 MATRIX

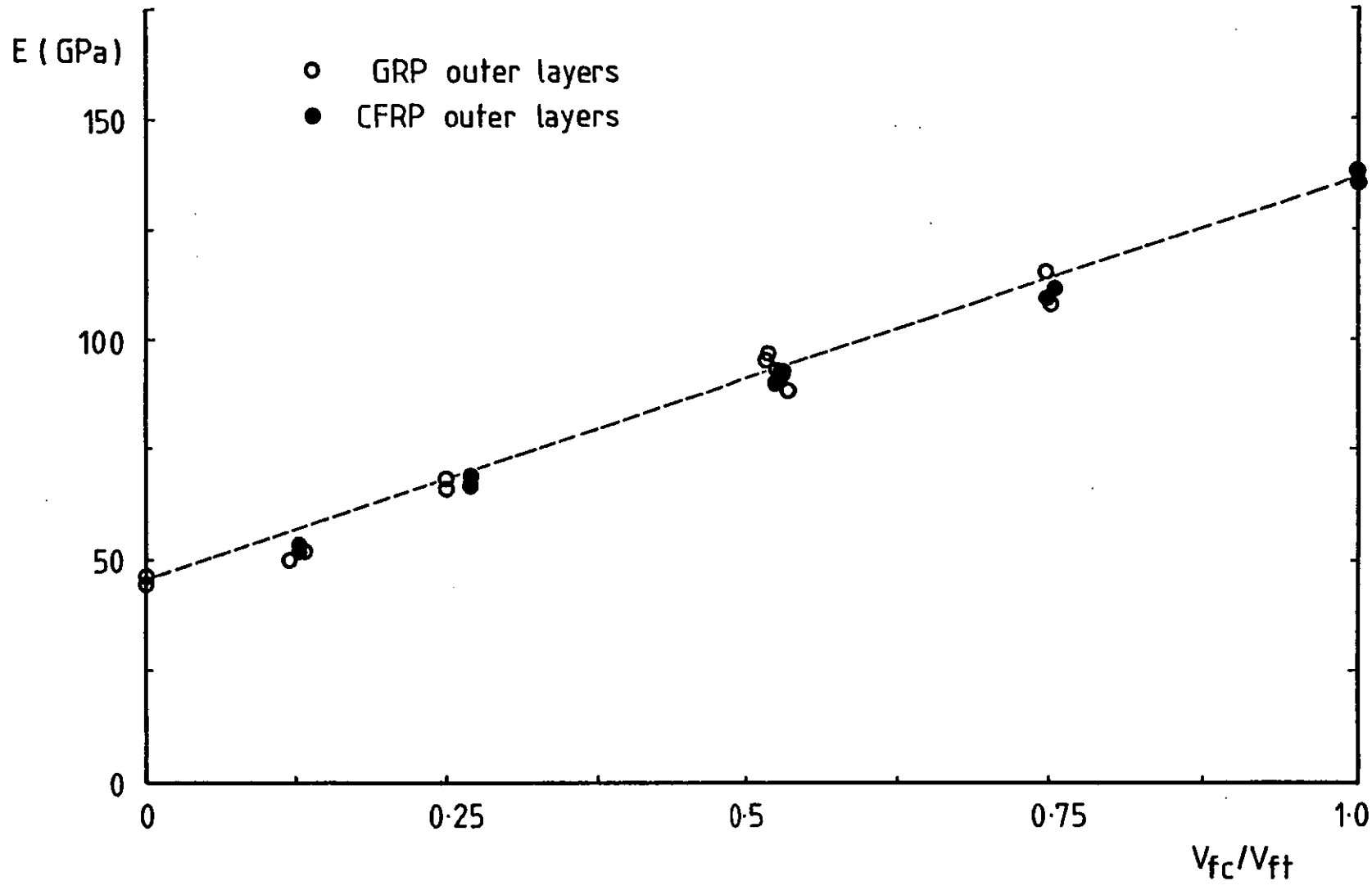

FIGURE 55: TENSILE MODULUS RESULTS AS A FUNCTION OF V_{fc}/V_{ft}, 913 MATRIX

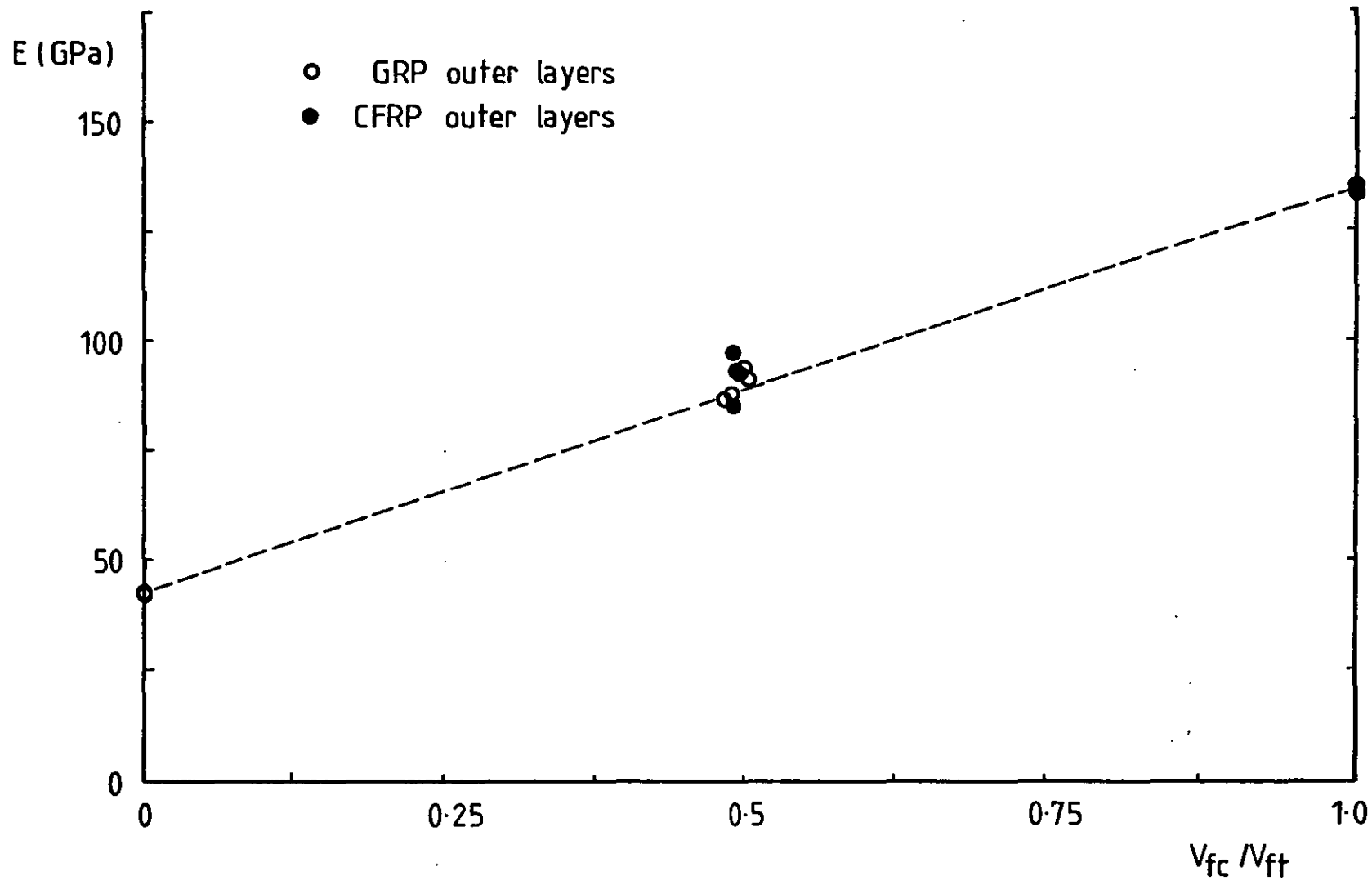

FIGURE 56: TENSILE MODULUS RESULTS AS A FUNCTION OF V_{fc}/V_{ft}, 914 MATRIX

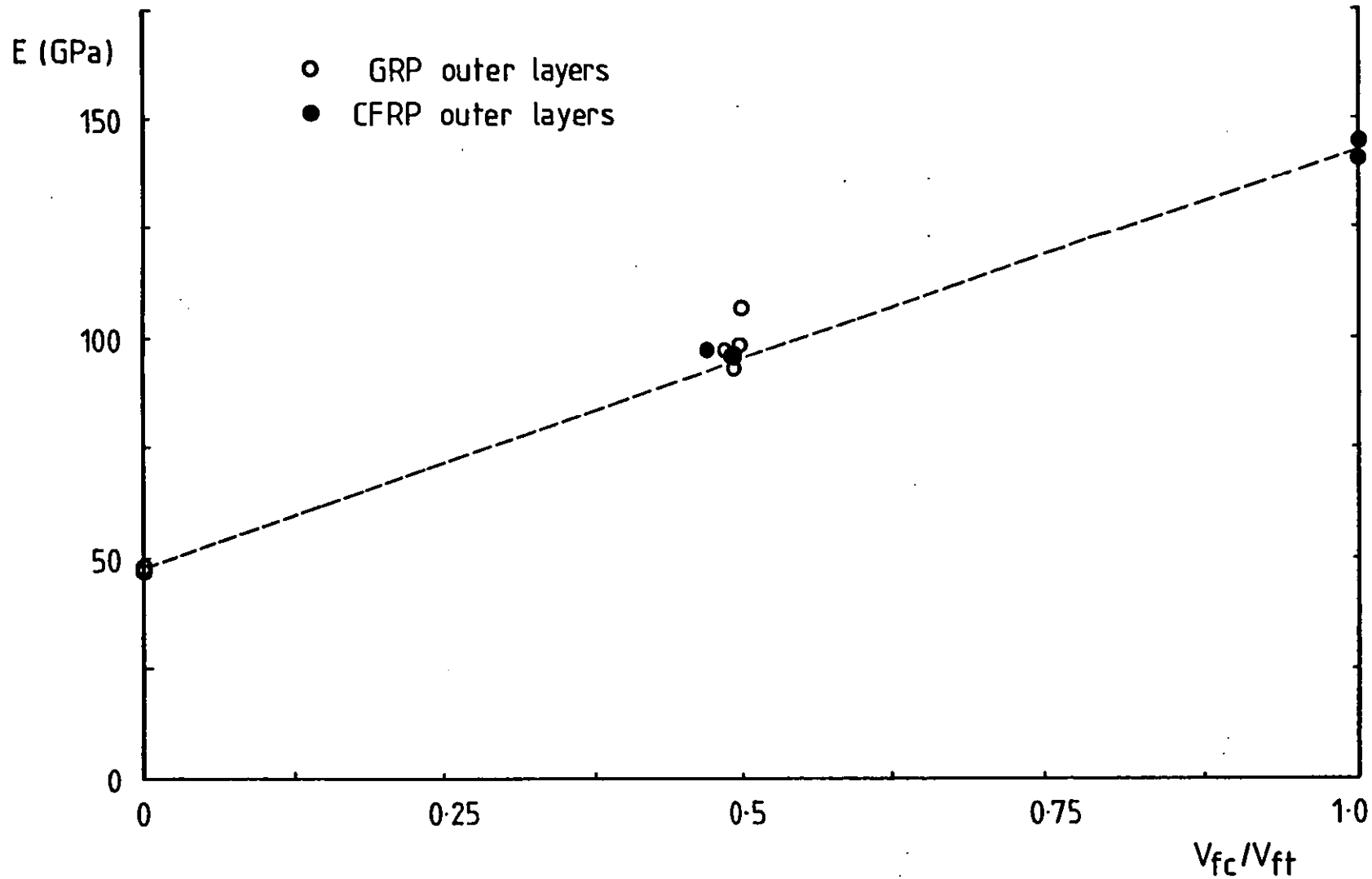

FIGURE 57: TENSILE MODULUS RESULTS AS A FUNCTION OF V_{fc}/V_{ft}, 411-45 MATRIX

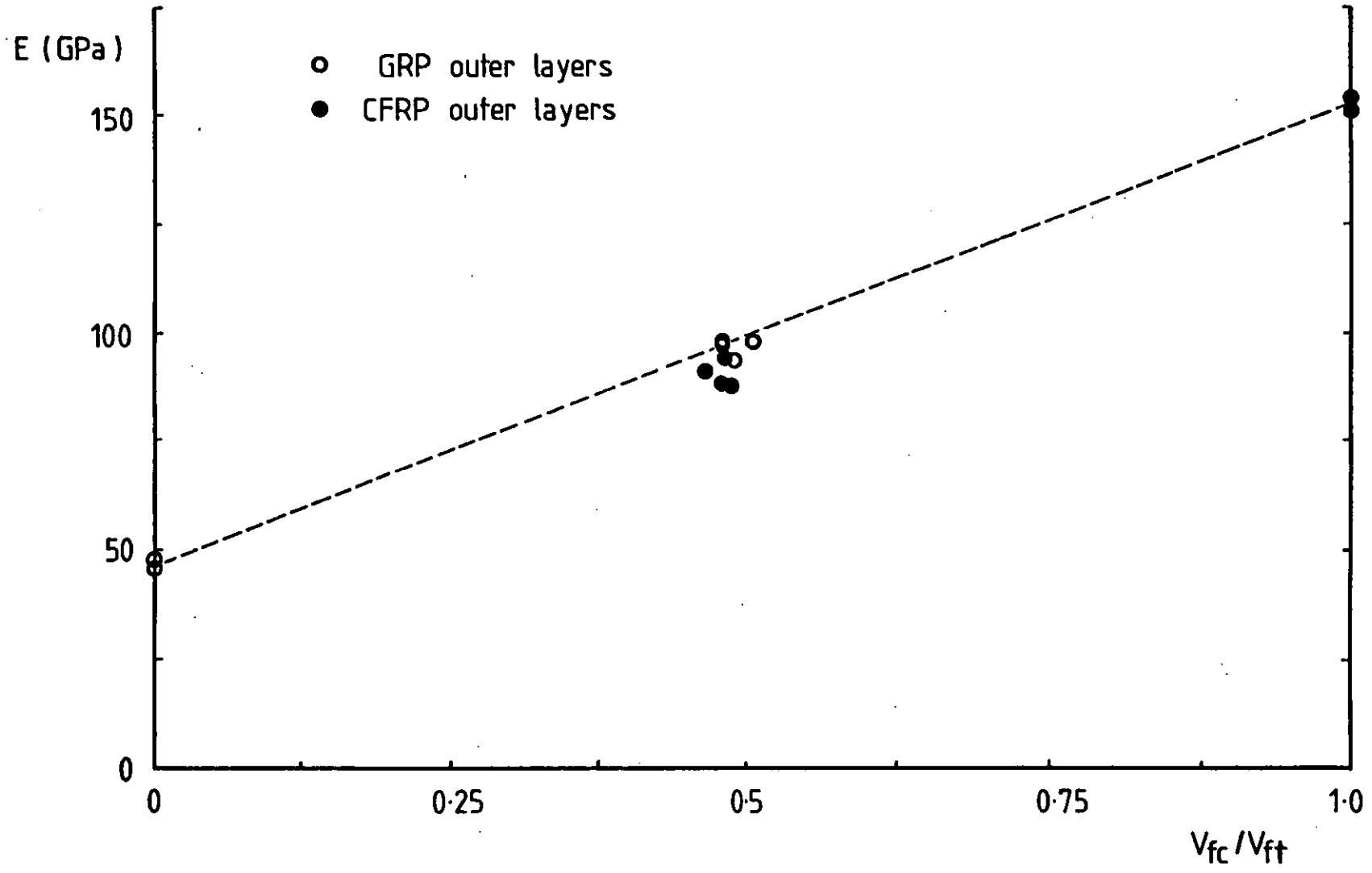

FIGURE 58: TENSILE MODULUS RESULTS AS A FUNCTION OF V_{fc}/V_{ft}, 470-36 MATRIX

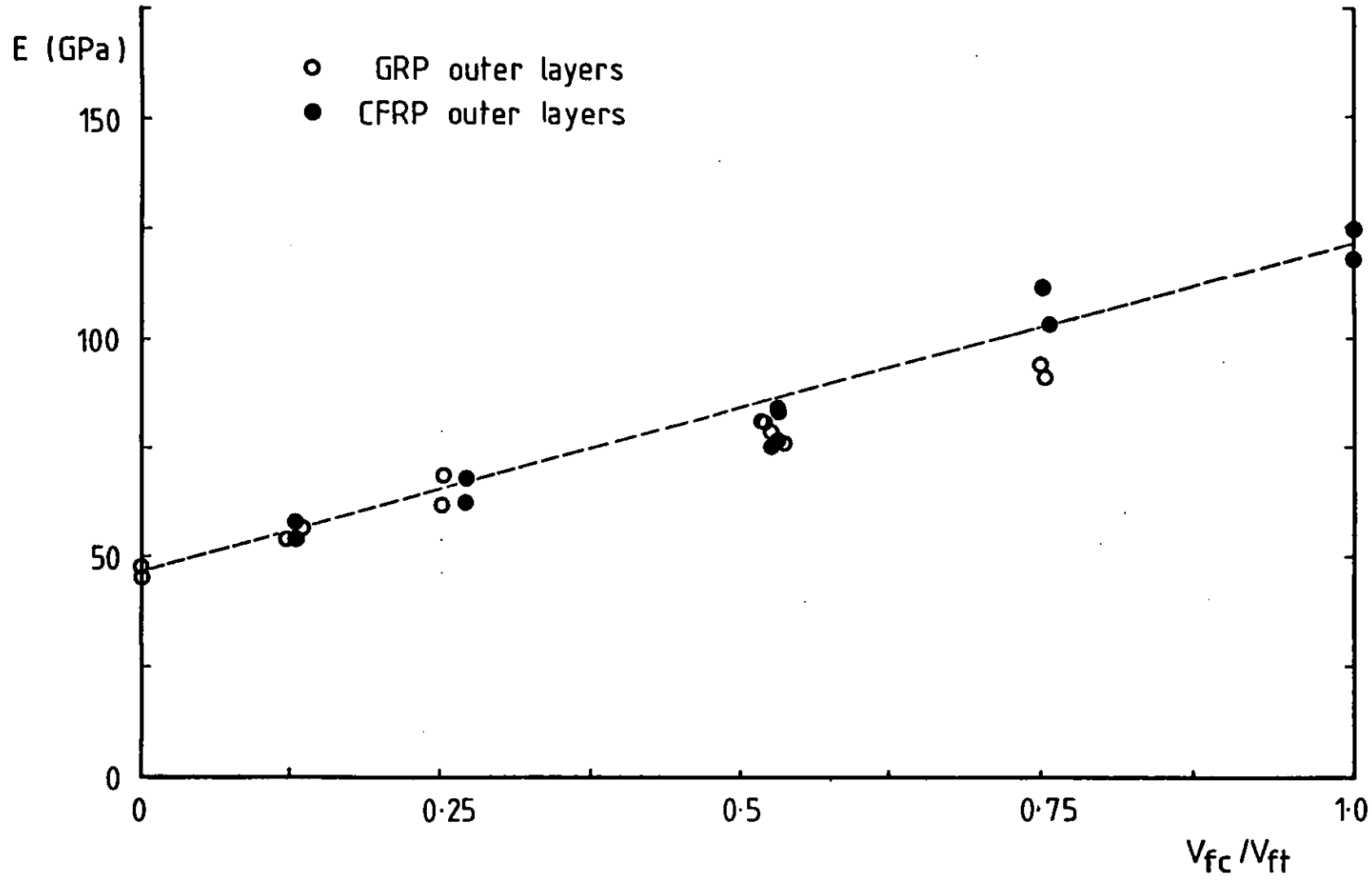

FIGURE 59: COMPRESSIVE MODULUS RESULTS AS A FUNCTION OF V_{fc}/V_{ft}, 913 MATRIX

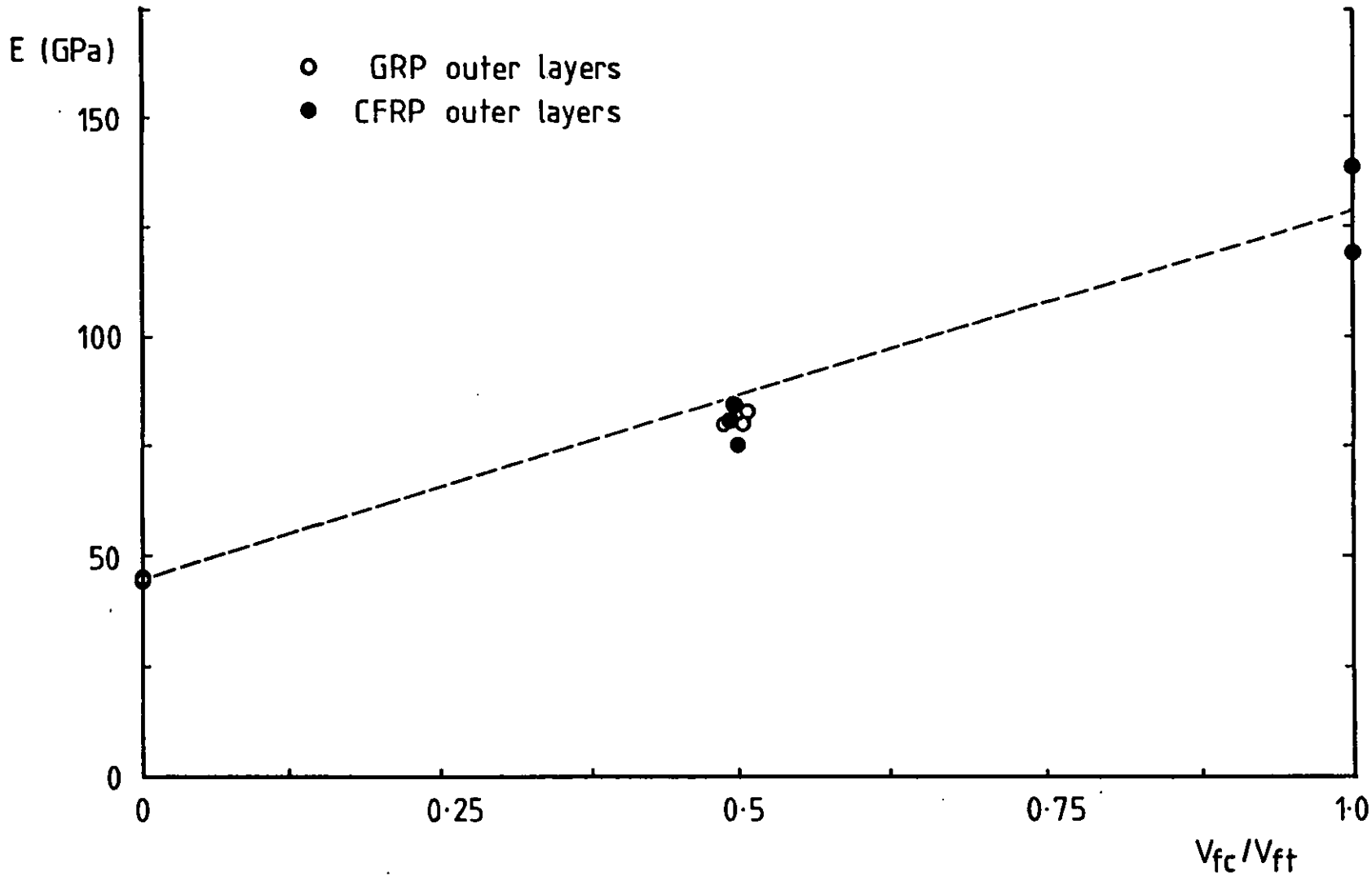

FIGURE 60: COMPRESSIVE MODULUS RESULTS AS A FUNCTION OF V_{fc}/V_{ft}, 914 MATRIX

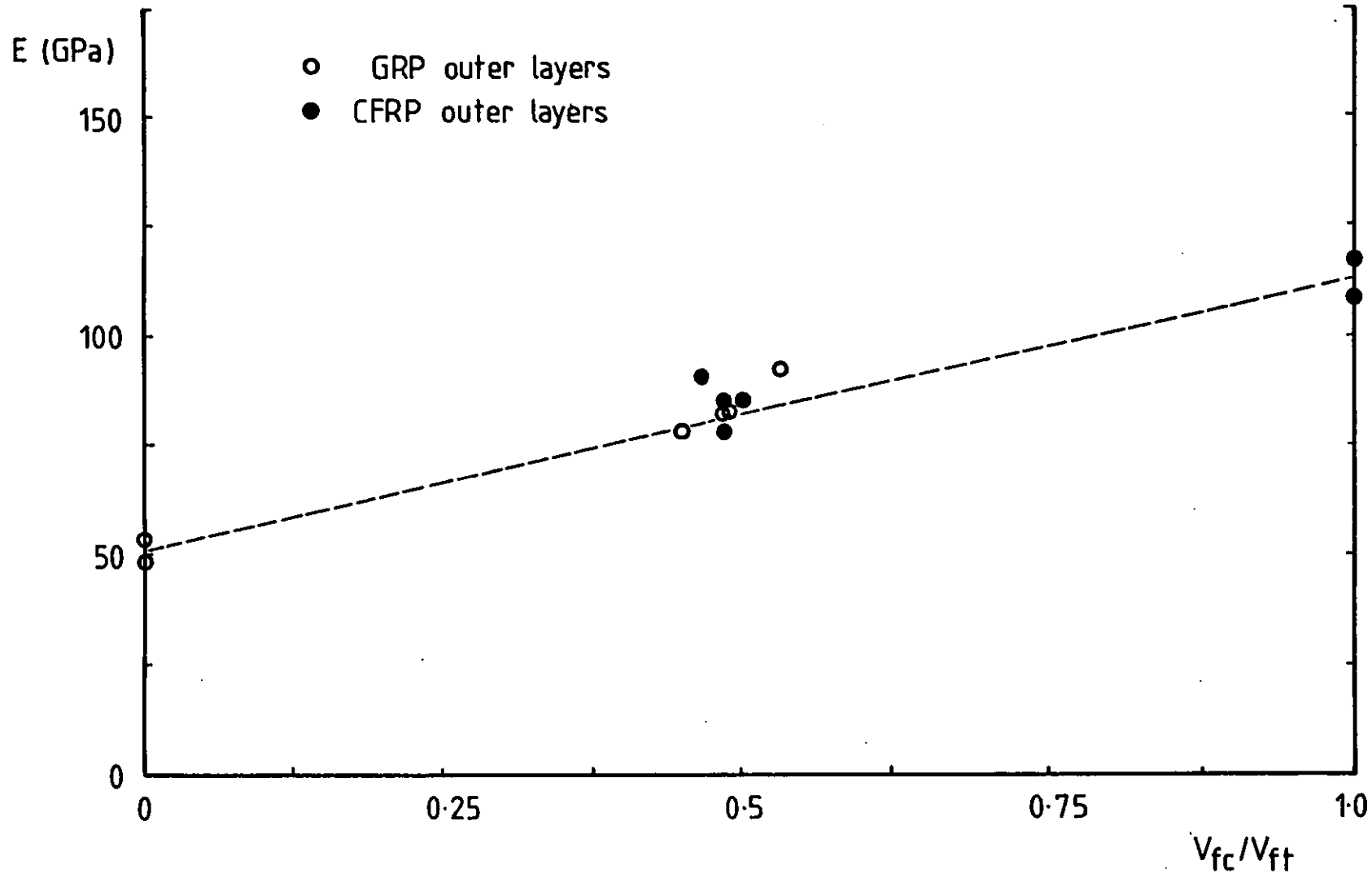

FIGURE 61: COMPRESSIVE MODULUS RESULTS AS A FUNCTION OF V_{fc}/V_{ft}, 411-45 MATRIX

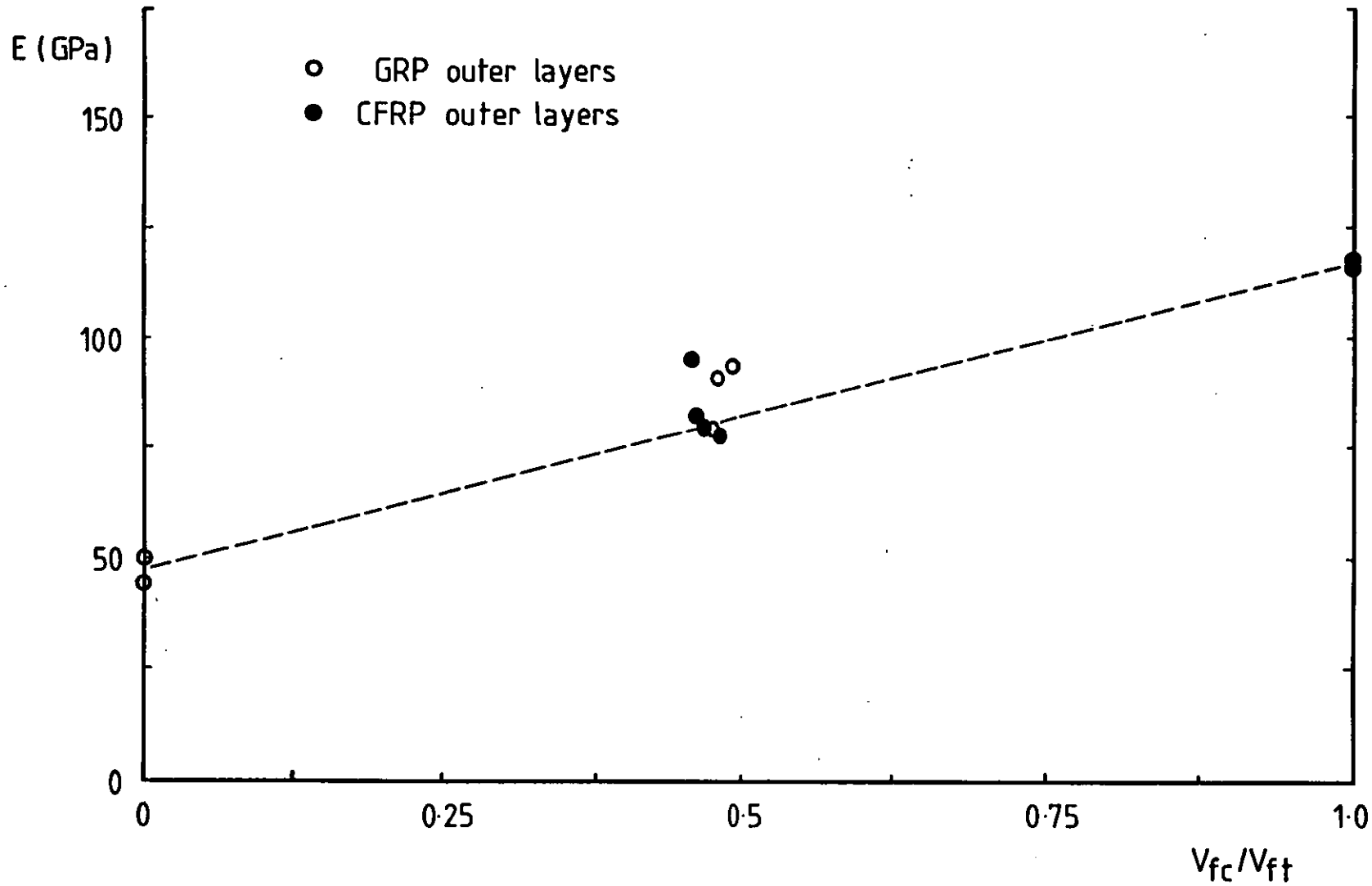

FIGURE 62: COMPRESSIVE MODULUS RESULTS AS A FUNCTION OF V_{fc}/V_{ft}, 470-36 MATRIX

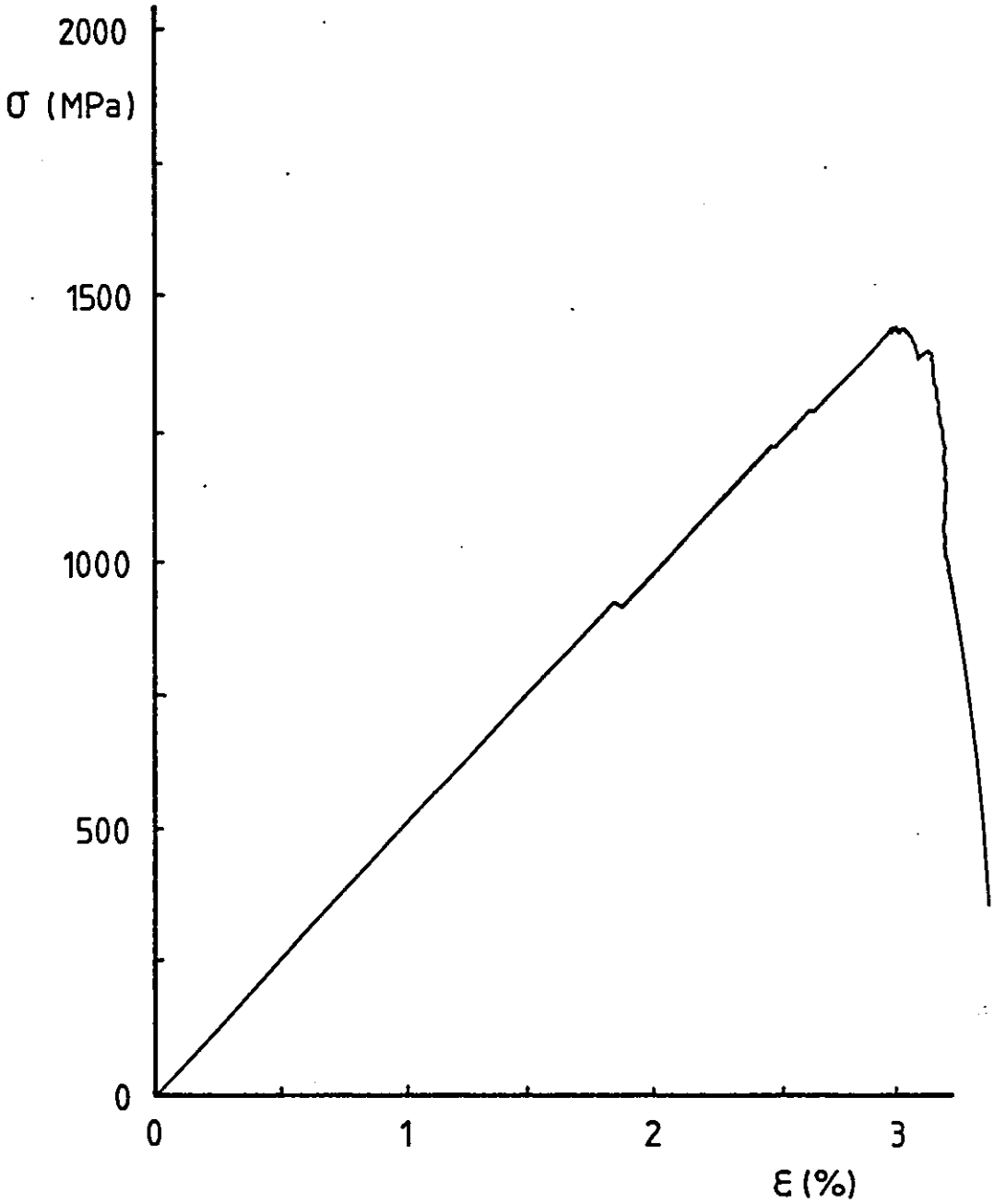

FIGURE 63: A TENSILE STRESS/STRAIN CURVE FROM A GRP LAMINATE, 913 MATRIX

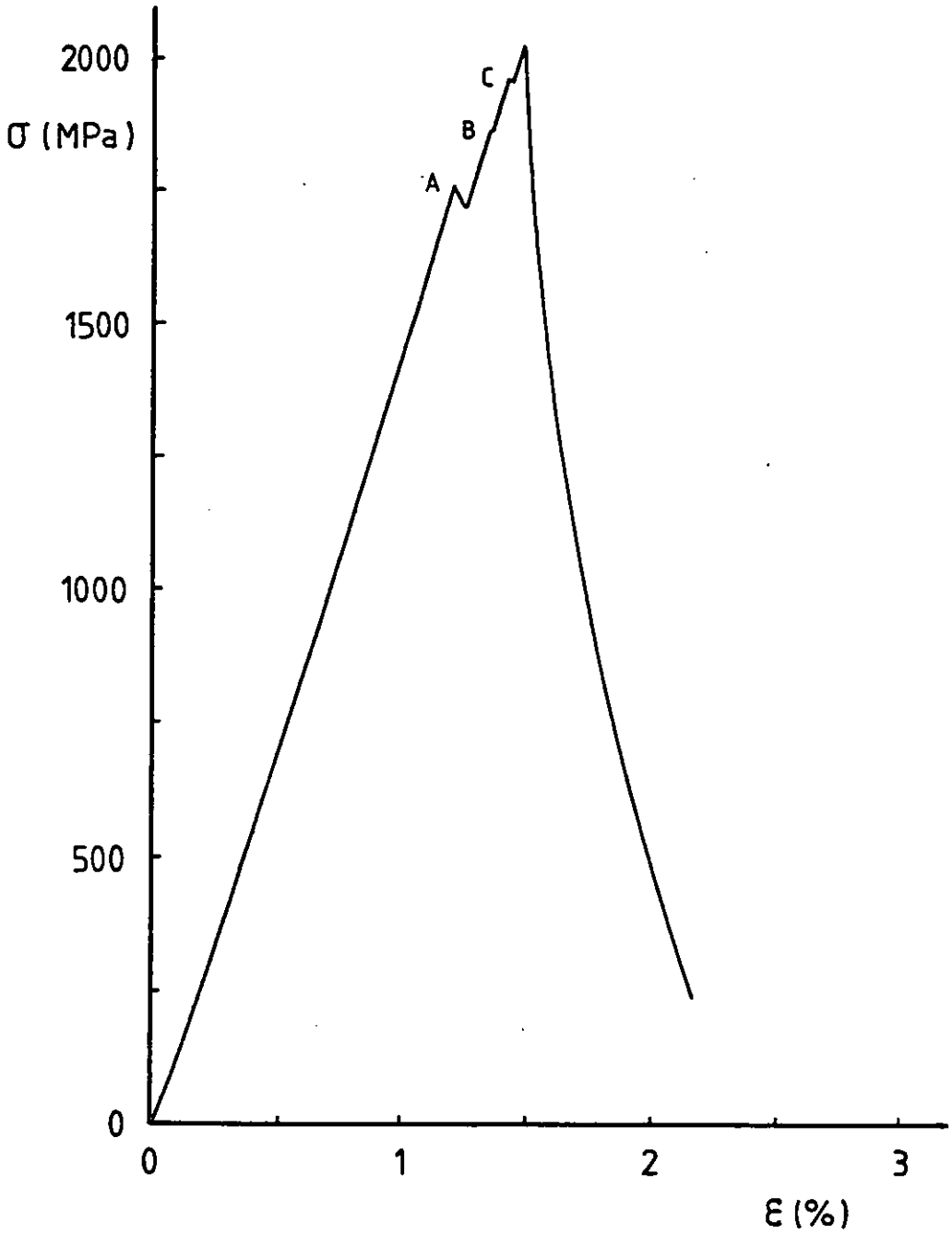

FIGURE 64: A TENSILE STRESS/STRAIN CURVE FROM A CFRP LAMINATE, 913 MATRIX

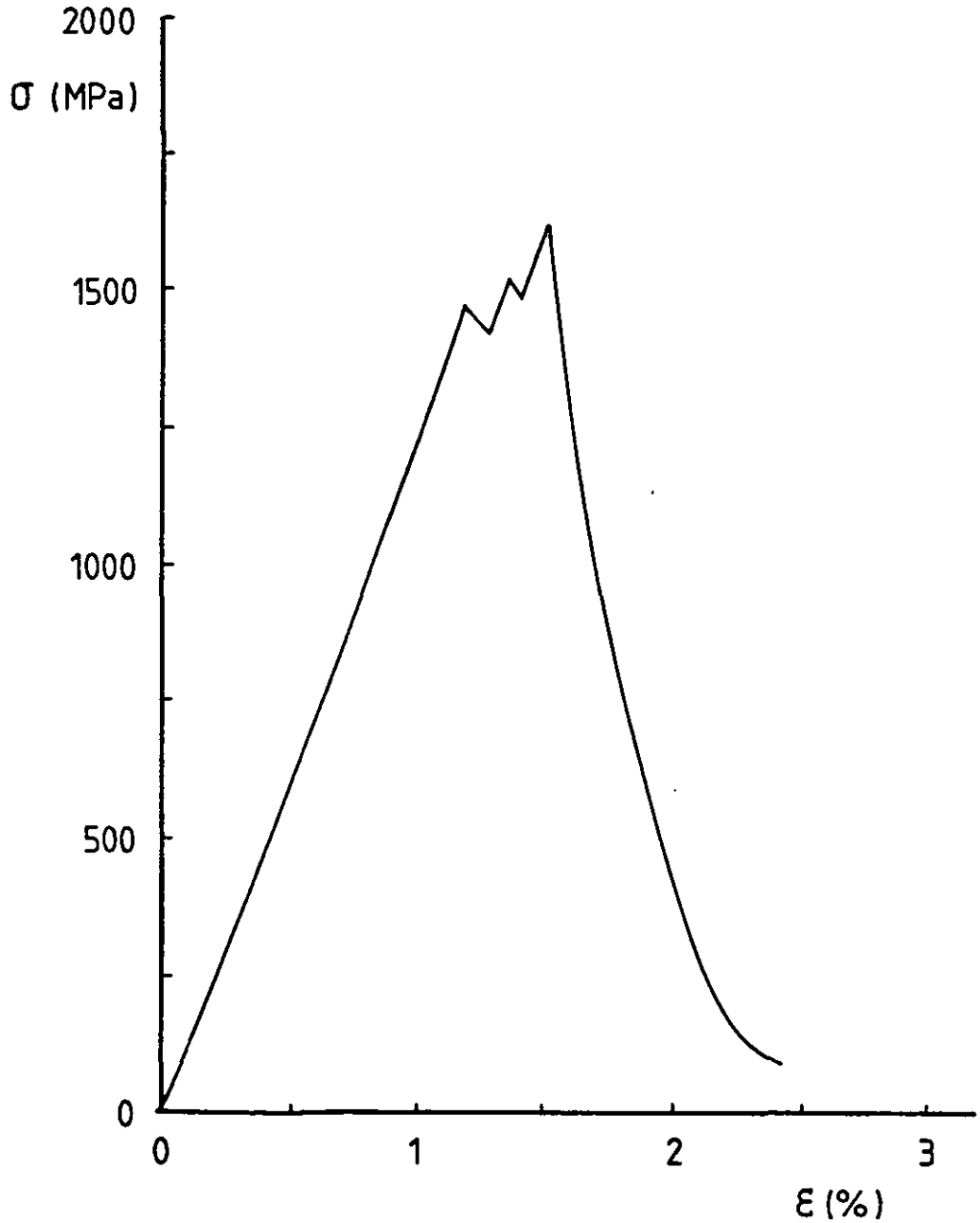

FIGURE 65: A TENSILE STRESS/STRAIN CURVE FROM A G_2C_6/C_6G_2 HYBRID LAMINATE, 913 MATRIX

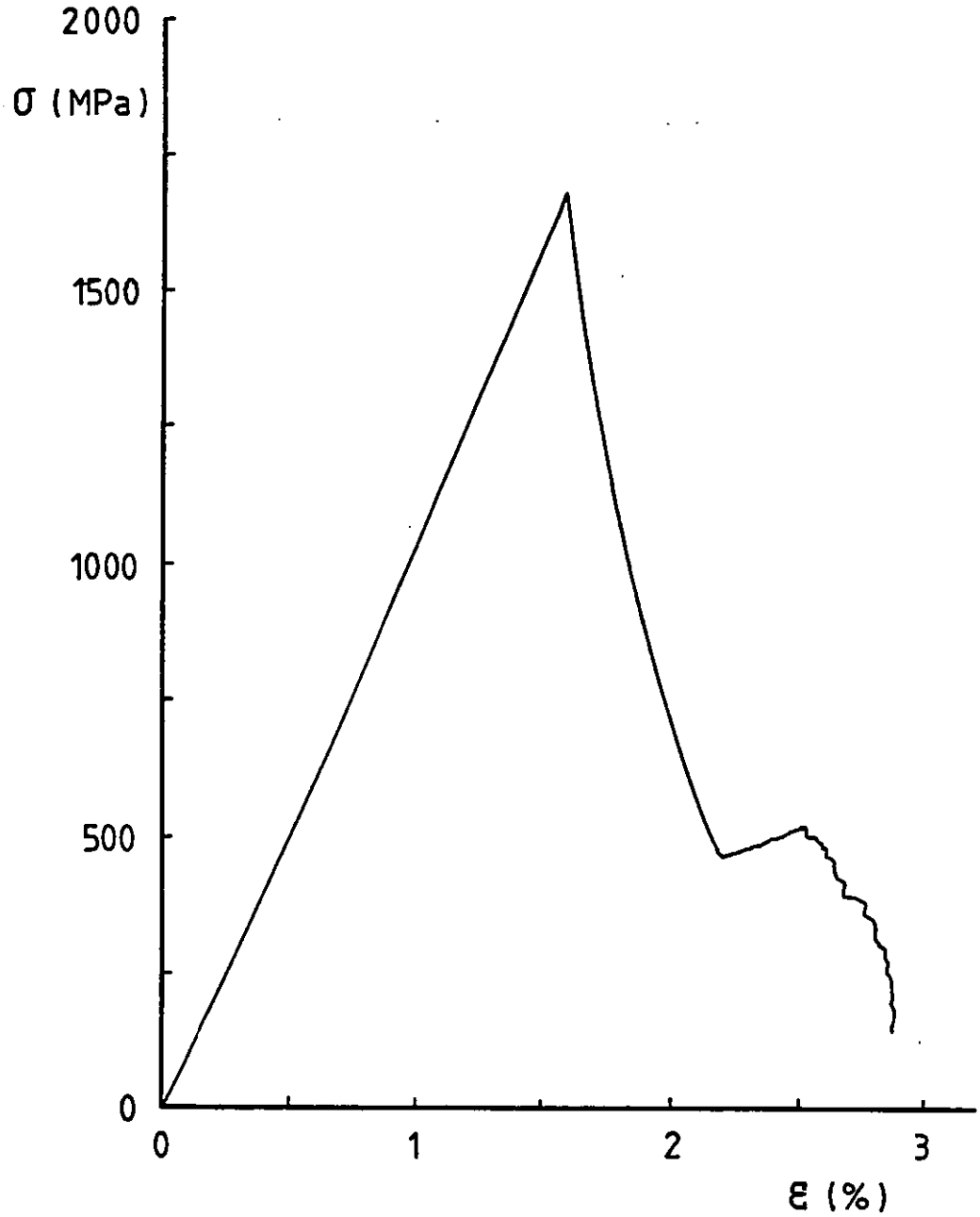

FIGURE 66: A TENSILE STRESS/STRAIN CURVE FROM A G_4C_4/C_4G_4 HYBRID LAMINATE, 913 MATRIX

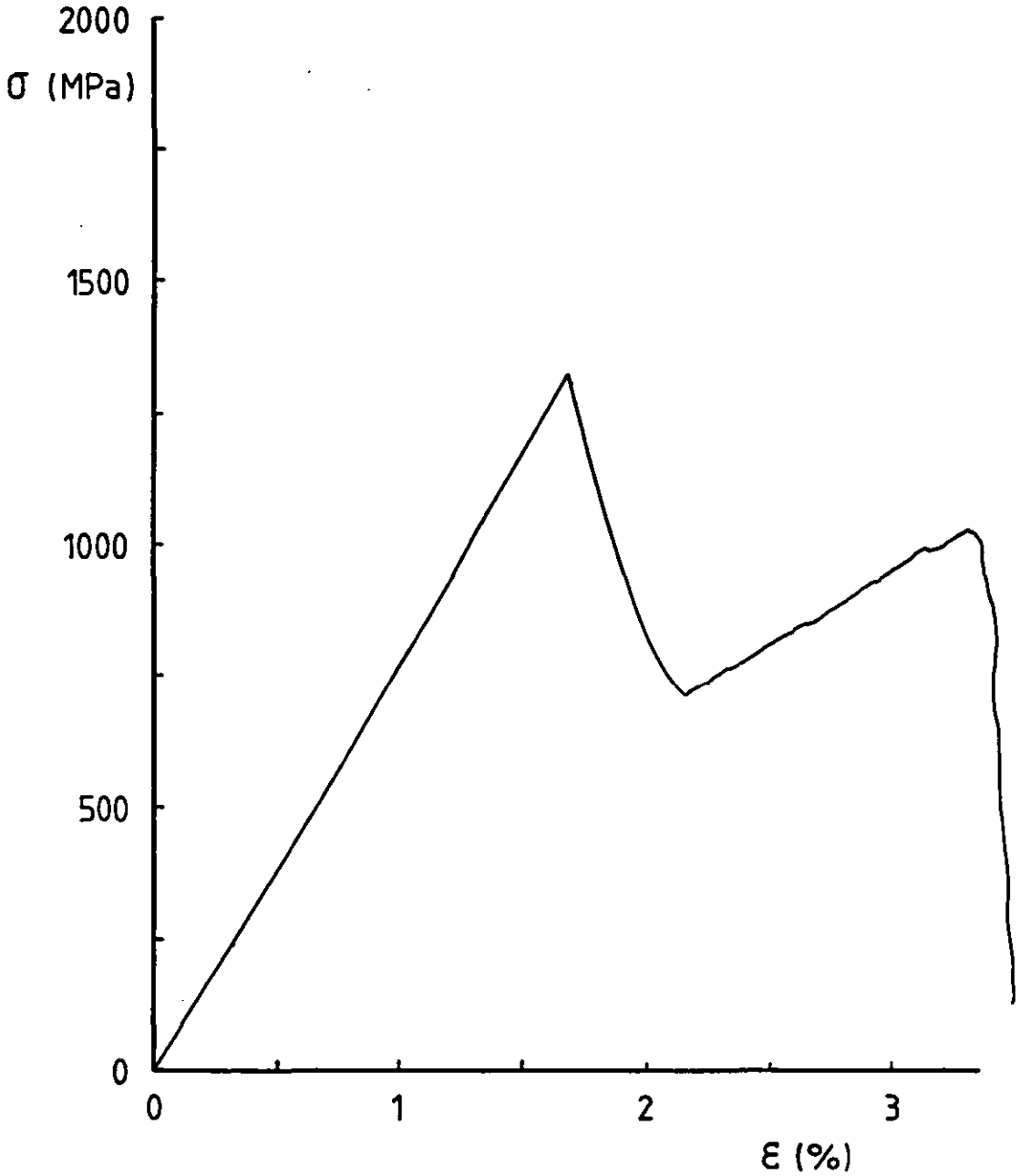

FIGURE 67: A TENSILE STRESS/STRAIN CURVE FROM A G_6C_2/C_2G_6 HYBRID LAMINATE, 913 MATRIX

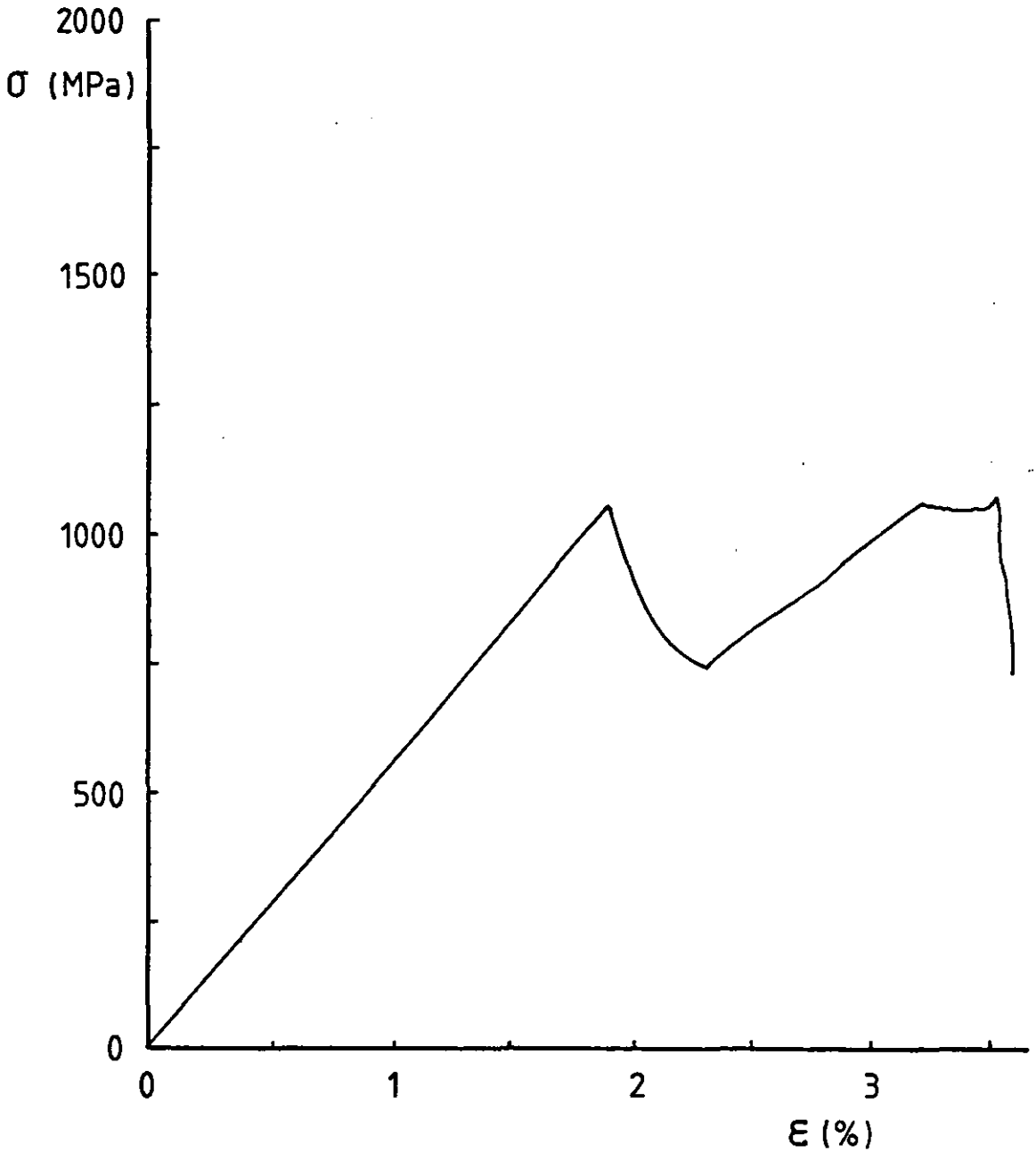

FIGURE 68: A TENSILE STRESS/STRAIN CURVE FROM A G_7C/CG_7 LAMINATE, 913 MATRIX

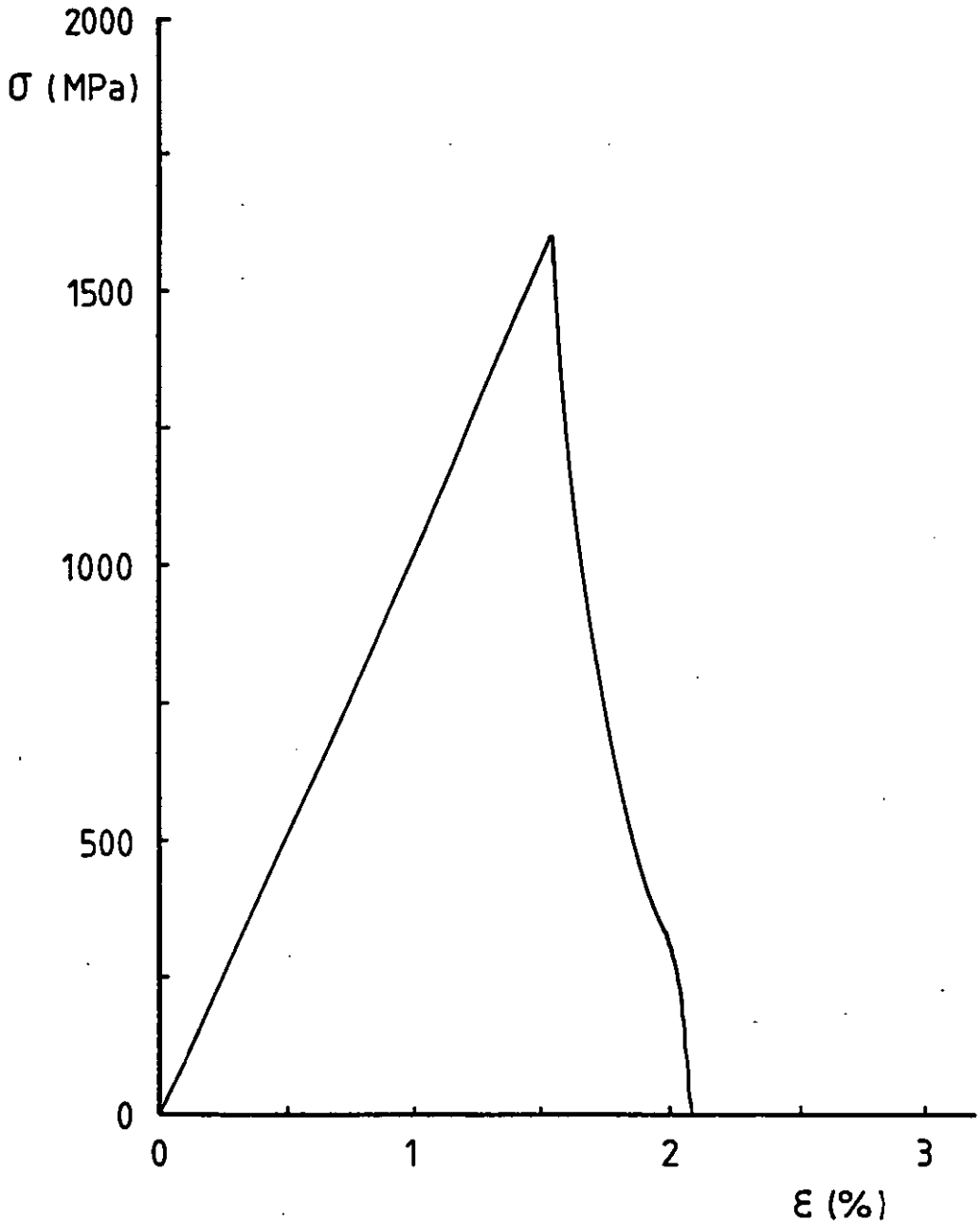

FIGURE 69: A TENSILE STRESS/STRAIN CURVE FROM A C_4G_4/G_4C_4 HYBRID LAMINATE, 913 MATRIX

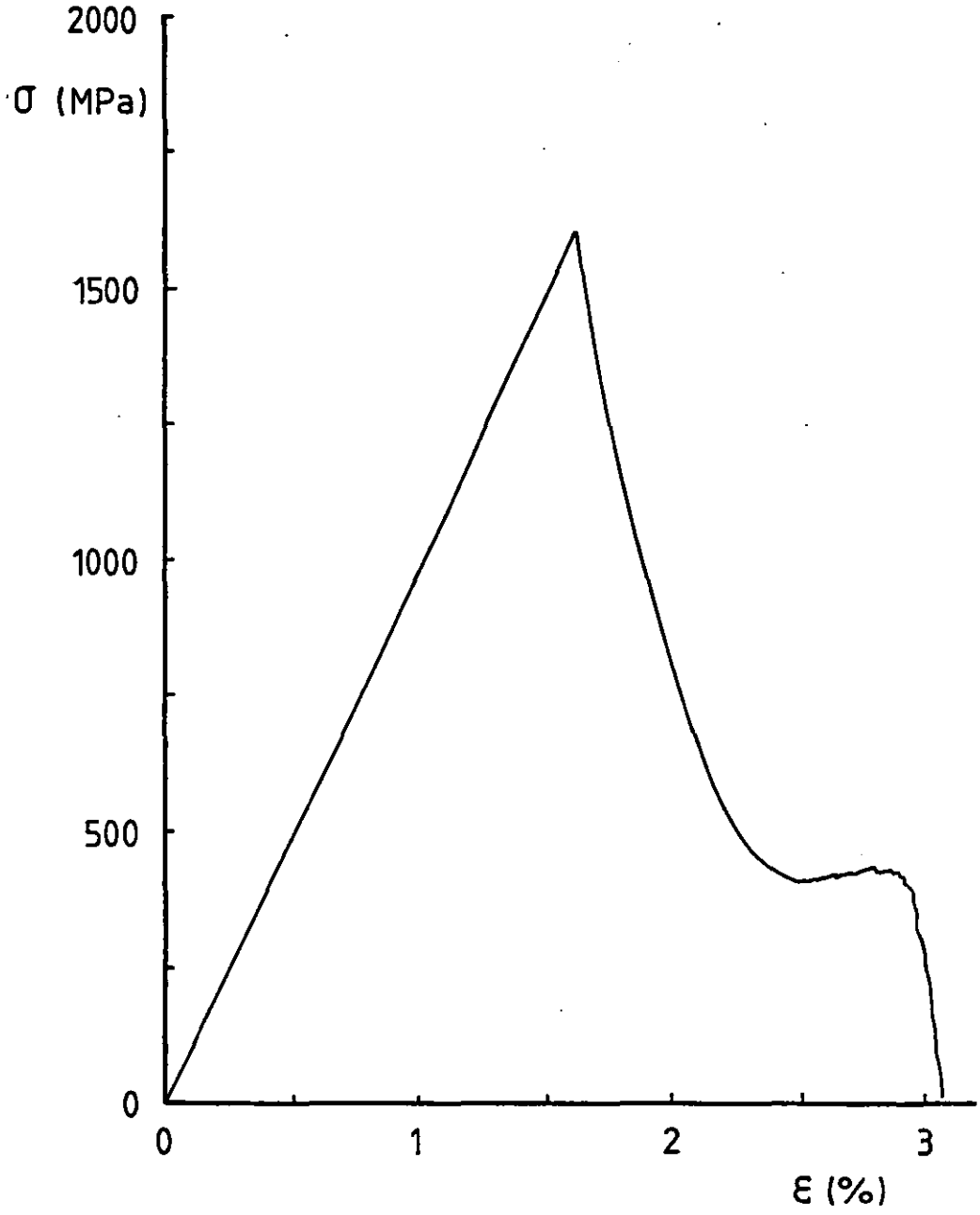

FIGURE 70: A TENSILE STRESS/STRAIN CURVE FROM A $G_2C_4G_2/G_2C_4G_2$ HYBRID LAMINATE, 913 MATRIX

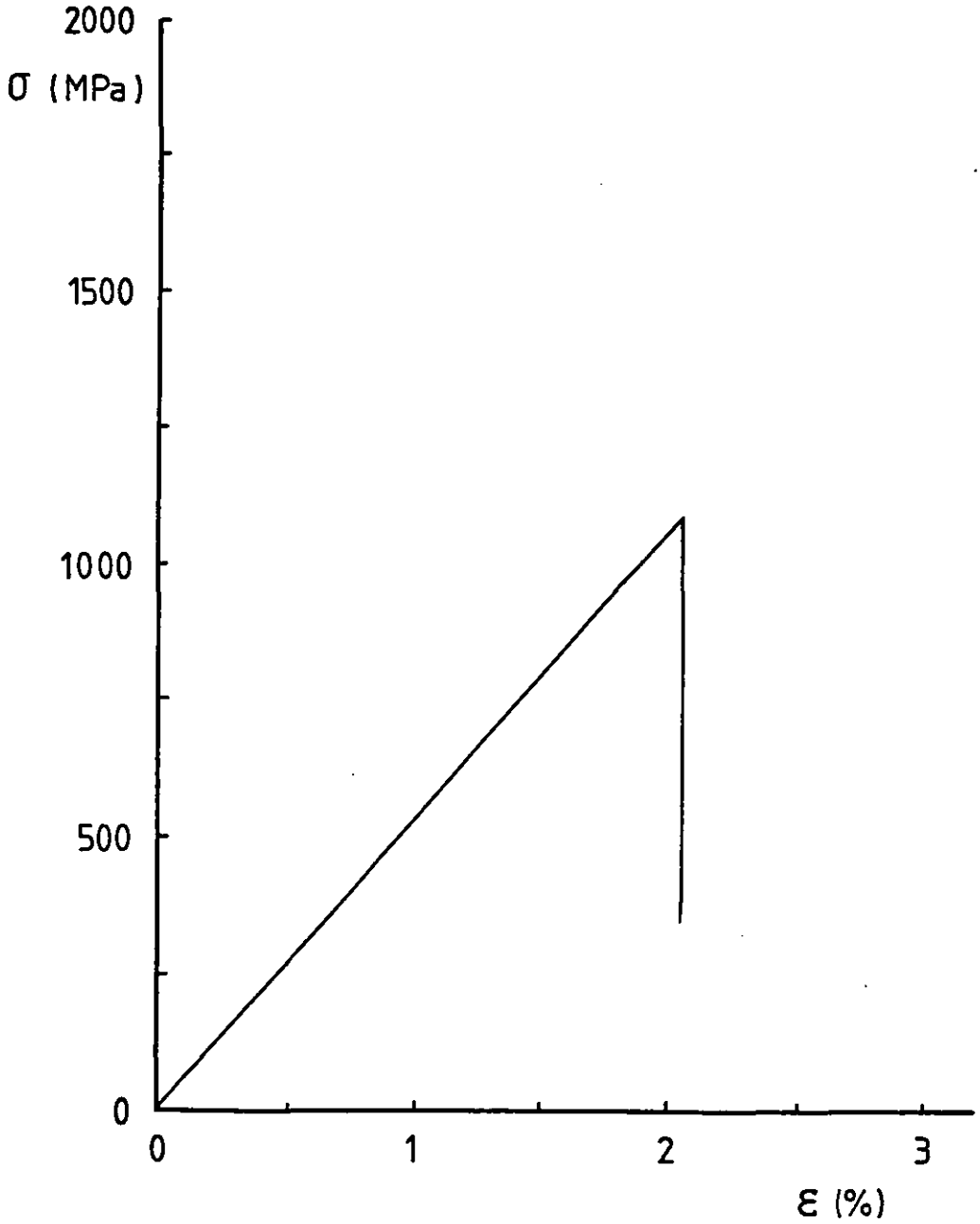

FIGURE 71: A COMPRESSIVE STRESS/STRAIN CURVE FROM A GRP LAMINATE, 913 MATRIX

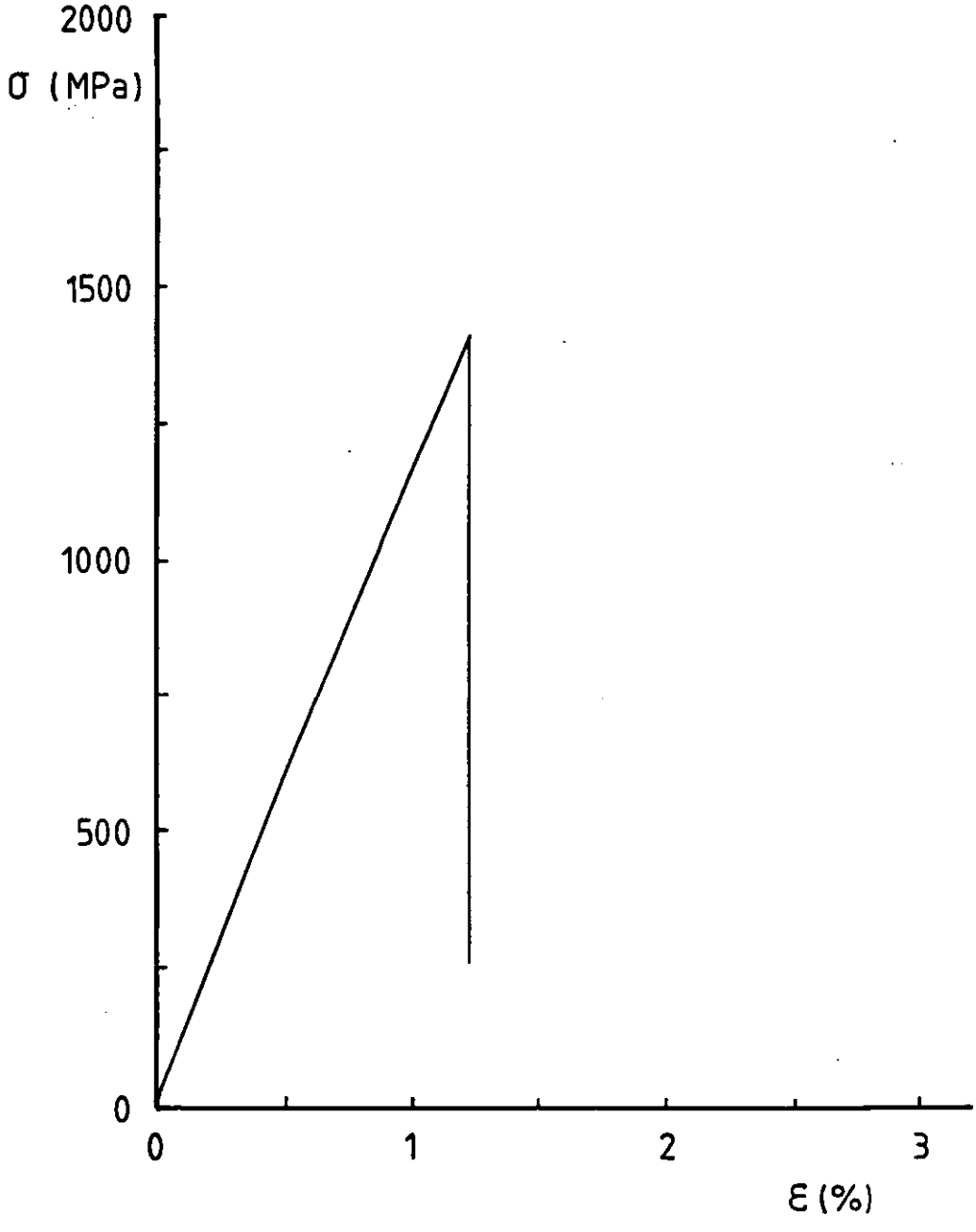

FIGURE 72: A COMPRESSIVE STRESS/STRAIN CURVE FROM A CFRP LAMINATE, 913 MATRIX

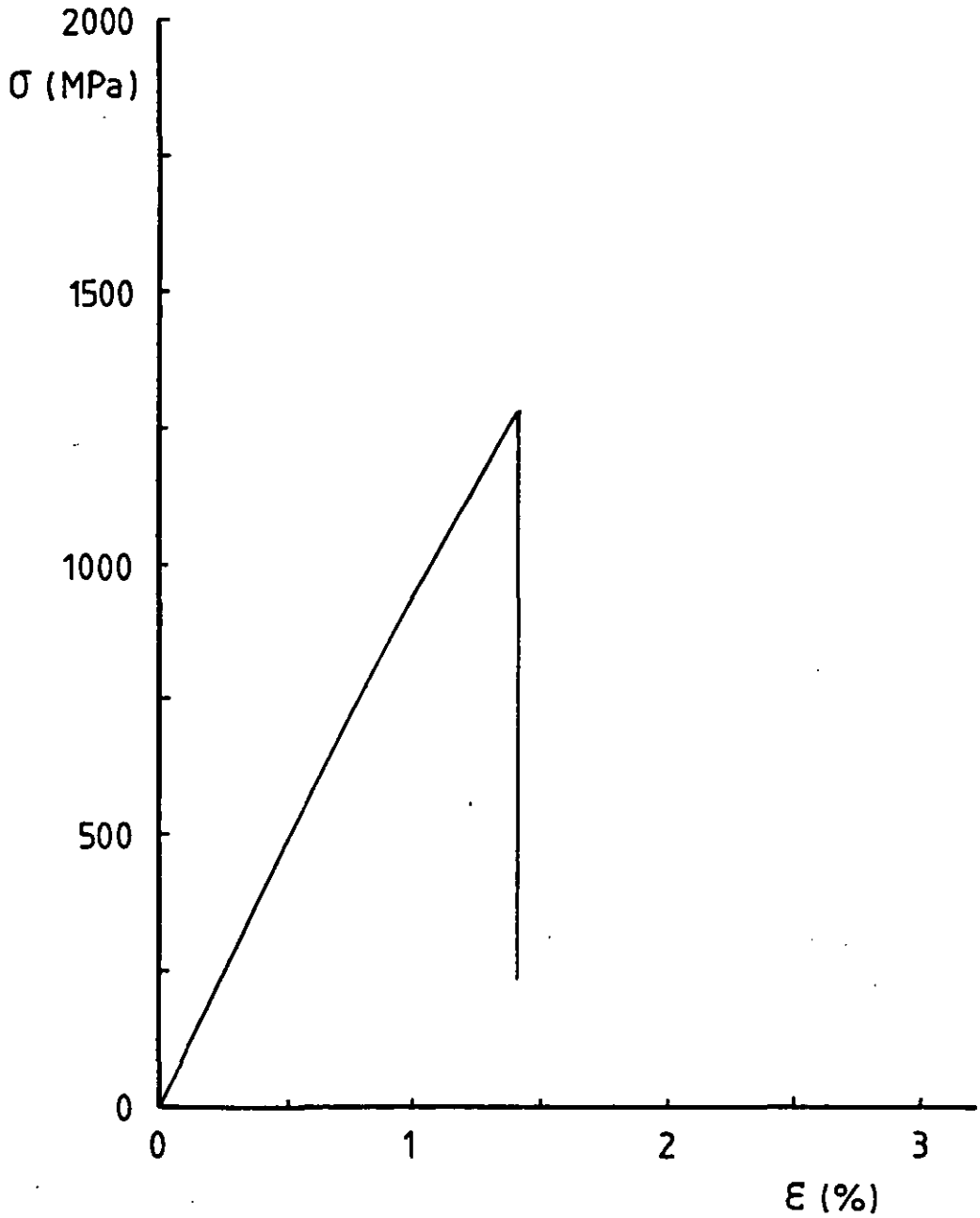

FIGURE 73: A COMPRESSIVE STRESS/STRAIN CURVE FROM A G_4C_4/C_4G_4 HYBRID LAMINATE, 913 MATRIX

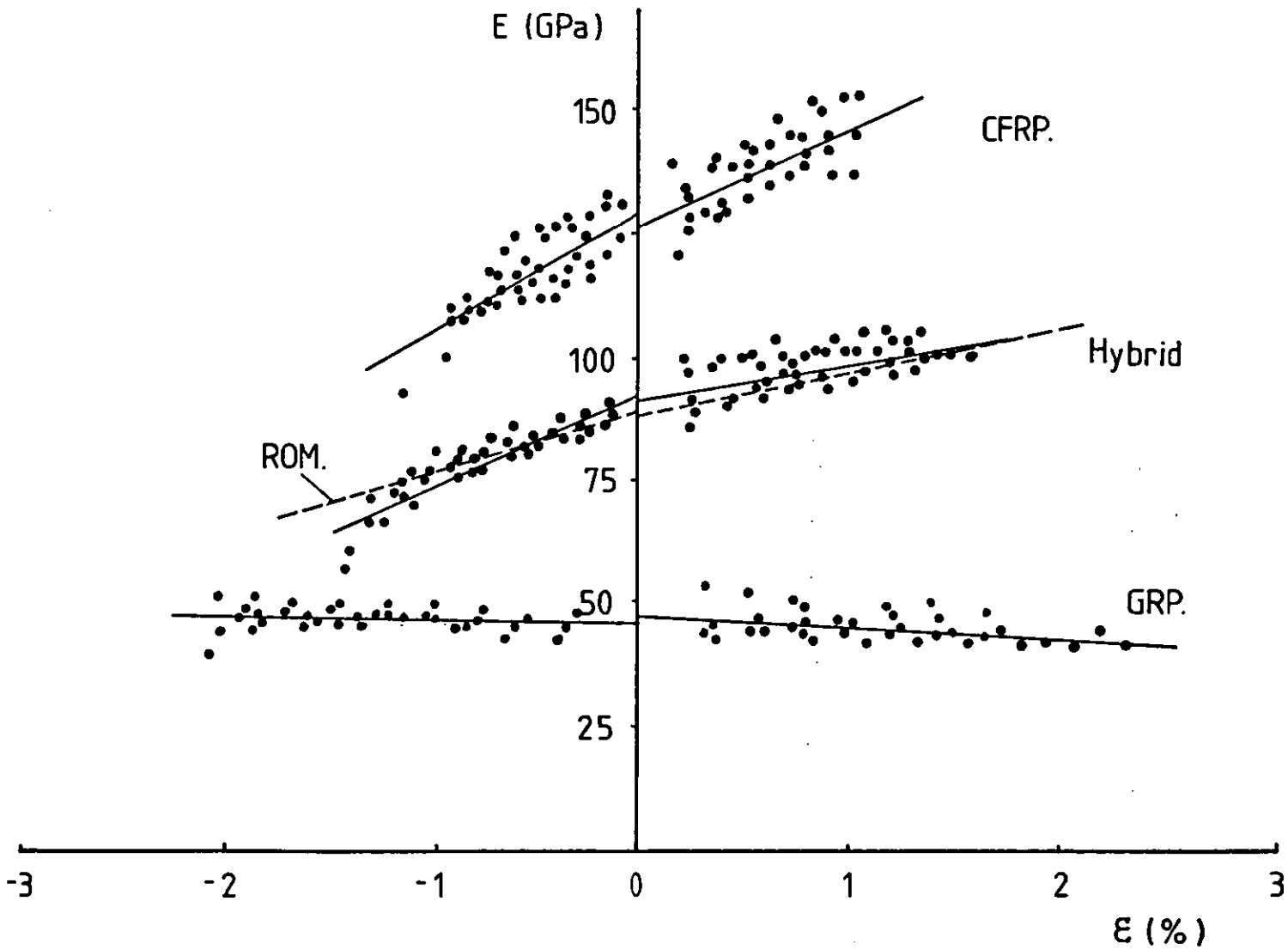

FIGURE 74: THE VARIATION OF TANGENT MODULUS AS A FUNCTION OF TENSILE AND COMPRESSIVE STRAIN IN GRP, CFRP AND G_4C_4/C_4G_4 HYBRID LAMINATES, 913 MATRIX

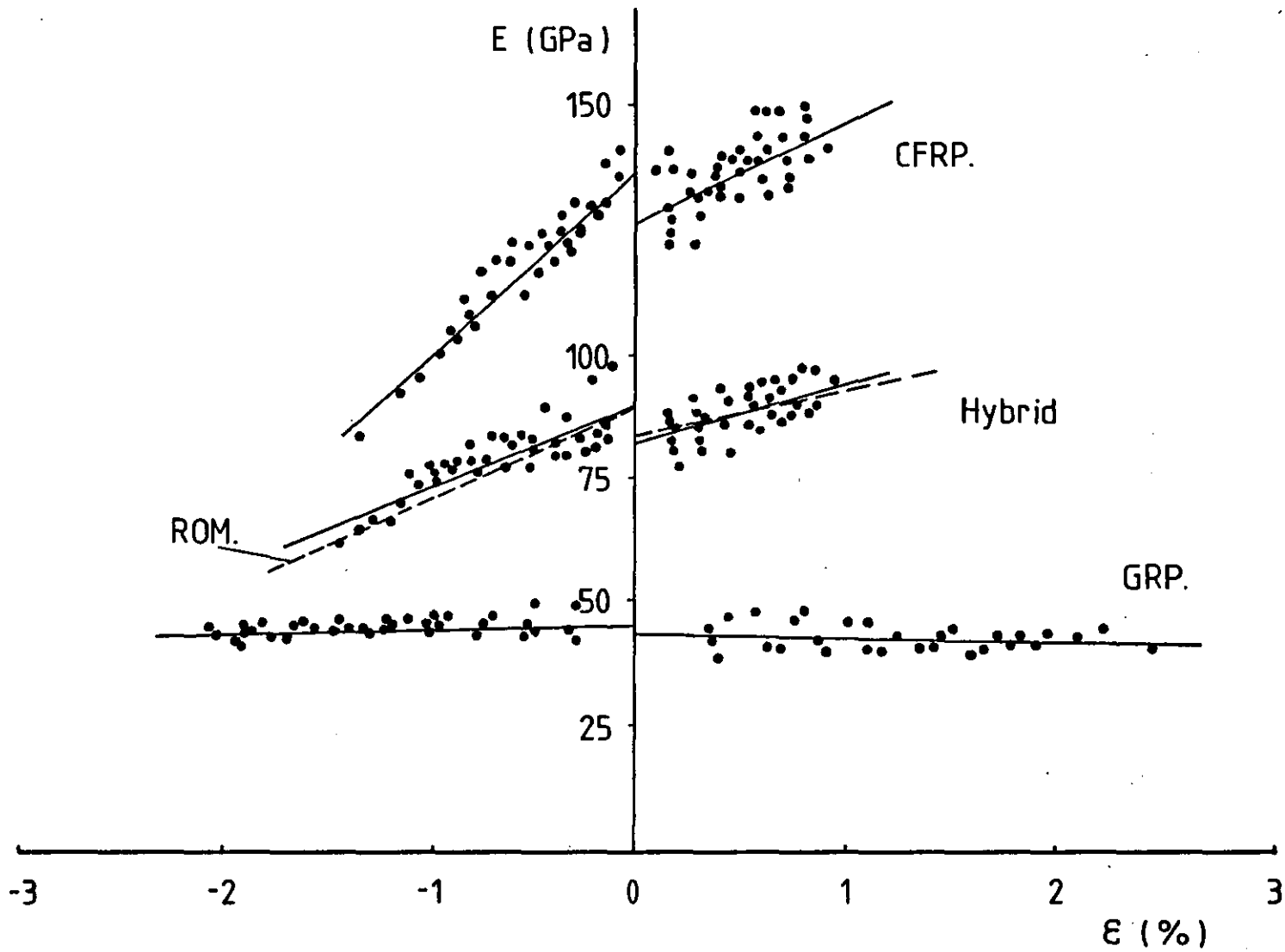

FIGURE 75: THE VARIATION OF TANGENT MODULUS AS A FUNCTION OF TENSILE AND COMPRESSIVE STRAIN IN GRP, CFRP AND G_4C_4/C_4G_4 HYBRID LAMINATES, 914 MATRIX

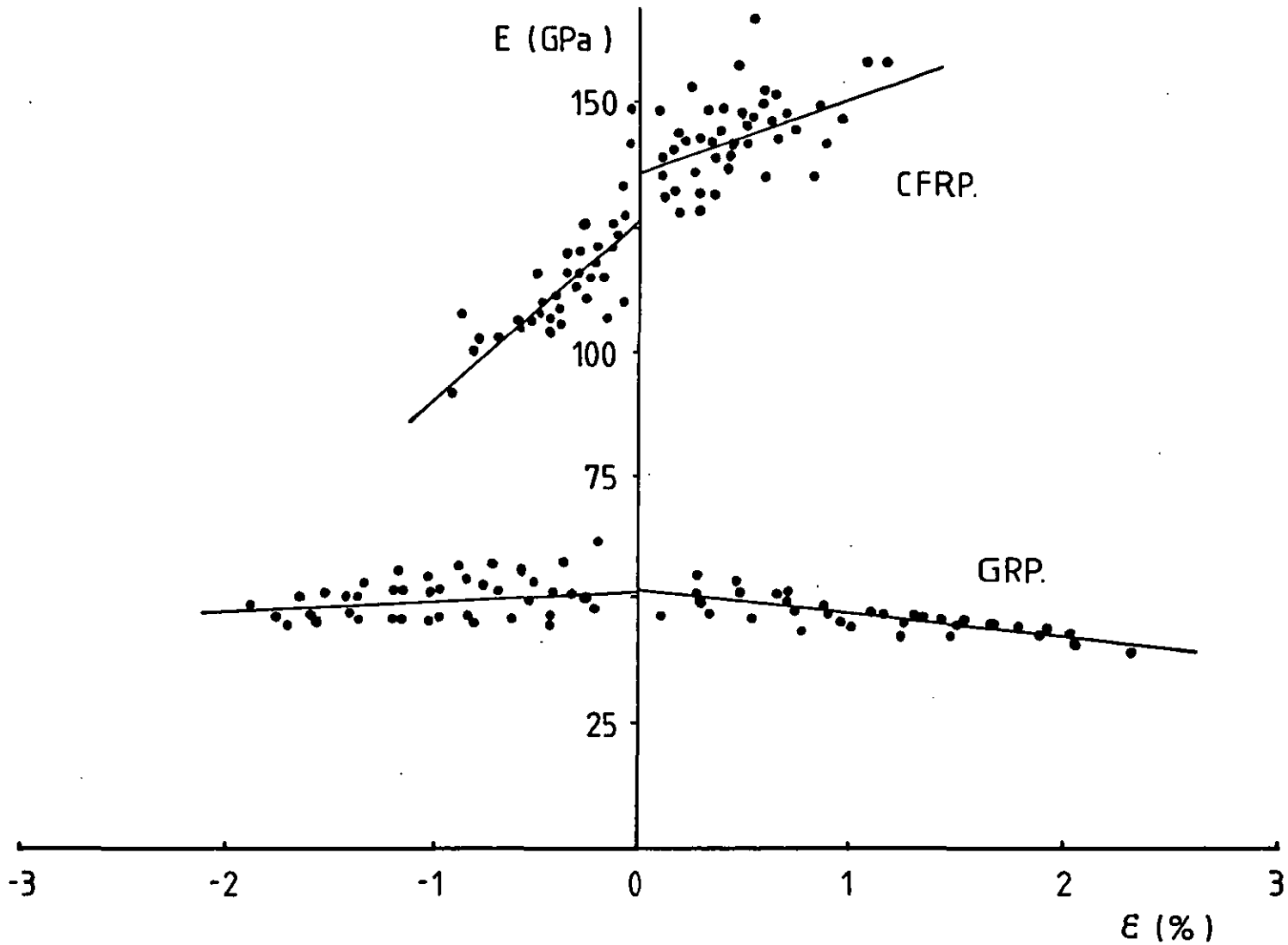

FIGURE 76: THE VARIATION OF TANGENT MODULUS AS A FUNCTION OF TENSILE AND COMPRESSIVE STRAIN IN GRP AND CFRP LAMINATES, 411-45 MATRIX

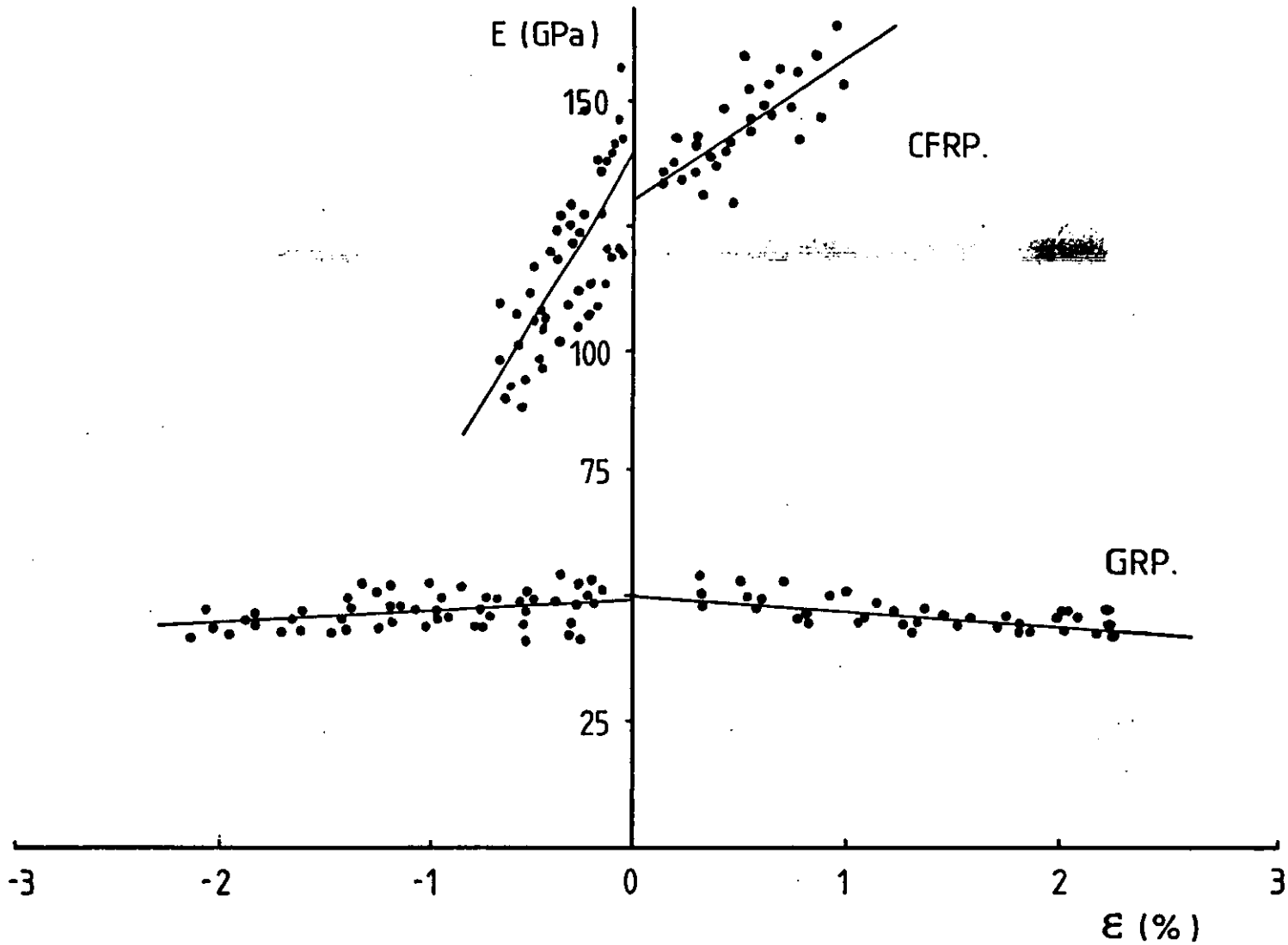

FIGURE 77: THE VARIATION OF TANGENT MODULUS AS A FUNCTION OF TENSILE AND COMPRESSIVE STRAIN IN GRP AND CFRP LAMINATES, 470-36 MATRIX

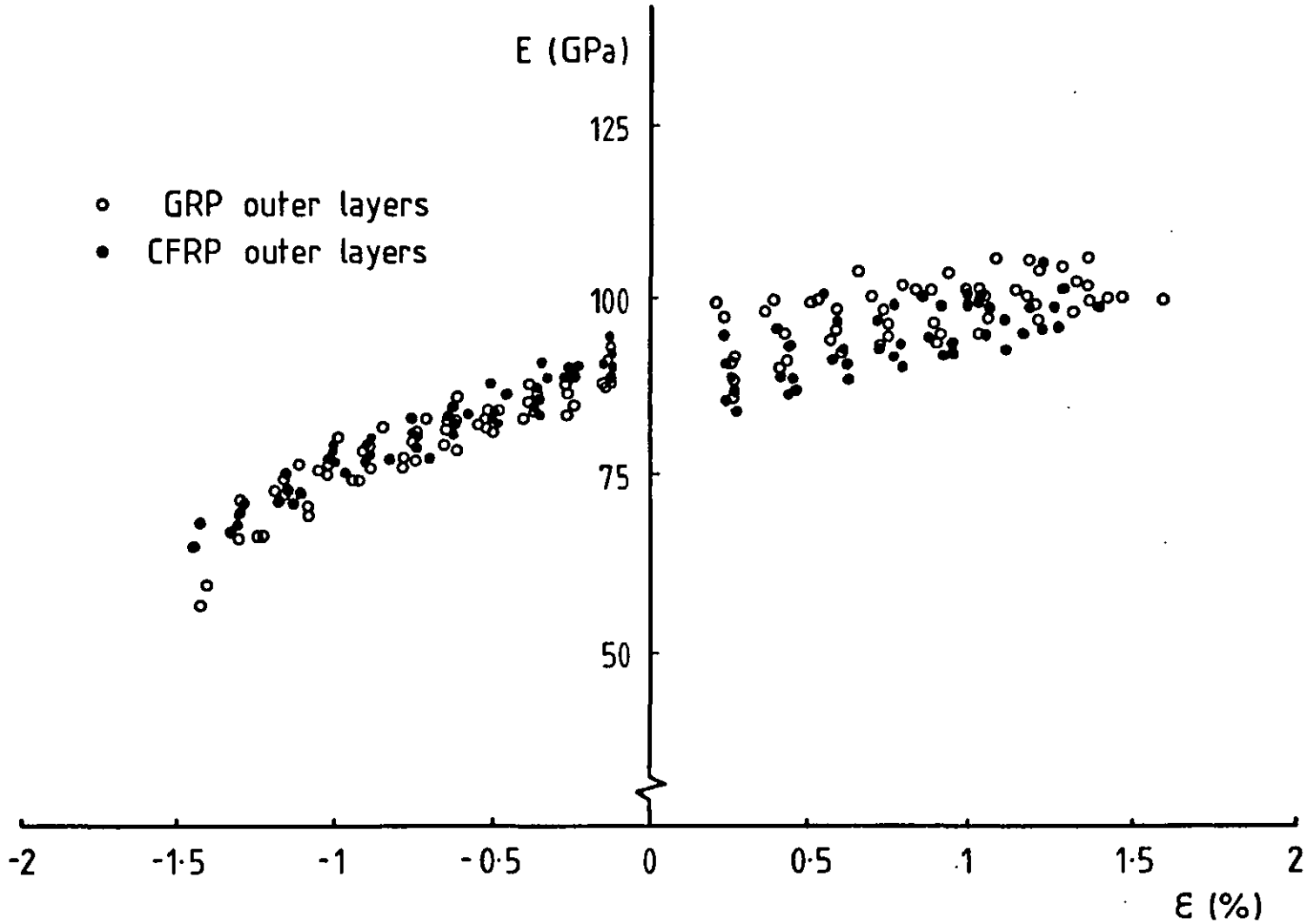

FIGURE 78: A COMPARISON OF THE TANGENT MODULUS VARIATION BETWEEN G_4C_4/C_4G_4 AND C_4G_4/G_4C_4 HYBRID LAMINATES AS A FUNCTION OF TENSILE AND COMPRESSIVE STRAIN, 913 MATRIX

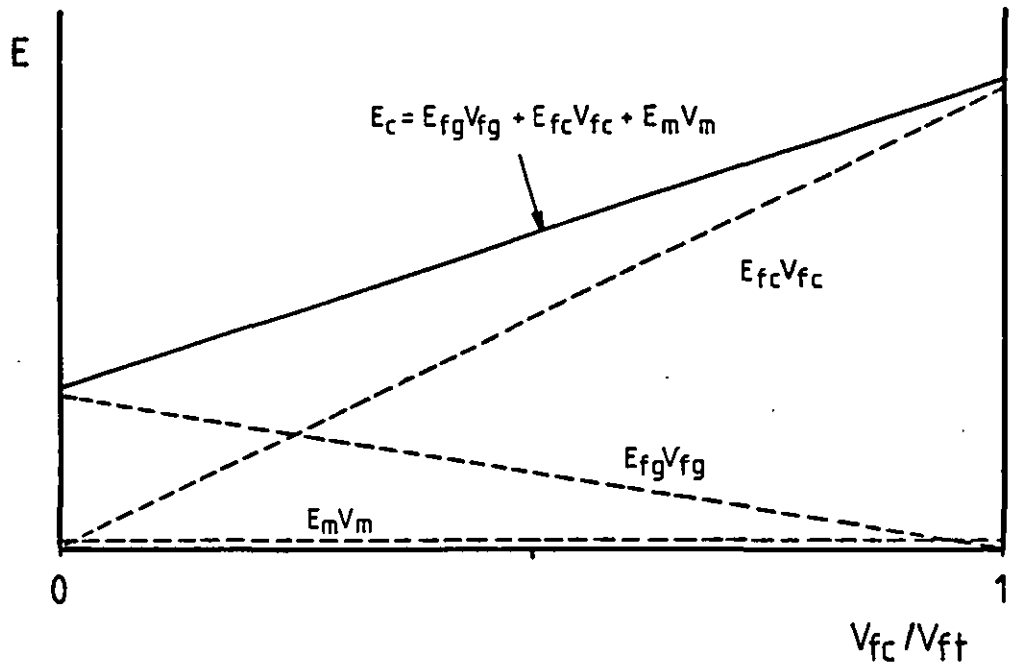

FIGURE 79: THE PROPORTIONAL CONTRIBUTIONS OF THE COMPONENTS OF A GLASS-CARBON HYBRID SYSTEM TO THE MODULUS, FOR COMPOSITES OF CONSTANT V_{ft}

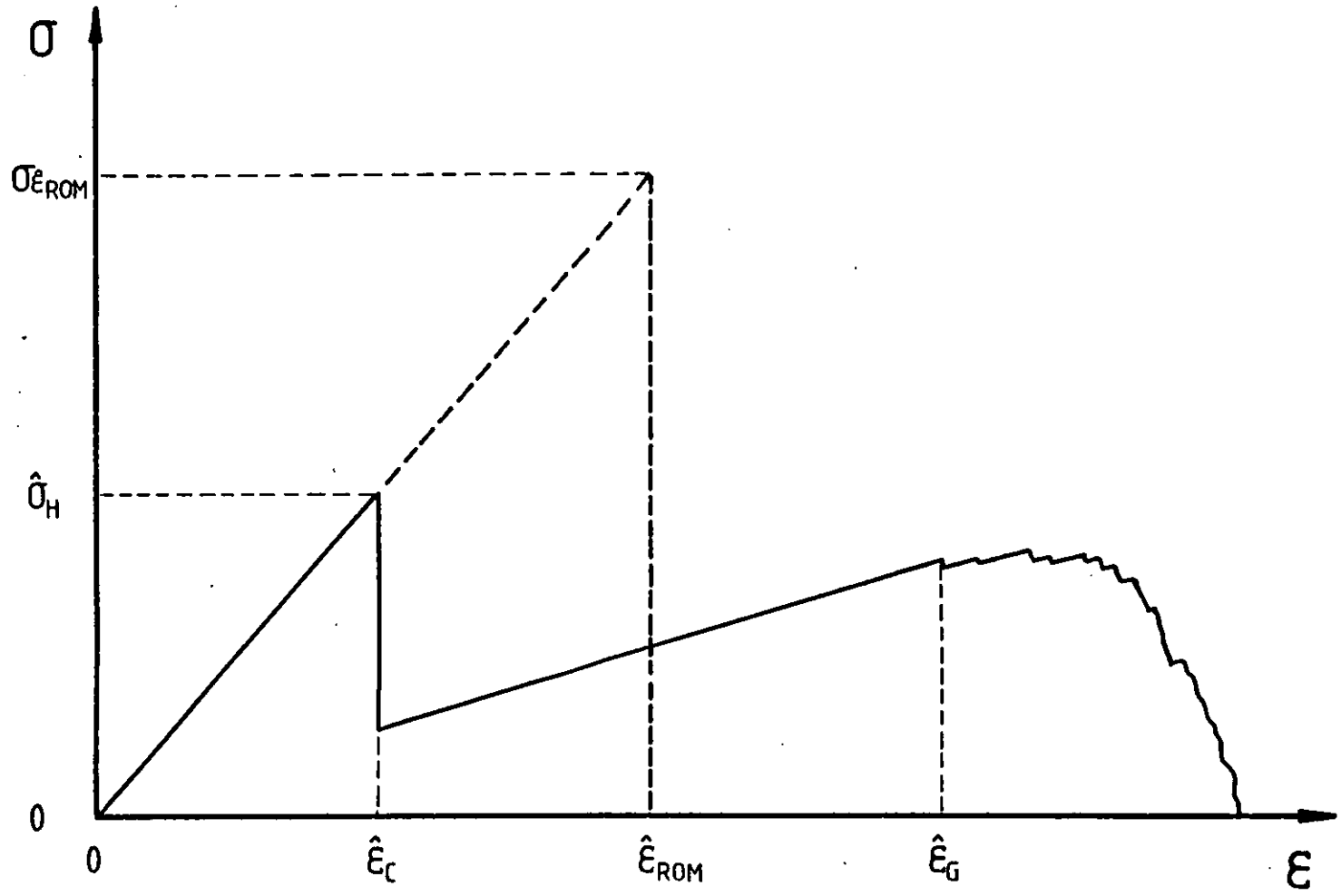

FIGURE 80: THE THEORETICAL STRESS/STRAIN CURVE OF A HYBRID COMPOSITE, SHOWING $\hat{\varepsilon}_{ROM}$

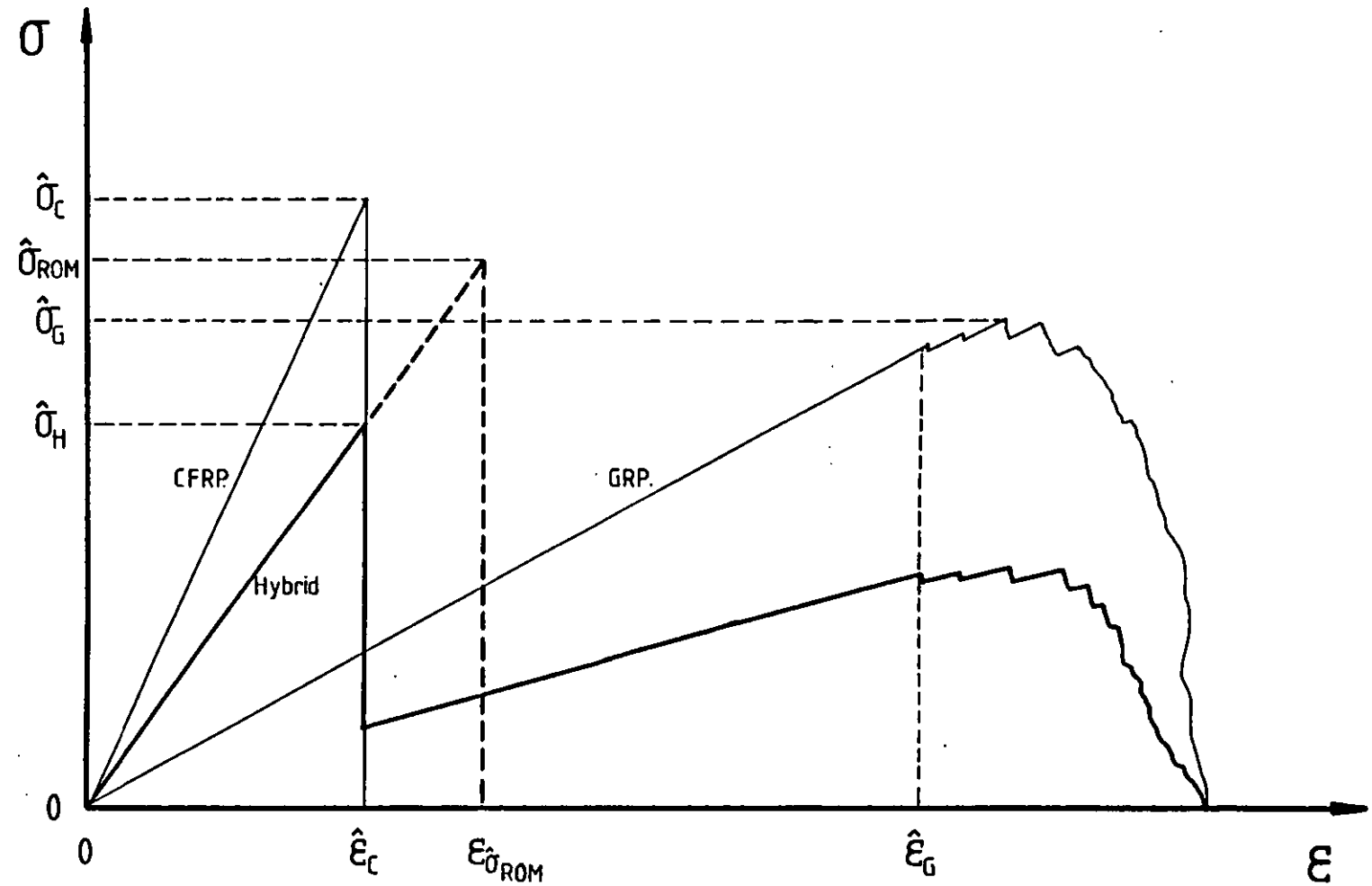

FIGURE 81: THE THEORETICAL STRESS/STRAIN CURVE OF A HYBRID COMPOSITE, SHOWING $\hat{\sigma}_{ROM}$ AND $\hat{\sigma}_H$

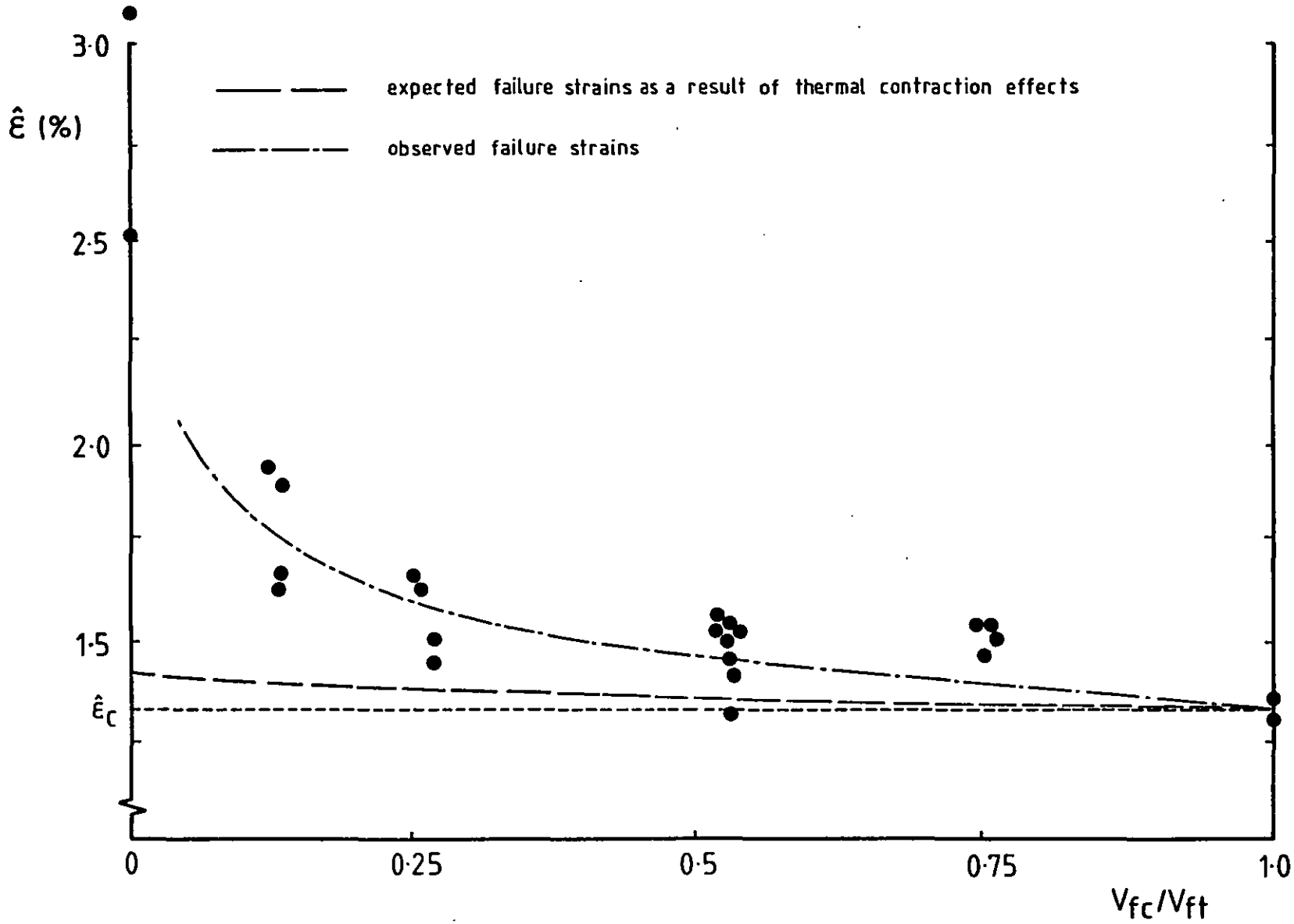

FIGURE 82: THE EXPECTED INCREASE IN TENSILE FAILURE STRAINS OF HYBRID LAMINATES AS A RESULT OF THERMAL CONTRACTION EFFECTS, IN COMPARISON WITH OBSERVED FAILURE STRAINS, 913 LAMINATES (ΔT = 115°C)

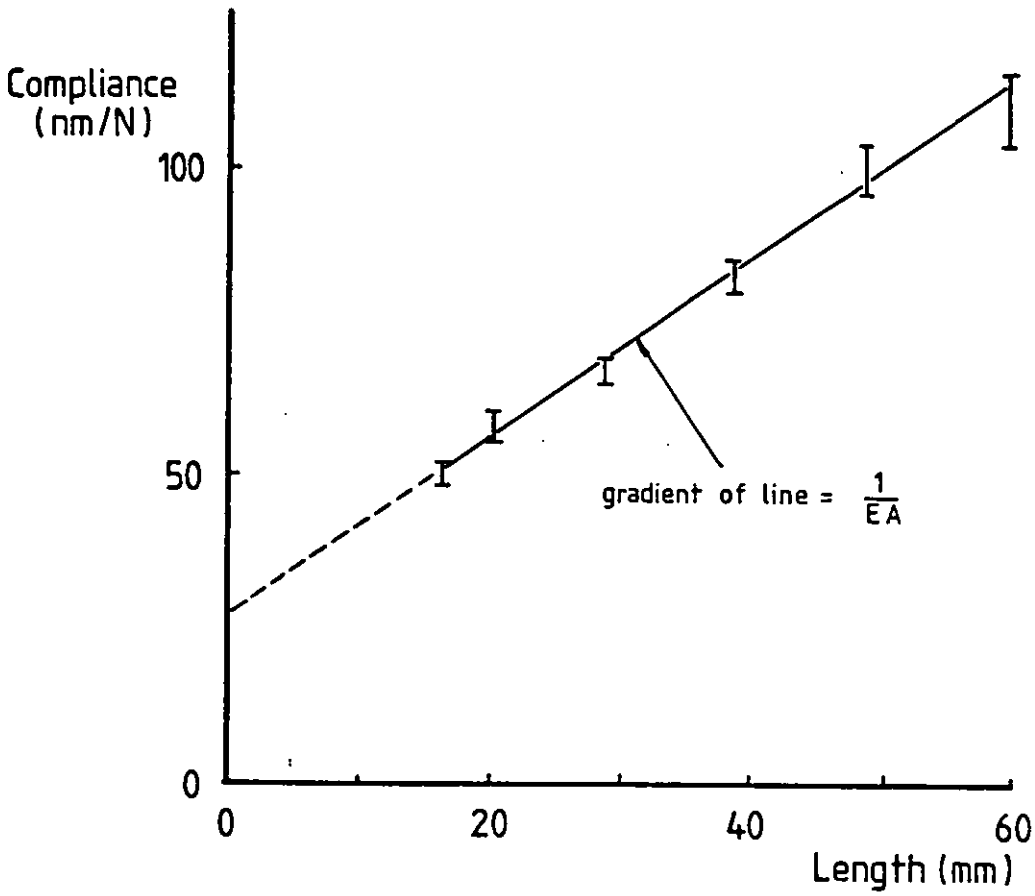

FIGURE 83: THE METHOD OF MODULUS MEASUREMENT EMPLOYED BY PIGGOTT AND HARRIS IN WHICH MACHINE DISPLACEMENT/ APPLIED FORCE IS PLOTTED AS A FUNCTION OF SPECIMEN LENGTH (From Ref 53)

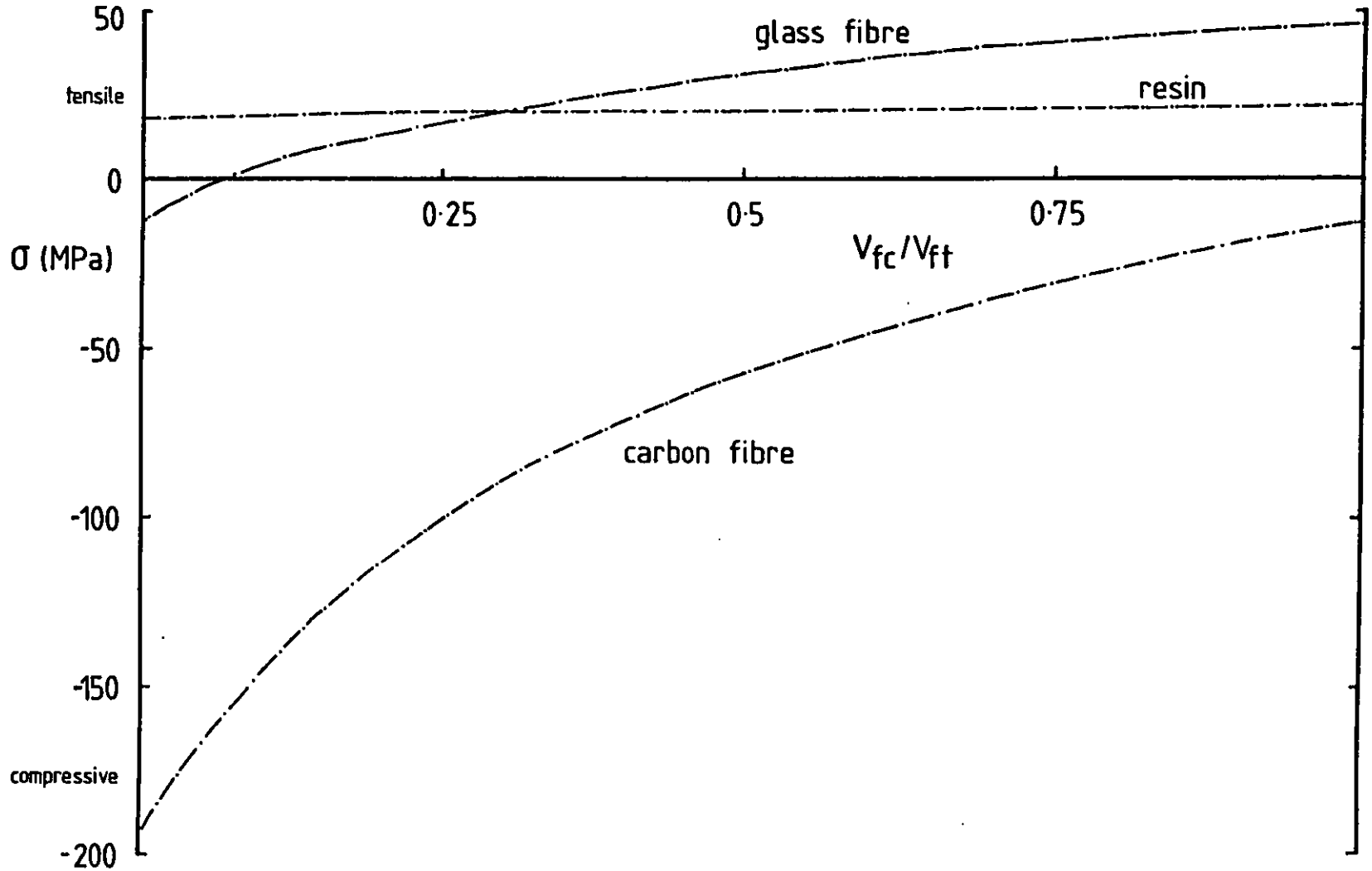

FIGURE 84: THE STRESSES IN THE INDIVIDUAL COMPONENTS OF HYBRID LAMINATES DUE TO COOLING FROM THE CURE TEMPERATURE, 913 MATRIX (ΔT = 115°C)

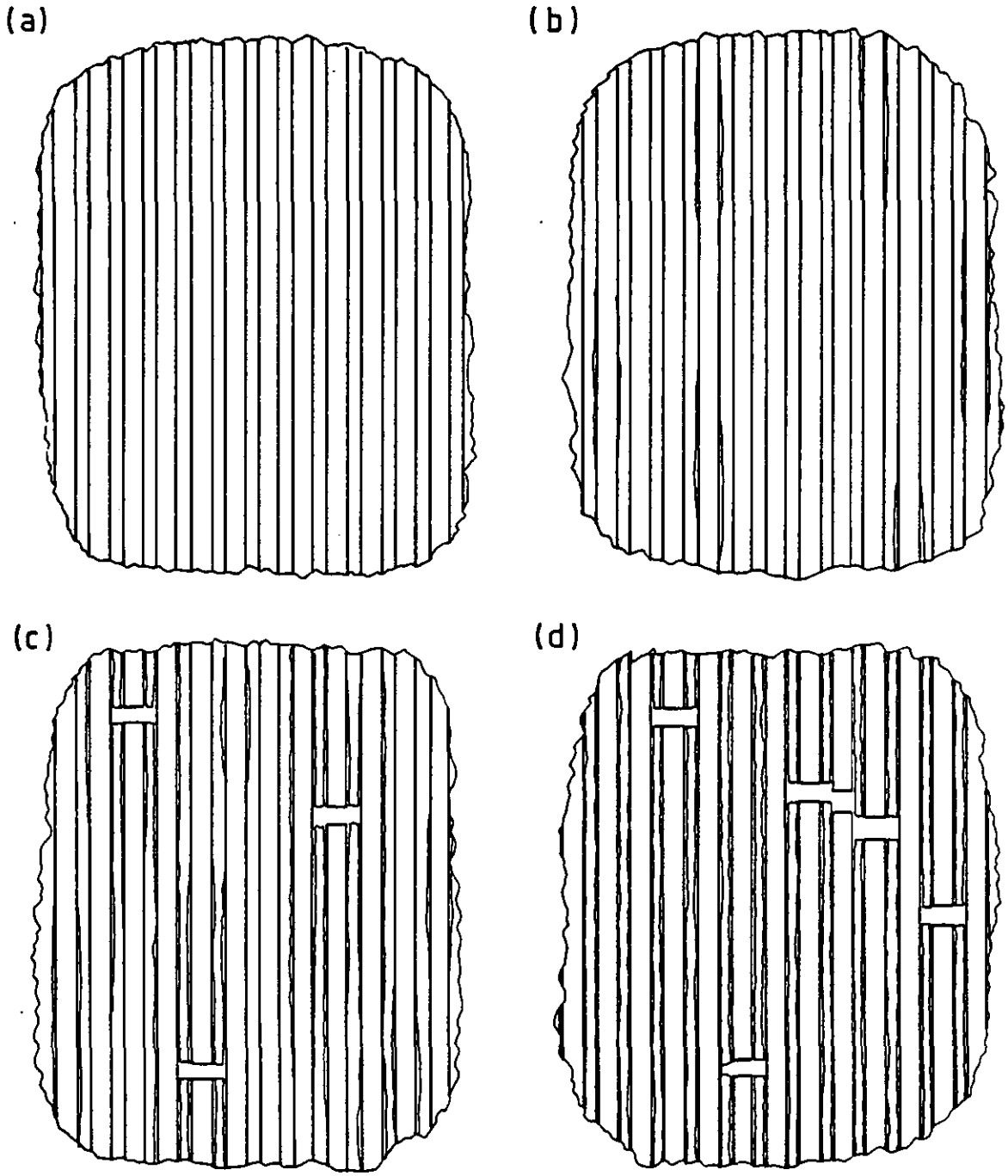

FIGURE 85: A TENSILE FAILURE MODEL FOR UNIDIRECTIONAL GRP MATERIAL

a) UNSTRESSED COMPOSITE WHICH CONTAINS DEFECTS
b) DEBONDING BEGINS TO OCCUR DUE TO DEFECTS
c) FIBRE FAILURE BEGINS TO OCCUR, AND CRACK PROPAGATION IS HALTED BY THE DEBONDING
d) FINAL FAILURE DUE TO FIBRE TENSILE FAILURE AND FIBRE-MATRIX SPLITTING

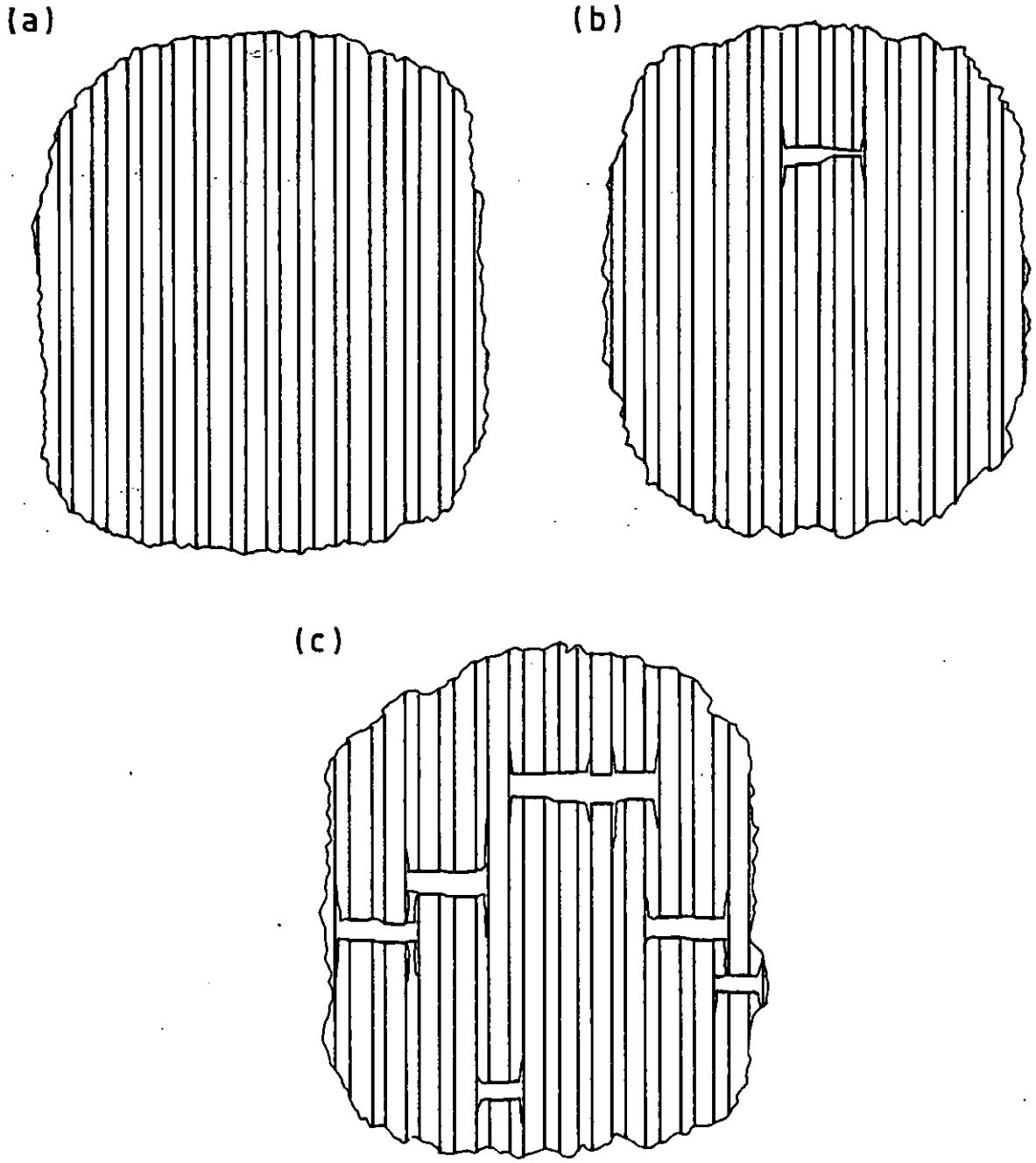

FIGURE 86: A TENSILE FAILURE MODEL FOR UNIDIRECTIONAL CFRP MATERIAL

a) UNSTRESSED COMPOSITE
b) AS FIBRE FAILURE BEGINS TO OCCUR THERE IS CONSIDERABLY LESS DEBONDING THAN IN GRP
c) FINAL FAILURE DUE MAINLY TO FIBRE AND RESIN TENSILE FAILURE

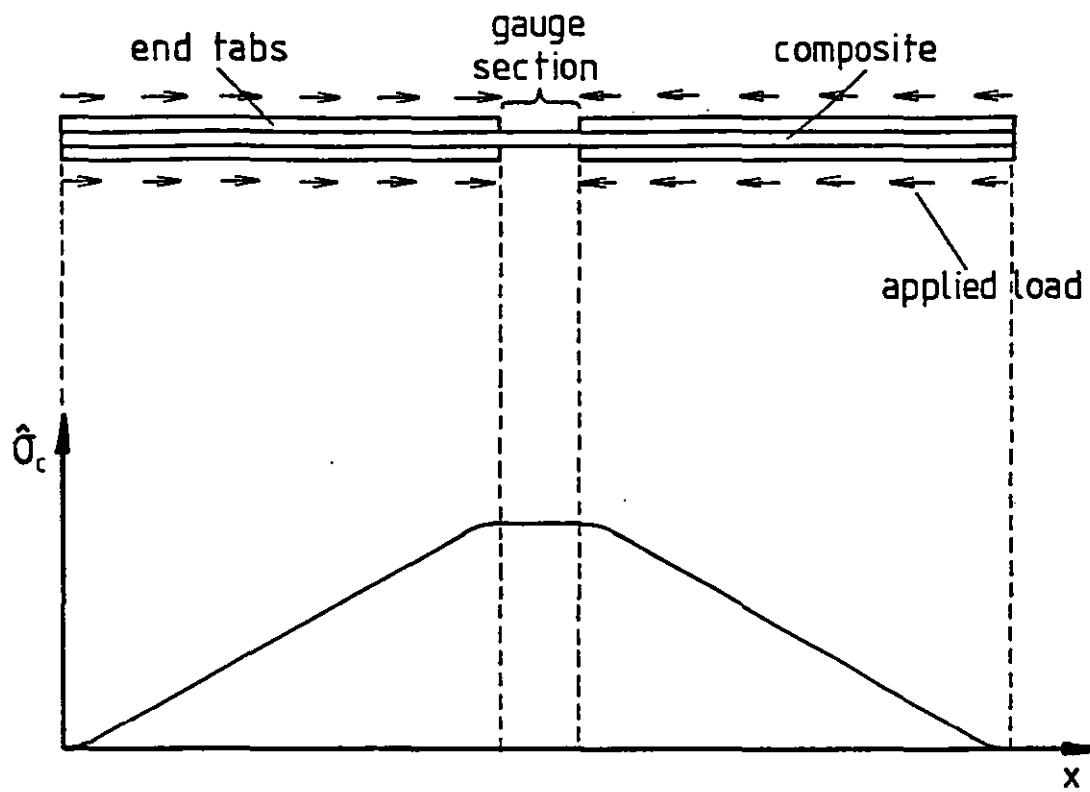

FIGURE 87: THE VARIATION OF COMPRESSIVE STRESS IN A LOADED COMPRESSION SPECIMEN

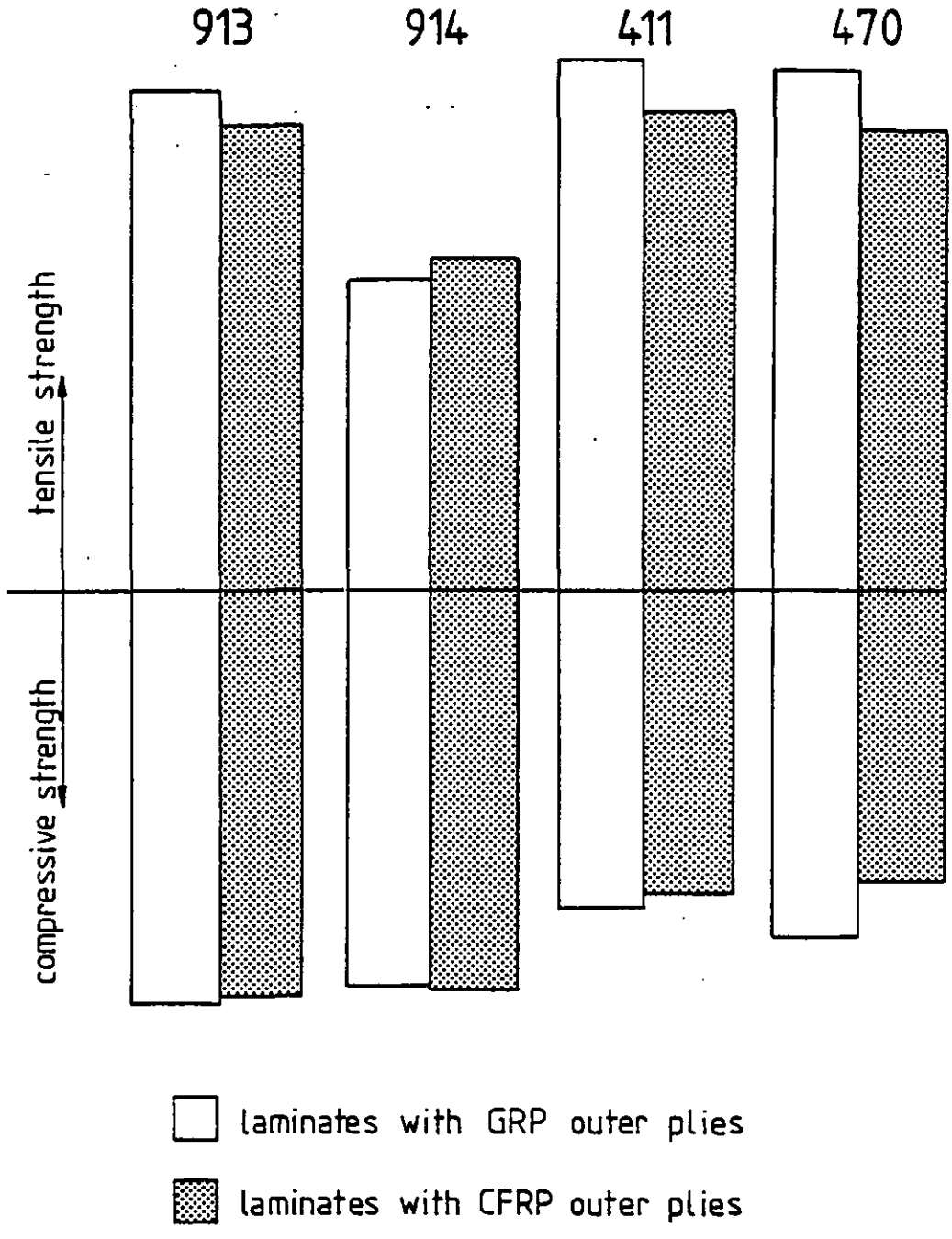

FIGURE 88: A COMPARATIVE REPRESENTATION OF THE STRESS RANGES OF UNIDIRECTIONAL HYBRID COMPOSITES CONTAINING EQUAL VOLUMES OF GLASS AND CARBON FIBRES

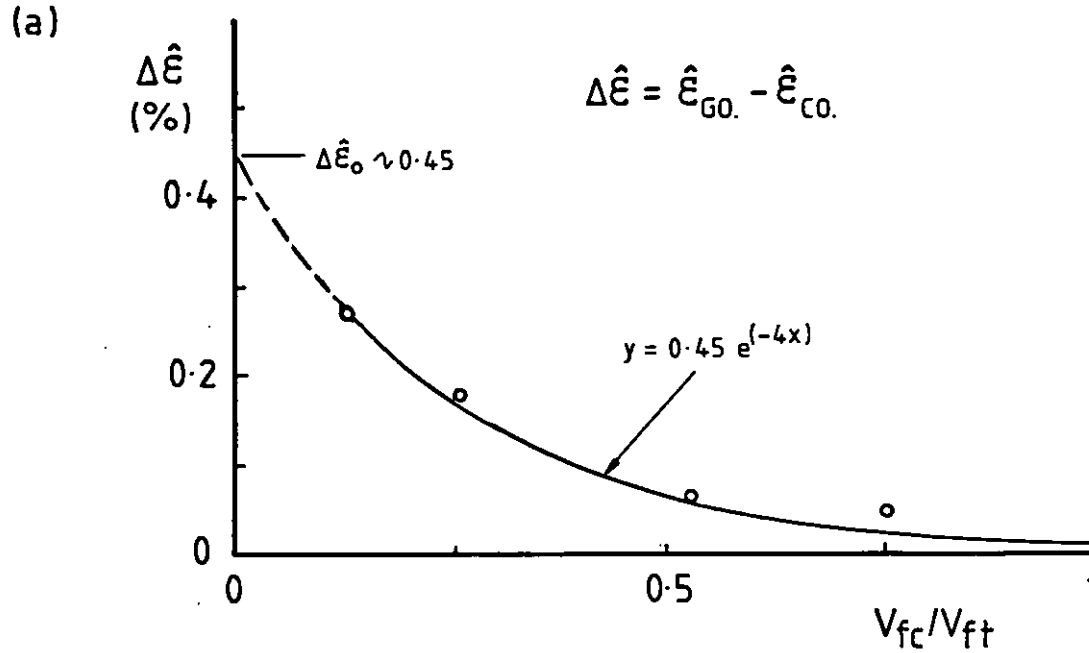

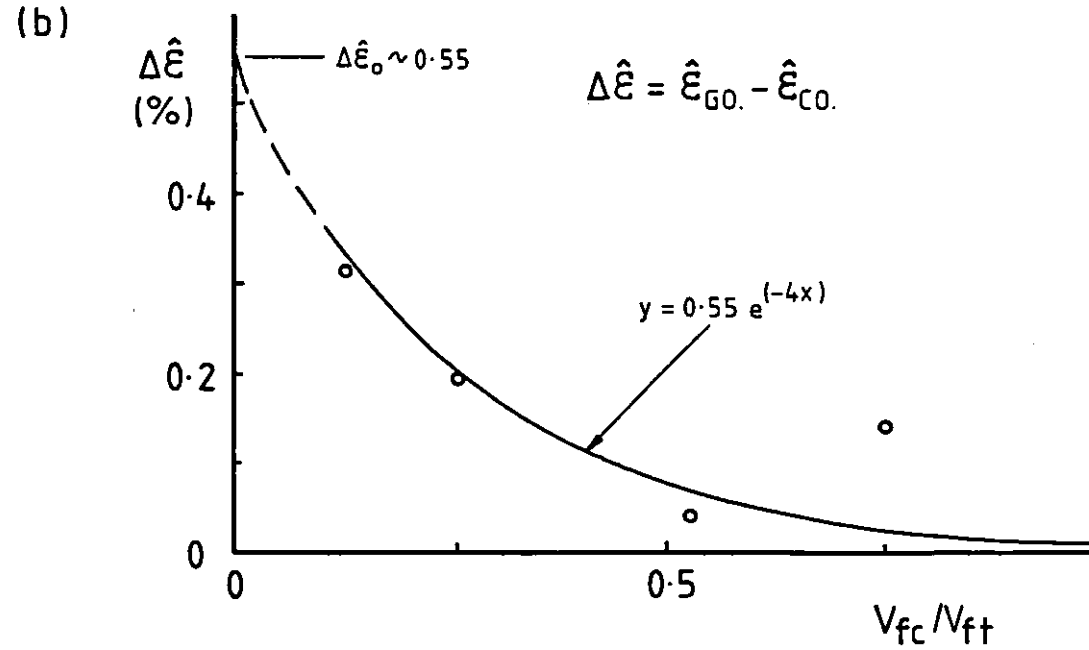

FIGURE 89: THE DIFFERENCE IN THE FAILURE STRAINS BETWEEN HYBRID LAMINATES WITH GRP IN THE OUTER LAYERS AND THOSE WITH CFRP IN THE OUTER LAYERS, 913 MATRIX
a) TENSILE FAILURE
b) COMPRESSIVE FAILURE

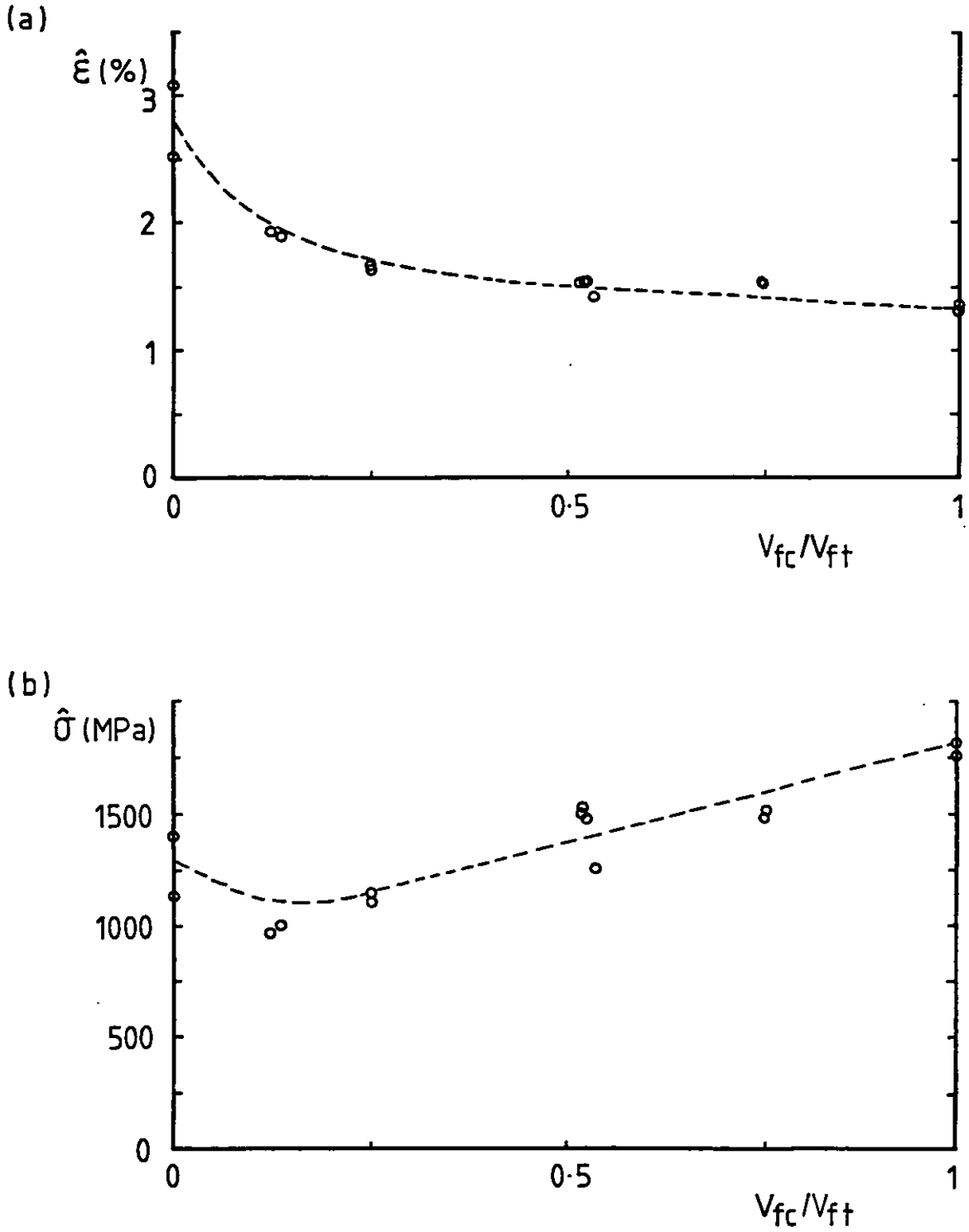

FIGURE 90: CHARACTERISATION OF THE 913 TENSILE FAILURE RESULTS FOR LAMINATES WITH GRP OUTER LAYERS
a) FAILURE STRAIN
b) STRENGTH

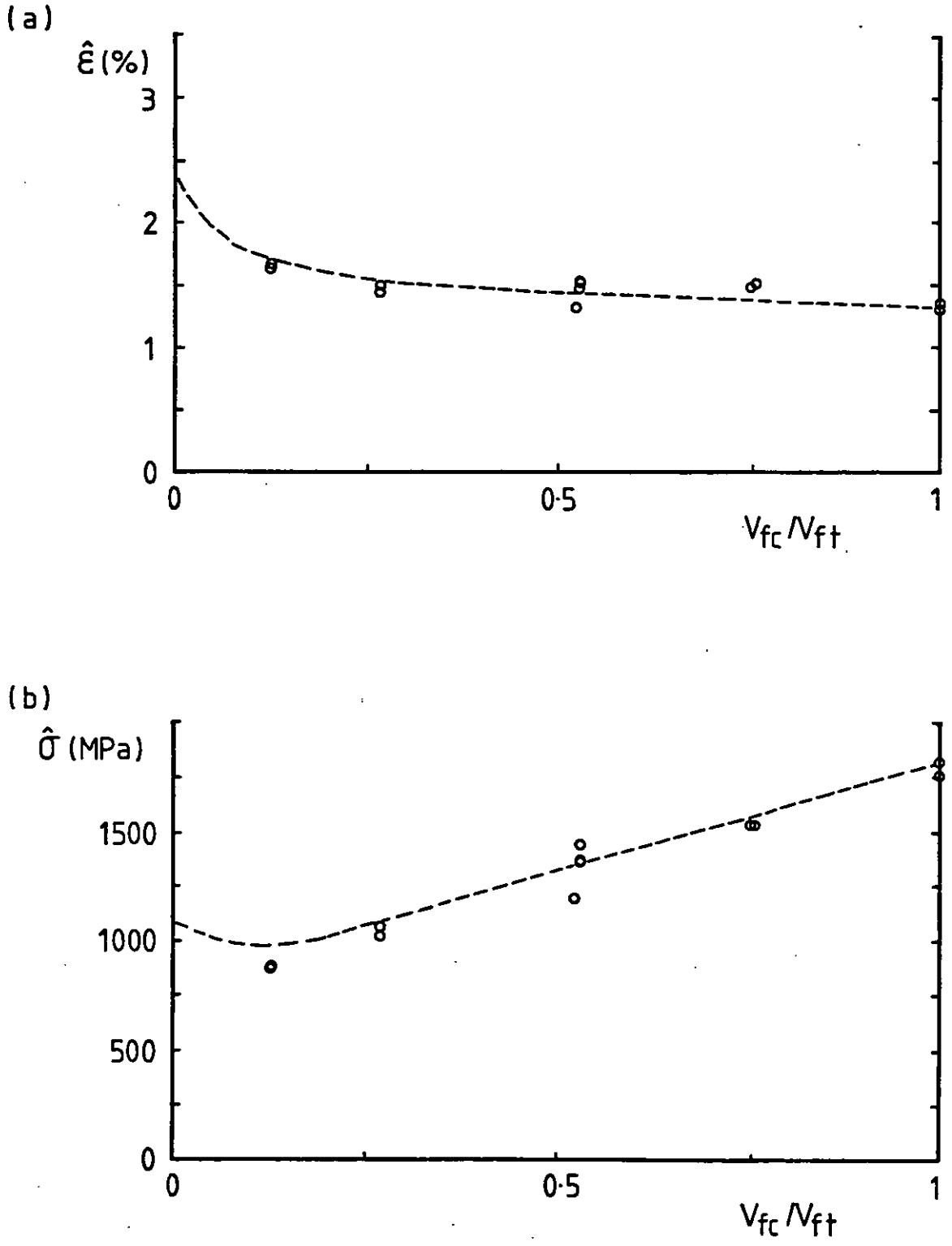

FIGURE 91: CHARACTERISATION OF THE 913 TENSILE FAILURE RESULTS FOR LAMINATES WITH CFRP OUTER LAYERS
a) FAILURE STRAIN
b) STRENGTH

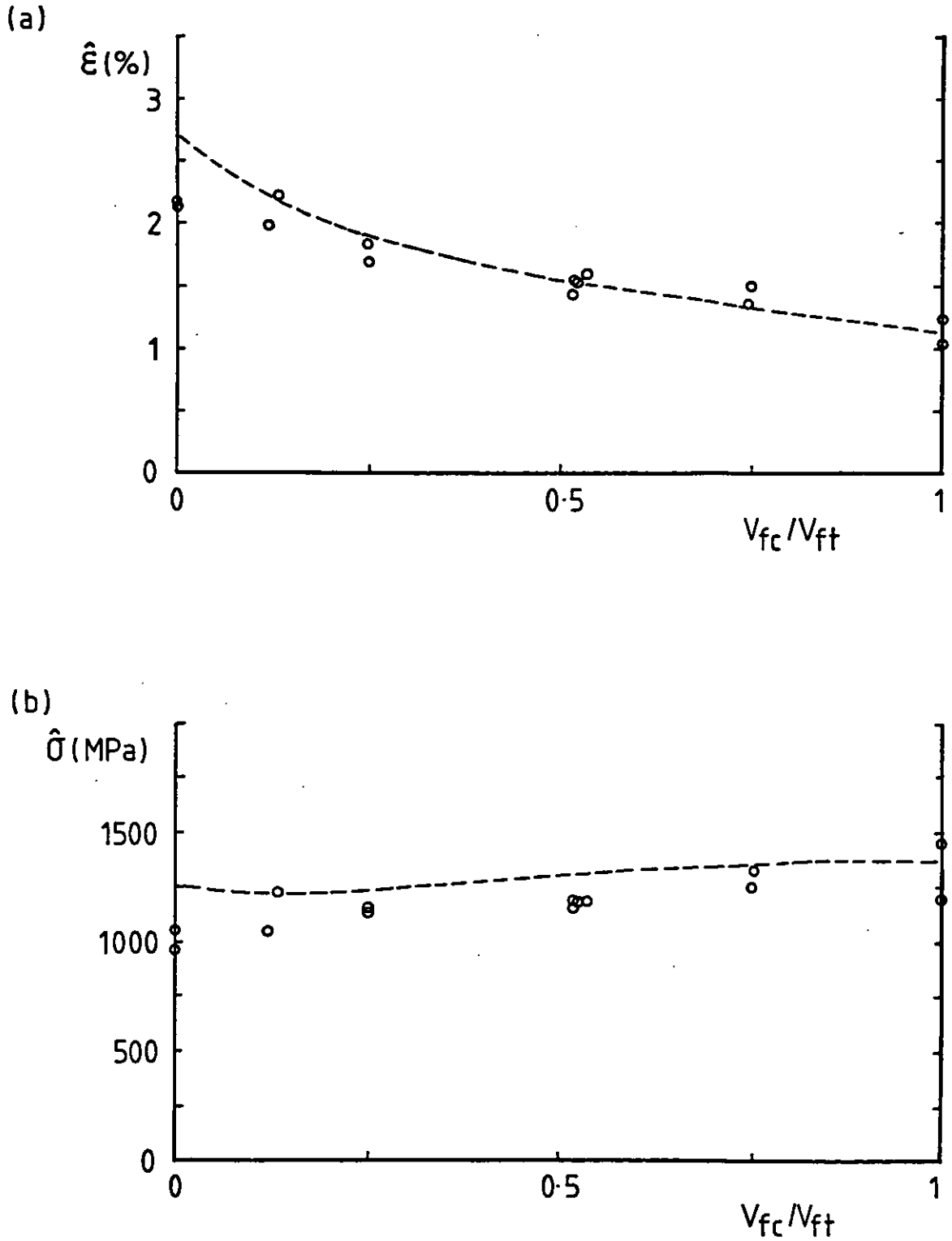

FIGURE 92: CHARACTERISATION OF THE 913 COMPRESSIVE FAILURE RESULTS FOR LAMINATES WITH GRP OUTER LAYERS
a) FAILURE STRAIN
b) STRENGTH

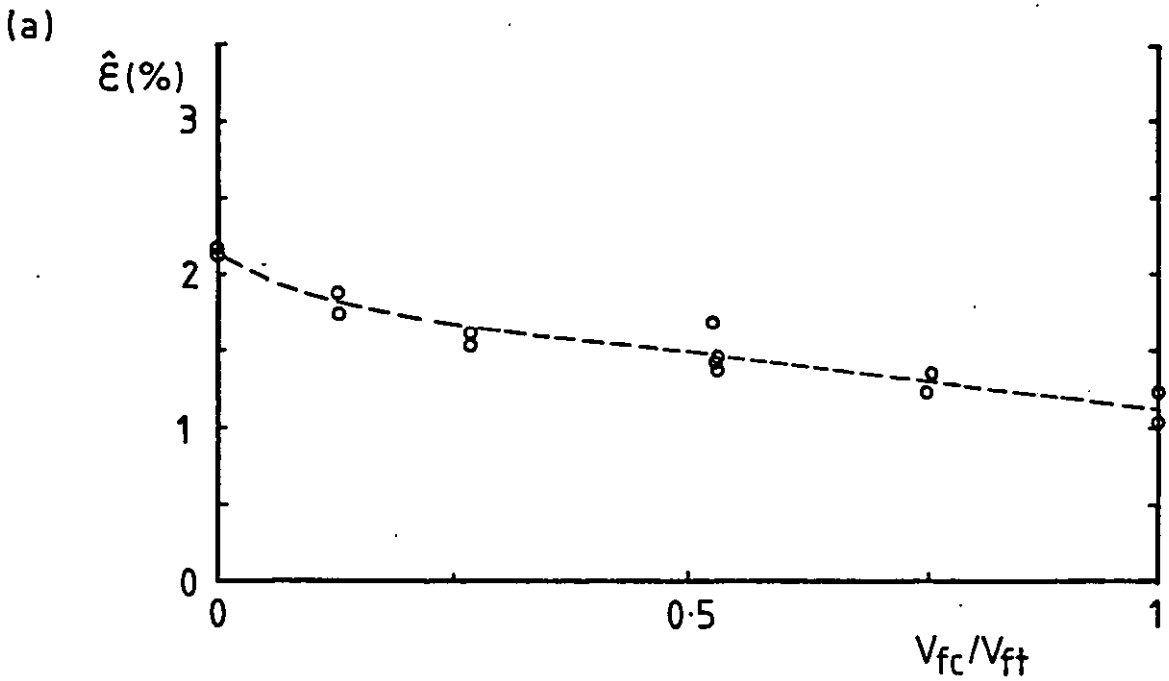

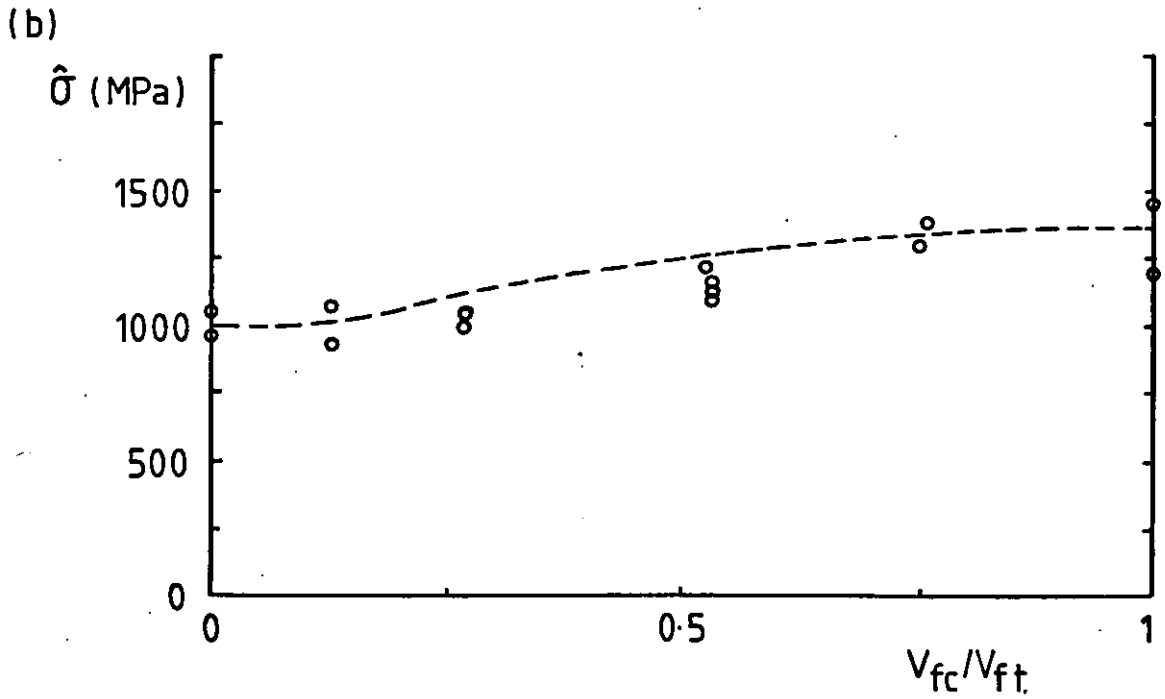

FIGURE 93: CHARACTERISATION OF THE 913 COMPRESSIVE FAILURE RESULTS FOR LAMINATES WITH CFRP OUTER LAYERS
a) FAILURE STRAIN
b) STRENGTH

PLATES

PLATE 1: The Dartec servohydraulic test machine with which tensile tests were performed

PLATE 2: The Mand servo-screw test machine with which compressive tests were performed

PLATE 3: The tensile failure of an epoxy GRP specimen, 913 matrix

PLATE 4: The tensile failure of a vinyl-ester GRP specimen, 411-45 matrix

PLATE 5: The tensile failure of a vinyl-ester GRP specimen, 470-36 matrix

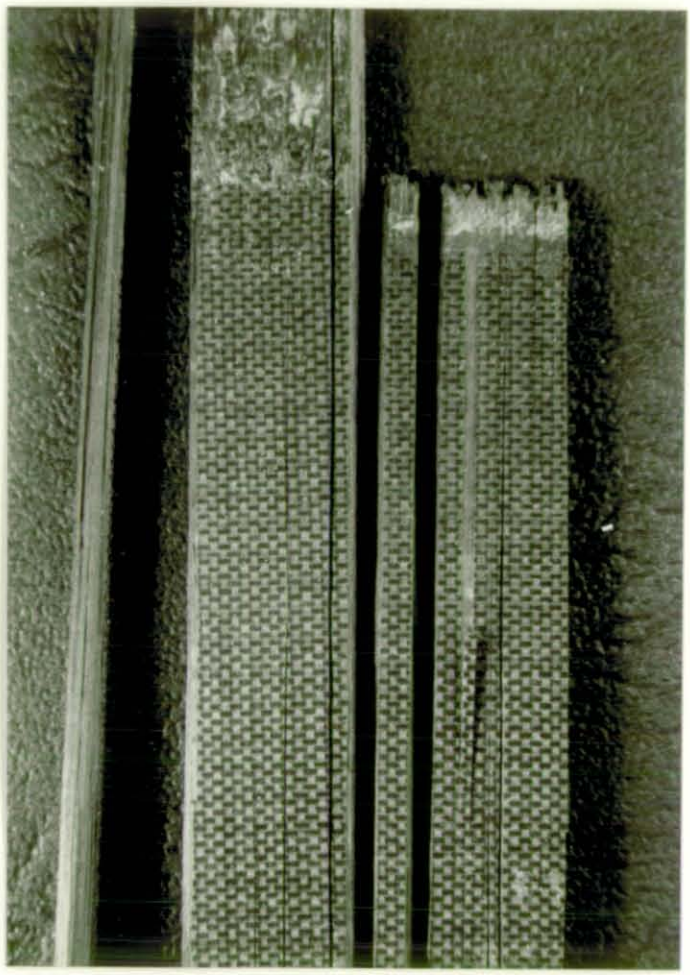

PLATE 6: The tensile failure of an epoxy CFRP specimen, 913 matrix

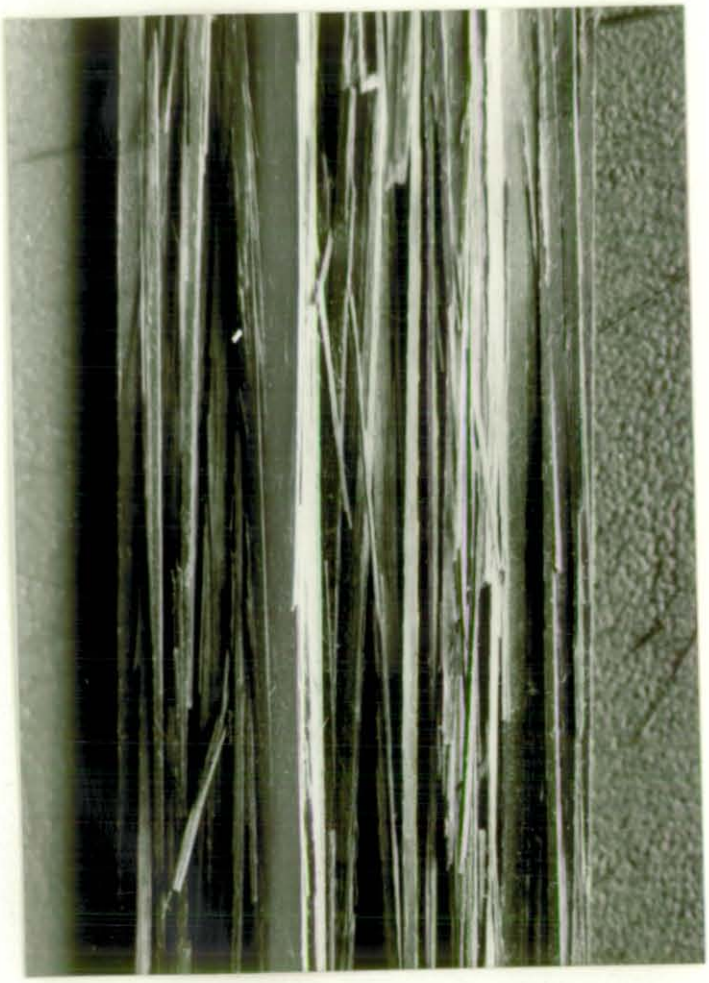

PLATE 7: The tensile failure of an vinyl-ester CFRP specimen, 411-415 matrix

PLATE 8: The tensile failure of an vinyl-ester CFRP specimen, 470-36 matrix

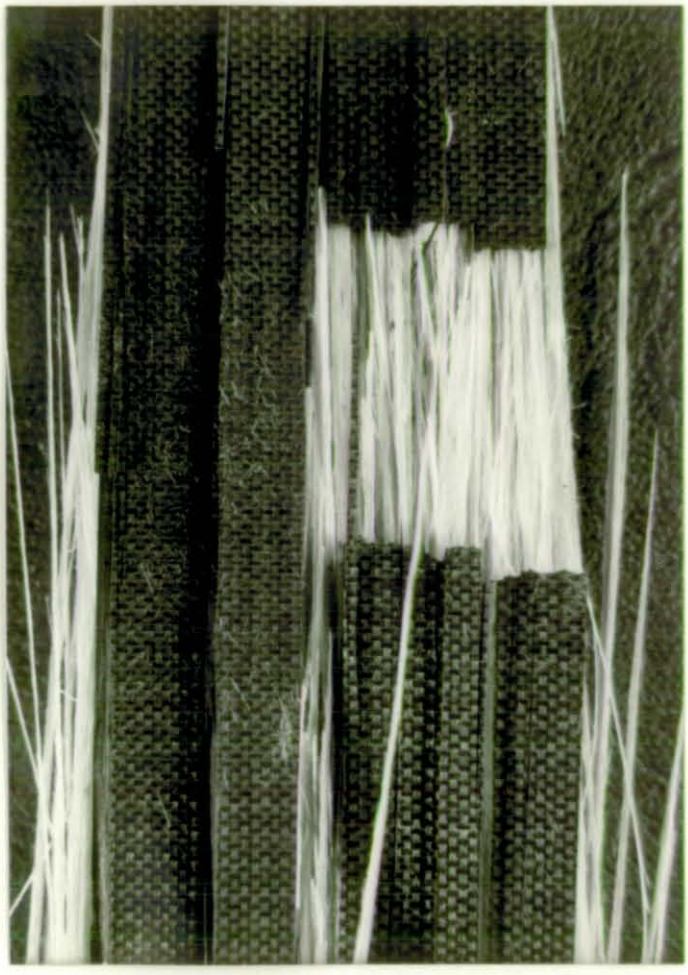

PLATE 9: The tensile failure of an epoxy C_4G_4/G_4C_4 hybrid specimen, 914 matrix

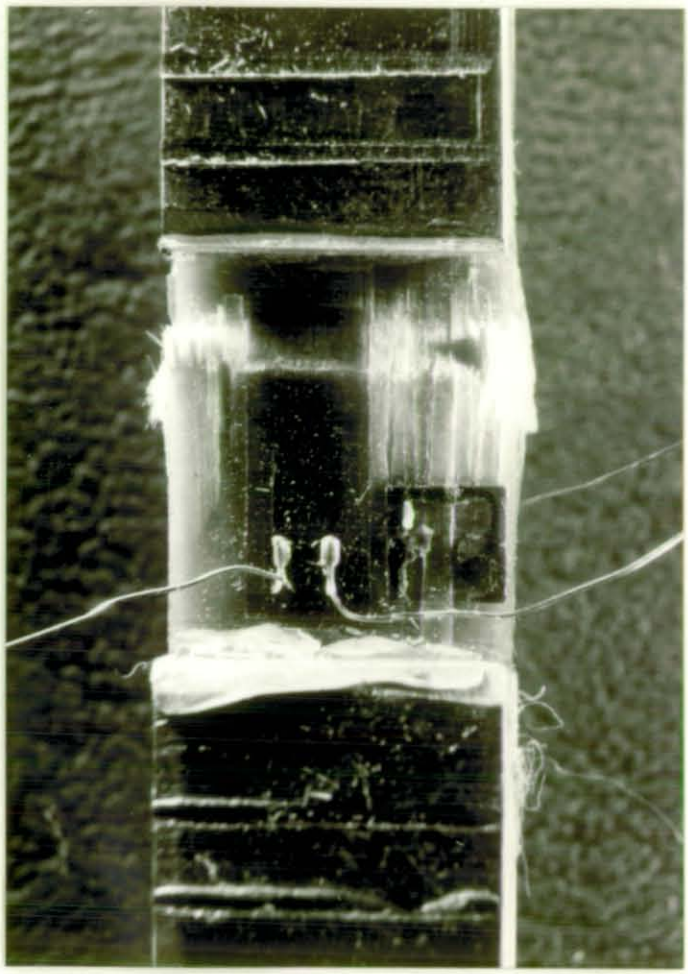

PLATE 10: The splitting mode of compressive failure observed in many of the GRP specimens, 913 matrix

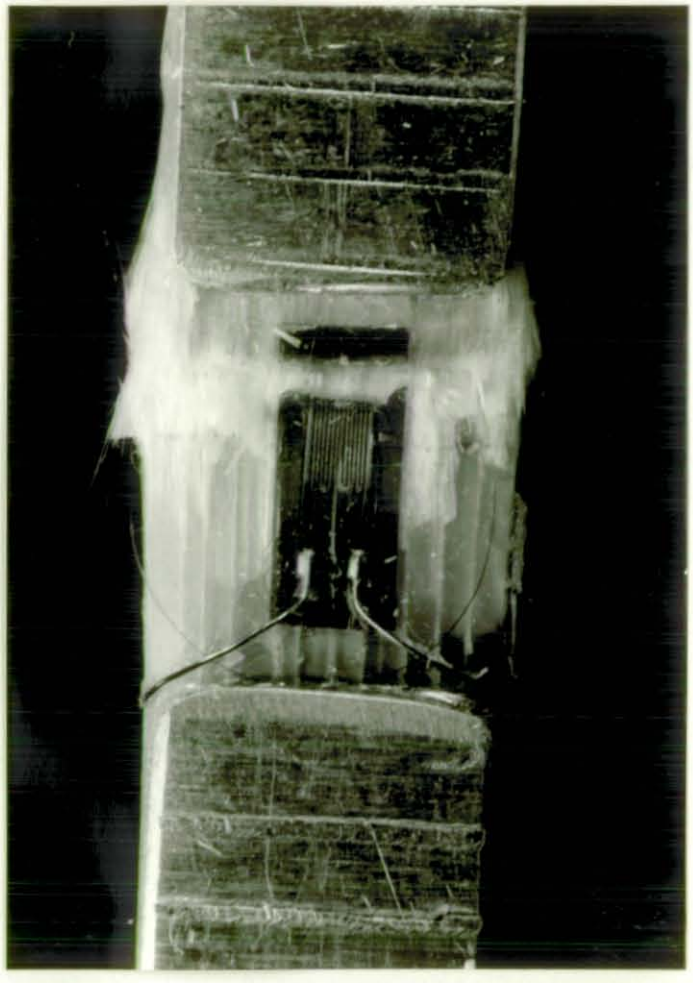

PLATE 11: The splitting mode of compressive failure observed in many of the GRP specimens, 470-36 matrix

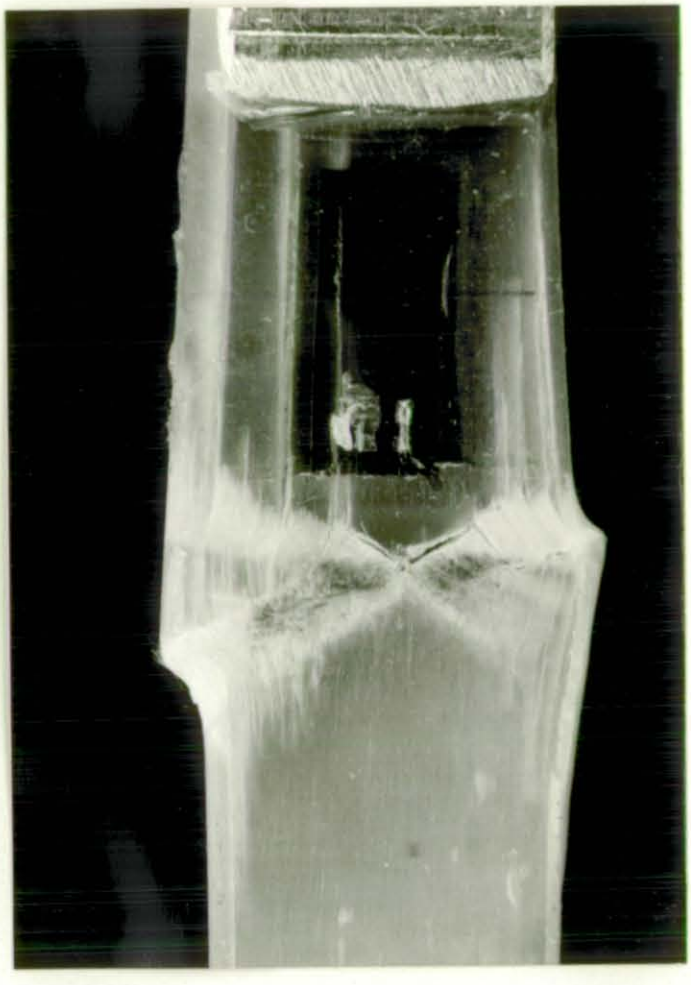

PLATE 12: The kink-band mode of compressive failure observed in some of the GRP specimens, 411-45 matrix

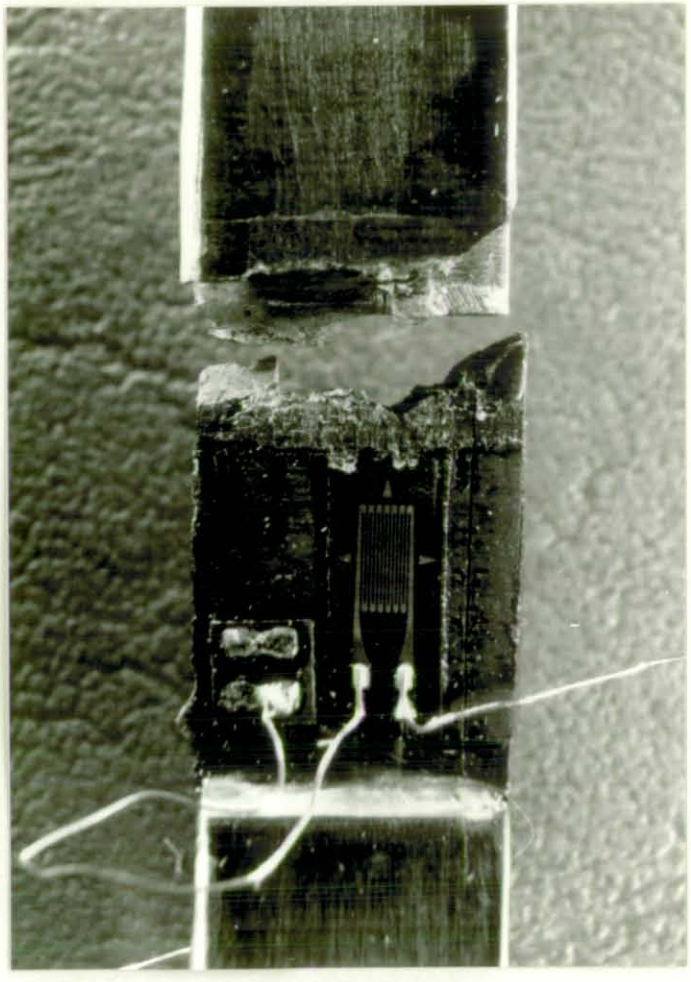

PLATE 13: The shear mode of compressive failure observed in the epoxy CFRP specimens, 913 matrix. The 45° failure plane is visible but not distinct because of the influence of the end tabs on the path of the fracture

×2·3K

PLATE 14: A high magnification SEM micrograph of the surface of the shear failure observed in epoxy CFRP specimens, 914 matrix

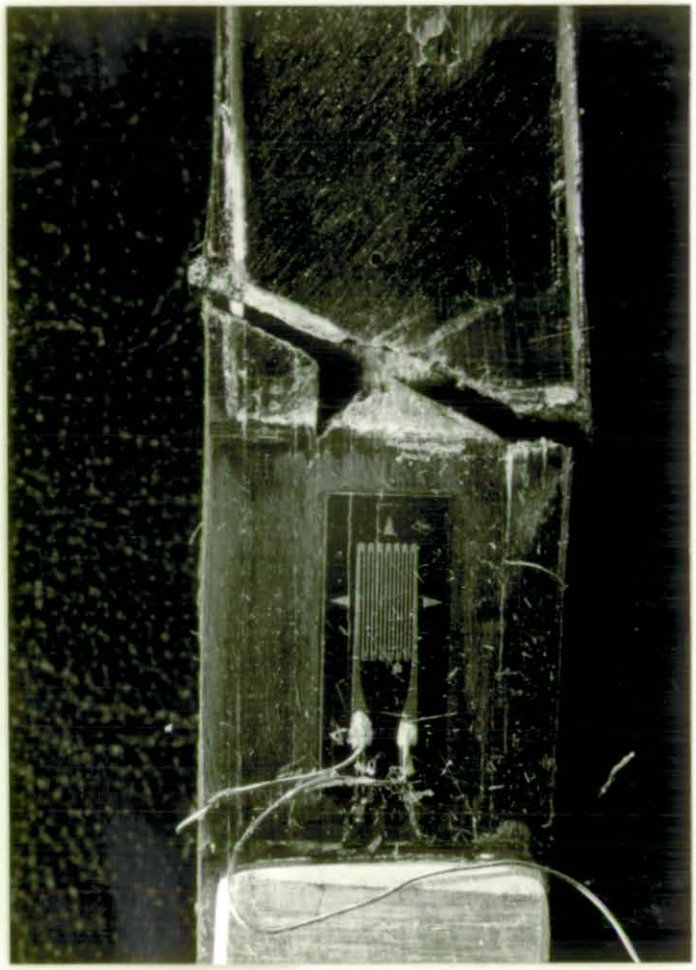

PLATE 15: The microbuckling mode of compressive failure observed in the vinyl-ester CFRP specimens, 411-45 matrix. The characteristic 70° plane of the fracture surface is clearly visible

×1·1K

PLATE 16: A high magnification SEM micrograph of part of the surface of a microbuckling failure observed in vinyl-ester CFRP specimens, 411-45 matrix

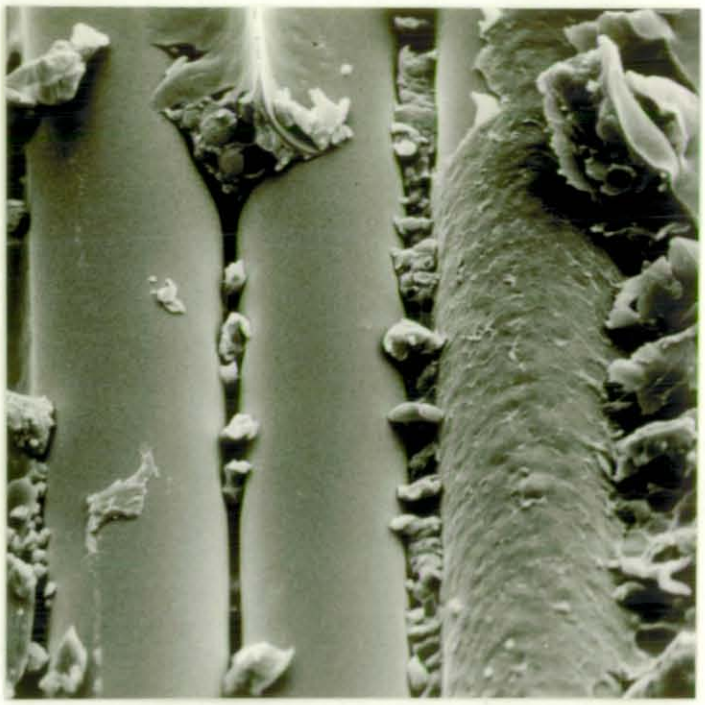

×1·8K

PLATE 17: A high magnification SEM micrograph of the fibres from an epoxy GRP inter-laminar shear failure, 913 matrix

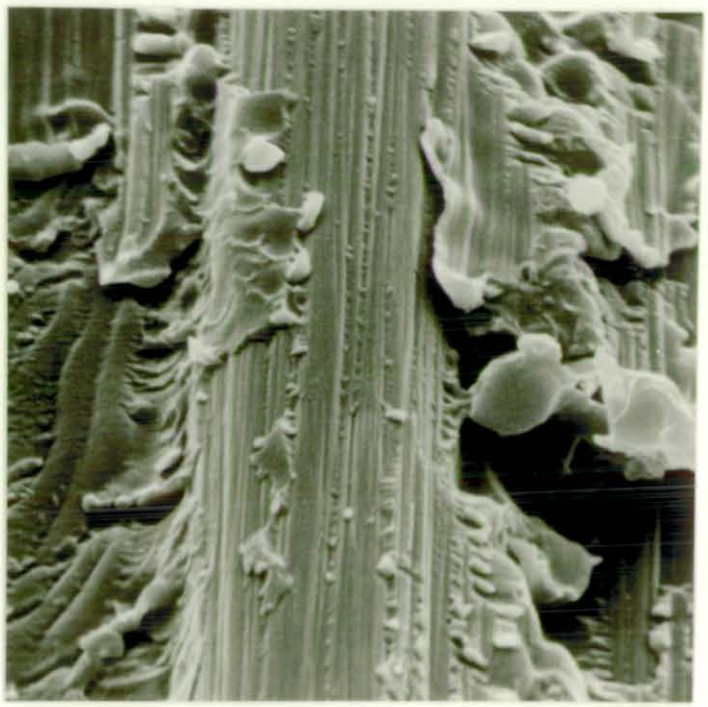

×4·5K

PLATE 18: A high magnification SEM micrograph of the fibres from an epoxy CFRP inter-laminar shear failure, 913 matrix

×4·5K

PLATE 19: A high magnification SEM micrograph of the fibres from a vinyl-ester GRP inter-laminar shear failure, 411-45 matrix

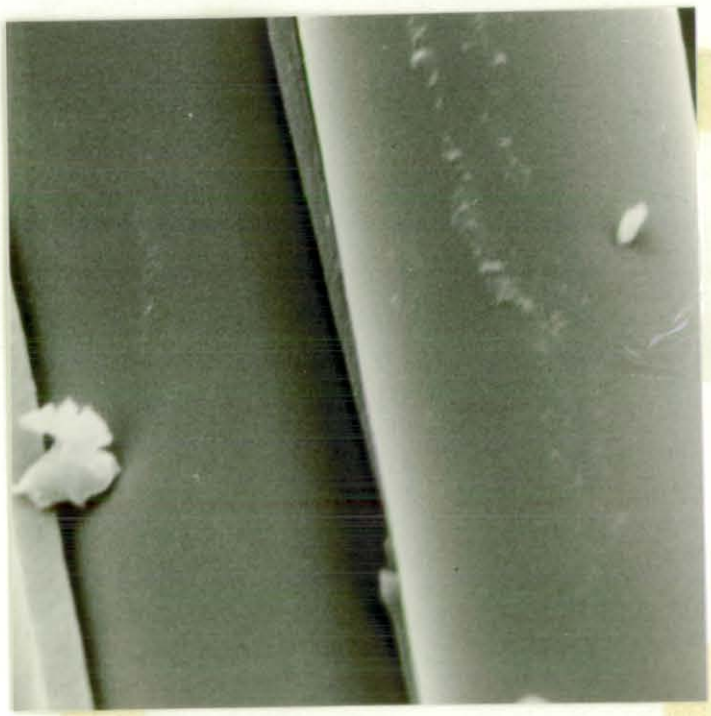

×5K

PLATE 20: A high magnification SEM micrograph of the fibres from a vinyl-ester CFRP inter-laminar shear failure, 411-45 matrix

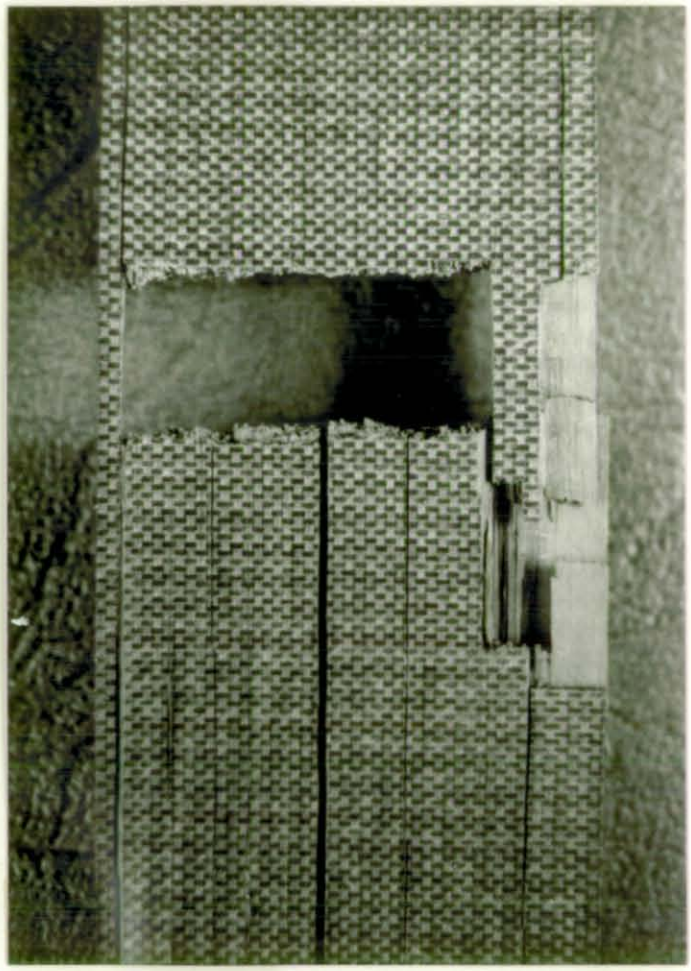

PLATE 21: The tensile failure of an epoxy CFRP specimen, 914 matrix

PLATE 22: A high magnification SEM micrograph of a fibre from an epoxy GRP transverse tensile failure, 913 matrix

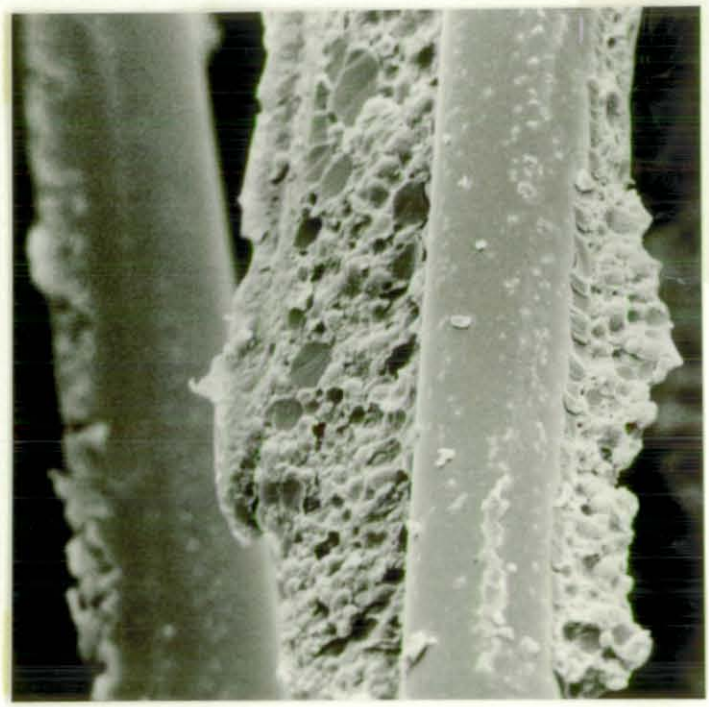

PLATE 23: A high magnification SEM micrograph of a fibre from an epoxy GRP transverse tensile failure, 914 matrix

×260

PLATE 24: An SEM micrograph of the compressive failure surface of a vinyl-ester CFRP specimen, 470-36 matrix. the characteristic steps which are the result of fibre microbuckling are clearly visible

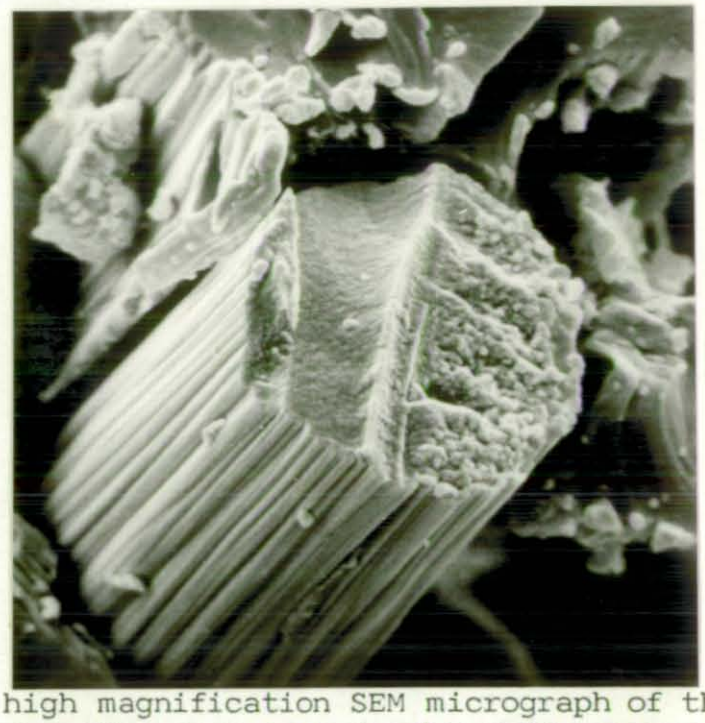

×6·5K

PLATE 25: A high magnification SEM micrograph of the end of a carbon fibre from a vinyl-ester CFRP compressive failure, 470-36 system. The fibre microbuckling failure has resulted in well defined tensile and compressive regions of fracture being visible

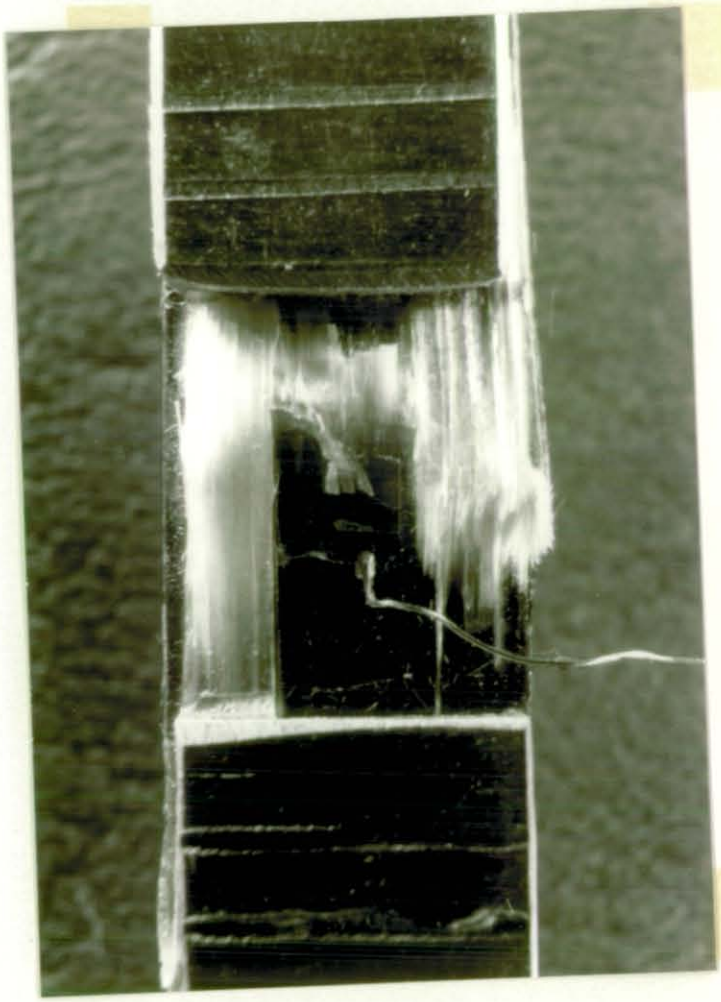

PLATE 26: The splitting mode of compressive failure in the GRP outer layers of a G_4C_4/C_4G_4 hybrid specimen, 470-36 matrix

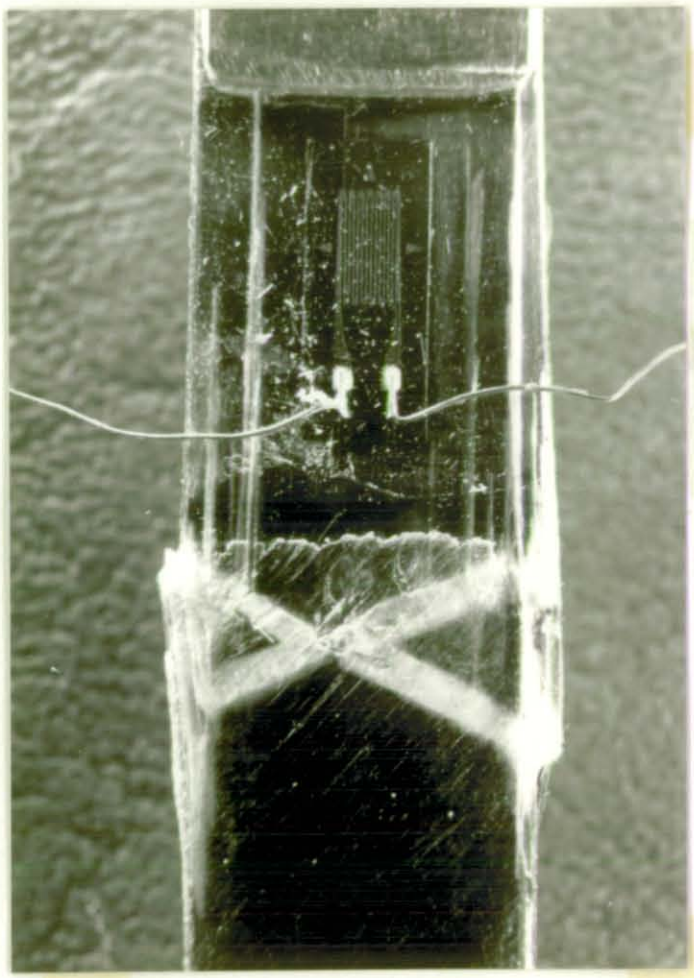

PLATE 27: The kink-band mode of compressive failure in the GRP outer layers of a G_4C_4/C_4G_4 hybrid specimen, 470-36 matrix

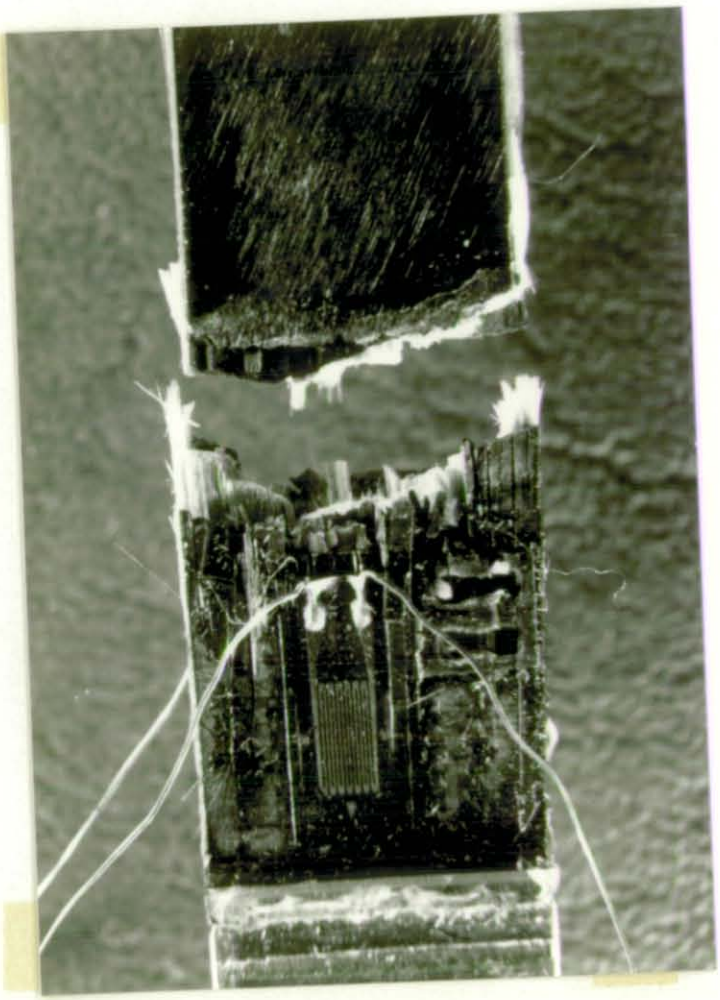

PLATE 28: The compressive failure of an epoxy C_4G_4/G_4C_4 hybrid specimen, 914 system. The influence of the end tabs on the path of the fracture is evident, but the 45° shear plane in the CFRP outer layers is also visible in places

×800

PLATE 29: An SEM micrograph of part of the tensile failure surface of an epoxy CFRP specimen, 913 matrix

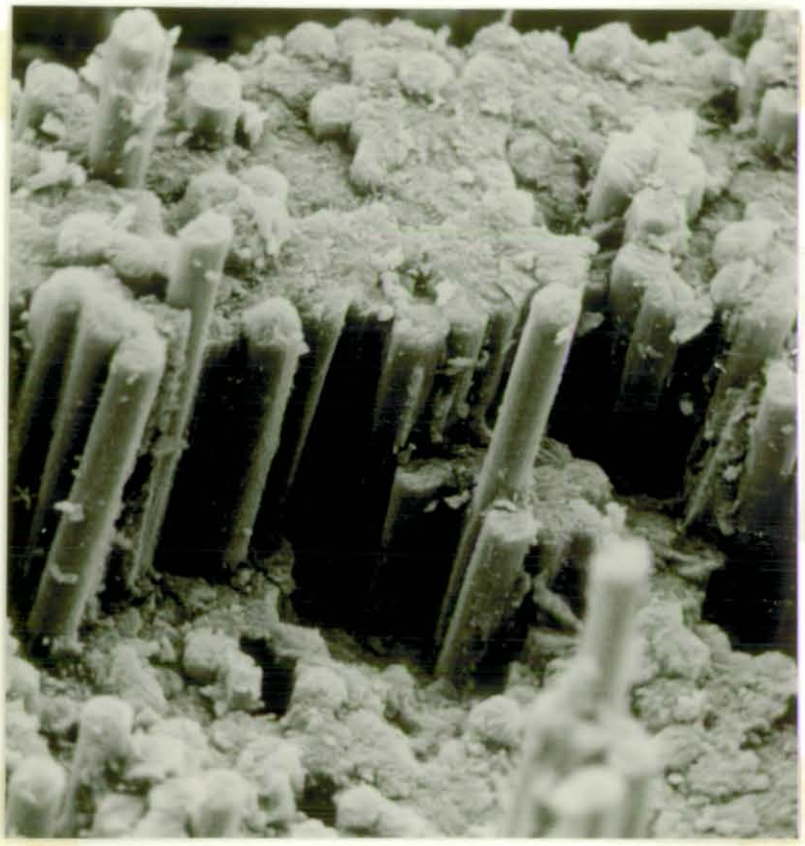

×800

PLATE 30: An SEM micrograph of part of the tensile failure surface of a 914 epoxy CFRP specimen. Comparison with Plate 29 reveals that in the 914, crack propagation through fibres and matrix has been aided

APPENDICES

APPENDIX 1

INDIVIDUAL TEST RESULTS

The individual specimen results are presented in Tables A48-A51 for the tensile tests and in Tables A52-A55 for the compressive tests. In cases where the value was not obtained for experimental reasons, it is denoted by "*". (Values in brackets are considered inaccurate for experimenal reasons).

TABLE A48: INDIVIDUAL TENSILE TEST RESULTS, 913 MATRIX

Lay-up	CSA (mm^2)	Max. Load (kN)	Failure Strain %	UTS (MPa)	E (GPa)	V_{fg} (%)	V_{fc} (%)	UTS (V_{ft}=0.6) (MPa)	E (V_{ft}=0.6) (GPa)
G_8/G_8	43.34	68.38	3.29	1577	47.8	67.4	0	1404	42.5
	43.26	68.12	2.94	1575	53.6	67.4	0	1402	47.7
	43.26	66.90	3.04	1547	50.7	67.4	0	1377	45.1
	40.82	50.29	2.13	1232	58.0	68.8	0	1074	50.5
	43.52	51.21	2.48	1177	51.9	68.8	0	1026	45.3
	45.43	65.53	2.96	1442	50.6	68.8	0	1258	44.1
C_8/C_8	50.90	103.48	1.48	2033	146.3	0	63.2	1930	138.9
	52.07	84.12	1.12	1616	142.8	0	63.2	1534	135.5
	51.91	87.94	1.30	1887	149.5	0	63.2	1791	141.9
	49.95	99.42	1.33	1990	147.6	0	64.6	1849	137.1
	50.60	98.96	1.43	1956	141.2	0	64.6	1816	131.1
	54.14	102.31	1.31	1890	150.2	0	64.6	1755	139.5
G_4C_4/C_4G_4	46.74	78.38	1.59	1677	105.1	30.9	33.5	1562	97.9
	47.69	73.47	1.51	1541	101.2	30.9	33.5	1435	94.3
	47.19	79.62	1.59	1687	107.1	30.9	33.5	1572	99.8
	48.32	77.36	1.44	1601	109.8	31.3	33.7	1478	101.4
	48.64	82.21	1.65	1690	101.5	31.3	33.7	1560	93.7
	47.63	73.78	1.54	1549	100.1	31.3	33.7	1430	92.4
C_4G_4/G_4C_4	45.45	67.91	1.51	1494	107.1	30.8	34.8	1367	98.0
	46.48	67.26	1.49	1447	96.9	30.8	34.8	1324	88.7
	47.31	71.33	1.54	1508	98.6	30.8	34.8	1379	90.1
	45.68	73.10	1.53	1600	103.2	30.4	34.3	1484	95.7
	45.86	62.96	1.39	1373	98.0	30.4	34.3	1273	90.9
	50.04	72.40	1.47	1447	98.6	30.4	34.3	1342	91.5
G_6C_2/C_2G_6	47.50	55.89	1.61	1177	72.7	49.6	16.6	1066	65.9
	46.74	57.65	1.67	1233	93.2	49.6	16.6	1118	66.3
	46.92	57.68	1.64	1229	74.5	49.6	16.6	1114	67.5
	45.86	55.49	1.66	1210	73.4	50.4	16.8	1080	65.5
	44.60	57.72	1.64	1294	80.0	50.4	16.8	1156	71.4
	44.28	58.67	1.69	1325	77.7	50.4	16.8	1183	69.4
C_6G_2/G_2C_6	49.41	83.28	1.57	1685	118.0	16.4	49.0	1546	108.2
	47.94	79.55	1.37	1659	122.4	16.4	49.0	1522	112.3
	48.77	80.25	1.48	1645	118.5	16.4	49.0	1510	108.8
	48.96	77.18	1.52	1574	123.6	16.0	49.4	1446	113.4
	48.38	77.22	1.46	1596	126.3	26.0	49.4	1464	115.9
	49.92	90.01	1.53	1803	116.6	16.0	49.4	1654	107.0

TABLE A48 (continued)

Lay-up	CSA (mm^2)	Max.Load (kN)	Failure Strain %	UTS (MPa)	E (GPa)	V_{fg} (%)	V_{fc} (%)	UTS (V_{ft}=0.6) (MPa)	E (V_{ft}=0.6) (MPa)
G_2C_6/	48.75	74.12	1.55	1520	121.0	16.2	47.9	1423	113.3
C_6G_2	52.12	84.01	1.52	1612	123.3	16.2	47.9	1509	115.4
	52.16	83.95	1.55	1609	126.7	16.2	47.9	1507	118.6
	49.75	78.52	1.48	1578	114.2	15.3	46.2	1540	111.4
	52.16	76.74	1.44	1471	111.2	15.3	46.2	1435	108.5
	53.46	85.31	1.69	1596	108.1	15.3	46.2	1557	105.5
C_2G_6/	45.61	52.73	1.55	1156	73.6	46.9	17.3	1080	68.8
G_6C_2	44.68	49.61	1.31	1110	73.7	46.9	17.3	1038	68.9
	46.38	52.17	1.48	1125	75.7	46.9	17.3	1052	70.7
	45.86	49.10	1.37	1071	76.4	48.0	17.7	978	69.8
	43.23	51.70	1.68	1196	69.7	48.0	17.7	1092	63.6
	45.24	48.69	1.45	1079	74.7	48.0	17.7	985	68.3
G_7C/CG_7	44.78	48.93	1.84	1093	59.6	60.3	8.2	957	52.2
	45.39	50.62	2.18	1115	52.2	60.3	8.2	977	45.7
	45.65	49.37	1.79	1081	60.7	60.3	8.2	947	53.2
	48.32	50.96	1.91	1055	55.2	54.9	8.4	1000	52.3
	46.69	49.30	1.85	1056	56.9	54.9	8.4	1001	53.9
	49.28	51.56	1.93	1046	54.4	54.9	8.4	992	51.5
CG_7/G_7C	45.29	43.89	1.60	969	59.7	60.2	8.8	843	51.9
	43.52	43.54	1.62	1000	61.8	60.2	8.8	870	53.8
	41.83	43.38	1.68	1037	63.9	60.2	8.8	902	55.6
	43.23	43.00	1.78	995	56.4	59.6	8.8	873	49.4
	43.93	43.90	1.67	999	60.4	59.6	8.8	877	53.0
	43.60	43.81	1.54	1005	62.6	59.6	8.8	881	54.9
$G_2C_4G_2$/	45.65	64.75	1.51	1418	92.5	30.7	35.4	1288	8.40
$G_2C_4G_2$	46.05	56.53	1.23	1228	100.2	30.7	35.4	1114	90.9
	50.09	74.78	1.53	1493	101.4	30.7	35.4	1355	92.1
	46.05	75.76	1.64	1645	99.1	31.0	34.3	1512	91.1
	46.74	75.13	1.60	1607	99.1	31.0	34.3	1477	91.1
	47.94	74.96	1.42	1564	107.3	31.0	34.3	1437	98.6
$C_2G_4C_2$/	45.54	53.51	1.23	1175	94.5	31.1	34.4	1076	86.5
$C_2G_4C_2$	47.50	61.01	1.28	1284	99.9	31.1	34.4	1177	91.5
	49.45	71.04	1.44	1437	102.1	31.1	34.4	1316	93.6
	46.87	72.27	1.52	1542	100.0	30.4	34.4	1428	92.6
	46.12	71.20	1.54	1544	99.5	30.4	34.4	1429	92.2
	47.19	73.32	1.53	1554	102.0	30.4	34.4	1439	94.5

TABLE A49: INDIVIDUAL TENSILE TEST RESULTS, 914 MATRIX

Lay-up	CSA (mm^2)	Max.Load (kN)	Failure Strain (%)	UTS (MPa)	E (GPa)	V_{fg} (%)	V_{fc} (%)	UTS (V_{ft}=0.6) (MPa)	E (V_{ft}=0.6) (MPa)
G_8	42.50	57.02	2.47	1342	52.9	70.4	0	1143	45.0
	40.32	50.39	*	1250	*	70.4	0	1065	*
	42.84	55.54	2.58	1296	47.8	70.4	0	1105	40.7
	41.75	57.17	2.80	1369	48.0	71.6	0	1148	40.3
	41.42	56.95	*	1375	*	71.6	0	1152	*
	40.75	58.15	2.63	1427	53.9	71.6	0	1196	45.1
C_8	46.23	61.22	0.87	1324	151.7	0	68.6	1158	132.7
	47.31	62.31	0.84	1317	154.1	0	68.6	1152	134.8
	45.11	61.08	0.95	1354	159.3	0	68.6	1184	139.4
	45.68	65.36	0.88	1431	160.5	0	69.3	1239	138.9
	47.31	65.42	0.93	1383	147.3	0	69.3	1197	127.6
	45.47	67.85	0.95	1492	154.2	0	69.3	1292	133.5
G_4C_4/ C_4G_4	43.67	43.27	0.95	991	102.6	36.3	34.4	841	87.1
	44.07	43.86	0.92	995	108.1	36.3	34.4	845	91.7
	42.92	37.23	0.90	867	96.4	36.3	34.4	736	81.8
	42.84	40.83	0.88	953	105.6	35.8	34.6	812	90.0
	43.90	42.63	0.96	971	99.5	35.8	34.6	828	84.8
	42.33	44.86	1.02	1060	104.6	35.8	34.6	903	89.4
C_4G_4 G_4C_4	43.42	47.15	1.16	1086	92.3	35.8	34.9	922	78.3
	43.93	48.50	1.01	1104	108.4	35.8	34.9	937	92.0
	42.67	*	*	*	*	35.8	34.9	*	*
	42.92	48.61	1.01	1133	106.3	36.0	35.0	957	89.8
	43.17	52.02	1.03	1205	101.7	36.0	35.0	1018	86.0
	41.99	53.54	0.80	1275	138.8	36.0	35.0	1078	117.3
$G_2C_4G_2$/ $G_2C_4G_2$	43.08	47.10	0.96	1093	112.4	35.0	35.9	925	95.1
	44.86	51.26	1.11	1143	101.9	35.0	35.9	967	86.3
	43.77	49.67	1.01	1135	110.8	35.0	35.9	960	93.7
	42.75	47.15	0.87	1103	126.2	35.5	35.9	927	106.0
	43.58	51.16	1.15	1174	101.0	35.5	35.9	986	84.9
	42.83	49.56	1.05	1157	109.9	35.5	35.9	972	92.3
$C_2G_4C_2$/ $C_2G_4C_2$	42.84	45.98	1.02	1073	103.8	35.4	35.2	912	88.2
	42.75	48.58	1.04	1136	103.4	35.4	35.2	966	87.9
	42.84	53.85	0.81	1257	121.0	35.4	35.2	1068	102.8
	43.50	44.04	0.94	1012	107.9	35.5	35.0	862	91.8
	44.43	47.68	1.02	1073	101.9	35.5	35.0	913	86.7
	42.50	44.48	0.87	1047	119.7	35.5	35.0	891	101.9

TABLE A50: INDIVIDUAL TENSILE TEST RESULTS, 411-45 MATRIX

Lay-up	CSA (mm^2)	Max. Load (kN)	Failure Strain %	UTS (MPa)	E (GPa)	V_{fg} (%)	V_{fc} (%)	UTS (V_{ft}=0.6) (MPa)	E (V_{ft}=0.6) (MPa)
G_8	49.75	52.90	2.32	1063	44.2	56.8	0	1123	46.7
	49.95	53.15	2.40	1064	46.3	56.8	0	1124	49.0
	49.60	53.80	2.21	1085	47.0	56.8	0	1146	49.7
	47.42	57.30	2.49	1208	48.7	60.9	0	1190	48.0
	47.19	47.00	1.96	996	49.6	60.9	0	981	48.8
	47.18	48.00	2.30	1017	45.2	60.9	0	1002	44.5
C_8	52.21	84.75	1.47	1623	120.9	0	53.5	1820	135.6
	52.16	88.90	1.24	1704	126.7	0	53.5	1911	142.1
	52.92	84.35	1.26	1594	129.9	0	53.5	1788	145.7
	48.44	72.35	1.22	1494	131.9	0	55.9	1603	141.5
	47.06	67.60	1.17	1436	132.8	0	55.9	1542	142.6
	48.95	81.00	1.33	1655	140.1	0	55.9	1776	150.3
G_4C_4/ C_4G_4	52.29	78.40	1.60	1499	93.6	25.8	25.7	1747	109.0
	52.08	70.60	1.59	1356	86.8	25.8	25.7	1579	101.1
	53.04	71.60	1.33	1350	96.2	25.8	25.7	1573	112.1
	47.50	60.15	(0.74)	1266	(122.1)	28.4	27.6	1357	(130.9)
	47.31	63.35	1.24	1339	91.6	28.4	27.6	1435	98.2
	49.05	67.60	1.45	1378	82.5	28.4	27.6	1477	88.4
C_4G_4/ G_4C_4	49.55	65.25	1.50	1317	86.6	27.9	26.8	1444	95.0
	50.09	63.05	1.51	1259	86.1	27.9	26.8	1381	94.4
	49.05	59.60	1.52	1215	90.4	27.9	26.8	1333	99.2
	49.45	71.40	1.68	1444	90.4	28.7	27.8	1533	96.1
	47.69	56.65	1.50	1188	88.4	28.7	27.8	1261	93.9
	48.36	54.65	1.03	1130	93.7	28.7	27.8	1200	99.5
$G_2C_4G_2$/ $G_2C_4G_2$	48.64	74.10	1.87	1523	89.3	28.9	27.0	1635	95.9
	48.50	65.10	1.66	1342	85.6	28.9	27.0	1441	91.9
	49.00	76.15	1.52	1554	98.3	28.9	27.0	1668	105.5
	48.95	67.20	1.71	1373	86.4	27.6	27.2	1503	94.6
	47.69	61.45	1.55	1289	91.5	27.6	27.2	1411	100.2
	48.83	69.65	1.35	1426	92.2	27.6	27.2	1562	101.0
$C_2G_4C_2$/ $C_2G_4C_2$	53.17	69.35	1.52	1304	84.3	27.3	23.9	1528	98.8
	53.38	63.20	1.35	1182	81.6	27.3	13.9	1385	95.6
	53.68	64.90	1.44	1209	83.7	27.3	23.9	1417	98.1
	47.12	58.85	1.34	1249	101.7	29.3	28.3	1301	105.9
	45.68	52.40	1.59	1147	86.7	29.3	28.3	1195	90.4
	48.07	68.40	1.76	1423	87.8	29.3	28.3	1482	91.5

TABLE A51: INDIVIDUAL TENSILE TEST RESULTS, 470-36 MATRIX

Lay-up	CSA (mm^2)	Max. Load (kN)	Failure Strain %	UTS (MPa)	E (GPa)	V_{fg} (%)	V_{fc} (%)	UTS (V_{ft}=0.6) (MPa)	E (V_{ft}=0.6) (MPa)
G_8	49.20	64.60	3.05	1313	41.9	55.3	0	1425	45.4
	49.35	55.40	2.59	1123	42.2	55.3	0	1218	45.7
	49.95	61.35	2.90	1228	42.6	55.3	0	1333	46.2
	47.34	62.15	2.98	1313	44.8	56.9	0	1384	47.3
	46.44	59.85	2.97	1289	43.4	56.9	0	1359	45.7
	47.81	52.55	2.30	1099	48.3	56.9	0	1159	50.9
C_8	49.39	83.30	1.31	1687	155.9	0	54.7	1850	171.0
	48.69	80.40	1.33	1651	129.4	0	54.7	1811	142.0
	49.00	75.10	1.20	1535	136.1	0	54.7	1683	149.2
	48.80	85.65	1.48	1755	132.0	0	56.0	1880	141.4
	47.56	81.00	1.12	1703	166.5	0	56.0	1825	178.4
	48.36	70.45	1.53	1457	124.6	0	56.0	1561	133.5
G_4C_4/ C_4G_4	48.41	70.40	1.65	1454	89.6	28.8	16.6	1575	97.0
	48.86	66.85	1.23	1368	90.4	28.8	26.6	1482	97.9
	48.41	61.60	1.10	1272	92.2	28.8	26.6	1378	99.9
	46.44	68.45	1.58	1474	95.2	30.5	28.2	1507	97.3
	44.35	63.35	1.47	1428	96.4	30.5	28.2	1460	98.5
	46.19	60.60	1.50	1312	95.5	30.5	28.2	1341	97.6
C_4G_4/ G_4C_4	49.25	66.30	1.36	1346	87.5	29.9	26.0	1445	93.9
	49.20	61.90	1.61	1258	84.1	29.9	26.0	1350	90.2
	49.20	66.95	1.74	1361	85.2	29.9	26.0	1461	91.4
	46.56	70.40	1.73	1512	90.6	30.5	28.4	1540	92.3
	44.46	50.40	1.49	1134	91.4	30.5	28.4	1155	93.1
	46.62	58.15	1.19	1247	97.7	30.5	28.4	1271	99.5
$G_2C_4G_2$/ $G_2C_4G_2$	49.95	72.85	1.74	1458	86.0	28.2	27.1	1582	93.3
	49.70	74.90	1.60	1507	89.2	28.2	27.1	1635	96.8
	49.14	66.90	1.75	1361	85.6	28.2	27.1	1477	92.9
	49.39	69.60	1.72	1409	90.4	27.8	28.6	1499	96.2
	47.56	65.55	1.11	1378	93.2	27.8	28.6	1466	99.2
	48.11	66.35	1.59	1379	94.5	27.8	28.6	1467	100.5
$C_2G_4C_2$/ $C_2G_4C_2$	49.30	65.90	1.63	1337	83.1	29.3	26.9	1427	88.7
	49.20	59.85	1.29	1216	86.9	29.3	26.9	1299	92.7
	48.56	52.05	1.48	1072	80.4	29.3	26.9	1144	85.9
	48.31	63.45	1.63	1313	81.4	29.7	28.3	1359	84.2
	46.49	51.60	1.37	1110	89.6	29.7	28.3	1148	92.7
	48.95	59.40	1.49	1213	85.8	29.7	28.3	1255	88.7

TABLE A52: INDIVIDUAL COMPRESSIVE TEST RESULTS, 913 MATRIX

Lay-up	CSA (mm^2)	Max. Load (kN)	Failure Strain %	UCS (MPa)	E (GPa)	V_{fg} (%)	V_{fc} (%)	UCS (V_{ft}=0.6) (MPa)	E (V_{ft}=0.6) (GPa)
G_8C_8	16.90	22.41	2.49	1326	52.9	67.4	0	1180	47.1
	16.63	18.44	2.05	1109	53.2	67.4	0	987	47.3
	16.04	17.89	1.98	1115	55.5	67.4	0	993	49.4
	15.68	17.20	2.09	1097	52.0	68.8	0	957	45.4
	15.81	17.27	2.09	1092	52.0	68.8	0	953	45.4
	15.60	17.65	2.22	1131	52.1	68.8	0	987	45.5
C_8/C_8	19.06	29.26	1.31	1535	125.2	0	63.2	1457	118.9
	19.21	27.12	1.12	1412	130.2	0	63.2	1340	123.6
	18.72	31.05	1.24	1659	139.6	0	63.2	1575	132.5
	19.36	25.47	1.05	1316	125.5	0	64.6	1222	116.6
	20.10	29.58	1.22	1472	122.8	0	64.6	1367	114.1
	19.89	22.04	0.84	1108	133.8	0	64.6	1029	124.3
G_4C_4/C_4G_4	17.51	22.60	1.57	1291	86.5	30.9	33.5	1203	80.6
	17.82	22.54	1.53	1265	85.3	30.9	33.5	1178	79.5
	18.33	23.95	1.55	1307	88.3	30.9	33.5	1217	82.3
	18.54	23.51	1.50	1268	85.5	31.3	33.7	1171	79.0
	18.03	21.87	1.39	1213	87.8	31.3	33.7	1120	81.1
	18.28	23.39	1.42	1280	90.8	31.3	33.7	1181	83.8
C_4G_4/G_4C_4	17.75	19.65	1.20	1107	92.0	30.8	34.8	1013	84.2
	17.85	22.23	1.40	1245	89.9	30.8	34.8	1139	82.2
	17.68	23.66	1.50	1338	91.8	30.8	34.8	1224	83.9
	18.82	20.59	1.19	1094	92.2	30.4	34.3	1015	85.5
	18.36	24.80	1.58	1351	89.3	30.4	34.3	1253	82.8
	18.00	24.04	1.51	1336	91.4	30.4	34.3	1239	84.7
G_6C_2/C_2G_6	17.53	24.79	1.92	1414	76.1	49.5	16.6	1284	69.1
	17.47	18.63	1.57	1066	68.6	49.5	16.6	968	62.3
	16.92	21.63	1.59	1278	82.1	49.5	16.6	1160	74.5
	18.78	20.87	1.67	1111	67.6	50.4	16.8	992	60.4
	18.44	27.01	1.85	1465	71.1	50.4	16.8	1308	63.5
	17.42	23.09	1.99	1325	68.3	50.4	16.8	1183	61.0
C_6G_2/G_2C_6	18.61	25.27	1.08	1358	129.1	16.4	49.0	1246	118.4
	19.16	27.94	1.41	1458	108.0	16.4	49.9	1338	99.1
	18.60	27.08	1.17	1456	129.4	16.4	49.0	1336	118.7
	17.81	29.16	1.44	1637	115.6	16.0	49.4	1502	106.0
	17.90	28.16	1.47	1573	110.4	16.0	49.4	1443	101.3
	19.22	25.27	1.15	1315	113.3	16.0	49.4	1206	103.9

TABLE A52 (continued):

Lay-up	CSA (mm^2)	Max:Load (kN)	Failure Strain (%)	UCS (MPa)	E (GPa)	V_{fg} (%)	V_{fc} (%)	UCS (V_{ft}=0.6) (MPa)	E (V_{ft}=0.6) (MPa)
G_2C_6/	19.46	29.32	1.45	1507	107.4	16.2	47.9	1419	100.5
C_6G_2	18.72	21.29	1.19	1137	97.4	16.2	47.9	1065	91.2
	18.87	26.11	1.44	1384	96.6	16.2	47.9	1295	90.4
	19.64	26.28	1.47	1338	92.5	15.3	46.2	1305	90.3
	19.64	24.82	1.34	1264	96.2	15.3	46.2	1233	93.9
	19.48	28.74	1.67	1475	92.1	15.3	46.2	1439	89.8
C_2G_6/	17.34	18.66	1.71	1076	63.9	46.9	17.3	1006	59.6
G_6C_2	18.53	19.31	1.46	1042	71.3	46.9	17.3	974	66.6
	18.24	19.88	1.67	1090	65.3	46.9	17.3	1019	61.0
	18.21	24.14	1.67	1326	80.2	48.0	17.7	1211	73.3
	18.87	20.79	1.48	1102	75.3	48.0	17.7	1006	68.8
	19.11	19.17	1.46	1003	66.9	48.0	17.7	916	61.1
G_7C/CG_7	17.89	23.24	*	1299	67.5	60.3	8.2	1138	59.1
	17.50	21.94	2.10	1254	60.2	60.3	8.2	1098	52.8
	17.79	18.90	1.85	1062	57.3	60.3	8.2	931	50.2
	19.92	25.07	2.17	1259	58.8	54.9	8.4	1193	55.7
	19.20	27.22	2.28	1418	63.6	54.9	8.4	1344	60.3
	19.13	23.40	2.20	1223	56.9	54.9	8.4	1159	54.0
CG_7/G_7C	16.57	21.49	1.96	1297	66.5	60.2	8.8	1128	57.8
	18.02	21.74	1.91	1206	64.4	60.2	8.8	1049	56.0
	17.92	21.49	1.76	1199	69.4	60.2	8.8	1043	60.3
	17.41	19.55	1.87	1123	62.0	59.6	8.8	985	54.4
	17.78	19.53	1.78	1098	62.6	59.6	8.8	964	54.9
	16.97	16.38	1.57	965	61.1	59.6	8.8	847	53.6
$G_2C_4G_2$/	18.96	26.22	1.66	1383	86.2	30.7	35.4	1255	78.3
$G_2C_4G_2$	18.80	23.53	1.52	1252	83.3	30.7	35.4	1136	75.6
	18.79	24.49	1.62	1303	82.1	30.7	35.4	1183	74.5
	19.17	23.84	1.54	1244	82.5	31.0	34.3	1143	75.8
	18.76	24.39	1.59	1300	82.6	31.0	34.3	1195	75.9
	18.74	24.73	1.47	1320	92.6	31.0	34.3	1213	85.1
$C_2G_4C_2$/	18.47	23.80	1.61	1289	82.6	31.1	34.4	1180	75.7
$C_2G_4C_2$	17.94	24.38	1.73	1359	80.9	31.1	34.4	1245	74.1
	18.87	25.66	1.75	1360	83.7	31.1	34.4	1246	76.7
	18.90	22.39	1.48	1185	83.8	30.4	34.4	1097	77.6
	18.83	23.25	1.59	1235	80.3	30.4	34.4	1143	74.3
	18.60	21.44	1.31	1153	85.3	30.4	34.4	1067	79.0

TABLE A53: INDIVIDUAL COMPRESSIVE TEST RESULTS, 914 MATRIX

Lay-up	CSA (mm^2)	Max.Load (kN)	Failure Strain %	UCS (MPa)	E (GPa)	V_{fg} (%)	V_{fc} (%)	UCS (V_{ft}=0.6 (MPa)	E (V_{ft}=0.6) (MPa)
G_8/G_8	16.80	18.75	2.09	1116	53.1	70.4	0	951	45.3
	17.01	18.11	2.06	1065	51.7	70.4	0	907	44.1
	17.89	23.04	2.46	1288	52.4	70.4	0	1098	44.7
	17.32	19.69	2.05	1137	56.0	71.6	0	953	46.9
	17.06	19.95	2.21	1169	52.8	71.6	0	980	44.2
	17.10	24.60	1.69	1439	53.4	71.6	0	1206	44.7
C_8/C_8	18.88	28.56	1.08	1513	141.3	0	68.6	1323	123.6
	18.78	35.05	1.49	1866	130.7	0	68.6	1632	114.3
	19.35	32.75	1.26	1693	137.4	0	68.6	1480	120.1
	18.59	32.56	1.08	1751	179.1	0	69.3	1516	155.1
	18.78	31.37	1.11	1670	164.1	0	69.3	1446	142.1
	18.52	31.22	1.30	1686	137.7	0	69.3	1460	119.2
$G_4C_4/$ C_4G_4	16.71	20.72	1.33	1240	97.3	36.3	34.4	1052	82.6
	17.80	25.90	1.65	1455	91.9	36.3	34.4	1235	78.0
	18.28	*	*	*	*	*	*	*	*
	17.92	22.02	1.34	1229	91.8	35.8	34.6	1047	78.3
	17.48	25.89	1.54	1481	98.8	35.8	34.6	1262	84.2
	18.43	20.78	1.19	1128	94.6	35.8	34.6	961	80.7
$C_4G_4/$ G_4C_4	18.11	22.88	1.33	1263	97.8	35.8	34.9	1072	83.0
	17.75	23.82	1.27	1342	103.4	35.8	34.9	1139	87.8
	17.73	24.02	1.38	1355	98.8	35.8	34.9	1150	83.9
	16.35	19.96	1.46	1221	87.9	36.0	35.0	1032	74.3
	18.06	24.65	1.33	1365	105.7	36.0	35.0	1153	89.3
	18.13	22.84	1.40	1260	94.6	36.0	35.0	1065	80.0
$G_2C_4G_2/$ $G_2C_4G_2$	17.42	24.72	1.51	1419	100.2	35.0	35.9	1201	84.8
	17.54	28.82	1.80	1643	98.2	35.0	35.9	1390	83.1
	18.22	19.68	1.12	1080	96.7	35.0	35.9	914	81.8
	17.52	22.72	1.47	1297	90.7	35.5	35.9	1090	76.2
	18.06	23.52	1.36	1302	97.3	35.5	35.9	1094	81.7
	18.41	27.10	1.61	1472	99.7	35.5	35.9	1237	83.8
$C_2G_4C_2/$ $C_2G_4C_2$	17.29	21.40	1.41	1238	91.4	35.4	35.2	1052	77.6
	17.72	23.98	1.61	1353	85.8	35.4	35.2	1150	72.9
	17.95	23.94	1.50	1334	89.8	35.4	35.2	1133	76.3
	17.87	25.15	1.52	1407	94.5	35.5	35.0	1198	80.5
	17.19	25.41	(1.30)	1478	(160.8)	35.5	35.0	1258	(136.9)
	17.34	26.77	1.57	1544	104.3	35.5	35.0	1314	88.7

TABLE A54: INDIVIDUAL COMPRESSIVE TEST RESULTS, 411 MATRIX

Lay-up	CSA (mm^2)	Max.Load (kN)	Failure Strain %	UCS (MPa)	E (GPa)	V_{fg} (%)	V_{fc} (%)	UCS (V_{ft}=0.6) (MPa)	E (V_{ft}=0.6) (GPa)
G_8/G_8	20.90	20.94	*	1002	*	55.7	–	1079	*
	20.66	21.17	*	1025	*	55.7	–	1104	*
	20.18	18.40	*	912	*	55.7	0	982	*
	18.55	17.69	2.22	954	42.8	55.7	0	1027	46.2
	19.15	19.53	2.39	1020	42.6	55.7	0	1099	45.9
	18.60	16.27	1.78	875	49.3	55.7	0	942	53.1
	20.78	23.20	*	1116	*	55.1	0	1216	*
	20.28	19.91	*	982	*	55.1	0	1069	*
	19.96	18.61	*	932	*	55.1	0	1015	*
	19.05	15.99	1.69	839	51.1	55.1	0	914	55.7
	18.91	*	*	*	*	55.1	0	*	*
	18.99	23.87	2.68	1257	47.0	55.1	0	1369	51.2
C_8/C_8	20.10	21.32	*	1061	*	0	56.2	1133	*
	20.18	17.88	*	886	*	0	56.2	946	*
	20.81	19.46	0.90	935	102.0	0	56.2	998	108.9
	20.12	20.73	1.01	1030	102.8	0	56.2	1100	109.8
	20.04	*	*	*	*	0	56.2	*	*
	18.66	10.58	0.60	567	126.6	0	63.6	535	119.4
	18.73	11.71	0.48	625	126.3	0	63.6	590	119.1
	18.55	12.89	0.55	695	122.5	0	63.6	656	115.6
$G_4C_4/$ C_4G_4	21.53	16.47	1.16	765	71.1	29.2	27.4	811	75.4
	20.92	20.80	1.16	994	83.9	29.2	27.4	1054	88.9
	20.32	20.83	1.47	1025	78.7	29.2	27.4	1087	83.5
	19.52	20.88	0.97	1070	111.4	27.8	31.7	1079	112.3
	19.48	17.12	1.07	879	83.1	27.8	31.7	886	83.8
	19.90	14.97	0.88	752	82.0	27.8	31.7	759	82.7
$C_4G_4/$ G_4C_4	19.62	10.02	(0.41)	511	(113.8)	30.2	28.5	522	(16.3)
	19.70	14.60	1.19	741	80.4	30.2	28.5	758	82.2
	18.97	14.06	1.03	741	72.9	30.2	28.5	758	74.5
	20.65	14.87	0.89	720	79.9	27.3	23.8	846	93.8
	20.67	16.74	1.16	810	67.8	27.3	23.8	951	79.6
	20.28	27.96	1.18	886	85.3	27.3	23.8	1040	100.2
$G_2C_4G_2/$ $G_2C_4G_2$	19.34	14.92	0.93	771	83.6	29.1	28.1	809	87.7
	19.52	19.21	1.29	984	79.5	29.1	28.1	1032	83.4
	19.36	14.45	1.02	746	74.7	29.1	28.1	783	78.4
	19.19	18.40	1.27	959	77.8	31.9	26.1	992	80.5
	19.10	16.62	1.16	870	75.9	31.9	26.1	900	78.5
	19.10	13.00	0.96	681	73.4	31.9	26.1	704	75.9

TABLE A54 (continued):

Lay-up	CSA (mm^2)	Max.Load (kN)	Failure Strain %	UCS (MPa)	E (GPa)	V_{fg} (%)	V_{fc} (%)	UCS (V_{ft}=0.6) (MPa)	E (V_{ft}=0.6) (GPa)
$C_2G_4C_2$/	19.68	14.04	0.80	713	76.6	28.3	26.8	777	83.4
$C_2G_4C_2$	20.32	18.16	1.10	894	82.1	28.3	26.8	973	89.4
	20.02	17.35	1.11	867	77.2	28.3	26.8	944	84.1
	19.35	15.40	0.92	796	93.4	28.9	29.0	825	96.8
	19.33	19.41	1.29	1004	78.5	28.9	29.0	1041	81.4
	19.13	17.78	1.22	929	75.8	28.9	29.0	963	78.5

TABLE A55: INDIVIDUAL COMPRESSIVE TEST RESULTS, 470-36 MATRIX

Lay-up	CSA (mm^2)	Max. Load (kN)	Failure Strain (%)	UCS (MPa)	E (GPa)	V_{fg} (%)	V_{fc} (%)	UCS (V_{ft}=0.6) (MPa)	E (V_{ft}=0.6) (GPa)
G_8/G_8	19.81	23.34	*	117.8	*	58.7	0	1204	*
	19.67	21.76	*	1106	*	58.7	0	1131	*
	18.89	21.44	*	1135	*	58.7	0	1160	*
	18.59	14.30	1.74	769	47.3	58.7	0	786	48.3
	18.62	21.50	2.36	1155	48.8	58.7	0	1180	49.8
	18.43	17.14	2.03	930	51.2	58.7	0	951	52.3
	19.93	18.59	*	933	*	65.9	0	849	*
	19.58	21.17	*	1081	*	65.9	0	984	*
	19.29	16.50	*	855	*	65.9	0	779	*
	17.62	20.09	2.41	1140	51.8	65.9	0	1038	47.2
	17.97	21.19	2.46	1179	47.7	65.9	0	1074	43.4
	19.06	21.81	2.36	1144	48.2	65.9	0	1042	43.9
C_8/C_8	20.60	20.10	1.10	976	112.7	0	56.1	1044	120.5
	20.40	19.36	0.80	949	115.8	0	56.1	1015	123.8
	20.40	13.80	0.62	676	103.2	0	56.1	723	110.4
	20.36	14.25	0.71	700	98.2	0	55.9	751	105.4
	20.15	12.74	0.52	632	127.3	0	55.9	679	136.6
	19.79	12.52	0.62	633	100.4	0	55.9	679	107.8
G_4C_4/C_4G_4	19.99	22.77	1.08	1139	103.9	29.5	28.5	1178	197.5
	19.69	22.33	1.14	1134	96.3	29.5	28.5	1173	99.7
	19.77	16.52	1.38	836	71.8	29.5	28.5	864	74.3
	20.33	15.46	0.89	760	94.1	29.1	26.5	821	101.5
	19.44	20.01	1.19	1029	94.4	29.1	26.5	1111	101.9
	19.63	16.50	1.36	841	65.1	29.1	26.5	907	70.3
C_4G_4/G_4C_4	19.64	15.15	1.04	771	73.3	30.8	26.7	805	76.5
	19.70	*	*	*	*	30.8	26.7	*	*
	19.50	10.80	0.65	554	80.6	30.8	26.7	578	84.1
	19.29	16.09	1.13	834	31.4	31.4	26.2	869	81.1
	19.24	17.99	1.05	935	93.0	31.4	26.2	974	96.9
	19.13	17.65	0.93	923	104.8	31.4	26.2	961	109.1
$G_2C_4G_2/G_2C_4G_2$	19.86	20.16	1.44	1015	72.4	29.5	25.5	1107	78.9
	19.86	17.02	1.15	857	74.9	29.5	25.5	935	81.7
	20.08	19.30	1.35	961	72.8	29.5	25.5	1049	79.4
	19.73	14.20	0.95	720	77.0	30.6	29.3	746	79.8
	19.11	20.50	1.48	1073	75.3	30.6	27.3	1112	78.0
	19.40	16.47	1.09	849	78.1	30.6	27.3	880	80.9

TABLE A55 (continued):

Lay-up	CSA (mm^2)	Max. Load (kN)	Failure Strain (%)	UCS (MPa)	E (GPa)	V_{fg} (%)	V_{fc} (%)	UCS (V_{ft}=0.6) (MPa)	E (V_{ft}=0.6) (GPa)
$C_2G_4C_2$/	19.23	11.90	0.91	619	70.8	29.3	27.0	659	75.5
$C_2G_4C_2$	19.11	19.06	1.38	997	74.0	29.3	27.0	1063	78.9
	19.42	17.87	1.23	920	74.0	29.3	27.0	981	78.9
	18.30	11.14	0.79	609	80.9	33.3	28.0	596	79.2
	17.71	16.15	0.97	912	92.7	33.3	28.0	893	90.7
	17.71	13.96	0.95	788	80.1	33.3	28.0	772	78.4

APPENDIX 2

STATISTICAL SIGNIFICANCE TESTS FOR THE HYBRID EFFECT

In order to show that the strain to failure of hybrid composite lay-ups is higher than that of the parent CFRP material, some form of statistical significance test is necessary. The "Student t" test was used for this purpose. The hybrid failure strain result samples were compared with the sample of CFRP failure strains, and the test was performed to determine whether the former was significantly different from the latter. The method adopted is described in greater detail by Chatfield[94]. An example calculation is as follows: Data obtained from the stress/strain test results:

Resin:fibre lay-up		913:C_8/C_8	913:G_4C_4/C_4G_4
Failure strain	1	1.48	1.59
results (%)	2	1.12	1.51
	3	1.30	1.57
	4	1.33	1.44
	5	1.43	1.65
	6	1.31	1.54
Mean, $\bar{x}$		1.328	1.550
Standard deviation, S		0.1248	0.0718

The standard deviation is calculated using the formula

$$S = \sqrt{\sum_{i=1}^{n} \frac{(x_i - \bar{x})^2}{n-1}}$$

where n = the number of items in the sample.

It is assumed that the two samples came from the same population.

The combined, unbiased estimate of the variance is given by

$$S^2 = \frac{(n_1-1)\ S_1^2 + (n_2-1)\ S_2^2}{n_1+n_2 - 2}$$

where n_1 = number of items in sample 1

n_2 = number of items in sample 2

S_1 = standard deviation of sample 1

S_2 = standard deviation of sample 2

The denominator in the above expression is the number of degrees of freedom (ν):

$$\nu = n_1 + n_2 - 2$$

Using the above data: $S = 0.1018$

and $\nu = 10$

The null hypothesis is given by $H_o: \mu_1 = \mu_2$ and the alternative hypothesis by H: $\mu_1 < \mu_2$. A one tailed test is appropriate.

The test statistic is given by

$$t = \frac{(\bar{x}_1 - \bar{x}_2)}{S(\frac{1}{n_1} + \frac{1}{n_2})^{\frac{1}{2}}}$$

Using the above data: $t = 3.777$

Since the estimate of S is based on ν degrees of freedom, if H_o is true, the sampling distribution of t is a t distribution with ν degrees of freedom.

From tables of Students t distribution:

$$t_{0.01,10} = 2.764$$

That is, the probability that $|t| > 2.764$ is 0.01. Therefore the result is significant at the 1% level, and it is very likely that H_o is untrue.

If the result were not significant at the 1% level, the test could be performed at, say, the 5% level of probability using

$$t_{0.05,10} = 1.812$$

These tests were carried out for all the hybrid fibre lay-ups in all four resin matrices and for both tensile and compressive tests. The results are presented in the following tables.

TABLE A56: 913 TENSILE TESTS

Lay-up	Sample Mean ($\bar{x}$)	Sample SD (S)	No. of dof (ν)	Test Statistic	SIGNIFICANT HYBRID EFFECT 90% Level	95% Level	99% Level
C_8/C_8	1.328	0.1248	-	-	-	-	-
G_7C/CG_7	1.917	0.1385	10	7.739	Yes	Yes	Yes
CG_7/G_7C	1.647	0.0848	10	5.179	Yes	Yes	Yes
G_6C_2/C_2G_6	1.652	0.0279	10	6.206	Yes	Yes	Yes
C_2G_6/G_6C_2	1.473	0.1316	10	1.958	Yes	Yes	No
G_4C_4/C_4G_4	1.550	0.0718	10	3.777	Yes	Yes	Yes
C_4G_4/G_4C_4	1.488	0.0546	10	2.877	Yes	Yes	Yes
$G_2C_4G_2/G_2C_4G_2$	1.488	0.1477	10	2.027	Yes	Yes	No
$C_2G_4C_2/C_2G_4C_2$	1.423	0.1360	10	1.261	No	No	No
G_2C_6/C_6G_2	1.528	0.0857	10	3398	Yes	Yes	Yes
C_6G_2/G_2C_6	1.488	0.0697	10	2.742	Yes	Yes	No

TABLE A57: 914 TENSILE TESTS

Lay-up	Sample Mean ($\bar{x}$)	Sample SD (S)	No. of dof (ν)	Test Statistic	SIGNIFICANT HYBRID EFFECT 90% Level	95% Level	99% Level
C_8/C_8	0.903	0.0463	-	-	-	-	-
G_4C_4/C_4G_4	0.938	0.0500	10	1.258	No	No	No
C_4G_4/G_4C_4	7.002	0.1291	9	1.763	Yes	No	No
$G_2C_4G_2/G_2C_4G_2$	1.025	0.1019	10	2.670	Yes	Yes	No
$C_2G_4C_2/C_2G_4C_2$	0.9500	0.0938	10	1.101	No	No	No

TABLE A58: 411-45 TENSILE TESTS

Lay-up	Sample Mean ($\bar{x}$)	Sample SD (S)	No. of dof (ν)	Test Statistic	SIGNIFICANT HYBRID EFFECT 90% Level	95% Level	99% Level
C_8/C_8	1.282	0.1061	-	-	-	-	-
G_4C_4/C_4G_4	1.442	0.1583	9	2.004	Yes	Yes	No
C_4G_4/G_4C_4	1.457	0.2202	10	1.754	Yes	No	No
$G_2C_4G_2/G_2C_4G_2$	1.610	0.1785	10	3.869	Yes	Yes	Yes
$C_2G_4C_2/C_2G_4C_2$	1.498	0.1597	10	2.760	Yes	Yes	No

TABLE A59: 470-36 TENSILE TESTS

Lay-up	Sample Mean ($\bar{x}$)	Sample SD (S)	No. of dof (ν)	Test Statistic	SIGNIFICANT HYBRID EFFECT 90% Level	95% Level	99% Level
C_8/C_8	1.328	0.1574	-	-	-	-	-
G_4C_4/C_4G_4	1.422	0.2125	10	0.871	No	No	No
C_4G_4/G_4C_4	1.520	0.2173	10	1.753	Yes	No	No
$G_2C_4G_2/G_2C_4G_2$	1.585	0.2430	10	2.174	Yes	Yes	No
$C_2G_4C_2/C_2G_4C_2$	1.482	0.1366	10	1.810	Yes	No	No

TABLE A60: 913 COMPRESSIVE TESTS

Lay-up	Sample Mean ($\bar{x}$)	Sample SD (S)	No. of dof (ν)	Test Statistic	SIGNIFICANT HYBRID EFFECT 90% Level	95% Level	99% Level
C_8/C_8	1.130	0.1692	-	-	-	-	-
G_7C/CG_7	2.120	0.1642	9	9.790	Yes	Yes	Yes
CG_7/G_7C	1.808	0.1393	10	7.578	Yes	Yes	Yes
G_6C_2/C_2G_6	1.765	0.1786	10	6.322	Yes	Yes	Yes
C_2G_6/G_6C_2	1.575	0.1198	10	5.258	Yes	Yes	Yes
G_4C_4/C_4G_4	1.493	0.0728	10	4.827	Yes	Yes	Yes
C_4G_4/G_4C_4	1.397	0.1665	10	2.755	Yes	Yes	No
$G_2C_4G_2/G_2C_4G_2$	1.567	0.0698	10	5.848	Yes	Yes	Yes
$C_2G_4C_2/C_2G_4C_2$	1.578	0.1645	10	4.650	Yes	Yes	Yes
G_2C_6/C_6G_2	1.427	0.1583	10	3.140	Yes	Yes	Yes
C_6G_2/G_2C_6	1.287	0.1717	10	1.595	Yes	No	No

TABLE A61: 914 COMPRESSIVE TESTS

Lay-up	Sample Mean ($\bar{x}$)	Sample SD (S)	No. of dof (ν)	Test Statistic	SIGNIFICANT HYBRID EFFECT 90% Level	95% Level	99% Level
C_8/C_8	1.220	0.1626	-	-	-	-	-
G_4C_4/C_4G_4	1.410	0.1832	9	1.824	Yes	No	No
C_4G_4/G_4C_4	1.362	0.0662	10	1.981	Yes	Yes	No
$G_2C_4G_2/G_2C_4G_2$	1.478	0.2299	10	2.244	Yes	Yes	No
$C_2G_4C_2/C_2G_4C_2$	1.524	0.0789	9	3.800	Yes	Yes	Yes

TABLE A62: 411-45 COMPRESSIVE TESTS

Lay-up	Sample Mean ($\bar{x}$)	Sample SD (S)	No. of dof (ν)	Test Statistic	SIGNIFICANT HYBRID EFFECT 90% Level	95% Level	99% Level
C_8/C_8	0.798	0.2327	-	-	-	-	-
G_4C_4/C_4G_4	1.118	0.2041	9	3.116	Yes	Yes	Yes
C_4G_4/G_4C_4	1.090	0.1290	8	3.210	Yes	Yes	Yes
$G_2C_4G_2/G_2C_4G_2$	1.105	0.1571	9	3.373	Yes	Yes	Yes
$C_2G_4C_2/C_2G_4C_2$	1.073	0.1837	9	2.913	Yes	Yes	Yes

TABLE A63: 470-36 COMPRESSIVE TESTS

Lay-up	Sample Mean ($\bar{x}$)	Sample SD (S)	No. of dof (ν)	Test Statistic	SIGNIFICANT HYBRID EFFECT 90% Level	95% Level	99% Level
C_8/C_8	0.728	0.2052	-	-	-	-	-
G_4C_4/C_4G_4	1.173	0.1833	10	3.962	Yes	Yes	Yes
C_4G_4/G_4C_4	0.9600	0.1873	9	1.940	Yes	Yes	No
$G_2C_4G_2/G_2C_4G_2$	1.243	0.2118	10	4.278	Yes	Yes	Yes
$C_2G_4C_2/C_2G_4C_2$	1.038	0.2209	10	2.519	Yes	Yes	No

It can be seen from Tables A56-A63 that, at the 90% confidence level, nearly every laminate lay-up passed the test, that is that the increase in the strain to failure of hybrids over CFRP was significant. At the 95% level, 20 out of 22 passed in compression, and 14 out of 22 in tension, while at the 99% confidence level, the pass rate fell to 15/22 in compression and 7/22 in tension.

Taking these results as a whole, it is clear that the hybrid effect is significant in both tension and compression. The greater increases in failure strain which the compressive specimens demonstrated gave the statistical analysis for those results a greater degree of confidence than those of the tensile tests. The reason why so many lay-ups did not pass the test at the 99% confidence level was the relatively large amount of scatter in the results which is an inherent characteristic of these materials. Because the system of lay-ups could be treated as a whole, the hybrid effect, if it occurs in one lay up, is likely to occur in the others too. For this reason, the level of confidence with which it can be concluded that a significant hybrid effect occurs, is effectively higher than that indicated by Tables A56-A63 for each individual lay-up.

APPENDIX 3

QUANTIFICATION OF THE VARIATION OF MODULUS WITH RESPECT TO STRAIN

The tangent modulus of an FRP laminate can be expressed as a function of the applied strain. For the purposes of this work the relationship in each case is considered to be straight lines through the tensile and compressive results independently. They can be expressed by the general equation

$$E(GPa) = A + B\varepsilon(\%) \qquad (A3.1)$$

The constants A and B have been calculated from the results and are presented in the following table:

TABLE A64: THE CONSTANTS A AND B (IN EQUATION A3.1) WHICH DEFINE THE STRAIGHT LINES THROUGH THE TANGENT MODULUS VS STRAIN RESULTS

a) 913 Matrix

Lay-up	Mode	V_{fc}/V_{ft}	A	B
G_8/G_8	tensile	0	48.2	-2.42
	compressive	0	45.7	-0.798
C_8/C_8	tensile	1.0	127.0	19.4
	compressive	1.0	129.9	24.1
G_4C_4/C_4G_4	tensile	0.519	91.6	7.34
	compressive	0.519	92.6	18.9
C_4G_4/G_4C_4	tensile	0.530	85.7	10.5
	compressive	0.530	94.8	19.5

b) 914 Matrix

Lay-up	Mode	V_{fc}/V_{ft}	A	B
G_8/G_8	tensile	0	43.8	-0.889
	compressive	0	45.5	0.686
C_8/C_8	tensile	1.0	127.1	20.2
	compressive	1.0	137.5	37.7
G_4C_4/C_4G_4	tensile	0.489	82.4	12.1
	compressive	0.489	90.4	17.0

TABLE A64 (continued)

c) 411-45 Matrix

Lay-up	Mode	V_{fc}/V_{ft}	A	B
G_8/G_8	tensile	0	52.0	-4.59
	compressive	0	52.2	2.16
C_8/C_8	tensile	1.0	136.0	15.0
	compressive	1.0	127.3	37.0

d) 470-36 Matrix

Lay-up	Mode	V_{fc}/V_{ft}	A	B
G_8/G_8	tensile	0	50.3	-3.06
	compressive	0	49.7	2.36
C_8/C_8	tensile	1.0	130.7	27.6
	compressive	1.0	138.6	67.4